Characterization of incompatible and compatible *Camellia-Ciborinia camelliae* plant-pathogen interactions

A thesis presented in partial fulfilment of the requirements for the degree of

Doctor of Philosophy in Plant Biology

at Massey University, Palmerston North, New Zealand

Matthew Denton-Giles

2014

Abstract

Many *Camellia* species and cultivars are susceptible to infection by the host-specific fungal phytopathogen *Ciborinia camelliae* L. M. Kohn (Sclerotiniaceae). This necrotrophic pathogen specifically infects floral tissue resulting in rapid development of host-cell death and premature flower fall. *C. camelliae* is considered to be the causal agent of '*Camellia* flower blight' and is an economically significant pest of both the *Camellia* floriculture and *Camellia* oil seed industries. This study sought to identify molecular components that contribute to incompatible and compatible interactions between *C. camelliae* and *Camellia* petal tissue.

Microscopic analyses of incompatible *C. camelliae-Camellia lutchuensis* interactions revealed several hallmarks of induced plant resistance, including papillae formation, H_2O_2 accumulation, and localized cell death. Extension of resistance analyses to an additional 39 *Camellia* spp. identified variable levels of resistance within the *Camellia* genus, with *Camellia lutchuensis, Camellia transnokoensis and Camellia yuhsienensis* exhibiting the strongest resistance phenotypes. Collectively, *Camellia* species of section Theopsis showed the highest levels of incompatibility. Based on this observation, a total of 18 *Camellia* interspecific hybrids with section Theopsis species in their parentage were tested for resistance to *C. camelliae*. The majority of hybrids developed disease symptoms, although the speed and intensity of disease development varied. Hybrids containing high genetic dosages of *C. lutchuensis* within their parentage were the most effective at resisting *C. camelliae* infection. Therefore, introgression of genetic information from *Camellia lutchuensis* into hybrids of *Camellia* is likely to be a valid approach for breeding *Camellia* hybrids with increased *C. camelliae* resistance. A comparison between transcriptomes of mock-infected and infected *C. lutchuensis* samples identified plant genes that may contribute to *C. camelliae* resistance, including two putative transcription factors.

C. camelliae growth in compatible tissue demonstrated a switch from biotrophy to necrotrophy, evident from the simultaneous development of secondary hyphae and necrotic lesions. The initial biotrophic-like period of *C. camelliae* growth *in planta* was asymptomatic; leading to the hypothesis that *C. camelliae* may secrete fungal effectors during infection. A bioinformatic approach was taken to identify putative effectors of *C. camelliae*. To facilitate this approach, a 40.7 MB draft genome of *C. camelliae* was assembled and validated. Genomic and transcriptomic data were used to predict a total of 14711 *C. camelliae* protein coding genes of which 749 were predicted to form the *C. camelliae* secretome. The secretome of *C. camelliae* was compared with the predicted secretomes of the closely related species, *Botrytis cinerea* (Sclerotiniaceae) and *Sclerotinia sclerotiorum* (Sclerotinaceae). Comparative analysis of the secretomes of these three species identified protein conservation within CAZyme (carbohydrate active enzyme) and protease categories. In contrast, the oxidoreducatase and small secreted protein (SSP) categories were less conserved. Further analysis of SSPs revealed a conserved family of putative effector proteins that appear to have undergone lineage-specific expansion within the host-specific pathogen *C. camelliae* (n = 73), but remain as single genes in the two host-generalists *B. cinerea* and *S. sclerotiorum*. Members of this *Ciborinia camelliae*-like small secreted protein (CCL-SSP) family share 10 conserved cysteine residues, are expressed during the early stages of infection and have homologs in other necrotrophic fungal phytopathogens. Functional assays of native recombinant CCL-SSPs indicate that the *B. cinerea* and *S. sclerotiorum* single gene homologs are able to induce necrosis when infiltrated into *Camellia* 'Nicky Crisp', *Camellia lutchuensis* and *Nicotiana benthamiana* host tissue. In comparison, nine native recombinant CCL-SSP homologs of *C. camelliae* were unable to replicate the necrosis phenotype when infiltrated into the same host tissue. This work identifies a previously uncharacterized family of fungal necrosis-inducing proteins that appear to have contrasting functions in related host-specific and host-generalist phytopathogens.

Acknowledgements

First and foremost I'd like to thank my supervisors, Dr. Paul Dijkwel, Assoc. Prof. Rosie Bradshaw and Assoc. Prof. Murray Cox. Your constructive advice and expert opinion has helped me considerably. I would particularly like to express my sincere gratitude to Paul who gave me the chance to enter into PhD studies. Paul has allowed me the freedom to develop as a scientist and has always encouraged me to do my very best. I would also like to thank Professor Michael McManus who has been supportive throughout my time at Massey University. Furthermore, I would like to thank Professor Tom Gordon and Sharon Kirkpatrick of UC Davis' plant pathology department for hosting my research trip to California.

I am grateful to the support and enthusiasm I have received from members of the New Zealand Camellia Society. A special thanks to Neville Haydon for his prowess and encouragement, Vince Neall for organizing speaking engagements, President Brian Hartley for inviting me to talk about my research, Vonnie Cave for my first introduction to *C. camelliae*, Blanche Lauridsen for helping me to source the best *Camellia* plants and to all the other New Zealand Camellia Society members who offered kind words and encouragement throughout the duration of my project. I would also like to extend my thanks to members of the International Camellia Society including, President Patricia Short, Bee Robson, Carmen Salinero and Professor Chuji Hiruki. Special thanks must go to Dan and Patty Charvet of Fort Bragg, California. Their passion for Camellia's left a lasting impression on me.

I would like to acknowledge the C5.19 lab community for their friendship and comradery. Thank you to Aakansha, Afsana, Alvina, Ameesha, Daniel R, Daniel M, Diantha, Happy, Jay, Jibran, Julia, Marion, Muhammad, Nikola, Rachael, Rubina, Sam, Shane, Srishti, Susanna, Tina, Willemien, Xiao and Yasmin. On a more personal note I would like to thank my family. To my wife Reganne, your support, love and encouragement have been unwavering. To my children Daisy and Moss, having you in my life has made this journey all the more worthwhile. I love you all.

None of this would have happened without financial support from the New Zealand Camellia Memorial Trust, The New Zealand Plant Protection Society, the Palmerston North Jaycee Trust Travelling Scholarship, New Zealand Genomics Ltd and Massey University's Institute of Fundamental Sciences. A special thanks to Mr and Mrs Riggall for your generous contribution towards post-graduate scientific research.

Table of Contents

Abstract i

Acknowledgements iii

List of Figures xi

List of Tables xiii

Abbreviations xiv

1. Introduction 1

 1.1. Background 2

 1.2. Plant resistance 3

  1.2.1. Preformed plant resistance 3

  1.2.2. Induced plant resistance 5

 1.3. Fungal phytopathogens 15

  1.3.1. The biotrophs and the hemibiotrophs 15

  1.3.2. The necrotophs 18

 1.4. *Botrytis cinerea* and *Sclerotinia sclerotiorum* 21

 1.5. *Ciborinia camelliae* 23

 1.6. Research Aims 27

2. Materials and Methods 31

 2.1. Plant and fungal material 32

 2.2. *Ciborinia camelliae* infection assays 32

 2.3. Microscopy 33

  2.3.1. Light microscopy 33

  2.3.2. Confocal laser scanning microscopy 34

  2.3.3. Scanning electron microscopy 34

 2.4. Image analysis 35

  2.4.1. Petal lesion area quantification using ImageJ 35

  2.4.2. Chemiluminescence quantification using ImageJ 35

 2.5. DNA and RNA manipulations 35

  2.5.1. Genomic DNA extraction 35

  2.5.2. Total RNA extraction 36

  2.5.3. Nucleic acid quantification 37

  2.5.4. Restriction endonuclease digests 37

2.5.5. General PCR 38
2.5.6. Colony PCR 38
2.5.7. Quantitative Real-Time PCR (qRT-PCR) 38
2.5.8. DNA and cDNA sequencing 40
2.6. Bioinformatic analyses 40
2.6.1. Post sequencing quality control 41
2.6.2. Draft genome assembly and validation 41
2.6.3. Transcriptome assembly and validation 42
2.6.4. Transcriptome quantification 43
2.6.5. *Ciborinia camelliae* EST identification and validation 44
2.6.6. *Ciborinia camelliae* protein prediction and validation 45
2.6.7. Fungal secretome prediction and validation 45
2.6.8. Secretome annotation 46
2.6.9. Comparative secretome analyses 47
2.6.10. Phylogenetic trees 47
2.6.11. Small secreted protein characterization 48
2.7. Cloning and recombinant protein expression 49
2.7.1. Host strains and growth conditions 49
2.7.2. *E. coli* plasmid DNA isolation 50
2.7.3. Construct and vector design 50
2.7.4. Site-directed mutagenesis 51
2.7.5. *E. coli* and *P. pastoris* transformation 52
2.7.6. Recombinant protein expression 53
2.8. Recombinant protein manipulations 54
2.8.1. *In planta* functional protein assays 54
2.8.2. Protein separation via SDS-PAGE 55
2.8.3. Western blotting 56
2.8.4. Chemiluminescence detection 56
2.9. Statistical analysis 57
2.9.1. *Ciborinia camelliae* host-resistance screening. 57
2.9.2. *Ciborinia camelliae* genome assembly calculations. 57
2.9.3. Statistical comparisons of secretome category raw counts. 58
3. *Ciborinia camelliae* plant resistance 59
3.1. Introduction 60

3.2. Results 62
3.2.1. *Camellia* genotype influences macroscopic disease development. 62
3.2.2. Compatible interactions involve cuticle penetration, intercellular growth and secondary hypha development. 62
3.2.3. Incompatible interactions induce characteristic plant defense responses. 67
3.2.4. Levels of incompatibility to *Ciborinia camelliae* vary within the *Camellia* genus..... 68
3.2.5. Interspecific hybrid resistance is influenced by parent genotype 71
3.3. Discussion.. 76
3.3.1. *Ciborinia camelliae* establishment and growth in compatible tissue 76
3.3.2. *Ciborinia camelliae* resistance in incompatible *Camellia lutchuensis* tissue 78
3.3.3. *Ciborinia camelliae* resistance within *Camellia* species.. 79
3.3.3. *Ciborinia camelliae* resistance within *Camellia* interspecific hybrids 81
3.4. Conclusions 83
4. The development of genomic and transcriptomic resources for the *Camellia-Ciborinia camelliae* interaction 85
4.1. Introduction 86
4.2. Results.. 87
4.2.1. *Ciborinia camelliae* draft genome sequencing and assembly................................. 87
4.2.2. *Ciborinia camelliae* shares genomic characteristics with close relatives *Botrytis cinerea* and *Sclerotinia sclerotiorum*.. 88
4.2.3. The *Ciborinia camelliae* MAT locus exhibits synteny with the heterothallic *Botrytis cinerea* B05.10 *MAT1-1* mating locus 88
4.2.4. *Camellia* 'Nicky Crisp' infected samples produce mixed origin transcriptomes....... 91
4.2.5. Fungal ESTs make up 10% of the *Camellia* 'Nicky Crisp' non-redundant transcriptome.. 96
4.2.6. Large changes in host-defense gene expression are induced in compatible *Camellia 'Nicky Crisp-Ciborinia camelliae* interactions.. 98
4.3. Discussion.. 101
4.3.1. RNA sequencing bias and *de novo* assembly limitations 101
4.3.2. Comparative genome analysis reveals potential heterothallism in *Ciborinia camelliae* 102
4.3.3. The *Ciborinia camelliae* transcriptome is estimated to be 94% complete 103
4.3.4. Compatible *Camellia* 'Nicky Crisp'-*Ciborinia camelliae* interactions induce dramatic changes in host gene expression 104
4.4. Conclusions 107
5. Comparative analysis of the secretomes of *Ciborinia camelliae*, *Botrytis cinerea* and *Sclerotinia sclerotiorum* 109

5.1. Introduction 110
5.2. Results 112
5.2.1. The *Ciborinia camelliae* genome is predicted to contain 14711 non-redundant proteins 112
5.2.2. The secretomes of *Ciborinia camelliae*, *Botrytis cinerea* and *Sclerotinia sclerotiorum* are estimated to be more than 80% complete. 112
5.2.3. Scatterplot analysis reveals differences in secretome composition between *Ciborinia camelliae*, *Botrytis cinerea* and *Sclerotinia sclerotiorum*. 113
5.2.4. Secretome annotation identifies conserved and divergent protein categories 115
5.2.5. Phylogenetic analysis reveals a conserved family of small secreted proteins that appear to be under diversifying selection in *Ciborinia camelliae*. 119
5.3. Discussion 124
5.3.1. Validating the secretomes of *Ciborinia camelliae*, *Botrytis cinerea* and *Sclerotinia sclerotiorum* 124
5.3.2. Two-dimensional scatterplot analysis enables visual comparison of related fungal secretomes. 126
5.3.3. CAZymes and proteases are highly conserved in all three secretomes 127
5.3.4. Diversity exists within the oxidoreductase and small secreted protein categories of each fungal secretome. 129
5.3.5. Half of the small secreted proteins are homologous. 130
5.4. Conclusions 132
6. *In silico* and functional characterization of a conserved family of small secreted proteins from *Ciborinia camelliae*, *Botrytis cinerea* and *Sclerotinia sclerotiorum* 133
6.1. Introduction 134
6.2. Results 135
6.2.1. *In silico Ciborinia camelliae*-like small secreted protein (CCL-SSP) characterization reveals conserved primary protein structure 135
6.2.2. CCL-SSP homologs are present across fungal classes but are confined to species with necrotrophic lifestyles 135
6.2.3. Members of the *CCL-SSP* family share genomic loci. 138
6.2.4. *Ciborinia camelliae CCL-SSP* family members are expressed during pre-lesion development 141
6.2.5. Recombinant *Botrytis cinerea* and *Sclerotinia sclerotiorum* CCL-SSP family members induce host-cell necrosis 144
6.2.6. *BcSSP2* and *SsSSP3* are expressed in *Pichia pastoris* post-induction and are highly stable 145
6.2.7. Tagged recombinant CCL-SSPs are compromised in their ability to induce host-cell necrosis 145

6.3. Discussion 150
6.3.1. CCL-SSP family members share a robust, heat tolerant structure. 150
6.3.2. CCL-SSP family members share characteristics with other necrosis-inducing fungal effectors. 152
6.3.3. *Ciborinia camelliae CCL-SSP* family members are likely to have undergone gene duplication. 154
6.3.4. *Ciborinia camelliae CCL-SSP* gene expression precedes host-cell necrosis 155
6.3.5. There is no evidence to suggest *Ciborinia camelliae* CCL-SSPs are functional homologs of BcSSP2 and SsSSP3. 156
6.4. Conclusions 158
7. General discussion 159
7.1. Breeding for *Ciborinia camelliae* resistance 160
7.2. Utilizing bioinformatics for fungal gene discovery 161
7.3. Putative necrosis-inducing mechanisms of BcSSP2 and SsSSP3 164
7.4. Adaptive evolution of *Ciborinia camelliae CCL-SSP* genes correlates with a loss of necrosis-inducing activity........ 166
7.5. Future directions 170
7.5. Concluding remarks 173
8. References 175
9. Appendices 199
Appendix 9.1A. Taxonomy, distribution and accession number information for *Camellia* species harvested from Auckland Botanic Gardens, New Zealand 200
Appendix 9.1B. *Camellia* species and interspecific hybrids harvested from Heartwood Nursery, CA 202
Appendix 9.2. Primers used in this study 203
Appendix 9.3. Aerial secondary hyphae of *Ciborinia camelliae* during infection of *Camellia* ‘Nicky Crisp’ 205
Appendix 9.4. Comparisons of host-resistance between *Camellia* sections using Tukey’s range test. 206
Appendix 9.5. A phylogenetic tree of the Sclerotiniaceae 207
Appendix 9.6. Determination of the ‘best’ k-mer length for *Ciborinia. camelliae* genome assembly (Velvet) 208
Appendix 9.7. Transcriptome validation results using BLASTN 209
Appendix 9.8. Defense gene homologs identification using BLASTN 212
Appendix 9.9. BLASTN alignments of the *Camellia* ‘Nicky Crisp’ non-redundant transcriptome to the *Ciborinia camelliae* genome. 213

Appendix 9.10A. Validation of a subset of *Ciborinia camelliae* proteins (*n* = 1472) using BLASTP and the Genbank non-redundant protein database 214

Appendix 9.10B. Validation of a subset of *Ciborinia camelliae* proteins (*n* = 1472) using BLASTP and the Genbank non-redundant protein database - top hit E-value distribution. . 214

Appendix 9.11. Secretome validation using previously published *Botrytis cinerea* secreted proteome data. 215

Appendix 9.12. Secretome annotation categories and protein counts. 216

Appendix 9.13. Secretome subcategory annotation and scatterplot analyses 218

Appendix 9.14. A phylogenetic tree of the conserved CCL-SSP family highlighting CCL-SSPs chosen for recombinant analysis. 219

Appendix 9.15. CCL-SSP family statistics 220

Appendix 9.16. An alignment of all CCL-SSP family members showing the conserved cysteine residues. 222

Appendix 9.17. Fungal gDNA accumulation *in planta* correlates with fungal NAD and TUB mRNA accumulation. 224

Appendix 9.18. Recombinant CCL-SSP construct sequences optimized for *Pichia pastoris* codon usage (note: these are not endogenous nucleotide sequences). 225

Appendix 9.19. Vector maps. 227

Appendix 9.20. Functional protein assays using native recombinant CCL-SSPs infiltrated into *Camellia lutchuensis* petal tissue. 229

Appendix 9.21. Functional protein assays using culture filtrate aliquots of BcSSP2 and SsSSP3 collected at different time-points post-induction. 230

Appendix 9.22. Western blot of tagged recombinant CCL-SSPs. 231

Appendix 9.23. Isoelectric point values of native and tagged recombinant proteins, not including the signal peptide. 232

Appendix 9.24. Coding sequences of all conserved CCL-SSPs from *Ciborinia camelliae, Botrytis cinerea* and *Sclerotinia sclerotiorum* (*n* = 75). 233

10. Publication 241

List of Figures

Figure 1.1. The two-branched plant immune system………………………………………………… 6

Figure 1.2. A fungal phylogeny based on 82 complete fungal genomes……………………….. 16

Figure 1.3. The lifecycle of *Ciborinia camelliae*……………………………………………………………. 24

Figure 3.1. Macroscopic assessment of *Ciborinia camelliae* infection on petals of *Camellia* 'Nicky Crisp' and *Camellia lutchuensis*... 63

Figure 3.2. The development and interaction of *Ciborinia camelliae* with host epidermal cells…….. 64

Figure 3.3. Subcuticular development of *Ciborinia camelliae* with host petal tissue………. 65

Figure 3.4. Analysis of macroscopic and microscopic parameters in 40 species and one interspecific hybrid of *Camellia*…………………………………………………………………………………… 70

Figure 3.5. A comparison of *Ciborinia camelliae* resistance within 18 interspecific hybrids and 1 species of *Camellia*……………………………………………………………………………………… 73

Figure 3.6. Examples of blooms from interspecific *Camellia* hybrids that are highly susceptible or semi-resistant to *Ciborinia camelliae* infection…………………………………….. 74

Figure 4.1. Mating (MAT) locus synteny comparisons between *Ciborinia camelliae* *Sclerotinia sclerotiorum* and *Botrytis cinerea*………………………………………………………………… 90

Figure 4.2. Validation of the origin of *Ciborinia camelliae* transcriptome ESTs using BLASTX and the Genbank non-redundant protein database……………………………………….. 94

Figure 4.3. *Camellia* 'Nicky Crisp' and *Camellia lutchuensis* infection-associated gene expression changes of ESTs homologous to 9 *Camellia* defense-related genes………………. 97

Figure 5.1. The *Ciborinia camelliae*, *Botrytis cinerea* and *Sclerotinia sclerotiorum* secretome prediction pipeline…………………………………………………………………………………… 114

Figure 5.2. Scatterplot analysis of secretome proteins from *Ciborinia camelliae*, *Botrytis cinerea* and *Sclerotinia sclerotiorum*……………………………………………………………………….. 116

Figure 5.3. A comparison of secretome composition and conservation between *Ciborinia camelliae*, *Botrytis cinerea* and *Sclerotinia sclerotiorum*………………………………….. 117

Figure 5.4. Analysis of the composition of the four most common secretome protein categories……… 120

Figure 5.5. Analysis of secretome subcategory conservation within the four most common secretome protein categories…………………………………………………………………… 121

Figure 5.6. A cladogram of the 149 small secreted proteins (SSPs) from *Ciborinia camelliae*, *Botrytis cinerea* and *Sclerotinia sclerotiorum*………………………………………………… 123
Figure 6.1. *In silico* characterization of the conserved *Ciborinia camelliae*-like small secreted protein (CCL-SSP) family……………………………………………………………………………….. 136
Figure 6.2. Clustering of 73 homologous *Ciborinia camelliae CCL-SSP* gene loci within the *Ciborinia camelliae* genome ……………………………………………………………………………….. 139
Figure 6.3. Quantitative real-time PCR data for a subset of 9 of the 73 *Ciborinia camelliae CCL-SSP* genes during host infection ……………………………………………………………. 140
Figure 6.4. Functional assays using native recombinant *Ciborinia camelliae*-like small secreted proteins (CCL-SSPs)…………………………………………………………………………………….. 142
Figure 6.5. Functional stability of the BcSSP2 and SsSSP3 proteins……………………………….. 143
Figure 6.6. Tagged recombinant *Ciborinia camelliae*-like small secreted protein (CCL-SSP) expression and functional assays……………………………………………………………………….. 149
Figure. 7.1. Backcrossing interspecific *Camellia* hybrids with *Camellia lutchuensis*……….. 162
Figure 7.2. Hypothesized molecular mechanisms of BcSSP2, SsSSP3 and the *Ciborinia camelliae* CCL-SSP homologs (CcSSPs). ……………………………………………………………………….. 167
Figure 7.3. A comparison of the native BcSSP2, SsSSP3 and CcSSP92 primary protein sequences…… 171

List of Tables

Table 3.1. Quantification of microscopic parameters associated with *Ciborinia camelliae* development in *Camellia* 'Nicky Crisp' and *Camellia lutchuensis* petal tissue..................... 66

Table 4.1. Comparative analysis of the *Ciborinia camelliae* draft genome with the *Botrytis cinerea* and *Sclerotinia sclerotiorum* genomes.. 89

Table 4.2. Transcriptome assembly statistics.. 92

Table 4.3. Comparative analysis of the *Camellia* 'Nicky Crisp' non-redundant transcriptome with the putative *Ciborinia camelliae* transcriptome.................................. 93

Table 4.4. The top 10 *Camellia* 'Nicky Crisp' and *Camellia lutchuensis* genes undergoing gene expression increases in response to *Ciborinia camelliae* infection............................ 99

Table 6.1. Characterization of CCL-SSP family homologs across different taxonomic classes of the fungal kingdom.. 137

Abbreviations

°C	Degrees Celsius
µl	Microlitre
µm	Micrometre
µmol m-2 s-1	Micromoles per square metre per second
AA	Amino acid
ACC	1-aminocyclopropane-1-carboxylate synthase
Avr	Avirulence
Avr2	Avirulence 2 protein of *Cladosporium fulvum*
BMGY	Buffered glycerol-complex medium
BMMY	Buffered methanol-complex medium
bp	Base pair
Ca^{2+}	Calcium ions
CAZyme	Carbohydrate active enzyme
CCL-SSPs	*Ciborinia camelliae*-like small secreted proteins
cDNA	Complementary deoxyribonucleic acid
Cf-2 R	*Cladosporium fulvum* 2 resistance protein
cm	Centimetre
CO_2	Carbon dioxide
Cq	Quantification cycle
CsCl	Caesium chloride
CTAB	Hexadecyltrimethylammonium bromide
CWDE	Cell wall degrading enzyme
DAB	3,3'-Diaminobenzidine
DAMP	Damage-associated molecular pattern
DEPC	Diethylpyrocarbonate
DNA	Deoxyribonucleic acid
DNase	Deoxyribonuclease
DTT	Dithiothreitol

EDTA	Ethylenediaminetetraacetic acid
Eff	Primer efficiency
EST	Expressed sequence tag
ET	Ethylene
ETI	Effector-triggered immunity
g	Gram
GABA	γ-aminobutyric acid
GB	Gigabase (1 billion bases)
GC	Guanine and cytosine
gDNA	Genomic deoxyribonucleic acid
h	Hour(s)
H_2O_2	Hydrogen peroxide
HCl	Hydrochloric acid
hpi	Hours postinoculation
HR	Hypersensitive response
HRP	Horseradish peroxidase
HST	Host-selective toxin
ICMP	International Collection of Microorganisms from Plants
JA	Jasmonic acid
Kb	Kilobase
L	Litre
LB	Luria-Bertani broth
LM	Light microscopy
LOV1	*Locus orchestrating victorin effects 1 gene*
LRR	Leucine rich repeat domain
M	Molar
MAMP	Microbe-associated molecular pattern
MAP	Mitogen-activated protein
MAT	Mating locus
MB	Megabase (1 million bases)
mg	Milligram
mins	Minutes

ml	Millilitre
mm	Millimetre
mM	Millimolar
MPa	Megapascal
mRNA	Messenger ribonucleic acid
N	Normal
$Na_2S_2O_5$	Sodium metabisulfite
NADPH	Nicotinamide adenine dinucleotide phosphate
NBS	Nucleotide binding site domain
NCBI	National Center for Biotechnology Information
NEP1	Necrosis and ethylene-inducing peptide 1
ng	Nanogram
NGS	Next generation sequencing
NLP	Necrosis and ethylene-inducing peptide 1-like protein
nm	Nanometre
NO	Nitric oxide
O^{2-}	Superoxide anion
OAH	Oxaloacetate acetylhydrolase
OD	Optical density
PAMP	Pathogen-associated molecular pattern
PDB	Potato dextrose broth
PCD	Programmed cell death
PCR	Polymerase chain reaction
PDA	Potato dextrose agar
PRR	Pathogen recognition receptor
PTI	PAMP-triggered immunity
pv.	Pathovar
PVDF	Polyvinylidene fluoride
qRT-PCR	Quantitative real-time polymerase chain reaction
RCR3	*Required for full Cladosporium fulvum resistance 3 gene*
R gene	Resistance gene
RIN	RNA integrity number

RNA	Ribonucleic acid
RNAi	RNA interference
RNase	Ribonuclease
RNA-seq	Ribonucleic acid sequencing
ROS	Reactive oxygen species
rpm	Revolutions per minute
RT	Room temperature
S/TPK	Serine/threonine protein kinase
SA	Salicylic acid
SAR	Systemic acquired resistance
SDS	Sodium dodecyl sulfate
SDS-PAGE	Sodium dodecyl sulfate-polyacrylamide gel electrophoresis
secs	Seconds
SEM	Scanning electron microscopy
Snn1	*Stagonospora nodorum toxin 1 sensitivity gene*
Snn3	*Stagonospora nodorum toxin 3 sensitivity gene*
SnTox1	*Stagonospora nodorum* toxin 1
SnTox3	*Stagonospora nodorum* toxin 3
SSITL	*Sclerotinia sclerotiorum integrin-like gene*
SSP	Small secreted protein
^{T}	Tagged
TBS	Tris buffered saline
TE	Tris-EDTA buffer
ToxA	Toxin A
Tris	Tris(hydroxymethyl) aminomethane
Tsn1	*ToxA sensitivity locus 1gene*
UV	Ultraviolet
w/v	Weight/volume
YPD	Yeast peptone dextrose medium
YPDS	Yeast peptone dextrose sorbitol medium

1. Introduction

1.1. Background

Necrotrophic fungal phytopathogens feed from dying host tissue. Unlike their biotrophic cousins, necrotophs are not obligated to reproduce within their hosts. Instead they are free to necrotize host tissue and plunder its nutritional resources (Glazebrook, 2005).

The Sclerotiniaceae is a family of fungi that contains some of the more anthropologically important necrotrophic fungal pathogens (Andrew et al., 2012). The host generalists *Botrytis cinerea* and *Sclerotinia sclerotiorum* are members of this family and have > 200 and > 400 plant hosts respectively (Amselem et al., 2011). Within this family of fungi there are also several host-specific necrotrophic fungi, including *Ciborinia camelliae*. *C. camelliae* specifically infects the petal tissue of *Camellia* plants and is the causal agent of '*Camellia* flower blight' (Kohn & Nagasawa, 1984). Despite their shared taxonomic classification in the Sclerotiniaceae, *C. camelliae*, *B. cinerea* and *S. sclerotiorum* have distinct differences in host specificity.

Recent research suggests that necrotrophic fungi secrete proteins into their hosts to establish disease (Liu et al., 2009; Liu et al 2012). These proteins are collectively termed 'effectors' and were originally thought to be exclusive to biotrophic fungi (Tan et al., 2010). The most well characterized necrotrophic effectors typically act to induce host-cell death. This contrasts with biotrophic fungal effectors, which typically act to suppress the plant immune system. More detailed observations of the lifestyles of necrotrophic fungi have indicated that asymptomatic growth is common during the establishment of these pathogens within their hosts, suggesting biotrophic-like 'effectors' may also be employed by necrotrophs (Gan et al., 2013).

In this thesis, the interaction between *C. camelliae* and its *Camellia* hosts are studied. The ability of taxonomically distinct *Camellia* hosts to resist *C. camelliae* infection is examined. Furthermore, putative fungal effector proteins that may contribute to *C. camelliae*, *B. cinerea* and *S. sclerotiorum* virulence are predicted and functionally characterized.

1.2. Plant resistance

The majority of microbes are unable to grow within plant tissue. This is because plants have evolved complex mechanisms that resist microbial infection. The major mechanisms that contribute to plant resistance can be separated into two groups; preformed plant resistance and induced plant resistance. Preformed plant resistance mechanisms are constitutive and protect plants from the majority of pathogens (Heath et al., 2000). Induced plant resistance mechanisms are invoked following recognition of foreign molecules *in planta* and involve activation of the plant immune system (Jones & Dangl, 2006). The type of plant resistance exhibited during a plant-pathogen interaction is dependent on how well adapted a pathogen is to a particular host (Schulze-Lefert & Panstruga, 2011). The mechanisms of preformed and induced plant resistance are introduced here, specifically in response to fungal infection.

1.2.1. Preformed plant resistance

Preformed plant resistance mechanisms vary in their form and structure and include; waxy exudates, cell wall components and phytoanticipins (Veronese et al., 2003). The observation that fungal pathogens have evolved mechanisms to degrade, penetrate and detoxify these components is evidence for their importance as structural and chemical barriers against pathogen attack.

Upon making contact with a plant host the first challenge a fungal pathogen must face is how to circumvent the waxy plant cuticle. Fungal pathogens have evolved several strategies to bypass this protective structure. The tomato leaf mould pathogen *Cladosporium fulvum* searches for natural openings in the leaf tissue created by stomata (Thomma et al., 2005). Some opportunist *Mycosphaerella* species infect through wounds in the plant tissue. Interestingly, transformation of *Mycosphaerella* sp. with a cutinase gene from *Fusarium solani* f. sp. *pisi* enabled direct penetration of intact host tissue, demonstrating the role of cutinase enzymes in overcoming preformed plant resistance (Dickman et al., 1989). Successful penetration or circumvention of the cuticle represents the first major accomplishment towards a compatible interaction between plant and pathogen.

The unmodified cell wall is also a formidable structure to most fungi. Its complex matrix of cellulose, hemicellulose, and pectin is able to prevent the passive movement of elongating hyphae into the protoplast and hence protect the valuable nutrients that are concentrated within the cell. *Magnaporthe grisea* produces appresoria, which are specialized penetration structures that penetrate the plant cuticle and cell wall directly. The turgor pressure created by a single cell appresorium of *M. grisea* was estimated to reach 8 MPa, which is the highest pressure known in any biological system (Howard et al., 1991). Furthermore, pathogenic fungi secrete a variety of cell wall degrading enzymes including pectinases, β-1,3-glucanases, cellulases, glycosidases and xylanases. These enzymes act to loosen the structure of the cell wall and, in turn, create a pool of nutrients for the initial nourishment of the advancing hyphae (Bolton et al., 2006).

In combination with structural resistance components, plants also constitutively produce a dynamic array of anti-fungal compounds including, antimicrobial proteins, peptides and non-proteinaceous secondary metabolites. These compounds are expressed prior to pathogen attack and are collectively termed phytoanticipins (Osbourn, 1996). Phytoanticipins are often localized to specific tissues. For example, diverse forms of antimicrobial glucosinolate metabolites are differentially localized in the leaves and roots of oilseed rape (Mithen, 1992). The saponin class of phytoanticipins are widely distributed throughout the plant kingdom, suggesting that they play an important functional role in preformed plant resistance. The significance of these molecules in preformed plant resistance has been demonstrated in saponin-deficient *Avena strigosa* plant lines. These lines are more susceptible to a variety of fungal pathogens as compared to wild-type controls (Papadopoulou et al., 1999). Furthermore, fungal pathogens have evolved enzymatic mechanisms to detoxify saponins. The saponin detoxifying enzyme avenacinase produced by the oat pathogen *Gaeumannomyces graminis* var. *avenae* is essential for the virulence of this pathogen on its host (Bowyer et al., 1995).

1.2.2. Induced plant resistance

Unlike mammals, plants lack a mobile adaptive immune system. Instead they rely on the ability of every cell to recognize and respond to invading microbial pathogens (Jones & Dangl, 2006). Millions of years of natural selection in a microbe-dominated environment has fashioned a two-branched plant immune system that can detect foreign molecules and induce resistance (Fig. 1.1).

PAMP-triggered immunity (PTI)

The first branch of the plant immune system relies on the ability of individual cells to recognize pathogen or microbe-associated molecular patterns (PAMPS or MAMPS) through the action of cell wall-associated pathogen recognition receptors (PRRs) This branch of the plant immune system is termed PAMP triggered immunity (PTI) (Uma et al., 2011). In addition, plants are able to specifically sense the archetypal damage caused by microbial pathogen infection, which may originate from degraded endogenous plant products or degraded pathogen structures. This form of recognition is termed damage or danger associated molecular patterns (DAMPs) and is also considered part of PTI (De Lorenzo et al., 2011).

The first phase of PTI relies on the recognition of 'non-self' (PAMPs) or 'damaged-self' (DAMPs), through the action of transmembrane PRRs (Jones & Dangl, 2006; Lotze et al., 2007). Perhaps the most well characterised PRR in plants is the *Arabidopsis FLS2* receptor (*Bak1*) which recognizes a conserved domain of bacterial flagella (Gomez-Gomez et al., 2001; Gomez-Gomez & Boller, 2002). The *WAK1* (*WALL-ASSOCIATED KINASE 1*) gene from *Arabidopsis* has recently been described as a PRR for a class of DAMPs known as the oligogalacturonides (De Lorenzo, et al., 2011). Oligogalacturonides are released from the plant cell wall during infection by fungal polygalacturonases and are able to induce downstream phytoalexin synthesis, which is a common PTI response (Hahn et al., 1981). Another example of a plant PRR that is linked to oligogalacturonide production is the plant cell wall polygalacturonase-inhibiting protein (PGIP). Like its name suggests, this PRR acts to inhibit fungal polygalacturonase enzymes culminating in the downstream induction of plant

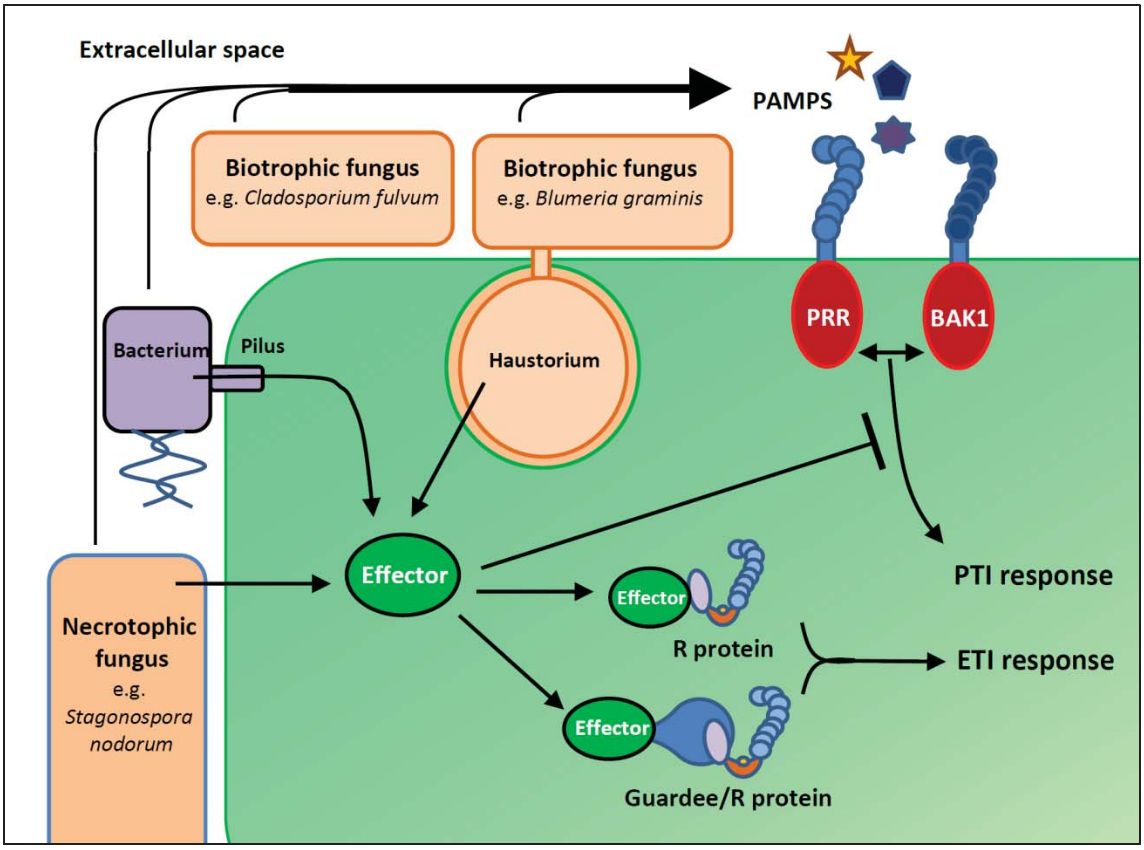

Figure 1.1. The two-branched plant immune system. Pathogen associated molecular patterns (PAMPs) from bacteria, biotrophic fungi and necrotrophic fungi are recognized by plant cell wall pathogen recognition receptors (PRRs), triggering PAMP triggered Immunity (PTI). Parallel secretion of effectors by pathogens can act to suppress PTI. Effector transmission can be via specialized pathogen structures or by diffusion. These effectors are directly or indirectly (via a guarded protein) recognized by host resistance (R) proteins, initiating effector triggered immunity (ETI). Fungal effectors can also have extracellular targets that can trigger ETI-like responses (not shown). ETI responses triggered by necrotrophic fungal effectors can lead to susceptibility whereas ETI responses triggered by biotrophic fungal effectors generally result in avirulence. Adapted from Dodds & Rathjen, (2010).

resistance through the concentration and self-recognition of oligogalacturonides (Di Matteo et al., 2003). Plants also produce peptides that are activated upon attempted infection. *Arabidopsis* produces an endogenous 23-amino acid peptide called Pep1 that is activated upon infection (Yamaguchi et al., 2010). Pep peptides are recognised by their corresponding PRRs, PEPR1 and PEPR2, resulting in PTI.

Recognition of PAMPS, MAMPS and or DAMPS by PRRs triggers a conserved mitogen activated protein (MAP) kinase signal cascade (Deller et al., 2011) together with an elevation in cytosolic Ca^{2+} levels (Ma & Berkowitz, 2007). The importance of the MAP kinase cascade for PTI was demonstrated during the interaction between a mutant strain of *Colletotrichum orbiculare* compromised in its ability to evade PTI and a line of *Nicotiana benthamiana* silenced for *MAP kinase kinase2*. The ensuing compatible interaction restored fungal virulence to wild-type levels (Tanaka et al., 2009). Overexpressing MAP kinase in *Brassica napus* led to enhanced resistance to the necrotrophic fungal pathogen *Sclerotinia sclerotiorum* (Wang et al., 2009). Furthermore, a direct link between the MAP kinase signal cascade and the induction of defense genes by WRKY transcription factors has been illustrated in *Nicotiana benthamiana* (Kim & Zhang, 2004). In *Arabidopsis*, there are 72 expressed WRKY transcription factors and many of them have been shown to be involved in the induction of defense responses downstream of PTI, including *WRKY23*, *WRKY29*, *WRKY33*, *WRKY53* and *WRKY55* (Yamaguchi, et al., 2010).

PTI-associated resistance responses

In response to PTI-associated pathogen recognition, plants are able to modify their cell wall structure, resulting in increased tensile strength. Cross-linking of the plant cell wall through the rapid insolubilization of proline-rich structural proteins has been shown to be one means of achieving this (Bradley et al., 1992). This modification is thought to involve H_2O_2-mediated oxidative cross-linking and correlates with the observation that H_2O_2 is often found in high concentrations around infection sites (Kogel et al., 1999). Plant cell walls can also be strengthened through the incorporation of lignin. Lignification not only increases penetration resistance but also provides the added property of making the cell wall insoluble to water, impeding the activity of pathogen cell-wall degrading enzymes. The importance of lignin in resistance to *Blumeria graminis* f. sp. *tritici* was demonstrated in an experiment where several wheat genes involved in the biosynthesis of the lignin monomer, monolignol, were silenced using RNA interference (Bhuiyan et al., 2009). *Blumeria graminis* f. sp. *tritici* is normally incompatible on this wheat cultivar but was able to successfully penetrate the compromised plant cell walls and establish a compatible interaction.

Papillae or cell wall appositions occur at sites of attempted pathogen penetration. One of the main structural components of a cell wall papilla is the plant polysaccharide callose, or β-1,3-glucan. Callose deposition often appears as concentric rings around the penetration site giving the papilla its characteristic spherical appearance (Zimmerli et al., 2004). *Arabidopsis* RNAi lines deficient in their ability to produce GLUCAN SYNTHASE-LIKE5 (GSL5) protein were unable to produce papillae-associated callose. This resulted in slightly enhanced penetration by the powdery mildew fungus *Blumeria graminis.* However, other non-host pathogens were still unable to establish compatibility highlighting the polygenic nature of PTI (Jacobs et al., 2003). Nishimura and colleagues mapped the *Arabidopsis powdery mildew resistant 4* (*pmr4*) mutant phenotype to a callose synthase gene. Unexpectedly, the mutant *pmr4* phenotype showed increased resistance to pathogens. This resistance phenotype was shown to be dependent on the salicylic acid (SA) defense signalling pathway which appeared to compensate for the loss of *pmr4* (Nishimura et al., 2003).

Actin filaments are actively reorganized into a radial pattern during papilla formation, creating a polarized cell (Takemoto et al., 2003). This rearrangement provides 'tracks' for the transportation of vesicles to the site of attempted penetration (Takemoto & Hardham, 2004). Inhibiting actin polymerization using cytochalasins, enabled *Erysiphe pisi* to penetrate the host cells of the non-hosts barley, wheat, cucumber and tobacco (Kobayashi et al., 1997). A similar experiment in *Arabidopsis* using cytochalasin E compromised resistance against *Blumeria graminis* f. sp. *hordei* (Yun et al., 2003).

The molecular components involved in regulating the transportation of antimicrobial vesicles to the site of papilla formation have recently been characterized in *Arabidopsis* using a forward genetics approach. Mutants that were unable to halt the penetration of *Blumeria graminis* f. sp. *hordei* were classified as *penetration* (*PEN*) mutants (Collins et al., 2003). The *PEN1* gene was characterized as a syntaxin (Assaad et al., 2004). Syntaxins have a C-terminal SNARE (SNAP receptor) domain that binds to SNAP-25 (synaptosome-associated protein, molecular mass 25 kDa) proteins, forming a stable complex that is involved in initiating fusion between vesicle membranes and plasma membranes (Pajonk et al., 2008). The *ROR2* barley homolog of *PEN1* also functions as part of a SNARE complex. This was demonstrated using a yeast-2-hybrid screen with the barley SNAP-34 protein as bait (Collins, et al., 2003). Two other *PEN* genes were identified to have a distinct role in secretion and accumulation of anti-microbial products at the site of papillae. *PEN2* is thought to be involved in metabolizing phytoalexins in the peroxisome (Lipka et al., 2005). *PEN3* was identified as the previously described *Arabidopsis* ATP binding cassette reporter *PDR8* and may be involved in toxin accumulation at attempted penetration points (Stein et al., 2006). Other components of the *Arabidopsis* vesicle transport system include the vesicle-associated membrane VAMP722 protein, which helps stabilise the SNARE complex and the SYP122 syntaxin. SYP122 and PEN1 have been shown to function as negative regulators of downstream defense pathways, including SA-associated defense and the hypersensitive response (HR) (Zhang et al 2007).

Phytoalexins are incredibly diverse compounds and include antimicrobial proteins, peptides and non-proteinaceous secondary metabolites that act as toxins to the invading pathogen (Hammerschmidt, 1999). They are synthesized *de novo* in response to pathogen recognition. The induced synthesis of phytoalexins sets them apart from the phytoanticipins, although the same compound can be included in both groups (Van Etten et al., 1994). Furthermore, a phytoalexin in one plant species may function as a constitutively expressed phytoanticipin in another species (Dixon, 2001). The majority of research in this field has concentrated on identifying phytoalexins and determining their degree of contribution to induced resistance.

The most well studied phytoalexin in *Arabidopsis* is the secondary metabolite camalexin (Mysore & Ryu, 2004). Camalexin is upregulated in response to infection by the fungal necrotroph *Alternaria brassicicola*. The *PAD3* (*phytoalexin deficient 3*) gene is required for camalexin biosynthesis in *Arabidopsis* and encodes a putative Cytochrome P450 monoxygenase. The *PAD3* mutant *pad3-1* is compromised in resistance to *Alternaria brassicicola*. However, it is not clear whether *PAD3* expression or camalexin induction has the same effect on other non-adapted fungal pathogens (Thomma et al., 1999).

Well adapted fungal pathogens are able to degrade phytoalexins using similar enzymatic pathways used for phytoanticipin detoxification. The existence of phytoalexin detoxification pathways in fungi provides insight into the importance of phytoalexins in induced resistance. These detoxification pathways represent a major area of interest for plant pathologists due to their potential as targets for pathogen control (Hammerschmidt, 1999). Examples of enzymes used by specific fungal pathogens to degrade phytoalexins include; pisatin demethylase from *Nectria hematococca* (Wasmann & Van Etten, 1996), brassinin oxidase from *Leptosphaeria maculans* (Pedras et al., 2009) and kievitone hydratase from *Fusarium solani* f. sp. *phaseoli* (Smith et al., 1981).

During PTI an influx of Ca^{2+} ions into the cytoplasm of plant cells stimulates an oxidative burst resulting in an increase in reactive oxygen species (ROS). Furthermore, ROS accumulation appears to feedback on cytosolic Ca^{2+} levels (Ranf et al., 2011). The most common plant resistance-associated ROS include; hydrogen peroxide (H_2O_2), the superoxide anion (O^{2-}) and nitric oxide (NO) (Ma & Berkowitz, 2007). Endogenous plant NADPH oxidases are thought to be the main enzymes involved in producing the oxidative burst. However, reduced H_2O_2 levels observed in *NADPH* compromised plant lines did not always correlate with reduced resistance (Torres et al., 2002). More recent research on the peroxisomal enzyme glycolate oxidase (GOX) suggests it acts as a source of H_2O_2 production during induced resistance (Rojas et al., 2012).

H_2O_2 plays a major role in PTI-associated resistance. It is often observed in high concentrations in the immediate vicinity of papillae and the surrounding cell walls (Thordal-Christensen et al., 1997). H_2O_2 is thought to be involved in mediating the cross-linking and lignification of papillae-associated cell walls, creating a toxic environment for the growth of some fungal pathogens and acting as a diffusible signalling molecule (Levine et al., 1994). The superoxide anion (O^{2-}) also localizes to infection sites (Huckelhoven & Kogel, 1998), although it is often only found to be present at low levels (Kang et al., 2010). A study in parsley cells demonstrated a role for O^{2-} in stimulating phytoalexin accumulation in response to fungal elicitors, indicating it too may act as a signal molecule during PTI-associated resistance (Jabs et al., 1997). NO is well characterized as a regulator of antimicrobial defense in mammals (Mur et al., 2006). This function appears to also be conserved in the plant kingdom. *In planta* NO is thought to inhibit the production of antioxidant enzymes resulting in an increase in defense-associated ROS production. *Arabidopsis* lines overexpressing a bacterial nitric oxide dioxygenase gene were impeded in their ability to regulate H_2O_2 production (Zeier et al., 2004).

PTI-associated resistance responses often culminate in an oxidative burst which can lead to an HR. The wheat pathogen *Blumeria graminis* f. sp. *tritici* has been shown to trigger an HR during interactions with non-hosts as diverse as *Hordeum vulgare* (Aghnoum & Niks, 2010; Huckelhoven et al., 2001; ThordalChristensen, et al., 1997) and *Capsicum frutescen*s (Hao et al., 2011). Other fungal pathogens, including *Botrytis cinerea* and *Puccinia triticina* f. sp. *tritici* have also been shown to trigger an HR in *Pinus pinaster* (Azevedo et al., 2008) and *Oryza sativa* (Li et al., 2012), respectively.

Compatible fungal pathogens have evolved means to cope with the oxidative burst by upregulating their own anti-oxidation enzymes. An ortholog of the yeast oxidative stress responsive *YAP1* (*YEAST AP-1*) transcription factor was identified in the maize pathogen *Ustilago maydis* (Molina & Kahmann, 2007). *U. maydis yap1* mutants displayed high sensitivity to H_2O_2 indicating this protein has a similar function to the yeast *YAP1*. Furthermore, a large set of *YAP1*-regulated genes were identified using microarray analysis, including two peroxidase genes which both act to detoxify ROS.

PTI-associated resistance responses to fungal infection involve diverse mechanisms and multiple genes. PTI accounts for the majority of incompatible reactions between fungal pathogens and plants and is considered a major factor in the evolution of host-specific compatibility, due to its role in restricting a pathogen's host range (Lipka et al., 2010; Mysore & Ryu, 2004).

Effector triggered immunity (ETI)

ETI-associated resistance or host resistance is defined as resistance that is exhibited by a cultivar within a species, which is normally susceptible to a particular pathogen species (Hadwiger & Culley, 1993). As mentioned previously, ETI involves the interaction of a single dominant plant resistance (R) protein with a corresponding pathogen effector protein (Fig. 1.1). A positive ETI recognition event typically leads to an increase in ROS, followed by an HR. *R* gene mediated ETI is thought to occur downstream of PTI and generally occurs when PTI-associated defense is compromised by the action of fungal effectors (Jones & Dangl, 2006).

Harold Flor was the first scientist to describe this branch of the plant immune system during his pioneering studies on flax and flax rust (Flor, 1942, 1956). He concluded that, for every dominant pathogen virulence gene there must exist a corresponding plant host-resistance gene (*R* gene), and that the interaction between these two products must lead to a defence response, primarily the HR. This hypothesis became known as the 'gene-for-gene hypothesis' and was not demonstrated until many years later with the discovery of a bacterial virulence protein that was recognized by a host *R* protein, resulting in avirulence (Staskawicz et al., 1984). Hence, microbial proteins that induce *R* protein mediated ETI are commonly referred to as avirluence proteins. Since this discovery, avirulence genes from bacteria, fungi and oomycetes have been cloned and identified along with their associated *R* genes (De Wit et al., 2009). The monogenic nature of this branch of the plant immune system has lent itself to molecular genetic studies. Literature concerning ETI has expanded dramatically over the last two decades, especially since the development of genomic, transcriptomic and proteomic techniques that allow for the identification of microbial effectors and host resistance genes (Jupe et al., 2012; Song et al., 2011; Vleeshouwers et al., 2008).

R genes code for highly stable proteins and are often constitutively expressed *in planta* (Gu et al., 2005). These proteins commonly have a conserved leucine rich-repeat (LRR) domain together with a nuclear binding site (NBS). LRR domains have been well characterized in biology and normally have a role in binding ligands or other proteins (Kobe & Kajava, 2001). Interestingly, the PRRs involved in PTI also have a conserved LRR domain. These conserved motifs provide a basis for identifying *R* gene candidates within genomic sequence data (Jupe et al., 2012).

Evidence suggests that two categories of *R* genes exist in plants, defined by their ability or inability to bind directly to avirulence gene products (Friedman & Baker, 2007). The first category binds directly to avirulence gene products and initiates a characteristic HR. *R* genes of this type must maintain diversity as their avirulence partners are constantly changing in order to avoid detection. Indeed, *R* gene clusters evolve more rapidly than other genomic loci (Richter & Ronald, 2000). Several studies have provided evidence in support of direct R protein/Avr protein interactions. Several previously identified flax rust fungus avirulence genes have been shown to bind specifically to their corresponding flax *R* protein partners (Dodds et al., 2006). An earlier study in rice demonstrated that the rice *R* gene *Pita* produces a protein that binds directly to the AVR-PITA protein of *Magnaporthe grisea*. Single amino acid substitutions that disrupted binding of PITA and AVR-PITA led to compatibility of *M. grisea* on normally resistant rise cultivars (Jia et al., 2000).

The second category of *R* gene products do not bind directly to their avirulence protein counterparts, but instead act to 'guard' host proteins that are targeted by fungal avirulence proteins (Friedman & Baker, 2007). Host proteins that are targeted by fungal avirulence proteins have been shown to function in plant defense (Jones & Dangl, 2006). By interacting with the host target protein, fungal avirulence proteins are able to suppress host defense. The 'guard hypothesis' was originally formulated based on the interaction between tomato and *Pseudomonas syringae* pv. *tomato* (Van der Biezen & Jones, 1998). R proteins of this category are believed to recognize uncharacteristic conformational changes to the 'target' protein caused by the action of pathogen effectors. By acting in this manner, one R protein can account for the action of several avirulence gene-products (Jones & Dangl, 2006). Support for the 'guard hypothesis' has been demonstrated during the interaction of effectors from two distinct eukaryotic plant pathogens with the tomato protease RCR3. An interaction between the CF-2 R protein of tomato and the Avr2 effector protein of *Cladosporium fulvum* was shown to be dependent on the presence of the tomato cysteine protease RCR3. This suggests that RCR3 is a target of Avr2 and is likely to be guarded by CF-2 (Rooney et al., 2005). The same RCR3 protein was shown to be inhibited by two effectors from the oomycete *Phytophthora infestans*, indicating a conserved role of RCR3 in pathogen resistance (Song et al., 2009). The importance of the *Rcr3* gene in wild-type defense against *P. infestans* was demonstrated by assessing the resistance of mutant *rcr3* tomato lines. These plants displayed increased susceptibility to infection, further supporting the hypothesis that RCR3 is a defense protein that is targeted by diverse pathogen effectors (Song et al., 2009).

ETI-associated resistance responses

Upon positive recognition of fungal effectors by *R* genes, a series of signals are initiated that stimulate the HR and downstream resistance responses (Jones & Dangl, 2006). These responses act to induce localized cell death as well as stimulate systemic acquired resistance (SAR).

The HR was first defined around 100 years ago as a result of observations during the interaction between cereal crops and *Puccinia graminis* (Stakman, 1915). The HR is a key hall mark of ETI and characteristically induces programmed cell death (PCD). HR-associated PCD exhibits characteristics of apoptosis such as DNA laddering and chromatin condensation, clearly discriminating it from unregulated plant cell death (Kiba et al., 2006). The role of the HR and PCD during pathogen infection is to kill and/or restrict the invading pathogen. This resistance strategy is particularly influential during incompatible interactions with biotrophic fungi but often fails to stop the invasion of HR-adapted necrotrophic fungi (Hammond-Kosack & Rudd, 2008).

The classic plant stress hormones salicylic acid (SA), jasmonic acid (JA) and ethylene (ET) all appear to play major roles in downstream signalling during ETI-associated resistance (Tsuda & Katagiri, 2010). In general terms, SA is particularly important for signalling during interactions with biotrophic fungal pathogens whereas JA and ET are important for interactions with necrotrophic fungal pathogens (Glazebrook, 2005; Tsuda & Katagiri, 2010). For example, a comprehensive study on hormone signalling during an interaction between *Arabidopsis* and the necrotroph *Alternaria brassicicola*, indicated that JA, SA and ET all contributed, with JA contributing the greatest (Tsuda et al., 2009). All three hormones are also induced during PTI-associated interactions suggesting that there is some cross-over of downstream PTI and ETI signalling pathways (Tsuda & Katagiri, 2010).

1.3. Fungal phytopathogens

Fungal phytopathogens are some of the most economically important eukaryotic phytopathogens (Dean et al., 2012). Confined mainly to the Ascomycota and Basidiomycota (Fig. 1.2), these fungi have evolved the means to penetrate plant tissue and sequester valuable nutrients, all at a great expense to the plant. The lifestyles of fungal phytopathogens vary, from obligate biotrophs that are unable to survive outside host-tissue, to plant cell-destroying necrotrophs that cause widespread necrosis (Oliver & Ipcho, 2004). Intermediate lifestyles that exhibit both biotrophy and necrotrophy (hemibiotrophy) have also been widely described, suggesting that biotrophic and necrotrophic lifestyles are not mutually exclusive (Lee & Rose, 2010). In addition, a study on the necrotrophic rich Sclerotiniaceae indicates that biotrophy has evolved from necrotrophy in at least two independent instances (Andrew et al., 2012).

1.3.1. The biotrophs and the hemibiotrophs

Biotrophic fungal pathogens have evolved complex mechanisms that allow them to survive within their hosts despite negative selection pressure (McDowell, 2011). To counteract the plant immune system, fungal biotrophs secrete a large number of fungal effector molecules. The genomes of the obligate biotrophs *Melampsora larici-populina* (poplar leaf rust) and *Puccinia graminis* f. sp. *tritici* (wheat and barley stem rust) were shown to have an extensive range of effector-like genes. It has been hypothesized that the constant selection pressure to retain and diversify effectors has

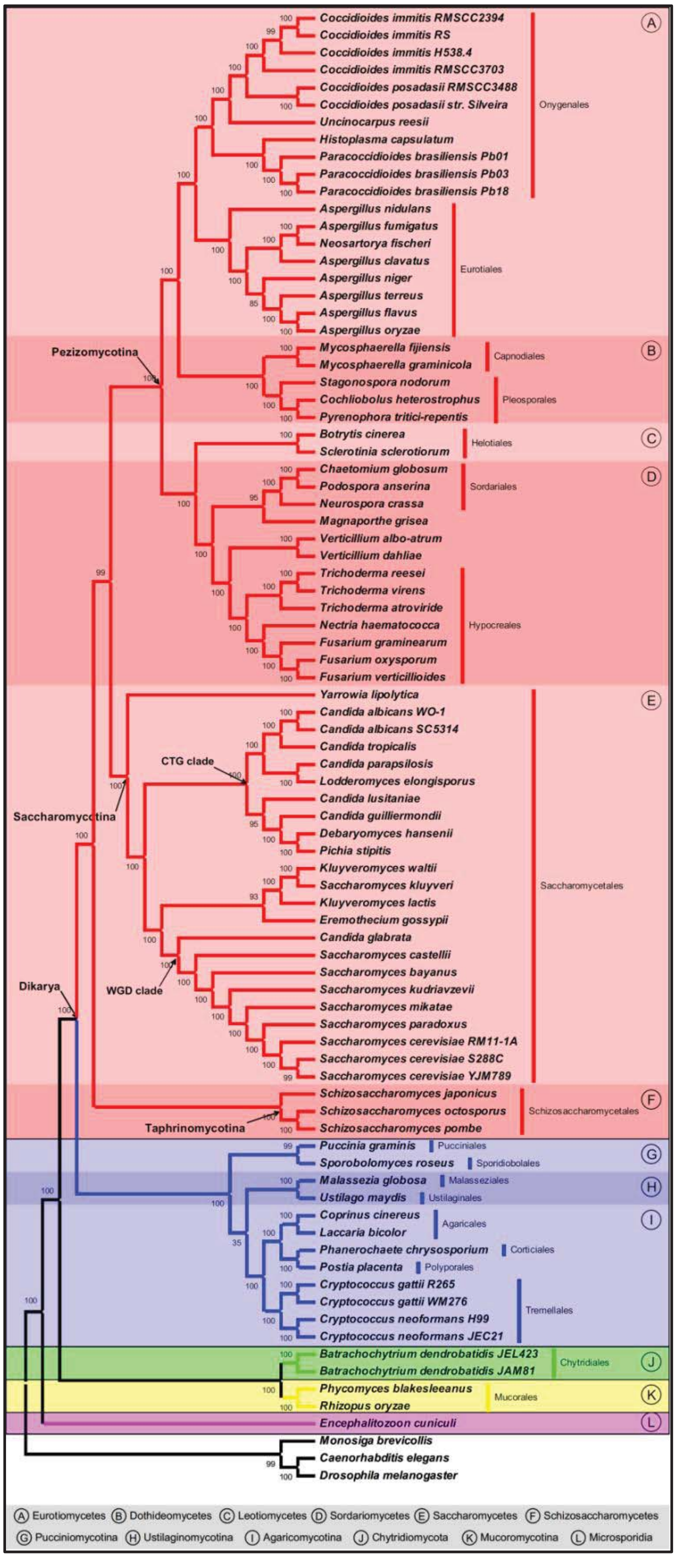

Figure 1.2. A fungal phylogeny based on 82 complete fungal genomes. Sections coloured red, blue, green, yellow and purple correspond to the Ascomycota, Basidiomycota, Chytridiomycota, Mucoromycotina and Microsporidia, respectively. Figure adapted from Hao et al., (2009).

contributed to these fungi having some of the biggest genomes in the fungal kingdom (Duplessis et al., 2011). Most biotrophic species develop specialized intracellular feeding structures that extend from the hyphae into the plant cells. These feeding structures are called haustoria and are thought to be directly involved in nutrient sequestration and effector secretion (Perfect & Green, 2001; Voegele et al., 2001). The presence of haustoria is often used to classify fungi as biotrophs, but it is important to note that not all biotrophs form haustoria. The biotroph *Cladosporium fulvum* exclusively grows in the apoplastic space without inducing cell lysis (Thomma, et al., 2005). It has been hypothesised that apoplastic γ-aminobutyric acid (GABA), which is generated during oxidative stress, may serve as a nutrient source for *C. fulvum* (Oliver & Solomon, 2004). This biotrophic pathogen is a model organism for the study of ETI (De Wit & Spikman, 1982). The discovery that the *C. fulvum* effector Avr2 directly inhibits the activity of the tomato cysteine protease RCR3 was one of the first described virulence roles for a fungal effector (Rooney et al., 2005). Furthermore, this interaction provided some of the first proof for the 'guard hypothesis' (Van der Biezen & Jones, 1998).

Hemibiotrophic fungal pathogens initiate early establishment as biotrophs, by secreting fungal effector proteins. After an asymptomatic biotrophic period they switch to a necrotrophic lifestyle by secreting toxins which cause host-cell death (Koeck et al., 2011). Many members of the *Colletotrichum* genus display a classic bi-phasic hemibiotrophic infection. These hemibiotrophs are initially confined to the apoplast and do not produce haustoria. The distinct second stage of infection by *Colletotrichum lindemuthianum* involves the production of secondary hyphae which is controlled by the *CLTA1* (*C. lindemuthianum TRANSCRIPTIONAL ACTIVATOR 1*) gene (Dufresne et al., 2000; Adaskaveg et al., 2005). Indeed several genes have been identified that control the switch from biotrophy to necrotrophy. The hemibiotrophic basidiomycete *Moniliopthora perniciosa* regulates its transition from biotrophy to necrotrophy through the temporal expression of an alternative oxidase (*AOX*) gene (Thomazella et al., 2012). Genetic control of the hemi-biotrophic switch has also been discovered in the fungal-like oomycetes *Phytophthora infestans* and *P. sojae*. The conserved *P. infestans* and *P. sojae Sne1* (*SUPPRESSOR OF NECROSIS1*) genes were identified as possible regulators of this process. *Sne1* was found to be expressed antagonistically to secreted cell-death inducing factors (Nep1-like proteins) and was shown to supresses their function (Kelley et al., 2010).

In contrast to the distinctly bi-phasic hemibiotrophs, some hemibiotrophs transfer from an asymptomatic biotrophic lifecycle to necrotrophic-mediated programmed cell death without a noticeable change in fungal morphology. The infection of wheat by *Mycosphaerella graminicola* exhibits a long symptomless period of intercellular growth followed by a swift transition to necrotrophic growth (Deller et al., 2011). The rice blast fungus *Magnaporthe grisea* exhibits a very short period of intercellular growth (24 hours) after which it begins to invade cells through their network of plasmodesmata (Ribot et al., 2008). In some instances hemibiotrophs can be concomitantly defined as necrotrophs, as is sometimes the case for *Mycosphaerella graminicola* (Hammond-Kosack & Rudd, 2008). In fact, it has even been postulated that hemibiotrophs may simply be a distinct class or subclass of necrotrophs (Oliver & Ipcho, 2004).

The reason why hemibiotrophs make the switch from a biotrophic lifestyle to a necrotrophic lifestyle is still not well understood. However, evidence suggests that the hemibiotroph *Colletotrichum graminicola* switches to necrotrophy because it is unable to sufficiently suppress plant defences during its biotrophic phase (Vargas et al., 2012).

1.3.2. The necrotophs

A large proportion of necrotrophic fungal phytopathogens belong to the Pezizomycotina, which is a subphylum of the Ascomycota (Fig. 1.2). They are scattered throughout this group with condensation in several orders including the Pleosporales and Helotiales. Some of the most well characterized necrotrophic fungi include *Alternaria brassicicola*, *Stagonospora nodorum*, *Pyrenophora tritici*, *Fusarium graminearum*, *Fusarium oxysporum, Cochliobolus victoriae*, *Sclerotinia sclerotiorum* and *Botrytis cinerea.*

Necrotrophic fungi characteristically produce a large number of cell wall-degrading enzymes (CWDEs), including pectin methylesterases, polygalacturanases and pectate lyases (Oliver & Ipcho, 2004). These enzymes stimulate host cell lysis and the subsequent release of cell nutrients into the surrounding tissue. Genomic studies have revealed the extent to which biotrophs and necrotrophs differ in their genomic fraction of CWDEs. The biotrophic smut fungus, *Ustilago maydis*, has relatively few CWDE encoding genes (n = 33), in contrast to the hemibiotroph *Magnaporthe grisea* (n = 138) and the necrotroph *Fusarium graminearum* (n = 103) (Cantu et al., 2008).

Previous opinion was that necrotrophs lacked the specialized effector repertoires present in their biotrophic counterparts. However, recent research suggests that some necrotrophs utilize effector molecules to manipulate the host and promote infection.

Necrotrophic phytopathogens *Stagonospora nodorum* and *Pyrenophora tritici-repentis* secrete effector molecules that induce susceptibility by co-opting the plant immune system's programmed-cell death pathway (Faris et al., 2010). Because susceptibility is determined by the presence of a single fungal effector protein and a single plant protein, these interactions have been termed inverse gene-for-gene interactions. These interactions contrast directly with the gene-for-gene hypothesis, where interactions between a single fungal effector protein and a single plant protein can result in ETI-associated resistance (Flor, 1942 & 1956).

The proteinaceous host-selective toxin (HST) ToxA is an example of a necrotrophic effector that initiates an inverse gene-for-gene interaction. ToxA indirectly interacts with the hosts *Tsn1* gene product, resulting in host-cell death. The cloning of *Tsn1* revealed its *R* gene like homology, including the presence of S/TPK and NBS-LRR domains (Faris, et al., 2010). In addition, targeted mutagenesis experiments indicated that these three domains were essential for ToxA susceptibility. Yeast-2-hybrid analysis between ToxA and *Tsn1* indicated that these two proteins do not interact, which is consistent with the guard hypothesis (Van der Biezen & Jones, 1998). Furthermore, only host genotypes that contain the *Tsn1* gene are susceptible to ToxA-mediated cell death. It is logical to suggest that the inverse gene-for-gene system described for *ToxA*

/*Tsn1* would be under negative selection in plants. However, of 53 wheat cultivars tested, 85% were positive for the *Tsn1* gene indicating that *Tsn1* may be required for resistance to unknown pathogens (Oliver et al., 2008). Additional *Tox* genes of *S. nodorum* have also been shown to act in an inverse gene-for-gene manner. SnTox1 and SnTox3 proteins are only active in wheat cultivars that contain the *Snn1* and *Snn3* genes (Liu et al., 2009; Liu et al., 2012).

A similar interaction has been described in detail for the *Cochliobolus victoriae* HST victorin and the *LOV1* gene of *Arabidopsis* (Sweat et al., 2008; Lorang et al., 2012). The victorin effector molecule targets an *Arabidopsis* thioredoxin that regulates the systemic acquired resistance pathway. This interaction is detected by the *R* gene product *LOV1*, which in turn incites cell death. *C. victoriae* is able to survive the subsequent HR response and benefits from ready access to necrotic tissue.

Mycosphaerella graminicola is thought to target the plant PCD-associated MAP Kinase (*TaMPK3*) signalling pathway during compatible interactions with wheat (Keon et al., 2007). Post-translational activation of the TaMPK3 protein coincides with PCD, suggesting a role for this gene product in PCD pathway signalling during biotrophic pathogen infection. In comparison, during an incompatible interaction with *M. graminicola*, *TaMPK3* is not post-translationally activated. The avirulence gene product that interacts with TaMPK3 remains to be identified (Hammond-Kosack & Rudd, 2008).

This plant HR-induction strategy suggests that necrotrophs are adapted to survive ETI-associated defense, including the oxidative burst and programmed cell death. It has been hypothesized that necrotrophs must have an effective ROS scavenging system that allows them to persist in such a hostile environment. Interestingly, studies on necrotrophs that are compromised in catalase activity (Schouten et al., 2002) and H_2O_2 detoxification-associated transcription factors (Temme & Tudzynski, 2009) showed that despite their inability to detoxify ROS they remained fully pathogenic on their hosts. It is possible that redundancy exists within ROS-detoxifying systems and that the deletion of one gene may not be sufficient to affect the ROS-scavenging ability of these fungi.

1.4. *Botrytis cinerea* and *Sclerotinia sclerotiorum*

The Sclerotiniaceae family includes two of the most economically important necrotrophic plant pathogens in *B. cinerea* and *S.sclerotiorum* (Boland & Hall, 1994; Bolton, et al., 2006; Dean et al., 2012; Williamson et al., 2007). These two necrotrophs exhibit strong genome synteny, and their genes share an average of 83% amino acid identity (Amselem et al., 2011). *S. sclerotiorum* and *B. cinerea* are able to each infect more than 200 angiosperm hosts, including the important crop species *Glycine max* (soybean), *Brassica napus* (canola) and *Cicer arietinum* (chickpea).

A major virulence factor of *S. sclerotiorum* infection is oxalic acid (Williams et al., 2011). During compatible interactions with *Helianthus annuus* (sunflower), *S. sclerotiorum* produces five times more oxalic acid compared to *B. cinerea* (Billon-Grand et al., 2011). A genetic screen for mutants defective in their ability to infect *Phaseolus vulgaris* led to the discovery that the oxaloacetate acetylhydrolase (*OAH*) gene is essential for *S. sclerotiorum* virulence (Godoy et al., 1990). Analysis of the OAH amino acid sequence identified a highly conserved serine residue that was shown to be important for the activity of this enzyme (Joosten et al., 2008). Research associated with this mutant *S. sclerotiorum oah* strain has shown that fungal oxalic acid production is involved in manipulating ROS homeostasis *in planta* and inducing PCD (Kim et al., 2011).

The decrease in pH associated with oxalic acid production is evident during compatible interactions involving both *B. cinerea* and *S. sclerotiorum*. A homolog of the *PacC* transcription factor of *Aspergillus nidulans* was identified and characterized in *S. sclerotiorum* (*Pac1*) (Rollins, 2003). This transcription factor regulates pH-sensitive genes and was found to be essential for full *S. sclerotiorum* virulence on tomato and *Arabidopsis*. A similar publication reported that *PacC* is also essential for full virulence in the necrotroph *Fusarium oxysporum* (Caracuel et al., 2003). *B. cinerea PacC* has been cloned but no functional studies have addressed its role in virulence. Site-specific likelihood analysis indicated that the *Pac1* gene is under positive selection in the *Sclerotiniaceae*, further suggesting that it plays an important role in these fungi (Andrew, et al., 2012). In addition, pH has been shown to be important for the activity of secreted proteases from *B. cinerea* (ten Have et al., 2004). Compared to *S. sclerotiorum*, *B. cinerea* secretes many more pH dependent CWDEs (Billon-Grand, et al., 2011), including *BcACP1* which is post-translationally modified in association with a drop in pH (Rolland et al., 2009).

Similar to other necrotrophs, the ability to trigger an oxidative burst is a key strategy employed by *B. cinerea* and *S. sclerotiorum*. In fact, the level of *B. cinerea* and *S. sclerotiorum* infection is directly proportional to the intensity of the HR. The oxidative burst is likely to be influenced by the endogenous activity of fungal NADPH oxidases during infection. Two NADPH oxidases were identified in the *S. sclerotiorum* genome (*SsNox1* and *SsNox2*) (Kim et al., 2011). The inability of *ssnox1* and *ssnox2* RNAi mutants to develop normally and establish compatible interactions highlighted the importance of these two genes in virulence and fungal development. In parallel, the NADPH-like genes *BcNoxA* and *BcNoxB* were also found to be essential for development and virulence in *B. cinerea* (Segmuller et al., 2008). H_2O_2 generated by the fungal protein BcSOD1 contributes to the oxidative burst associated with appresoria penetration (Rolke et al., 2004). These fungal ROS-generation mechanisms appear to function in parallel with the plant's own oxidative burst.

B. cinerea and *S. sclerotiorum* are known to secrete proteins that trigger host-cell necrosis. Two necrosis and ethylene-inducing peptide 1 (Nep1)-like proteins (NLPs) of *B. cinerea* specifically induce cell death in dicotyledonous plants (Schouten et al., 2008). *S. sclerotiorum* also has two functional NLP proteins although their specificity to dicotyledonous hosts has not been established (Dallal et al., 2010). These four proteins share the heptapeptide sequence 'GHRHDWE' which is conserved across all characterized NLP proteins (Qutob et al., 2006). The cerato-platanin protein, BcSpl1 is highly expressed during the late stages of *B. cinerea* host infection and is also capable of inducing host-cell necrosis (Frías et al., 2011). The virulence of *B. cinerea bcspl1* mutant strains was compromised, indicating a role for this gene in pathogenicity. The *Xyn11A* gene of *B. cinerea* encodes a catalytically-impaired xylanase that has a necrosis-inducing function. This gene has also been shown to be required for full virulence (Noda et al., 2010). As yet there is no evidence that these *B. cinerea* and *S.*

sclerotiorum host-cell death-inducing proteins share the inverse gene-for-gene mechanisms of other necrotrophic fungi.

Recently, the first host-immune suppressing effector of *S. sclerotiorum* was characterized (Zhu et al., 2013). The SSITL secreted integrin-like protein contributes to the virulence of *S. sclerotiorum* and is thought to delay the activation of plant defense responses by suppressing the jasmonic acid/ethylene signal pathway in *Arabidopsis*. This discovery supports the hypothesis that necrotrophic fungi share host-immune suppressive effectors with their biotrophic counterparts.

1.5. *Ciborinia camelliae*

C. camelliae L. M. Kohn is a host-specific organ-specific necrotroph of the Sclerotiniaceae (Kohn & Nagasawa, 1984; Whetzel, 1945). This pathogen specifically infects the floral tissue of *Camellia* species and interspecific hybrids and is the causal agent of '*Camellia* flower blight' (Kohn & Nagasawa, 1984). Within the *Ciborinia* genus 21 species are described, all of which are host-specific plant pathogens (Saito & Kaji, 2006). Members of this genus usually attack the flowers or leaves of their hosts but have also been observed on bark, bulbs and stolons (Batra & Korf, 1959; Groves & Bowerman, 1955). The life cycle of *C. camelliae* closely resembles that of the teleomorph of *B. cinerea* (Fig. 1.3) (Amselem et al., 2011).

The genus *Camellia* is the largest genus of the family Theaceae (Chen et al., 2006; Vijayan et al., 2009). The two most economically important species are *Camellia sinensis var. sinensis* and *Camellia sinensis var. assamica*, which are cultivated for the production of tea (Chen et al., 2006). *Camellia* species are also valued as ornamental shrubs, being especially popular in temperate regions of the world, including North America, Europe and Australasia (Ackerman, 1973; Taylor & Long, 2000). Intraspecific and interspecific hybrids of *Camellia japonica*, *Camellia sasanqua* and *Camellia reticulata* form the basis of more than 20,000 registered ornamental *Camellia* cultivars (Sfondrini & Guadenzi, 2012). The majority of *Camellia* species and interspecific hybrids are susceptible to *C. camelliae*, including the interspecific hybrids of *Camellia*

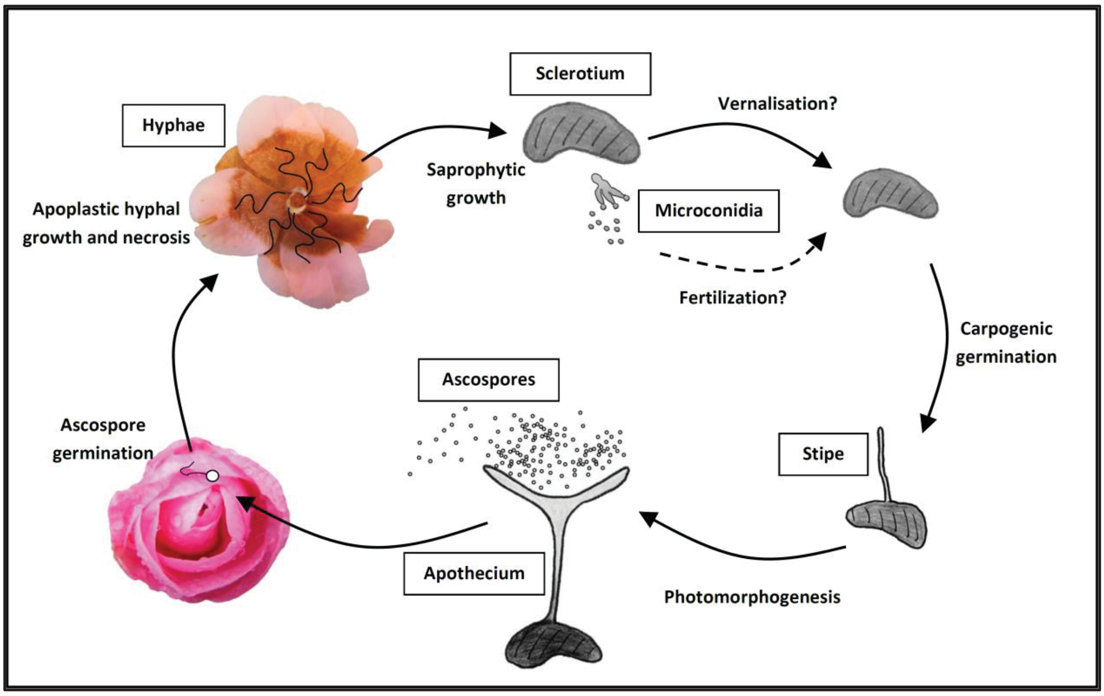

Figure 1.3. The lifecycle of *Ciborinia camelliae*. Apothecia emerge from dormant sclerotia at the beginning of winter. The maturation of emerging apothecia is light-dependent, a trait observed in several other species of the Sclerotiniaceae (Henson & Valleau, 1940; Taylor, 2004). Ascospores are produced within each apothecium and are thought to be the primary means of infection (Anzalone, 1959; Zummo & Plakidas, 1961). Upon contacting susceptible *Camellia* floral tissue, ascospores germinate to produce single unbranched hyphae. The hyphae grow across the phylloplane and then directly penetrate the cuticle of the floral tissue (Vingnanasingam, 2002). Once penetration has occurred the fungus grows exclusively in the apoplastic space for the first 72 h postinoculation (Vingnanasingam, 2002). Brown lesions can be observed on the surface of petals within 24 h postinoculation (Taylor, 2004). As the infection matures, melanised sclerotia form at the base of the petals and continue to increase in size after flower fall. Microconidia are not thought to be capable of initiating secondary infection (Zummo, 1960) but may be involved in fertilizing receptive sclerotial tissue. It is not known whether *C. camelliae* sclerotia require vernalisation prior to carpogenic germination. Carpogenic germination produces a stipe which matures into an apothecium. Figure adapted from Amselem et al., 2011.

japonica, *Camellia sasanqua* and *Camellia reticulata* (Taylor, 2004).

C. camelliae specifically infects the floral organs of *Camellia*, including the androecium, gynoecium, petals and sepals. Other members of the Sclerotiniaceae are also prolific flower infectors including *Botrytis cinerea*, *B. tulipae*, *B. elliptica*, *B. gladiolorum*, *Monilinia laxa*, *M. fructigena*, *M. fructicola*, *M. vaccinii-corymbosi* and *S. sclerotiorum* (Ngugi & Scherm, 2006). *S. sclerotiorum* often invades hosts by establishing in senescing host floral tissue before penetrating stems and leaves (Olivier et al., 2008). Sclerotia of *S. sclerotiorum* are a major contaminant of sunflower heads as they tend to develop in the floral receptacle (Bolton et al., 2006).

There are several reasons why floral organs may be attractive to these fungal phytopathogens. The petals and stigmatic surfaces are thin walled and more susceptible to penetration than leaves. Furthermore, petal cell walls are usually not lignified (Ngugi & Scherm, 2006). Floral organs are natural nutrient sinks and are also often equipped with nutrient-rich nectaries. *Colletotrichum acutatum* infects the floral organs of almond more readily than the leaf tissue (Adaskaveg, et al., 2005). However, floral organs are often well protected. Nectary-associated defense gene expression in tobacco is higher than in other parts of the plant (Thornburg et al., 2003). A stamen-specific plant defensin from Chinese cabbage (BSD1) was shown to be toxic against *Phytophthora parasitica* when overexpressed in tobacco (Park et al., 2002). Due to the existence of floral-specific defense genes it is possible that floral-specific fungal pathogens have evolved novel effectors to combat these defense mechanisms. Indeed, the maize pathogen *Ustilago maydis* has evolved tissue-specific effectors that initiate tumorigenesis in above ground organs of maize, by targeting cell division-associated genes (Skibbe et al., 2010). The restriction of *C. camelliae* to the floral organs of *Camellia* may be an evolutionary adaptation selected for by this pathogen. By infecting and developing on floral organs *C. camelliae* is able to maintain host viability and proximity, increasing the probability of annual infections. Despite its necrotrophic lifestyle, this pathogen appears to have evolved to keep its perrenial host plant alive.

Originally, all *Camellia* varieties were thought to be equally susceptible to *C. camelliae* infection (Hansen & Thomas, 1940). However, recent research has indicated that variable levels of resistance to *C. camelliae* exist in the *Camellia* genus, from highly susceptible to highly resistant phenotypes (Taylor, 2004). Resistant species show almost no visual sign of petal lesion development. In contrast, petals of highly susceptible species can be completely covered by lesions by 72 h postinoculation. A colour change in the petals of several semi-resistant *Camellia* hybrids has been observed in response to infection (Taylor, 2004). Confocal microscopy revealed that ascospores deposited on resistant petals failed to penetrate the tissue after germination (Vingnanasingam, 2002). Papillae formation, chitinase activity and lignin-associated cell wall modifications were identified in most of the resistant species but only in a few susceptible species (Taylor, 2004; Vingnanasingam, 2002).

1.6. Research Aims

Interactions between fungal phytopathogens can result in either compatible or incompatible outcomes. A combination of plant-specific and fungal-specific factors contribute to these interactions and ultimately determine which organism is successful. This thesis aims to investigate interactions between the host-specific necrotrophic fungal pathogen *C. camelliae*, and host *Camellia* petal tissue.

Species and interspecific hybrids of *Camellia* have previously been shown to resist *C. camelliae* infection (Taylor, 2004). Initial observations indicated that resistance correlated with species that had small, white, fragrant blooms. In addition, *C. camelliae* tissue penetration was thought to be absent in resistant species (Vingnanasingam, 2002). These observations led to the initial hypothesis: that *C. camelliae*/*Camellia* incompatibility was a result of preformed resistance.

To test this hypothesis the following aims were established:

1. To determine whether *C. camelliae* incompatibility resembles preformed, PTI or ETI-associated resistance. To address this, microscopic observations of incompatible and compatible interactions were performed using common histological techniques. Plant resistance responses were observed and quantified together with complementary fungal growth measurements.

2. To screen the *Camellia* genus for species that exhibit incompatibility to *C. camelliae*. To address this, macroscopic and microscopic observations of plant resistance and fungal growth responses were quantified for interactions between *C. camelliae* and 40 *Camellia* species.

3. To determine whether *C. camelliae* incompatibility is heritable. To address this, macroscopic and microscopic observations of plant resistance and fungal growth responses were quantified for interactions between *C. camelliae* and 18 interspecific *Camellia* hybrids.

The second objective of this project was to identify plant and fungal genes that influence incompatible and compatible *C. camelliae-Camellia* interactions. Observations made during the first stage of the project had revealed that a) incompatibility appeared to be governed by induced plant resistance and b) compatible interactions included an initial asymptomatic period of growth *in planta*. These two observations led to the hypotheses: (1) that incompatible *Camellia* species actively supress *C. camelliae* infection via PTI-associated resistance responses and (2) that *C. camelliae* secretes fungal effectors during the initial stage of host-establishment.

To test these hypotheses the following aims were established:

1. To identify *Camellia* genes contributing to *C. camelliae* incompatibility. To address this, the transcriptome of incompatible *C. camelliae-Camellia lutchuensis* interactions was sequenced and assembled. Comparisons between mock-inoculated and infected tissue were used to identify plant genes that responded to *C. camelliae* infection.

2. To identify *C. camelliae* genes that act as virulence factors. To address this, the transcriptome of compatible *C. camelliae-Camellia* 'Nicky Crisp' interactions was sequenced and assembled. *C. camelliae*-specific ESTs were identified in the transcriptome by comparing them to the sequenced *C. camelliae* genome. Expressed genes that resembled secreted fungal effector proteins were identified.

The third objective of this project was to compare the predicted secretome of *C. camelliae* with the secretomes of *B.cinerea* and *S. sclerotiorum*. It was proposed that comparative secretome analysis would help to characterise components of the *C. camelliae* secretome. It was hypothesized that (1) the conserved components of the *C. camelliae*, *B. cinerea* and *S. sclerotiorum* secretomes embody the core necrotrophic fungal virulence genes and (2) that diversifying, or unique components of the *C.*

camelliae secretome specifically contribute to the compatible *C. camelliae-Camellia* interaction.

To test these hypotheses the following aim was established:

1. To identify conserved, diversifying and species-specific secretome components. To address this, secretomes were predicted from predicted protein sequences of *C. camelliae*, *B. cinerea* and *S. sclerotiorum*. Secretomes were compared based on protein sequence homology. Each protein was annotated and classified based on its sequence homology. Information about secretome conservation, secretome diversification and species-specific proteins was obtained. Putative fungal effectors were identified based on protein size (< 200 AA), cysteine content (> 4%) and the presence of an N-terminal signal peptide.

2. Materials and Methods

2.1. Plant and fungal material

Five year old shrubs of *Camellia* ‘Nicky Crisp’ (*Camellia japonica* x *Camellia pitardii var. pitardii*) (*n* = 12) and *Camellia lutchuensis* (*n* = 12) were maintained in a sealed glasshouse at outside ambient temperature. All other *Camellia* petal tissue was sampled from species or interspecific hybrids growing in the Auckland Botanic Gardens (coordinates 37°00'40’S 174°54'25’E) or Heartwood Nursery, Fort Bragg, California (coordinates 39°25'48’N 123°47'8’W) (Appendix 9.1A & 9.1B). Flowers of similar developmental age were chosen for infection experiments, as determined by the presence of undehisced pollen. *Nicotiana benthamiana* plants were grown on seed raising mix (Daltons) at 22°C and were subjected to a 12 hour/12 hour light/dark photoperiod.

Isolates of *C. camelliae* were collected from wild populations located either in the Massey University Arboretum (coordinates 40°38’37’S 176°62’12’E) or Heartwood Nursery. Freshly collected apothecia were inverted in 50 ml universal bottles, and left at room temperature to release their ascospores over a period of 2 days. Ascospores were suspended in sterile milliQ water, quantified using a haemocytometer and diluted to a concentration of 8×10^5 spores/ml immediately prior to petal inoculation. Fungal isolates were cultured and maintained on potato dextrose agar (PDA) and potato dextrose broth (PDB). The *C. camelliae* isolate that was chosen for genome sequencing was sub-cultured on PDA and deposited in Landcare Research’s International Collection of Microorganisms from Plants (ICMP) under the reference barcode ICMP 19812.

2.2. *Ciborinia camelliae* infection assays

Ascospores were sprayed onto the adaxial surface of detached *Camellia* petals using a 15 ml atomizer with an estimated coverage of 500 to 1000 ascospores/cm^2. Sterile MilliQ water was used for all mock inoculations. Trays of inoculated and mock-inoculated petals were sealed and incubated in a growth cabinet at 21°C under a 12 hour/12 hour light/dark photoperiod at a light intensity of 90 µmol m^{-2} s^{-1}. Petals that potentially developed infection from pre-inoculation contamination (based on observations of mock inoculated control petals) were omitted from all subsequent analyses. Petals were removed for experimental analyses at pre-determined time intervals.

2.3. Microscopy

2.3.1. Light microscopy

Fungal infection assays performed at Massey University (section 3.2.1 to 3.2.4) were visualized and captured using a Leica DM500 light microscope equipped with a Leica D5C295 digital camera (Leica, Germany). Infection assays performed at UC Davis (section 3.2.5) were visualized and captured using an Olympus CH30 light microscope equipped with a Dinolite digital camera.

For Trypan Blue (Sigma-Aldrich) staining of fungal hyphae, 10 mm diameter petal tissue discs were excised, fixed and cleared in 3:1 ethanol: acetic acid overnight. Discs were stained in a solution of 0.1% (w/v) Trypan blue in lactophenol for 2 to 3 hours, washed twice in MilliQ water and stored in 30% (w/v) glycerol until examined. For dual 3,3'-diaminobenzidine (DAB) (Sigma-Aldrich) and Trypan blue staining, 10 mm diameter discs were excised from live tissue 2 hours before their pre-determined assessment time, vacuum infiltrated with a solution of 1 mg/ml DAB pH 5.0 and dark incubated. At the time of assessment, discs were fixed and cleared in 3:1 ethanol: acetic acid and stained with Trypan blue.

Quantification of microscopic parameters for *Camellia* 'Nicky Crisp' and *Camellia lutchuensis* petals (section 3.2.2 & 3.2.3) was performed by assessing 50 germinated ascospores at 12, 24, 36 and 48 h postinoculation. Ascospores were considered to have germinated if their oval shape had become polarized or if primary hyphae were visible. Papilla formation was quantified by counting the number of interactions that produced a DAB stained halo at the point of penetration. Intercellular H_2O_2 was quantified by counting the number of interactions with DAB staining at the cellular periphery of afflicted epidermal cells. Collapsed/DAB stained cells were quantified by counting the number of interactions that exhibited a depressed cuticle and simultaneously exhibited DAB staining. Lengthened primary hyphae were quantified by counting the number of interactions that produced a primary hypha with a length greater than its associated ascospore. Sub-cuticular hyphae were quantified by counting the number of interactions that gave rise to hyphae below the petal cuticle and, in turn, grew as far as the epidermal intercellular space. Sub-epidermal hyphae were quantified by counting the number of interactions that successfully gave rise to hyphae that were visible at a sub-epidermal focal plane. Auckland Botanical Gardens and Heartwood Nursery *Camellia* petal samples (*n* = 3 unless stated) were analyzed similarly at 24 h postinoculation, with the exception that all analyses were performed blind.

2.3.2. Confocal laser scanning microscopy

Plant cell autofluorescence associated with *C. camelliae* infection was captured using a Leica SP5 DM6000B confocal microscope (Leica, Germany). An argon laser was used for excitation at 488 nm and epidermal cell autofluorescence was collected using photomultiplier tube detectors set for detection between 499 and 676 nm. A Z-stack of 41 sequential scans through the infected epidermal cell at intervals of 0.46 µm was performed in order to determine the localization of epidermal cell autofluorescence and to visualize papillae in the cell wall (Fig. 3.2E').

2.3.3. Scanning electron microscopy

Scanning electron microscopy (SEM) was performed as described by Eaton et al., 2010. Petal tissue was fixed in 0.1 M phosphate buffer pH 7.2 containing 3% glutaraldehyde and 2% formaldehyde for 24 hours. Following fixation, tissue was washed with 0.1 M phosphate buffer pH 7.2, passed through an ethanol series, critical point dried using liquid CO_2, mounted on stubs and sputter-coated with gold particles. An FEI Quanta 200 environmental scanning electron microscope with digital image capture (FEI, The Netherlands) was used to visualize *Camellia* 'Nicky Crisp'-*C. camelliae* and *Camellia lutchuensis*-*C. camelliae* interactions at 24 h postinoculation.

2.4. Image analysis

2.4.1. Petal lesion area quantification using ImageJ

Images used for macroscopic lesion analysis were taken using a Fujifilm FinePix Z digital camera. A total of six single-petal replicates from two separate experiments were used to profile lesion development in *Camellia* 'Nicky Crisp' and *Camellia lutchuensis* (Fig. 3.1). Three single-petal replicates were used for the analysis of *Camellia* genotypes from Auckland Botanical Gardens and Heartwood Nursery, unless otherwise stated. ImageJ software (NIH, USA, http://rsb.info.nih.gov/ij/) was used to quantify lesion area at selected post inoculation time points using the 'colour threshold' tool. Lesion pixel colour was calibrated by measuring the pixel colour range within fully established petal lesions.

2.4.2. Chemiluminescence quantification using ImageJ

Images of the light emitted from HRP-probed membrane-bound proteins were processed using ImageJ's gel quantification plugin. Gel lanes were manually selected and the band intensity was calculated and plotted for each individual protein band. The band intensity area within each plot was measured and used for semi-quantitative comparison (Fig. 6.6C & 6.6D).

2.5. DNA and RNA manipulations

2.5.1. Genomic DNA extraction

Genomic DNA was routinely extracted from fungal apothecia and infected plant tissue using a CTAB based DNA extraction protocol. DNA extraction buffer was prepared by combining 0.35 M sorbitol, 0.1 M Tris.HCl and 0.005 M EDTA in a final volume of 1 litre of milliQ H_20. The pH of the extraction buffer was adjusted to 7.5 and the solution was autoclaved. Prior to use, $Na_2S_2O_5$ was added to the extraction buffer (0.38 g/ 100 ml). Nuclear lysis buffer was prepared by combining 0.2 M Tris.HCl (pH 7.5), 0.05 M EDTA, 2 M NaCl and 2% CTAB (does not solubilize well, stir O/N). A 5 % solution of sarkosyl (in milliQ H_20) was prepared by adding 5 g of sarkosyl to 100 ml of milliQ water.

Briefly, 0.5 to 1.0 g of ground tissue was suspended in a solution made up of 2 parts extraction buffer, 3 parts nuclear lysis buffer and 1 part 5% sarkosyl. After 1 hour incubation at 65°C, solutions were partitioned into aqueous and non-polar phases using 24:1 chloroform/isoamyl alcohol. DNA dissolved in the aqueous phase was precipitated using isopropanol and pelleted by centrifugation at 17,000 g for 10 minutes. The pelleted DNA was washed with 70% ethanol and then re-dissolved in TE (pH 8.0) or sterile milliQ H_2O.

For fungal genome sequencing, a modified CTAB method was used to extract DNA from an axenic culture of *C. camelliae*. Briefly, an isolate of *C. camelliae* was grown in PDA broth for 12 days without shaking. Mycelia were collected, ground in liquid nitrogen and processed until the liquid/liquid partition step of the CTAB genomic DNA extraction protocol. The aqueous phase was added to a 6 ml solution of caesium chloride (1.01 g per 1.0 g of solution) and ethidium bromide (10 µg/ml), and heated at 30°C to facilitate the dissolution of CsCl. Ultracentrifuge tubes were balanced, crimp sealed and centrifuged for 18 hours at 55,000 rpm / 18°C. Following ultracentrifugation, genomic DNA was visualized under UV light and extracted by inserting an 18-gauge syringe below the DNA band and gently drawing it into the chamber. An equal volume of TE-saturated isoamyl alcohol was added to the extracted DNA solution and the upper pink layer of ethidium bromide was discarded. Next, the solution was diluted 3-fold in TE buffer and DNA was precipitated with two volumes of 100% ethanol. After pelleting the DNA by centrifugation, the DNA was washed twice in 70% ethanol, re-suspended in TE and used for *C. camelliae* genome sequencing (section 2.5.8).

2.5.2. Total RNA extraction

Total RNA was extracted from 0.5 g of ground plant tissue using the ZymoResearch Plant RNA-miniprep Kit (see http://www.zymoresearch.com/ for the full protocol). The optional Zymo-Spin IV HRC spin filter system was used to improve the quality of the RNA. A final volume of 40 µl was eluted from the spin columns and 0.5 µl of RNase inhibitor (Roche) was added to maintain the integrity of the RNA. RNA was treated with RNase free DNaseI (Roche) at 37°C for 15 minutes. DNaseI was deactivated by the addition of 2 µl of 0.2 M EDTA at 75°C for 5 minutes. RNA was precipitated via the addition of 3 M sodium acetate (1/10 original volume) and 100% ethanol (2 ½ original volume). Following centrifugation, the RNA pellet was washed with 75% ethanol in DEPC H_2O and re-suspended in 25 µl of RNase-free H_2O.

2.5.3. Nucleic acid quantification

Solutions of DNA and RNA were routinely quantified using a Nanodrop spectrophotometer (Thermo Scientific). Sample purity was determined by comparing the absorbance ratios of 260 nm/ 280 nm and 260 nm/ 230 nm, which were ideally ≥ 1.8. To confirm Nanodrop results, DNA was quantified by agarose gel. DNA concentration was determined by directly comparing sample DNA band intensity with the band intensity of known standard DNA concentrations on a 1-2% TAE Agarose gel run at 100 volts for 45 to 60 minutes. The commercially available 1Kb Hyperladder (Bioline) was used as the DNA standard.

For instances where highly accurate DNA and RNA quantification was required, samples were submitted to the Massey University genome service for analysis. Fungal and plant genomic DNA aliquots used to create a standard curve for converting qRT-PCR crossing point values to gDNA concentrations (data not shown), were quantified using a Quant-iT™ dsDNA Assay Kit (Life Technologies) and a Qubit™ Flurometer (Life Technologies). Total RNA used for cDNA library preparation and Illumina high-throughput sequencing (section 2.5.8) was quantified using a Bioanalyzer (Agilent). RNA samples that produced RNA integrity number (RIN) values of ≥ 8.0 were considered suitable for deep sequencing.

2.5.4. Restriction endonuclease digests

Restriction endonuclease digests were performed routinely on plasmid DNA to confirm positive transformation events, to cleave DNA fragments in preparation for cloning and to linearize pPICZA prior to *Pichia pastoris* transformation (see section 2.8.5). Typically 1-10 ug of DNA was digested with 1-3 units of restriction enzyme (New England Biolabs) in a 50 µl volume of buffered solution. Incubation temperatures and deactivation requirements were dependant on the enzyme and buffer used.

2.5.5. General PCR

Standard PCR was used for a wide range of different applications including; amplifying target genes for sequencing, checking RNA for genomic DNA contamination, colony PCR, PCR-based cloning and site-directed mutagenesis. PCR primers were designed using the opensource software Primer3 (http://primer3.sourceforge.net/). Primers used in this project are listed in Appendix 9.2. PCR master mix (Promega) was used for all amplifications with a final reaction volume of 20 µl. A standard PCR programme consisted of an initial 3 minute denaturing step at 95°C followed by 30 to 40 cycles of 95°C/20 secs, 50-60°C/15 secs, 72°C/10-60 secs and a final extension of 72°C/3mins. Primer annealing temperatures and extension times were dependant on the specifications of the primer pair used and the length of the PCR fragment to be amplified.

2.5.6. Colony PCR

Colony PCR was used to screen *Escherichia coli* and *Pichia pastoris* putative transformants for the presence of transgenes. *E. coli* colonies were picked from selective media using sterile pipette tips and transferred to PCR tubes containing 15 µl of sterile milliQ H_2O. Pipette tips was gently agitated and 1 µl of each solution was used as the template for downstream PCR reactions. A standard PCR programme was used, except that the initial denaturing step was extended to 5 mins. For *P. pastoris*, sampled colonies were agitated in a 15 µl solution of lyticase (1 unit) and 100 mM pH 7.0 phosphate buffer. Samples were incubated at room temperature for 2 hours and then placed in a PCR block at 37°C for 15 minutes followed by 95°C for 15 minutes. The lysate was diluted with 34 µl of sterile milliQ H_2O and 5 µl was used as template for downstream PCR reactions.

2.5.7. Quantitative Real-Time PCR (qRT-PCR)

Genomic DNA and total RNA of *C. camelliae* infected *Camellia* petal tissue were subjected to qRT-PCR analysis. Total RNA samples were converted to cDNA using the Transcriptor First Strand cDNA synthesis Kit (Roche), utilizing oligo (dT) primers.

qRT-PCR reactions were made up in LightCycler® 480 multi-well plates with each biological replicate being analysed in triplicate. A single qRT-PCR reaction consisted of 2.5 µl of template DNA (10 ng of total genomic DNA or diluted cDNA (20 fold)), 0.5 µl of forward primer (10 pmol/ul), 0.5 µl of reverse primer (10 pmol/ul), 1.5 µl of PCR grade H_2O and 5 µl of LightCycler® 480 SYBR Green I PCR master mix (Roche). Primers (Appendix 9.2) were designed to amplify regions of DNA between 75 and 200 bp in length and were pre-screened using standard PCR. cDNA primers were designed to span exon/intron boundaries in order to limit the effect of gDNA contamination. Completed multi-well plates were pulse centrifuged (1000 g) and inserted into a LightCycler® 480 II instrument for analysis.

The qRT-PCR programme consisted of an initial 5 minute denaturing step at 95°C followed by 45 cycles of 95°C/10 secs, 60°C/10 secs and 72°C/10 secs. A melting curve was generated at the end of the programme (95°C/5 secs, 65°C/60 secs, 40°C/30 secs) to check that only a single product was amplified. SYBR Green fluorescence readings were recorded after each cycle and continuously during melting curve profiling. Raw data was analysed using the EXOR software (Roche) and primer efficiency measurements and quantification cycle (Cq) values were calculated using the opensource LinRegPCR software (http://LinRegPCR.HFRC.nl). Relative mRNA levels were determined by comparative quantification of two housekeeping genes (plant GADPH and Actin, fungal NAD and tubulin) using the following calculation:

$$\mathbf{R} = \frac{\left.\mathbf{Eff}^{(\mathbf{Cq}_{\mathbf{calibrator}} - \mathbf{Cq}_{\mathbf{sample}})}\right\}\ \textbf{Gene of interest}}{\left.\mathbf{Eff}^{(\mathbf{Cq}_{\mathbf{calibrator}} - \mathbf{Cq}_{\mathbf{sample}})}\right\}\ \textbf{Housekeeping gene}}$$

R = relative expression

Cq = qRT-PCR quantification cycle

Eff = Primer efficiency.

2.5.8. DNA and cDNA sequencing

PCR fragments and plasmids were routinely sequenced by the Massey genome service using BigDye™ Terminator v3.1 chemistry. Samples were submitted in 20 µl reaction volumes consisting of template DNA (100 to 500 ng), sequencing primer (5 to 10 pg) and milliQ H_2O.

A total of ~1.5 µg of high quality *C. camelliae* genomic DNA was sent to New Zealand Genomics Ltd. for sequencing on the Illumina MiSeq platform (project NZGL00386). After checking gDNA for RNA contamination (< 10% threshold) using a Qubit™ Flurometer (Life Technologies) a gDNA library was prepared using a TruSeq DNA Library Preparation Kit (Illumina). Deep sequencing produced 8.6 gigabases (GB) of 250 bp paired end reads.

Four samples of total RNA were sent to New Zealand Genomics Ltd for sequencing on the Illumina HiSeq2000 platform (project NZGL00013). The four samples were; infected/compatible plant petal tissue, uninfected/compatible plant petal tissue, infected/incompatible plant petal tissue and uninfected/incompatible plant petal tissue. Each sample of high quality RNA (RIN ≥ 8) was subjected to mRNA enrichment, cDNA synthesis and cDNA library preparation using the TruSeq RNA sample prep kit (Illumina). The cDNA libraries were indexed and split run on 2 lanes of an Illumina HiSeq2000 instrument. Deep sequencing produced a combined total of around 80 gigabases (GB) of 100 bp paired end reads.

2.6. Bioinformatic analyses

Genome and transcriptome assembly were performed on a Unix server containing 16 cores and 72 gigabytes of RAM. All other bioinformatic analyses were performed on a stand-alone 64-bit Linux desktop computer containing 8 cores and 16 gigabytes of RAM.

2.6.1. Post sequencing quality control

The SolexaQA package of bioinformatic tools (Cox et al., 2010) were used to analyse and process the genome and transcriptome sequence read data. Using a combination of the DynamicTrim.pl and LengthSort.pl programs, reads were assessed for quality based on their phred quality scores and lengths.

Genomic reads that had a phred quality score of ≤ Q20 (i.e. a probability that ≤ 1/100 bases are called incorrectly) and were ≤ 65 bp in length were excluded from the genome assembly.

Transcriptomic reads that had a phred quality score of less than ≤ Q20 and were ≤ 51 bp in length were excluded from the transcriptome assembly. All single, unpaired reads were also excluded from the transcriptome assembly.
Software commands:

DynamicTrim.pl genome_pair1.fastq -p 0.01 –d ./

DynamicTrim.pl genome_pair2.fastq -p 0.01 –d ./

LengthSort.pl –d ./ -l 65 genome_pair1_trimmed.fastq genome_pair2_trimmed.fastq

DynamicTrim.pl transcriptome_pair1.fastq –p 0.01 –d./

DynamicTrim.pl transcriptome_pair2.fastq –p 0.01 –d./

LengthSort.pl –d ./ -l 51 transcript_pair1.trimmed.fastq transcript_pair2.trimmed.fastq

2.6.2. Draft genome assembly and validation

De novo C. camelliae genome assembly was performed by the staff of New Zealand Genomics Ltd. using the assembly software Velvet (Zerbino & Birney, 2008). A variety of assembly k-mers, ranging from 31 to 121 were tested. The choice of the 'optimal' k-mer was made using two common *de novo* assembly metrics: the number of contigs and the n50 statistic. The n50 is a statistical measure defined as the contig length for which 50% of all bases are contained within contigs of that length or longer. The assembly for k-mer 69 was chosen for the final assembly as it yielded the fewest contigs with the highest n50 (Appendix 9.6). The software SSPACE (Boetzer et al., 2011) was used to combine contigs into larger scaffolds. To check the accuracy of the genome assembly, *C. camelliae* sequences used for phylogenetic analysis (Appendix 9.5) were successfully mapped to the contigs. Contigs were also mapped against the NCBI nucleotide database using BLASTN.

Software commands:

velveth assembly_69 69 -fastq -shortPaired –separate

genome_pair1_trimmed.fastq

genome_pair2_trimmed.fastq

genome_single_trimmed.fastq

velvetg assembly_69 -ins_length 300 -ins_length_sd 30 -cov_cutoff auto -exp_cov auto

SSPACE_Basic_v2.0.pl -l library.lib -s assembly_69/contigs.fa -m 50 -o 20 -b final

2.6.3. Transcriptome assembly and validation

The sample read libraries of *Camellia lutchuensis* and *Camellia* 'Nicky Crisp' mock and infected plant petal tissue were independently assembled using the *de novo* transcriptome assembly software Trinity (Grabherr et al., 2011). Reference transcriptomes were made by combining mock and infected expressed sequence tag (EST) libraries and removing redundant sequences using cd-hit-est (Li and Godzic, 2006). ESTs with greater than 90% nucleotide identity were considered 'redundant'. The longest redundant ESTs were retained and added to their respective non-redundant datasets.

To validate the infected/compatible and uninfected/compatible transcriptomes, previously published sequences of *Camellia sinensis* (*n* = 21), *B. cinerea* (*n* = 53) and *S. sclerotiorum* (*n* = 16) were aligned to the transcriptome using a local installation of BLASTN. Results of the alignments and the accession numbers of the published gene sequences used are included in Appendix 9.7.

Software commands:

Trinity --seqType fq --kmer_method inchworm --left transcript_pair1.trimmed.fastq --right transcript_pair2.trimmed.fastq --cpu 8 *cd-hit-est –i Trinity_output.fa -c 0.9 -n 8 -o Trinity_ouput_nonredundant.fa*

formatdb –p F –i Trinity_output.fa –n Trinity_output.db

blast2 -p blastn -i query.fa -d Trinity_output.db -F F -b 1 -v 1 -m8 -o querytosubject

2.6.4. Transcriptome quantification

Assembled reads of the infected/compatible and uninfected/compatible plant petal tissue datasets were independently mapped to the reference transcriptome using bowtie2 (Langmead & Salzberg, 2012). Reference ESTs were first indexed using bowtie2-build and then each set of pre-assembled reads were aligned to the ESTs using bowtie2-align. The in-house script map_count.pl (written by Dr Murray Cox) was used to count the number of reads that align to each EST. Read count normalization between the two datasets was based on the total read count ratio of the two datasets. Analysis of differential expression between the two datasets was performed using the *R*-based programme DEGseq (Wang et al., 2010). The tabulated results were imported into excel and sorted based on the fold change of the reads counts and the false discovery rate (Benjamini & Hochberg, 1995).

Software commands:

bowtie2-build Trinity_ouput_nonredundant.fa indexed_reference_transcriptome.fa -p 8

bowtie2-align -p 6 -x indexed_reference_transcriptome.fa -1 transcript_pair1.trimmed.fastq -2 transcript_pair2.trimmed.fastq –S bowtie_output.sam

map_count.pl -f Trinity_ouput_nonredundant.fa -s bowtie_output.sam -o count_output –p

> library('DEGseq')

> geneExpMatrix1 = readGeneExp('~/Desktop/DEGseq/count_output ', header=TRUE, geneCol=1, valCol=2)

> geneExpMatrix2 = readGeneExp('~/Desktop/DEGseq/ count_output ', header=TRUE, geneCol=1, valCol=3)

> DEGexp(geneExpMatrix1 = geneExpMatrix1, geneCol1 = 1, expCol1 = 2, groupLabel1 = ' uninfected/compatible ', geneExpMatrix2 = geneExpMatrix2, geneCol2 = 1, expCol2 = 2, groupLabel2 = ' infected/compatible ', method = 'FET', outputDir='~/Desktop/DEGseq/Output')

2.6.5. *Ciborinia camelliae* EST identification and validation

C. camelliae ESTs were identified in the reference transcriptome by aligning the transcriptome to the *C. camelliae* genome using BLASTN. Differential expression data were also used to further screen for candidate fungal ESTs. All ESTs designated as fungal passed the following three threshold parameters; (1) a *C. camelliae* genome alignment E-value ≤ 1e-100. (2) ≥ 50 fold increase in read counts between the uninfected/compatible and infected/ compatible transcriptomes. (3) ≤ 20 read counts in the uninfected/compatible transcriptome.

BLASTX was used to validate the selection of the fungal ESTs (Fig. 4.2). A subset of randomly selected fungal ESTs (*n* = 1325) were aligned to protein sequences from the Genbank non-redundant protein database using BLAST2GO (Conesa & Götz, 2008). Alignments that scored below the BLASTX E-value cut-off of ≤ 1e-03 were considered to be successful matches. Successful alignments were categorized into six groups; fungi, green plants, moss, algae, other and unknown. The 'other' category refers to ESTs that successfully aligned with unannotated proteins. The 'no hits' category refers to ESTs that did not align with a protein in the Genbank non-redundant database.

Software commands:

formatdb –p F –i assembly_69/contigs.fa –n genome_output.db

blast2 -p blastn -i fungalESTs.fa -d genome_output.db -F F -b 1 -v 1 -m8 -o validatedESTs

2.6.6. *Ciborinia camelliae* protein prediction and validation

The MAKER2 software (Holt & Yandell, 2011) was used to predict *C. camelliae* protein coding sequences using both genome and EST data. MAKER2 utilized the *ab-initio* gene prediction software AUGUSTUS (Stanke et al., 2004), which was trained for *B. cinerea* gene prediction. In addition, *C. camelliae* proteins were predicted directly from EST sequences using OrfPredictor (Min et al., 2005). The output sequences of all three prediction strategies were combined and redundant sequences (i.e. ≥ 90% identity) were removed using the program CD-HIT (Fu et al., 2012). A total of 14711 non-redundant *C. camelliae* protein coding sequences were predicted.

BLASTP was used to validate the predicted *C. camelliae* protein sequences (Appendix 9.10A). A subset of 10% randomly selected protein sequences (*n* =1472) were aligned to protein sequences from the Genbank non-redundant protein database using BLAST2GO. Alignments that scored below the BLASTP E-value cut-off of ≤ 1e-03 were considered to be successful matches.

Software commands:

cd-hit –i all_three_protien_predictions.fa -c 0.9 -n 8 –o
fungal_proteins_nonredundant.fa

2.6.7. Fungal secretome prediction and validation

The secretomes of *C. camelliae*, *B. cinerea and S. sclerotiorum* were predicted using a bioinformatic pipeline (Fig. 5.1). *B. cinerea* and *S. sclerotiorum* protein sequences were downloaded from the Broad Institute's fungal genome database (Retrieved from http://www.Broadinstitute.org/ 1 Jun 2013).

For secretome prediction, protein sequences were first subjected to signal peptide prediction using SignalP-4.0 (Petersen et al., 2011). Sequences that passed the D-score cut-off of ≥ 0.45 were considered to have a putative signal peptide. Secondly, TargetP-1.1 (Emanuelsson et al., 2000) was used to classify the proteins based on their predicted subcellular localization (mitochondrial or secreted). Proteins that were deemed to be secreted by TargetP-1.1 were used for further analysis. Thirdly, protein sequences were assessed for the presence of transmembrane domains using TMHMM-2.0 (Krogh et al., 2001). Only sequences that were ≥ 90 amino acids in length and had a methionine in the first position of their N-terminus were considered for TMHMM-2.0 analysis. In addition, 30 amino acids were deleted from the N-terminus, as signal peptides can be predicted as transmembrane domains by TMHMM (Krogh et al., 2001). A final total of 749 *C. camelliae*, 754 *B. cinerea* and 677 *S. sclerotiorum* full length proteins were predicted to be secreted.

To validate the secretome prediction pipeline, the *B. cinerea* secretome was compared with previously published *B. cinerea* secreted proteome data (Shah et al., 2009, Espino et al., 2010, Gonzalez-Fernandez et al., 2014) (Appendix 9.11). All three published studies used the Broad institute's *B. cinerea* gene IDs for proteome annotation. For each dataset, the number of proteome genes that had matching secretome gene IDs was calculated. Shah et al. Espino et al. and Gonzalez-Fernandez et al. detected 60, 105 and 67 individual proteins respectively.

Software commands:

signalp -t euk -f short fungal_proteins_nonredundant.fasta > passed_signalP.fasta

targetp -N passed_signalP.fasta > passed_targetP.fasta

cat Monly_-30_length_passed_targetP.fasta | decodeanhmm.Linux_x86_64 -f ~/TMHMM2.0.options -modelfile ~/TMHMM2.0.model > passed_TMHMM.fasta
tmhmmformat.pl passed_TMHMM.fasta > formatted_ passed_TMHMM.fasta

2.6.8. Secretome annotation

Secretome proteins were annotated using the BLAST2GO software. Genbank BLAST annotations and enzyme codes were used to group the majority of the proteins into 32 designated categories (Appendix 9.12). Proteins were annotated as small secreted proteins (SSPs) if they were less than 200 amino acids in length and had ≥ 4% cysteine content. Unannotated proteins were categorized as 'predicted protein'.

2.6.9. Comparative secretome analyses

The three secretomes of *C. camelliae*, *B. cinerea* and *S. sclerotiorum* were compared to each other using BLASTP alignments. Alignments that produced an E value ≤ 1e-03 and included at least 10% of the length of the queried sequence were designated as matches. The amino acid identity values were extracted from each successful match. Unsuccessful matches were given an identity of 0%. Alignments of < 20% amino acid identity were not considered as matches by the BLASTP program. Each query sequence produced two amino acid identity scores and these were graphed using the two dimensional *R* 'smoothScatter' scatterplot function. Three graphs were independently generated for each of the three secretomes and were overlaid for comparison using ImageJ's 'Z project' function.

To identify the dominant protein categories within each secretome, the number of proteins per category were calculated (Fig. 5.3 & Appendix 9.12). In addition, a measure of protein conservation within a category was devised, by counting the number of proteins in each category that produced alignments ≥ 50% amino acid identity for both species, and dividing this number by the total number of proteins in that category. The same calculations were also performed on four of the most common secretome categories; carbohydrate active enzymes (CAZymes), oxidoreductase proteins, small secreted proteins and proteases. Each of these four categories was further divided into subcategories (Fig. 5.4 & Appendix 9.12).

2.6.10. Phylogenetic trees

The Geneious™ software package (version 6.1.5) http://www.geneious.com was used for all phylogenetic analyses. The phylogenetic tree of the Sclerotiniaceae (Appendix 9.5) was created from a CLUSTALW alignment of 23 concatenated housekeeping gene sequences. Each concatenated sequence included; calmodulin (CAL), glyceraldehyde-3-phosphate dehydrogenase (G3PDH) and heat-shock protein 60 (HSP60) sequences. The default Geneious™ neighbour-joining algorithm was used to produce the phylogenetic tree from 1000 bootstrap samples. *Sclerotinia homeocarpa* was designated as the out-group based on the recommendation in Andrew et al., 2012.

The phylogenetic tree of the secretome-derived *C. camelliae*, *B. cinerea* and *S. sclerotiorum* small secreted proteins (Fig. 5.6) was created from a CLUSTALW protein alignment of the SSP secretome data. The Geneious™ PHYML plugin was used to build the tree from 1000 bootstrap samples. The same approach was used to build the phylogenetic trees shown in Fig. 6.6B and Appendix 9.14.

2.6.11. Small secreted protein characterization

The 46 homologous SSPs identified in the *C. camelliae* secretome were used to screen the *C. camelliae* draft genome for additional family members, using BLASTN. An alignment E-value cut-off of ≤ 1e-05 identified 27 additional non-redundant ESTs. These sequences had not been predicted in the secretome due to their inferior length, absence of an N-terminal methionine, or due to other unknown limitations. *C. camelliae* EST sequences were identified for all 27 additional non redundant ESTs. The full coding sequences of all 73 small secreted proteins were identified by aligning the ESTs with the *C. camelliae* genome sequence in Geneious™. Full-length protein sequences were derived from the predicted coding sequences. The amino acid length, coding sequence length, intron length, intron/exon boundary location, EST transcriptome abundance and the ID of the aligned genome scaffold were recorded for each member of protein family (Appendix 9.15).

The CodeML program of the PAML software (version 4.7) (Xu and Yang, 2013) was used to identify amino acids within the protein family (n = 75) that were under positive selection. The CodeML tree was created in Geneious™ (default neighbour-joining algorithm) and then modified manually to work in PAML. Model M8 of CodeML was used to identify codons under positive selection and the Bayes empirical Bayes method was used to calculate posterior probability. The results were plotted with each amino acid position on the x-axis and the posterior probability for positive selection on the y-axis (Fig. 6.1). Disulphide bond prediction was performed using the web-based program DISULPHIND (Ceroni et al., 2006). The probability that each cysteine residue was involved in disulphide bridge formation was calculated together with the proposed connectivity pattern. SSPs were manually screened for previously characterized fungal effector motifs using Geneious™.

All 73 *C. camelliae* small secreted proteins were aligned to the Genbank non-redundant protein database using Geneious' BLASTP default parameters. For each of the top alignments (E-value cut-off of ≤ 1e.03) the number of non-redundant homologs was tallied for each fungal species. Information about each SSP homolog was recorded including; its hosts taxonomic class and fungal lifestyle, the amino acid pairwise identity score to *C. camelliae*'s CcSSP92 protein, its cysteine residue content and its Genbank accession number (Table 6.1).

2.7. Cloning and recombinant protein expression

Ten *C. camelliae* small secreted proteins, CcSSP31, CcSSP33, CcSSP36, CcSSP37, CcSSP41, CcSSP43, CcSSP81, CcSSP92, CcSSP93, CcSSP94 and the single copy genes from *B. cinerea* (BcSSP2) and *S. sclerotiorum* (SsSSP3) were chosen for cloning and recombinant protein expression. BcSSP2 and SsSSP3 are synonymous with the BC1T_01444 and SS1G_06068 genes predicted by the Broad institute. The selected *C. camelliae* small secreted proteins were chosen based on their phylogenetic distance from the BcSSP2 and SsSSP3 genes (Appendix 9.14). The EasySelect™ *Pichia* Expression Kit (Life Technologies) was used for downstream recombinant protein expression.

2.7.1. Host strains and growth conditions

The *E. coli* strain TOP10F' and the *P. pastoris* wild-type strain X-33 were used in this study. The incubation temperatures used for *E. coli* and *P.* pastoris cultures were 37°C and 30°C respectively. Due to the reduced activity of Zeocin in high salt medium, *E. coli* was cultured in low salt LB when the Zeocin selectable marker was utilized. Low salt LB liquid media consisted of 1% peptone, 0.5% yeast extract and 0.5% NaCl. The solution was adjusted to a pH of 7.5 using NaOH and autoclaved. Solid media was prepared in the same way except for the addition of 15 g/L of bactoagar. Zeocin was added to a concentration of 25 µg/ml, once the media had cooled to < 55°C. When Ampicillin was used as the selectable marker the NaCl concentration was increased to a final concentration of 1%.

Pichia pastoris colonies were routinely cultured in liquid and solid YPD media, without antibiotic selection. YPD liquid media consisted of 2% peptone, 1% yeast extract and 2% dextrose. The solution was mixed and autoclaved. Solid media was created by adding 4% bactoagar.

2.7.2. *E. coli* plasmid DNA isolation

The alkaline-lysis method was used to extract plasmid DNA form *E. coli*. Cultured cells were transferred to a 1.5 ml microcentrifuge tube, centrifuged at 6,000g for 5 minutes and re-suspended in 200 µl of an ice-cold solution of 50 mM Glucose, 25 mM Tis (pH 8.0), 10 mM EDTA and 4 mg/ml of lysozyme. Next, 300 µl of a 200 mM NaOH and 1% SDS was added to the solution and samples were incubated at RT for 5 minutes prior to the addition of 300 µl of 3 M Sodium acetate (pH 4.8). Following a 5 min incubation on ice, the samples were centrifuged at top speed for 10 mins at RT. The supernatant was transferred to a new tube and incubated with 4 µl of RNaseA (10mg/ml) for 30 minutes at 37°C. Next, samples were partitioned with 400 µl of 24:1 chloroform/isoamyl alcohol and centrifuged at 13,000 rpm for 1 min. The aqueous layer was transferred to a new tube and 500 µl of isopropanol was added to facilitate DNA precipitation. Plasmid DNA was pelleted by centrifugation at 13,000 rpm for 10 mins, washed with 70% ethanol and re-suspended in 10 mM Tris-HCl (pH 8.0) or sterile milliQ H_2O.

2.7.3. Construct and vector design

The coding sequences of the 12 selected genes were synthesized by the biotech company GenScript (http://www.genscript.com/) under the project ID 367346 (see Appendix 9.18 for sequence information). The *EcoRI* restriction site was added upstream of the start codon and the *ApaI* restriction site was added immediately downstream of the stop codon. In addition the tri-nucleotide sequence ACT was inserted between the *EcoRI* restriction site and the start codon in order to create a yeast consensus sequence for translation efficiency. Codon optimization was performed by GenScript based on *Pichia pastoris* codon usage.

The extended coding sequences were cloned into the intermediate vector pUC57 and then into the pPICZA expression vector by GenScript (see Appendix 9.19 for vector maps). Transformants were selected based on their ability to grow in the presence of 100 µg/ml of ampicillin for puc57 and 25 µg/ml of Zeocin for pPICZA. Positive transformants were confirmed via sequencing and restriction digest, using SacI and SalI for puc57 and SacI and HindIII for pPICZA.

2.7.4. Site-directed mutagenesis

PCR-based site-directed mutagenesis was used to mutate the stop codons of the 12 original constructs in order to allow translation of the C-terminal c-Myc 6xHis tag. Construct CcSSP92 was mutated by Genscript under the project ID 449332.

Reverse primers were designed with a single nucleotide mismatch at the thymine position of the stop codon so that the stop codons TAA and TAG were mutated to lysine codons AAA and AAG. The *ApaI* restriction site was included within each reverse primer in order to facilitate restriction endonuclease digestion and cloning. The commercially supplied 5' AOX primer was used as the forward primer for all reactions (Appendix 9.2).

For the CcSSP33^{T}, BcSSP2^{T} and SsSSP3^{T} constructs, amplified PCR products were double digested with *EcoRI* and *ApaI*, gel purified using the ZymoClean Gel DNA Recovery Kit (ZymoResearch) and ligated into the empty pPICZA vector using T4 DNA Ligase (Roche). An intermediate cloning step using the PGEM-T easy vector (Appendix 9.19) was used to facilitate cloning of the other eight constructs. Briefly, PCR products were directly ligated into the linearized PGEM-T easy vector by means of the vector's 3' T-overhang technology and transformed into *E. coli* TOP10F'. Positive transformants were identified via blue white selection on LB plates supplemented with 100 µg/ml of ampicillin and confirmed by colony PCR, restriction digest and sequencing. Following confirmation, constructs were excised from PGEM-T-easy using *EcoRI* and *ApaI*, ligated into pPICZA using T4 DNA Ligase and transformed into *E. coli* Top10F'. Cloning of constructs CcSSP36^T and CcSSP41^T failed due to ligation and sequence polymorphism issues. Due to their phylogenetic redundancy with CcSSP31^T (Appendix 9.14) they were deemed surplus to requirement for comparative analysis.

2.7.5. *E. coli* and *P. pastoris* transformation

Both *E. coli* and *P. pastoris* competent cells were transformed using electroporation.

Electro-competent *E. coli* Top10F' cells were prepared by culturing a single colony isolate starter culture overnight at 37°C in 5 ml of LB media with 10 µg/ml tetracycline for selection. A 1/100 dilution of the starter culture was grown until an OD600 of 0.6 to 0.7. Cells were placed on ice for 30 mins and pelleted at 5000 rpm for 15 mins at 4°C. Care was taken to keep the cells cold at all times. Next, the cells were washed twice in 10% glycerol and re-suspended in 1 ml of 10% glycerol. 50 µl aliquots of cell suspension were flash frozen in liquid N_2 and stored at -80°C.

Electro-competent *P. pastoris* X33 cells were prepared by culturing a starter culture overnight at 30°C in 5 ml of YPD broth. A 1/500 dilution of the starter culture was grown until an OD600 of 1.3 to 1.5. The cells were cooled on ice and pelleted at 2800 rpm for 5 mins at 4°C. Next, the cells were washed twice in cold, sterile H_2O followed by a final wash in cold 1 M sorbitol. 100 µl aliquots of cell suspension were flash frozen in liquid N_2 and stored at -80°C.

In preparation for electroporation, defrosted cells were mixed with the appropriate plasmid, linearized plasmid or ligation mix, and pipetted into 0.2 mm electroporation cuvettes (Biorad). *E. coli* cells were electroporated using a Micropulser™ (Biorad) instrument set to 'Ec2'. Immediately following the pulse, 1 ml of low salt LB was added to the cells. The *E. coli* cells were incubated at 37°C with shaking (200 rpm) for 2 hours before plating on low salt LB solid media, supplemented with 25 µg/ml of Zeocin. *P.*

pastoris cells were electroporated using a Micropulser™ (Biorad) instrument set to 'Pic'. Immediately following the pulse, 1 ml of 1 M sorbitol was added to the cells. The *P. pastoris* cells were incubated at 30°C without shaking for 2 hours before plating on YPDS solid media supplemented with 100 µg/ml of Zeocin. Plated cells were grown until putative transformants were visible. pPICZA transformants were confirmed via colony PCR.

2.7.6. Recombinant protein expression

Following transformation, *P. pastoris* strains were grown on YPDS plates supplemented with 100 µg/ml of Zeocin. YPDS plates consisted of 2% peptone, 1% yeast extract, 2% dextrose, 1 M sorbitol and 2% bactoagar. Dextrose and Zeocin were added once the autoclaved solution had cooled to < 55°C.

For the induction of protein expression*,* single colony isolates of transformed *P. pastoris* strains were grown overnight in 5 ml of liquid BMGY media, without antibiotic selection. BMGY cultured cells were separated into two 2.5 ml homogeneous solutions, centrifuged at 2000 rpm for 3 mins and re-suspended in BMMY protein induction media. Every 24 h methanol was added to each culture to a final concentration of 0.05%. BMGY media consisted of 2% peptone, 1% yeast extract, 100 mM potassium phosphate (pH 6.0), 1.34% yeast nitrogen base, 4 x 10^{-5} % biotin and 1% glycerol. The 100 mM potassium phosphate (pH 6.0), 1.34% yeast nitrogen base, 4 x 10^{5}% biotin and 1% glycerol solutions were added to the autoclaved peptone/yeast extract solution after it had cooled to room temperature. BMMY media was prepared similarly except for the substitution of 0.5% methanol for 1% glycerol.

P. *pastoris* cells were harvested after 48 hours of growth in induction conditions. Culture aliquots of 1 ml were centrifuged at 13,000 rpm for 3 minutes to facilitate the separation of the culture supernatant from the pellet. Both the supernatant and pellet were snap frozen in liquid N_2 and stored at -80°C.

2.8. Recombinant protein manipulations

2.8.1. *In planta* functional protein assays

Prior to recombinant protein infiltration, frozen culture filtrate supernatant was defrosted to room temperature and passed through a 0.2 µm filter syringe to remove any yeast or contaminating microorganisms. Next, the sterile culture filtrate was drawn into a sterile 1 ml, 29-gauge needle and the tip of the needle was inserted below the petal cuticle. Around 100 µl of culture filtrate was injected into the apoplastic space of the petal tissue. Empty vector culture filtrate was co-infiltrated into the same petal tissue as recombinant culture filtrate in order to serve as a negative control. Photographs of the petals were taken using a Canon PowerShot SX110 IS digital camera at 0, 1, 2, 3, 4, 8 and 24 h postinoculation. Infiltration of culture filtrates into *N. benthamiana* was performed similarly, except that photos were taken at 48 h postinoculation only. Dilutions of recombinant protein culture filtrates were always performed using empty vector culture filtrate as the diluent.

Several manipulations of the basic recombinant protein *Camellia* petal assay were developed to assess protein expression and function. To determine if the active component of the culture filtrate was present prior to protein induction, samples of the culture filtrate were collected over a time-course. A total of 250 µl was removed from each 5 ml BMMY-based recombinant protein culture at 0 h, 3 h, 6 h, 9 h, 12 h, 24 h and 48 h post-induction. Aliquots were centrifuged at 13,000 rpm for 3 minutes, snap frozen in liquid N_2 and stored at -80°C. Defrosted, sterile aliquots were infiltrated into petal tissue and temporally assessed as described above.

To confirm that the active component of the culture filtrate was proteinaceous in nature, sterile culture filtrates were subjected to denaturing conditions prior to infiltration. Culture filtrates were incubated with 50 mM or 100 mM DTT for 2 hours, or boiled for 30 minutes in a water bath. Treated culture filtrates were infiltrated into petal tissue and temporally assessed.

2.8.2. Protein separation via SDS-PAGE

To concentrate the protein 150 µl of 100% Trichloroacetic acid (TCA) was added to 1 ml of culture filtrate. The solution was stored at 4°C overnight and then centrifuged for 15 min at 4°C. The supernatant was removed and the pellet was air-dried for 15 mins. The pellet was re-suspended in 50 µl of potassium phosphate buffer (pH 6.0) at 37°C.

In preparation for SDS-PAGE analysis several buffers were prepared. The 4x TRIS/SDS (ph8.8) resolving gel buffer was prepared by dissolving 91 g of Tris-base in 300 ml H_2O and adjusting the pH to 8.8 with 1 N HCl. In addition, 2 g of SDS and 500 ml of H_2O were added to the solution. THe 4x TRIS/SDS (ph6.8) stacking gel buffer was prepared by dissolving 6.05 g of Tris-base in 40 ml H_2O. The pH was adjusted to 6.8 with 1 N HCl. In addition, 0.4g of SDS and 100 ml of H_2O were added. The 10x SDS electrophoresis buffer was prepared by combining 30.2 g of Tris-base, 144 g of glycine, 10 g of SDS and 1 L of H_2O. The 6x SDS reducing buffer was prepared by combining 20.0 ml of 4x Tris/SDS (pH 6.8) buffer, 5.0 g of SDS, 30 µl of 150 mg/ml bromophenol blue and 15 ml of glycerol. Following autoclaving, 300 µl of B-mercaptoethanol was added to 700 µl aliquots of the 6x SDS reducing buffer.

A total of 20 µl of 6x SDS reducing buffer was added to each sample. If the solution appeared yellow in colour, 2 µl of 1 M Tris (pH 8.9) was also added. Next, samples were boiled for 10 minutes and pulse centrifuged.

Tris-glycine polyacrylamide gels were used for separating the proteins in the culture filtrate supernatant. The resolving gel (12%) was prepared by combining 2.5 ml of 4x TRIS/SDS (pH 8.8), 3 ml of 40% Acrylamide (29.1:0.9), 4.5 ml of H_2O, 100uL of 10% APS and 20ul of TEMED. The stacking gel (4%) was prepared by combining 1 ml of 4x TRIS/SDS (pH 6.8), 0.4 ml of 40% acrylamide (29.1:0.9), 2.6 ml of H_2O, 40uL of 10% APS, and 8ul of TEMED.

A total of 15 µl of each sample was loaded into each well. In addition, 2.5 µl of PageRuler™ pre-stained ladder (Thermo scientific) was also loaded. Gels were run at 0.03 constant amperage for 60 to 90 minutes.

2.8.3. Western blotting

Western blotting was performed to detect the presence of tagged recombinant proteins in culture filtrates. In preparation for Western blotting several buffers were prepared. Western transfer buffer: Combine 3.025 g of Tris, 14.42 g of Glycine and 800 ml of H_2O. Solubilize all components and then add 200 ml of low grade methanol. 10x Tris buffered saline (TBS): Combine 12.1 g of Tris base, 87.6 g of NaCl and 1 L of H_2O. Adjust the pH of the solution to 7.6 with HCl. Dilute TBS to 1x prior to use. Wash buffer: Combine 100 ml of 10 x TBS, 2 ml of Tween-20, and 898 ml of H_2O. Blocking buffer: Make up a 5% nonfat dry milk powder solution in wash buffer. Antibody dilution buffer: Dilute blocking buffer by a factor of 10.

Briefly, protein was blotted from an SDS-PAGE gel onto a PVDF membrane at 0.150 constant amperage for 2 hours. All blotting was performed at temperatures < 4°C. Prior to the addition of blocking buffer, aliquots of primary antibody (mouse monoclonal [9E10] to c-Myc) and secondary antibody (anti-mouse horseradish peroxidase conjugate) were dabbed onto the corners of the PVDF membrane to control for antibody binding specificity. Non-fat milk powder was used to block the PVDF membrane. After 30 min of blocking, the PVDF membrane was washed in TBS (3 x 1 min) and incubated overnight in a 1/1000 diluted primary antibody solution at 4°C. Multiple wash steps were performed using TBS (3 x 5 min) prior to a 2 h incubation with the diluted secondary antibody (1/40000). After the final TBS washes (4 x 15 min), 2 ml of BM Chemiluminescence blotting substrate (Roche) was pipetted onto the membrane and allowed to incubate for 1 min. Membranes were drip-dried, sealed in plastic and exposed to x-ray film.

2.8.4. Chemiluminescence detection

PVDF membranes were subjected to chemiluminescence detection following x-ray exposure. Membranes were placed on a tray and loaded into a Fujitsu Intelligent Dark Box II equipped with an LAS-1000 Camera. Light emission was recorded by collecting cumulative images every 60 sec for a total of 16 mins using the LAS-1000 Pro software.

The final image was used for semi-quantification of the tagged recombinant protein (Fig. 6.6C & 6.6D).

2.9. Statistical analysis

2.9.1. *Ciborinia camelliae* host-resistance screening.

Percentage data for macroscopic and microscopic analyses were calculated from biological replicates and presented as mean percentage ± one standard deviation. The heat-maps (Figs. 3.4 & 3.5) were generated from mean percentage values for each microscopic parameter using MeV software (Institute for Genomic Research, Rockville, USA, http://www.tm4.org/mev/). Papilla formation data were converted to papilla absence (inverse measurement of papilla formation) in order to conform with the high to low trend of the other heat-map data. The software package *R* (R foundation for statistical computing, Austria, http://www.r-project.org/) was used for statistical analyses of the data. To compare significance between quantified microscopic resistance parameters, raw data from the *Camellia* 'Nicky Crisp' control samples was compared with other *Camellia* species/interspecific hybrids using multiple two-tailed Student's t-tests. P values were adjusted for multiple testing using a false discovery rate correction (Benjamini et al., 1995). One-way ANOVA and Tukey's range test was used to determine whether *Camellia* sections were significantly different from each other for each microscopic resistance parameter (Appendix 9.4). Resistance scores (Fig 3.5, column F) were calculated by ranking each *Camellia* genotype from 20 to 1 for each resistance parameter and then calculating the sum of the combined ranking values.

2.9.2. *Ciborinia camelliae* genome assembly calculations.

Several calculations were used to compare the *C. camelliae* draft genome assembly to the published *B. cinerea* and *S. sclerotiorum* genomes (Table 4.1). Genome coverage was calculated by dividing the total number of sequenced nucleotides by the predicted genome size. The total contig length was calculated by counting the total number of nucleotides contained within all contigs. The contig and scaffold n50 values were calculated using abyss-fac.pl perl code (https://github.com/bcgsc/abyss/blob/

master/bin/abyss-fac.pl). The n50 is defined as the contig or scaffold length for which 50% of all bases are contained within contigs or scaffolds of that length or longer. Guanine and cytosine (GC) content was calculated by counting the number of guanine and cytosine residues in all contigs and expressing this number as a percentage of the total number of nucleotides.

2.9.3. Statistical comparisons of secretome category raw counts.

The total number of proteins in each individual secretome protein category was compared for all three fungal species using *R* (R foundation for statistical computing, Austria, http://www.r-project.org/). Fisher's exact test was chosen to look for significant differences between *C. camelliae* and *B. cinerea*, or *C. camelliae* and *S. sclerotiorum* protein categories (Figs. 5.3A & 5.4 and Appendix 9.12). *P* values were adjusted for multiple testing using a false discovery rate correction (Benjamini et al., 1995).

3. *Ciborinia camelliae* plant resistance

3.1. Introduction

Since the detection of *'Camellia* flower blight' in the USA in 1939 (Hansen & Thomas, 1940), concerted attempts have been made to control *Ciborinia camelliae*. Previous methods have included the collection and destruction of infected blooms (Anzalone, 1959), the application of soil drenches, contact fungicides and systemic fungicides (Taylor & Long, 2000), as well as the inoculation of biological control agents (van Toor et al., 2005b; van Toor et al., 2005c). Although several of these methods have shown promise in reducing the incidence of '*Camellia* flower blight', none have been able to stop the annual re-incursion of this disease into treated areas. The recent discovery of natural resistance to *C. camelliae* in several species of the genus *Camellia* has revealed an opportunity to control this pathogen using conventional resistance breeding techniques (Taylor, 2004).

Fungi that are able to successfully bypass the plant epidermis are destined to interact with the plant's dual-branched immune system. Well adapted fungal pathogens suppress (van Esse et al., 2008) or evade (van Esse et al., 2007) the plant immune system through the action of fungal effector molecules. Non-adapted or semi-adapted fungal pathogens are unable to fully supress and/or evade detection, resulting in the initiation of the plant immune system (Heath, 2000; Uma et al., 2011).

The plant immune system consists of two branches that have separate molecular mechanisms for detecting pathogen infection (Jones & Dangl, 2006). The first branch recognizes conserved PAMPs/MAMPs at the cell wall, through the action of PRRs (Gomez-Gomez & Boller, 2002). PAMP-triggered immunity (PTI) characteristically stimulates downstream defense responses that include cell wall modifications, papillae formation, phytoalexin biosynthesis, and reactive oxygen species (ROS) accumulation (Huckelhoven et al., 2001; Lipka et al., 2008; Thordal-Christensen et al., 1997).

The second branch of the plant immune system involves the detection of pathogen effector molecules by plant resistance (R) proteins. Effector-triggered immunity (ETI) characteristically culminates in a hypersensitive response (HR) and is a more rapid response than PTI (Jones & Dangl, 2006). Many plant–pathogen interactions stimulate characteristics of both branches of the plant immune system (Huckelhoven et al., 2001).

Within this chapter, interactions of *C. camelliae* with *Camellia* 'Nicky Crisp' and *Camellia lutchuensis* host petal tissue are characterized based on macroscopic and microscopic observations of *in planta* fungal development and host immune responses. These observations were used to develop a phenotypic screen for assessing *C. camelliae* resistance levels within species and interspecific hybrids of *Camellia*.

3.2. Results

3.2.1. *Camellia* genotype influences macroscopic disease development.

C. camelliae infection was quantified macroscopically by spray-inoculating detached petals of *Camellia* 'Nicky Crisp' and *Camellia lutchuensis* with 8×10^5 ascospores/ml of inoculum suspension and assessing lesion development. *Camellia* 'Nicky Crisp' petals formed lesions 24 h postinoculation (hpi) (Fig. 3.1). By 72 hpi these lesions had coalesced to cover > 95% of the petal area. In contrast, *Camellia lutchuensis* petals failed to develop any detectable lesions before 42 hpi and reached a maximum lesion area of 13% by 72 hpi. Mock infected petals failed to produce any lesions in both genotypes, indicating that foreign ascospore levels were low (data not shown). Based on this bioassay, *C. camelliae* was deemed to be compatible with *Camellia* 'Nicky Crisp' and incompatible with *Camellia lutchuensis*.

3.2.2. Compatible interactions involve cuticle penetration, intercellular growth and secondary hypha development.

Microscopic characterization of compatible *Camellia* 'Nicky Crisp'-*C. camelliae* interactions used a combination of scanning electron microscopy (SEM) and light microscopy (LM). Direct penetration of the petal cuticle by *C. camelliae* was observed at 24 hpi using SEM (Fig. 3.2A). Penetration was achieved by the action of an appressorium-like structure at one end of the germinated ascospore. Instances where penetration occurred after a period of surface hyphal growth were also observed (Fig. 3.2B). Histological analysis indicated that cuticle penetration was followed by sub-cuticular growth of the primary hypha (Figs. 3.2D & 3.3A). Upon reaching the epidermal intercellular space, sub-cuticular hyphae commenced an apoplastic growth phenotype. Apoplastic growth was maintained in the lower epidermal tissue prior to 24 hpi (Fig. 3.3B). The majority of *in planta* fungal hyphae were localized to the petal mesophyll tissue at 24 hpi (Fig. 3.3C). From 36 hpi a change in fungal development in the epidermal tissue was observed, underlined by broadening of sub-cuticular primary hyphae and initiation of secondary hyphal development (Fig. 3.3D). As secondary hyphal growth radiated, some of the hyphae became aerial (Appendix 9.3). This change in hyphal growth correlated with the proliferation of lesions observed in the

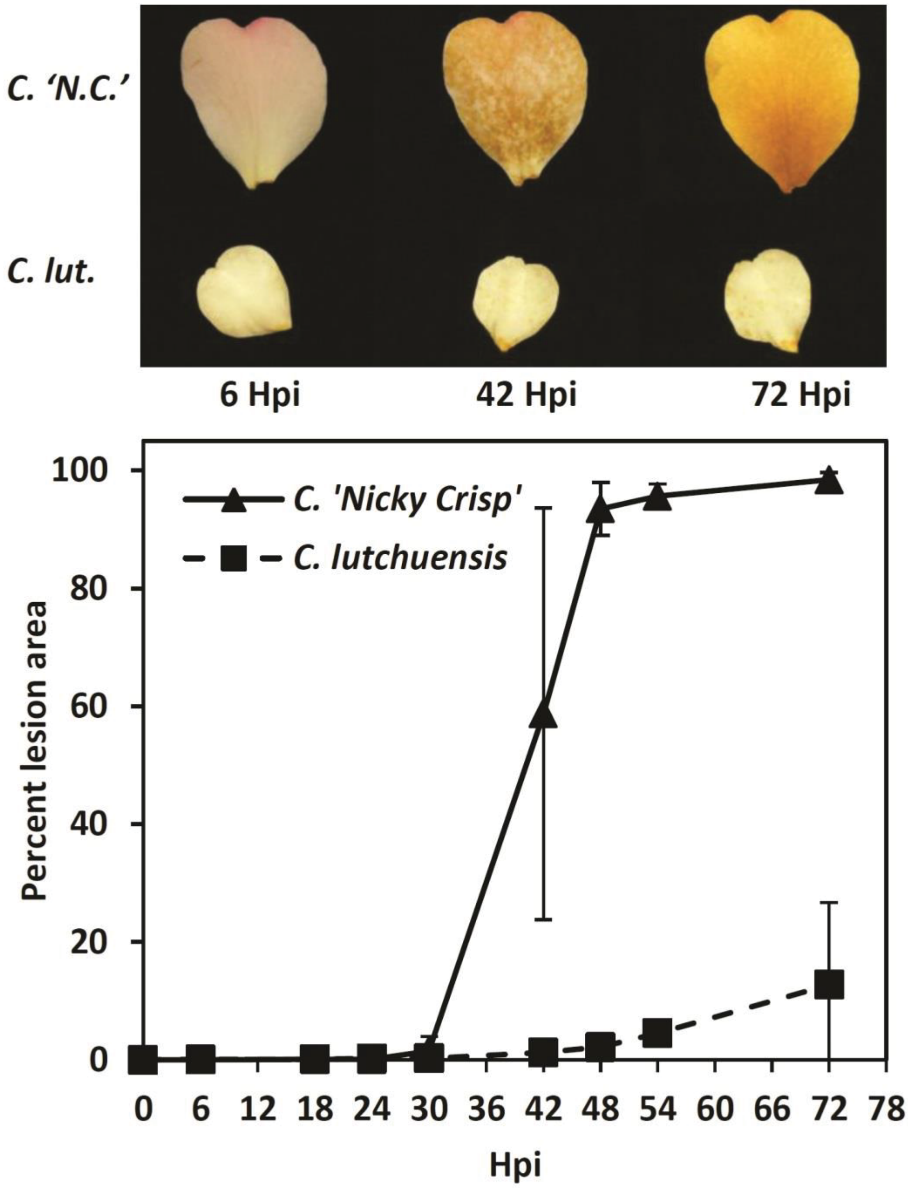

Figure 3.1. Macroscopic assessment of *Ciborinia camelliae* infection on petals of *Camellia* 'Nicky Crisp' and *Camellia lutchuensis*. Images show disease progression in infected petals of *Camellia* 'Nicky Crisp' (*C. 'N.C.'*) and *C. lutchuensis* (*C. lut.*) at 6, 42 and 72 h postinoculation (hpi). The graph shows percent petal lesion area at 6, 18, 24, 30, 42, 48, 54 and 72 hpi. Each data point corresponds to the mean percentage lesion area of six single-petal replicates ± one standard deviation.

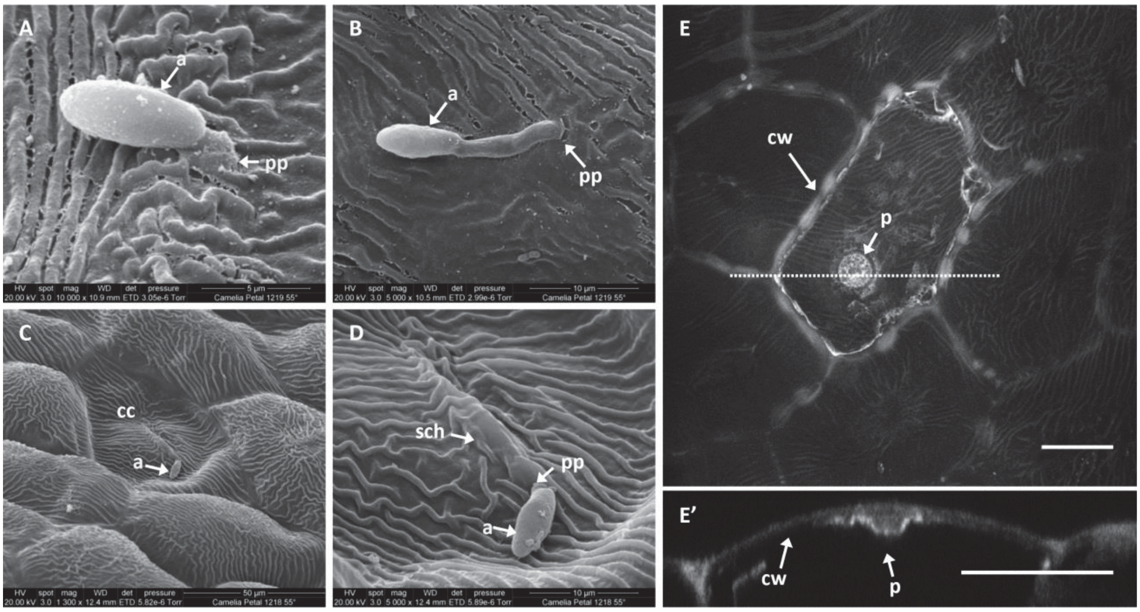

Figure 3.2. Scanning electron and confocal micrographs show the development and interaction of *Ciborinia camelliae* with epidermal cells of **A and B**, *Camellia* 'Nicky Crisp' and **C, D, E, and E'**, *Camellia lutchuensis*. Penetration of the petal cuticle by appressorium-like structures occurred directly from the ascospore (A) or following a period of hyphal growth (B). Incompatible interactions occasionally triggered epidermal cell collapse (C). A collapsed cell reveals the subcuticular growth habit of *C. camelliae* (D). A merged Z-stack of 41 images reveals localized autofluorescence associated with the cell wall and papilla of an afflicted epidermal cell (E). An orthogonal view of the same Z-stack through the site of papilla formation (indicated by the dotted line) reveals thickening of the cell wall at the position of papilla formation (E'). Symbols: a = ascospore; pp = penetration point; cc = collapsed cell; sch = subcuticular hyphae; cw = cell wall; p = papilla. All images were taken at 24 h postinoculation. Scale bar = 25 µm.

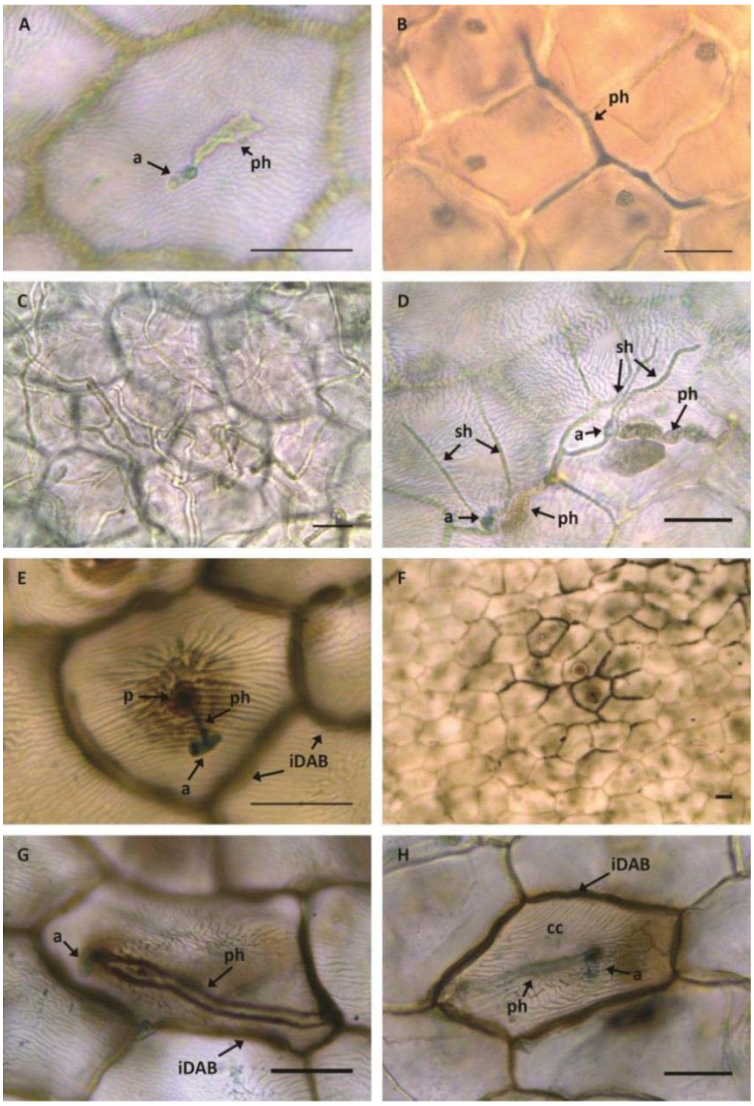

Figure 3.3. Light micrographs showing the development and interaction of *Ciborinia camelliae* with **A to D**, compatible *Camellia* 'Nicky Crisp' and **E to H**, incompatible *Camellia lutchuensis* petal tissue. All samples were stained with Trypan Blue. Samples A and C to H were co-stained with 3,3′-diaminobenzidine (DAB). **A**, Penetration and subcuticular growth occurred prior to 12 h postinoculation (hpi) and failed to induce localized DAB staining in compatible *Camellia* 'Nicky Crisp' petal tissue. **B**, A primary hypha exhibited apoplastic growth in the lower epidermis at 24 hpi. **C**, Translucent primary hyphae concentrated within the mesophyll tissue at 24 hpi. **D**, From 36 hpi, primary hyphae broadened and secondary hyphae developed. **E**, Papilla formation and intercellular DAB staining occurred in response to attempted cuticle penetration of *C. lutchuensis* petal tissue by *C. camelliae*, prior to 12 hpi. **F**, Intercellular DAB staining diffused outward from the afflicted epidermal cells. **G**, DAB staining localized to the cell wall of a subcuticular primary hypha at 24 hpi. **H**, Collapse of a DAB-stained epidermal cell was denoted by the lower focal plane of the cell's cuticle compared with surrounding cells at 36 hpi. Symbols: a = ascospore; ph = primary hypha; sh = secondary hypha; p = papilla; iDAB = intercellular DAB; cc = collapsed cell. Scale bar = 25 µm.

Table 3.1. Quantification of microscopic parameters associated with *Ciborinia camelliae* development in compatible *Camellia* 'Nicky Crisp' and incompatible *Camellia lutchuensis* petal tissue[a]

Camellia 'Nicky Crisp'			*Camellia lutchuensis*			
12 hpi	24 hpi	36 hpi	12 hpi	24 hpi	36 hpi	48 hpi
0 ± 0	0 ± 0	0 ± 0	50 ± 12	61 ± 15	76 ± 7	81 ± 10
0 ± 0	2 ± 1	6 ± 7	76 ± 15	90 ± 6	84 ± 10	88 ± 10
0 ± 0	0 ± 0	0 ± 0	0 ± 0	1 ± 2	5 ± 3	2 ± 2
87 ± 7	96 ±3	99 ± 1	19 ± 10	52 ± 20	46 ± 12	31 ± 18
39 ± 7	91 ± 4	95 ± 3	1 ± 1	32 ± 14	33 ± 14	24 ± 20
0 ± 0	90 ± 5	86 ± 22	0 ± 0	1 ± 1	0 ± 0	2 ± 2

[a] Data were collected at 12, 24, 36 and 48 h postinoculation (hpi) for each microscopic parameter by assessing 50 germinated ascospores per biological replicate (*n* = 5). Data were not recorded for *Camellia* 'Nicky Crisp' at 48 hpi due to disease-associated deterioration of the petal tissue. Mean percentage values are shown for each analysis ± one standard deviation.

compatible *Camellia* 'Nicky Crisp' detached petal bioassay (Fig. 3.1).

3.2.3. Incompatible interactions induce characteristic plant defense responses.

A series of temporal microscopic analyses were carried out to investigate the mechanism of defense in petal tissue of *Camellia lutchuensis*. SEM analysis revealed that the petal cuticle of the incompatible tissue was also penetrated directly by *C. camelliae* (Fig. 3.2D). However, unlike the compatible interaction, penetration was frequently accompanied by the formation of plant papillae in epidermal cell walls (Figs. 3.2E, 3.3E & Table 3.1). DAB staining revealed an accumulation of H_2O_2 at the site of papilla formation as well as at the periphery of the epidermal cell. This is consistent with reports that describe papilla formation and H_2O_2 accumulation in response to attempted pathogen penetration (Huckelhoven et al., 2001; Thordal-Christensen et al., 1997). An orthogonal cross-section through a single papilla showed thickening of the cell wall, further confirming this structure as a papilla (Figs. 3.2E & 3.2E'). Quantification of the number of papillae showed that they increased significantly ($P < 0.01$) during the incompatible interaction from 12 hpi to 48 hpi (Table 3.1). H_2O_2 appeared to diffuse from the afflicted cell to the walls of neighboring epidermal cells (Fig. 3.3F). Intercellular H_2O_2 was occasionally observed during the *Camellia* 'Nicky Crisp'-*C. camelliae* compatible interaction suggesting that this phenotype is not exclusive to the *Camellia lutchuensis-C. camelliae* incompatible interaction (Table 3.1).

A small percentage of *Camellia lutchuensis* epidermal cells exhibited a collapsed phenotype in response to infection by *C. camelliae* from 24 hpi (Figs. 3.2C, 3.3H & Table 3.1). Collapsed cells stained intensely with DAB indicating that H_2O_2 levels were elevated (Fig. 3.3H). In contrast, collapsed cells were not observed during the compatible *Camellia* 'Nicky Crisp'-*C. camelliae* interaction (Table 3.1).

Hyphal development was used as a second, DAB-independent strategy for quantifying resistance to *C. camelliae in planta*. The number of germinated ascospores that produced hyphae that were greater than their ascospore length, increased over time for both compatible and incompatible interactions. By 36 hpi, 99% of primary hyphae were longer than their associated ascospores in susceptible tissue, whereas only 46% reached this threshold length in resistant tissue (Table 3.1). It is possible that the formation of papillae contributed to the reduced hyphal length in resistant tissue.

In support of this hypothesis, papilla formation inversely correlated with the number of sub-cuticular hyphae observed from 24 hpi (Table 3.1). Primary hyphae that managed to successfully penetrate the cuticle of *Camellia lutchuensis* epidermal cells established sub-cuticular growth. However, only 8% of these sub-cuticular hyphae developed into sub-epidermal hyphae by 48 hpi, suggesting that further defense mechanisms contribute to the restriction of fungal development *in planta*.

3.2.4. Levels of incompatibility to *Ciborinia camelliae* vary within the *Camellia* genus

The frequency and intensity of *C. camelliae* incompatibility within the *Camellia* genus was assessed by extending the described analyses to 39 additional *Camellia* species collected from the Auckland Botanic Gardens (ABG) (Fig. 3.4). Colour-converted mean percentage data depicted a gradient of resistance across the *Camellia* genus, from highly compatible phenotypes (light grey) to comparatively incompatible phenotypes (black). Statistical comparisons (Student's t-test) of the susceptible *Camellia* 'Nicky Crisp' ABG genotype with each *Camellia* species, further defined the levels of resistance within the *Camellia* genus (Fig. 3.4). *Camellia lutchuensis*, *Camellia yuhsienensis* and *Camellia transnokoensis* scores were significantly different to the *Camellia* 'Nicky Crisp' ABG genotype, with significantly lower values for at least four of the five assessed parameters. *Camellia xichengensis, Camellia mairei var. mairei*, *Camellia granthamiana*, *Camellia japonica* ssp. *japonica, Camellia sinensis var. sinensis, Camellia saluenensis, Camellia jinshajiangica, Camellia pitardii var. yunnanica* and *Camellia puniceiflora* were not significantly different from the *Camellia* 'Nicky Crisp' ABG phenotype for all assessed parameters, suggesting that these genotypes were compatible with *C. camelliae*. All other species exhibited a range of intermediate phenotypes with significance in one, two or three of the five analyses. Statistical

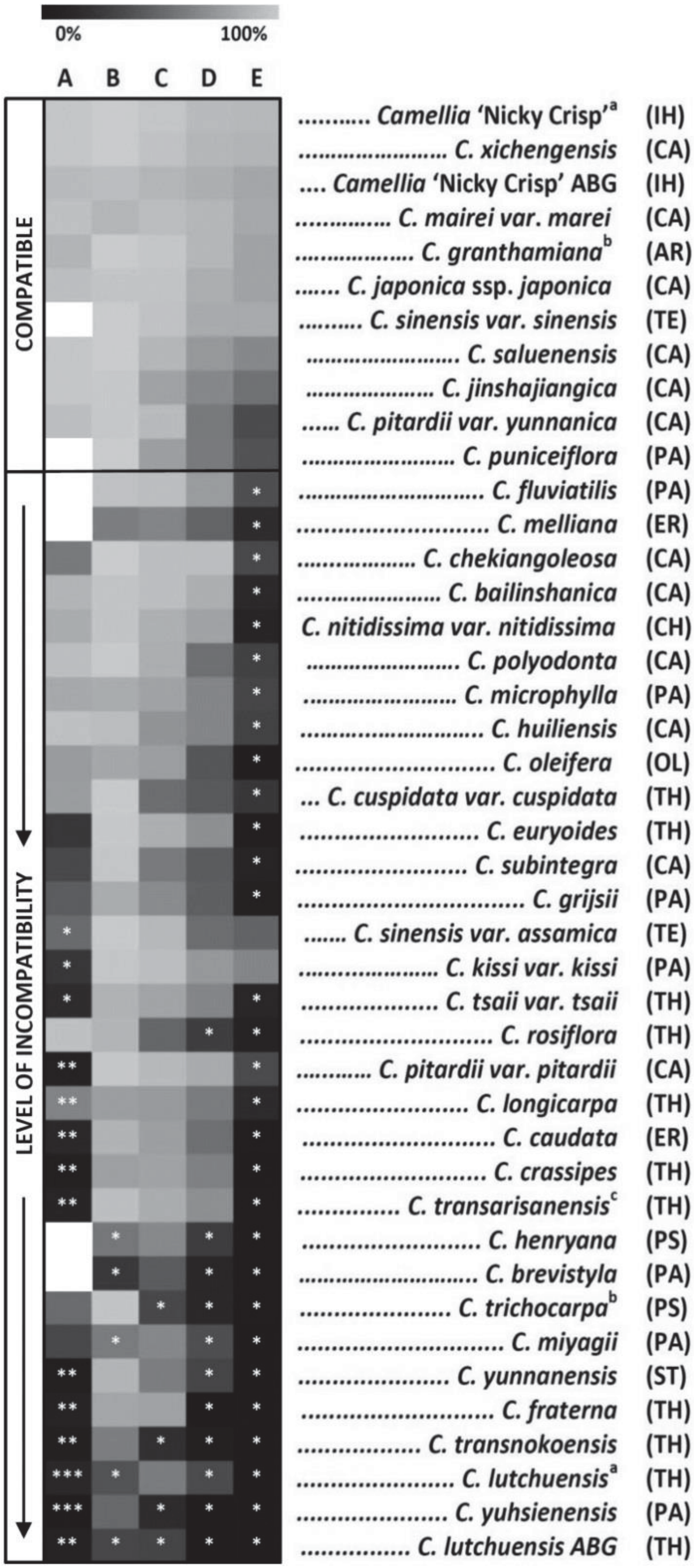
0%
100%
A B C D E
COMPATIBLE
LEVEL OF INCOMPATIBILITY
Camellia 'Nicky Crisp'[a] (IH)
C. xichengensis (CA)
Camellia 'Nicky Crisp' ABG (IH)
C. mairei var. marei (CA)
C. granthamiana[b] (AR)
C. japonica ssp. japonica (CA)
C. sinensis var. sinensis (TE)
C. saluenensis (CA)
C. jinshajiangica (CA)
C. pitardii var. yunnanica (CA)
C. puniceiflora (PA)
C. fluviatilis (PA)
C. melliana (ER)
C. chekiangoleosa (CA)
C. bailinshanica (CA)
C. nitidissima var. nitidissima (CH)
C. polyodonta (CA)
C. microphylla (PA)
C. huiliensis (CA)
C. oleifera (OL)
C. cuspidata var. cuspidata (TH)
C. euryoides (TH)
C. subintegra (CA)
C. grijsii (PA)
C. sinensis var. assamica (TE)
C. kissi var. kissi (PA)
C. tsaii var. tsaii (TH)
C. rosiflora (TH)
C. pitardii var. pitardii (CA)
C. longicarpa (TH)
C. caudata (ER)
C. crassipes (TH)
C. transarisanensis[c] (TH)
C. henryana (PS)
C. brevistyla (PA)
C. trichocarpa[b] (PS)
C. miyagii (PA)
C. yunnanensis (ST)
C. fraterna (TH)
C. transnokoensis (TH)
C. lutchuensis[a] (TH)
C. yuhsienensis (PA)
C. lutchuensis ABG (TH)

Figure 3.4. Analysis of macroscopic and microscopic parameters in 40 species and one interspecific hybrid of *Camellia*. Column A = percent lesion area at 72 h postinoculation (hpi); B = papillae absence, C = lengthened primary hyphae, D = subcuticular hyphal growth, and E = subepidermal hyphae at 24 hpi. Tile color coding represents mean percentage data of three biological replicates (unless specified), ranging from highly compatible phenotypes (light gray) to comparatively incompatible phenotypes (black). White tiles represent 'no data'. Multiple two-tailed Student's t tests were applied to raw data for each independent column, comparing each species with the susceptible *Camellia* 'Nicky Crisp' Auckland Botanic Gardens (ABG) genotype; *, **, and *** indicate values significantly less than *Camellia* 'Nicky Crisp' ABG values at $P \leq 0.05$, 0.01, and 0.001 respectively. The absence of asterisks represents no significant difference. Incompatible species were manually sorted and ranked based on the number of parameters that showed significant difference to the compatible control, *Camellia* 'Nicky Crisp' ABG. Camellia sections are abbreviated as CA (Camellia), AR (Archecamellia), TE (Thea), CH (Chrysantha), PA (Paracamellia), OL (Oleifera), TH (Theopsis), ER (Eriandria), PS (Pseudocamellia), and ST (Stereocarpus). IH = interspecific hybrid. Superscript a: Data from original *Camellia* 'Nicky Crisp' and *Camellia lutchuensis* samples were included for comparison. Superscript b: Column A data based on two biological replicates. Superscript c: Column B, C, D, and E data based on two biological replicates.

comparisons made between the data for the *Camellia* 'Nicky Crisp' ABG genotype and the previously examined *Camellia* 'Nicky Crisp' genotype showed no significant difference for the parameters presented (Fig. 3.4), suggesting that comparable analyses were reproducible. In addition to lesion analysis at 72 hpi, further observations of lesion development were made at 113 hpi. *Camellia lutchuensis, Camellia yuhsienensis*, *Camellia transnokoensis*, *Camellia fraterna*, *Camellia transarianensis, Camellia longicarpa* and *Camellia caudata* were the only assessed species that failed to fully develop visible petal lesions by this time.

To determine whether the selected *Camellia* taxonomical sections were significantly different from each other, ANOVA was performed independently for each assessed parameter. *Camellia* sections appeared to be significantly different from one another for each of the assessed infection parameters, including lesion area at 72 hpi ($P < 0.001$), papillae absence ($P < 0.001$), lengthened primary hyphae ($P < 0.001$), sub-cuticular hyphae ($P < 0.001$) and sub-epidermal hyphae ($P < 0.001$). Further statistical analysis (Tukey's range test) highlighted specific differences between sections (Appendix 9.4). Section Camellia was significantly different to section Paracamellia and section Theopsis for all of the quantified parameters. Furthermore, sections Thea and Archecamellia were found to be not significantly different from section Camellia for all of the quantified parameters, although the number of replicate species within these two sections was low (n = 2). This result suggests that resistance to *C. camelliae* is confined to certain sections of the *Camellia* genus.

3.2.5. Interspecific hybrid resistance is influenced by parent genotype

Many of the most popular ornamental *Camellia* shrubs exist as interspecific hybrids. A proportion of these hybrids have previously been bred from species that were shown to be resistant to *C. camelliae* (Fig. 3.4). Interspecific hybrids that included *C. lutchuensis*, *C. transnokoensis*, *C. fraterna* or *C. forrestii* within their parentage were specifically chosen for resistance screening. This choice was based on the observation that section Theopsis species appear to be the most resistant to *C. camelliae* (Fig. 3.4). The parentage of each of the 18 chosen hybrids consisted of 2 to 7 contributing parents (Appendix 9.1B). The degree of *C. camelliae* resistance was determined by measuring the same macroscopic and microscopic parameters previously used to screen *Camellia* species.

Papillae were absent from the majority of the tested interactions (Fig. 3.5, column A). Furthermore, *C. camelliae in planta* development was unhindered in the majority of the interspecific hybrids tested. Hybrid No. 18 (*C. japonica* x *C. transnokoensis*) was the only hybrid genotype to have significantly lower levels of lengthened primary hyphae and subcuticular hyphal growth (Fig. 3.5, columns B & C). Less than 2% of ascospores produced subepidermal hyphae when applied to hybrid No. 18 (*C. japonica* x *C. transnokoensis*) petal tissue, although these numbers weren't significantly different to the susceptible control (Fig. 3.5. column D). Hybrid No. 15 (*C. pitardii* var. *yunnanica* x *C. yunnanensis*) x (*C. japonica* x *C. lutchuensis*) also exhibited low levels of subepidermal hyphae (< 2%), although fungal penetration and subcuticular growth was not significantly different from the susceptible control.

Only 9 of the 20 genotypes had a mean lesion area average of less than 10% by 48 hpi (Figure 3.5, column E), suggesting that disease was developing quickly in the majority of the tested hybrids. *C. lutchuensis* petals also had a considerable degree (6 to 18%) of browning by this time, although it was unclear whether this was due to lesion development or tissue desiccation. Only hybrids No. 17 (*C. japonica* x *C. lutchuensis*) and No. 15 (*C. pitardii* var. *yunnanica* x *C. yunnanensis*) x (*C. japonica* x *C. lutchuensis*) failed to develop all enveloping disease-associated lesions by 96 hpi. Surprisingly, the mock-inoculated control of hybrid No. 17 (*C. japonica* x *C. lutchuensis*) did develop brown lesions, but it is unclear whether this was due to *C. camelliae* infection, or as a result of pre-experiment infection from an unknown *Camellia* pathogen. Despite observations that *C. camelliae* was being actively resisted in hybrid No. 18 (*C. japonica* x *C. transnokoensis*) this genotype also developed lesions by 96 hpi.

Hybrid resistance scores (Figure 3.5, column F) were calculated by ranking each hybrid from 20 to 1 for each resistance parameter, and then calculating the sum of the

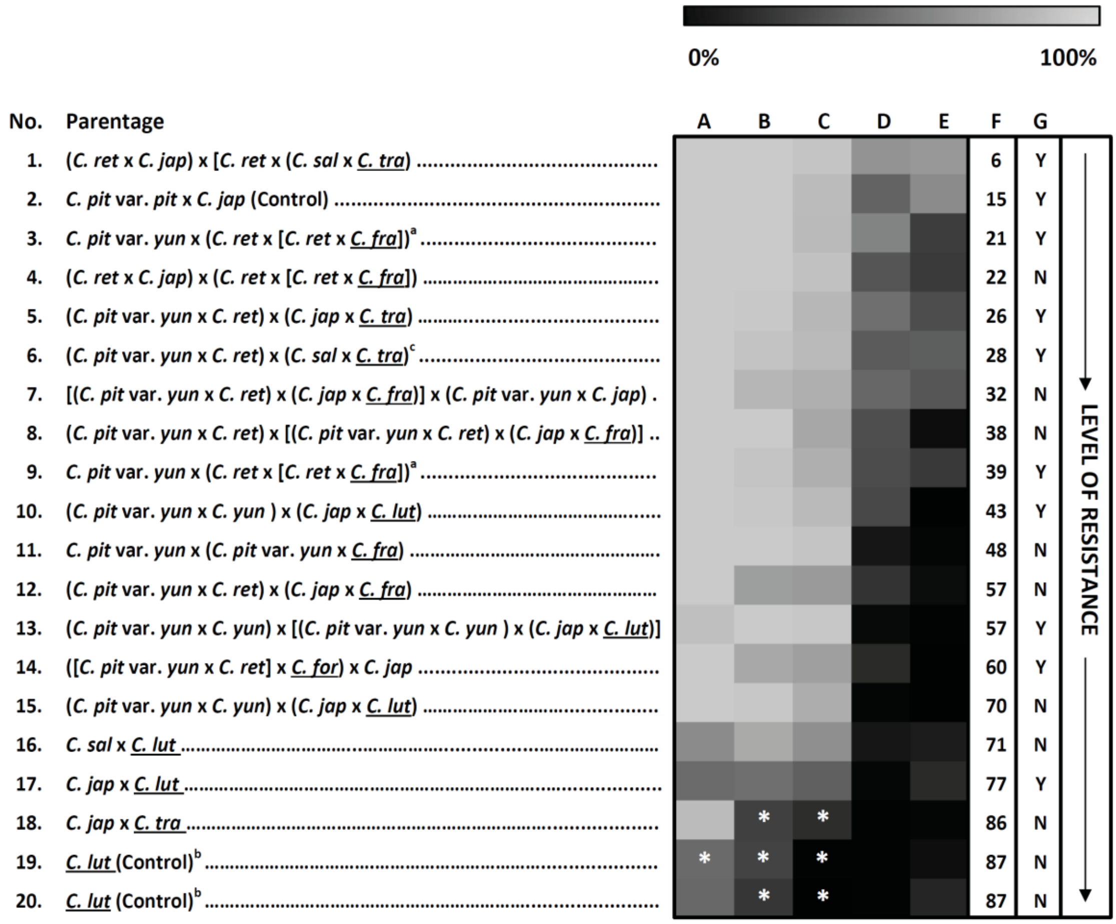

Figure 3.5. A comparison of *Ciborinia camelliae* resistance within 18 interspecific hybrids and 1 species of *Camellia*. Column A= papillae absence, B = lengthened primary hyphae, C = subcuticular hyphal growth, D = subepidermal hyphae at 24 h postinoculation (hpi), E = percent lesion area at 48 hpi, F = combined resistance score, and G = lesion development in mock-inoculated controls by 96 hpi (Y = yes, N = no). Tile colour coding represents mean percentage data of three biological replicates (unless specified), ranging from highly susceptible phenotypes (light gray) to comparatively resistant phenotypes (black). The displayed order of the *Camellia* genotypes is replicated in Appendix 9.1B and is based on the combined resistance score (F). Multiple two-tailed Student's t tests were applied to raw data for each independent column, comparing each genotype with the susceptible *Camellia* 'Nicky Crisp' (hybrid No. 2) genotype; * indicate values significantly less than *Camellia* 'Nicky Crisp' values at P ≤ 0.1. The absence of asterisks represents no significant difference. *Camellia* species names are abbreviated as *C. jap* (*C. japonica*), *C. pit* var. *pit*, (*C. pitardii* var. *pitardii*), *C. sal* (*C. saluenensis*), *C. pit* var. *yun* (*C. pitardii* var. *yunnanica*), *C. ret* (*C. reticulata*), *C. fra* (*C. fraterna*), *C. tra* (*C. transnokoensis*), *C. for* (*C. forrestii*), *C. lut* (*C. lutchuensis*), *C. yun* (*C. yunnanensis*). All section Theopsis species are underlined. Superscript a: morphologically diverse offspring from the same original cross. Superscript b: *C. lutchuensis* individuals from two different localities. Superscript c: data based on two biological replicates.

Figure 3.6. Examples of blooms from interspecific *Camellia* hybrids that are highly susceptible (A to C), or semi-resistant (D to F) to *Ciborinia camelliae* infection. Image **A**, No. 1 (*C. reticulata* x *C. japonica*) x [*C. reticulata* x (*C. saluenensis x C. transnokoensis*), **B**, No. 3 *C. pitardii* var. *yunnanica* x (*C. reticulata* x [*C. reticulata* x *C. fraterna*]), **C**, No. 5 (*C. pitardii var. yunnanica x C. reticulata*) x (*C. japonica x C. transnokoensis*), **D**, No. 15 (*C. pitardii* var. *yunnanica* x *C. yunnanensis*) x (*C. japonica* x *C. lutchuensis*), **E**, No. 16 *C. saluenensis* x *C. lutchuensis*, **F**, No. 17 *C. japonica* x *C. lutchuensis*.

combined rank values. Hybrids that exhibited relatively high resistance for a particular parameter were given a higher rank. Hybrid No. 1 (*C. reticulata* x *C. japonica*) x [*C.reticulata* x (*C. saluenensis x C. transnokoensis*) ranked poorly in 4 of the 5 resistance parameter categories, and therefore, produced a low combined resistance score (Fig. 3.5). Interspecific hybrids with large resistance scores tended to have *C. lutchuensis* as their contributing Theopsis parent, with the exception of hybrid No. 18 (*C. japonica* x *C. transnokoensis*). In general, hybrids with *C. lutchuensis* and one additional parent species appeared to be more resistant than those hybrids that had two or three non-Theopsis species contributing to their parentage. This suggested that the greater the proportion of *C. lutchuensis* within a hybrid genotype, the stronger the resistance to *C. camelliae.* However, hybrid No. 15 (*C. pitardii* var. *yunnanica* x *C. yunnanensis*) x (*C. japonica* x *C. lutchuensis*) was an exception to this trend. Despite multiple parents, hybrid No. 15 was the only interspecific *Camellia* hybrid that failed to develop disease. Images of the susceptible and semi-resistant *C. lutchuensis* hybrids are shown (Fig. 3.6).

3.3. Discussion

Breeding pathogen resistant crops has been a common goal of plant breeders for many years and still remains a preferred option for controlling plant disease (Moose & Mumm, 2008). The discovery of natural resistance to *C. camelliae* in several species of the *Camellia* genus has revealed a new opportunity that has potential to control this pathogen using a traditional plant breeding strategy (Taylor, 2004). In this chapter the response of different *Camellia* genotypes to *C. camelliae* ascospore infection was characterized using both macroscopic and microscopic analyses. Compatible *Camellia* 'Nicky Crisp'-*C. camelliae* interactions failed to display visible signs of resistance. In comparison, the incompatible *Camellia lutchuensis*-*C. camelliae* interaction showed strong signs of an induced resistance response. Assessment of 40 *Camellia* species indicated that incompatibility is variable across the *Camellia* genus with prevalence being higher in sections Theopsis and Paracamellia. *Camellia lutchuensis*-derived interspecific hybrids exhibited resistance to *C. camelliae*, although all but one genotype ultimately developed disease.

3.3.1. *Ciborinia camelliae* establishment and growth in compatible tissue

Penetration of the compatible *Camellia* 'Nicky Crisp' petal cuticle by *C. camelliae* was achieved by appressorium-like structures that differ from the classic polarized appressoria produced by *Colletotrichum* and *Magnaporthe* species (Kleemann et al., 2012; Wilson & Talbot, 2009). However, *C. camelliae* appressorium-like structures were morphologically similar to those of other members of the Sclerotiniaceae, including *B. cinerea*, *S. sclerotiorum* and *Monilinia fructicola* (Fourie & Holtz, 1995; Jurick & Rollins, 2007; Lee & Bostock, 2006).

Following cuticle penetration of the susceptible tissue, initial asymptomatic growth of *C. camelliae* was confined to the apoplast. The well characterized biotrophic fungus *Cladosporium fulvum* also confines its growth to the apoplast (De Wit, 1977) and is thought to modulate the supply of host-derived nutrients as it grows (Solomon & Oliver, 2001; Solomon & Oliver 2002). The AVR2 and AVR4 proteinaceous effectors of *Cladosporium fulvum* have been shown to localize specifically to the apoplast of tomato leaves where they act to indirectly inhibit plant protease activity (Rooney et al., 2005) as well as recognition by PRRs (van Esse et al., 2008). It is plausible that *C. camelliae* may also produce apoplastic effectors that act to suppress PTI during compatible interactions.

Following radiation of fungal hyphae in the apoplast there is a switch in the growth habit of *C. camelliae*. Broadening of the sub-cuticular primary hyphae was observed at 36 hpi, together with the development of secondary hyphae in the vicinity of the cuticle penetration site (Fig. 3.3D). It is unclear whether the secondary hyphae of *C. camelliae* directly penetrate host petal cells. However, secondary hyphal growth appears to coincide with the first signs of macroscopic lesion development and necrosis. These observations are very similar to the growth habit of the hemibiotroph *Colletotrichum acutatum* (Adaskaveg et al., 2005). Initial biotrophic growth of *Colletotrichum acutatum* on almond petal tissue is confined to the apoplast, with broad intercellular sub-cuticular hyphae observed between 24 and 48 hpi. Similarly, the switch to necrotrophy is hallmarked by the initiation of secondary hyphae that directly penetrate host cells.

The Sclerotiniaceae is well-known as a necrotrophic-rich family of fungi, where necrotrophy is thought to be the ancestral state (Andrew et al., 2012). It has recently been suggested that the well-established necrotroph *Sclerotinia sclerotiorum* exhibits characteristics of biotrophy during its early pathogenic phase (Williams et al., 2011). Similarly, *C. camelliae* exhibits an asymptomatic biotrophic-like phase during establishment *in planta*, that later transitions to necrotrophy. However, it is difficult to deduce whether this is a true hemibiotrophic lifestyle, based on observational data alone. Transcriptomic and genomic studies, such as those used to characterize and confirm the switch from biotrophy to necrotrophy in *Colletotrichum* fungi (Gan et al., 2013), would help to determine if a similar switch occurs in *C. camelliae*.

3.3.2. *Ciborinia camelliae* resistance in incompatible *Camellia lutchuensis* tissue

Incompatibility observed during the *Camellia lutchuensis*-*C. camelliae* interactions resembled previous descriptions of induced plant resistance (Thordal-Christensen et al., 1997; Huckelhoven et al., 2001; Fan & Doerner, 2012). The formation of pre-invasive papillae in *Camellia lutchuensis* epidermal cells was observed, together with localized H_2O_2 at infection sites. Temporal quantification of papilla induction showed that the induced response to *C. camelliae* in plant epidermal cells was gradual over time (Table 3.1). This slow, steady increase in the intensity of the defense response is consistent with the gradual induction of PTI-associated responses (Jones & Dangl, 2006).

The accumulation of H_2O_2 is thought to be involved in several processes during induced plant resistance, including strengthening the cell wall (Levine et al., 1994) and contributing to the oxidative burst/HR (Lamb & Dixon, 1997; Molina & Kahmann, 2007). During the *Camellia lutchuensis*-*C. camelliae* interaction, H_2O_2 localization at papillae formation sites was observed, suggesting that cross-linking of the cell wall may occur during this interaction. However, it is unclear whether mechanical resistance is important for impeding the development of *C. camelliae*, as the initial sub-cuticular and apoplastic growth habit does not appear to require penetration of the plant cell wall (Figs. 3.3A & 3.3B).

H_2O_2 is localized to the intercellular spaces of petal epidermal cells in proximity to cuticle penetration sites. Intercellular H_2O_2 appeared to diffuse outwards from the penetration site suggesting that its accumulation and localization is in response to cuticle penetration. Intercellular H_2O_2 was occasionally observed during penetration of some of the susceptible species including the *Camellia* 'Nicky Crisp' ABG control (data not shown). It is plausible that some of the H_2O_2 observed during the plant-pathogen interactions, is derived from *C. camelliae*, as several members of the Sclerotiniaceae are believed to produce H_2O_2 through the action of their own NADPH oxidase enzymes (Kim et al., 2011; Segmuller et al., 2008) and via secreted oxalic acid-mediated plant programmed cell death (Kim et al., 2008). Therefore, it is unclear whether intercellular H_2O_2 acts to suppress or promote the growth of *C. camelliae* in *Camellia* petal tissue.

A small percentage of epidermal cells exhibited DAB staining and a depressed cuticle during the *Camellia lutchuensis-C. camelliae* interaction. Previous reports have attributed observations of this kind to an ETI-mediated HR, which leads to localized cell death (Thordal-Christensen et al., 1997). This phenotype is consistent with the weak ETI previously observed in other induced plant-pathogen interactions, including the barley-powdery mildew interaction (Huckelhoven et al., 2001; Thordal-Christensen et al., 1997), and the pepper-powdery mildew interaction (Hao et al., 2011). The low frequency of the ETI response is thought to be due to weak recognition of effectors by plant R proteins (Jones & Dangl, 2006). It is possible that the cell death associated with ETI also contributed to lesion area measurements, particularly during incompatible interactions.

These results suggest that *Camellia lutchuensis* defense responses to *C. camelliae* are initially induced at the point of attempted cuticle penetration. Furthermore, the impaired development of sub-cuticular and sub-epidermal fungal hyphae, together with localized cell death, suggests that *Camellia lutchuensis-C. camelliae* incompatibility involves multiple mechanisms of defense.

3.3.3. *Ciborinia camelliae* resistance within *Camellia* species

The extension of macroscopic and microscopic analyses to a further 39 species of *Camellia* revealed significant phenotypic variation in resistance to *C. camelliae* (Fig. 3.4). *Camellia lutchuensis*, *Camellia yuhsienensis* and *Camellia transnokoensis* showed the strongest resistance phenotypes to *C. camelliae* infection and also failed to fully develop petal lesions by 113 hpi. The species *Camellia fraterna*, *Camellia transarianensis*, *Camellia longicarpa* and *Camellia caudata* also failed to fully develop petal lesions by 113 hpi, but exhibited comparatively weaker resistance phenotypes than *Camellia lutchuensis*, *Camellia yuhsienensis* and *Camellia transnokoensis* (Fig. 3.4). These results suggest that variable strengths of resistance to *C. camelliae* exist within the *Camellia* genus.

A large proportion of analyzed species showed defense responses, but ultimately failed to resist the establishment of *C. camelliae*. This phenotype is consistent with the definition of basal resistance, which is described as resistance that reduces pathogen spread during compatible plant-pathogen interactions (Niks & Marcel, 2009). Many *Camellia* species were able to delay the onset of necrotic lesion formation and the establishment of sub-epidermal hyphae as compared to the compatible *Camellia* 'Nicky Crisp' ABG genotype (Fig. 3.4). Consistent with Jones and Dangl's description of basal resistance (Jones & Dangl, 2006), both PTI and ETI specific responses (papillae formation and HR) were observed in epidermal cells of these species (Fig. 3.4). Schulze-Lefert and Panstruga suggest a model whereby the contribution of the two branches of plant immunity to resistance varies depending on how well adapted a pathogen is to a potential host (Schulze-Lefert & Panstruga, 2011). In their model, high incompatibility between host and pathogen is due to a strong PTI-associated response, which in turn is a result of an ineffective pathogen-effector repertoire. Weaker incompatibility to a different host is the result of a weaker PTI-associated response and a more effective pathogen-effector repertoire. Here it is hypothesized that the variable levels of basal resistance observed during interactions between *C. camelliae* and *Camellia* species are also due to the variable effectiveness of *C. camelliae*'s effectors in phylogenetically divergent hosts.

The susceptibility of the common ornamental species *Camellia japonica* ssp. *japonica* was confirmed (Fig. 3.4). Two other common ornamental species, *Camellia reticulata* and *Camellia sasanqua* were not examined in this study. However, *Camellia* species belonging to the same sections as *Camellia reticulata* and *Camellia sasanqua* (section Camellia and section Oleifera) were all susceptible to *C. camelliae* infection. Confirmation that both *Camellia sinensis* var. *sinensis* and *Camellia sinensis* var. *assamica* form compatible interactions with *C. camelliae* (Fig. 3.4) may have implications for tea breeding, as fruit production is thought to be affected by this disease (Hara, 1919).

3.3.3. *Ciborinia camelliae* resistance within *Camellia* interspecific hybrids

Based on the observation that section Theopsis species of genus *Camellia* have high resistance to *C. camelliae* (Fig. 3.4), it was hypothesized that hybrids with section Theopsis parentage may also exhibit high levels of resistance to *C. camelliae*. The majority of the interspecific *Camellia* hybrids tested were susceptible to *C. camelliae*. However, observations of lesion development at 16, 24 and 48 hpi indicated that the rate at which disease developed varied between hybrids. Furthermore, several hybrids that exhibited a low incidence of lesion development at 48 hpi went on to develop lesions by 96 hpi, including hybrid No. 14 ([*C. pitardii* var. *yunnanica* x *C. reticulata*] x *C. forrestii*) x *C. japonica*, hybrid No. 16 (*C. saluenensis* x *C. lutchuensis*) and hybrid No. 18 (*C. japonica* x *C. transnokoensis*). This basal resistance phenotype offers an alternative strategy for reducing '*Camellia* flower blight' symptoms on hosts. If this trait were to be selected in hybrids that have short-lived blooms, disease could potentially be abscised from the plant before it had a chance to negatively affect the aesthetic value of the bloom. However, this strategy may not reduce the incidence of *C. camelliae* in the environment, as it can persist as a saprophyte (Kohn & Nagasawa, 1984).

Interestingly, hybrids with identical or similar parentage did not respond in the same way to *C. camelliae* infection. The strong resistance phenotype demonstrated by hybrid No. 15 (*C. pitardii* var. *yunnanica* x *C. yunnanensis*) x (*C. japonica* x *C. lutchuensis*) was not conserved in hybrid No. 10 (*C. pitardii* var. *yunnanica* x *C. yunnanensis*) x (*C. japonica* x *C. lutchuensis*). Furthermore, hybrids that were derived from exactly the same parent plants (i.e. hybrid Nos. 3 and 9) also scored differently during macroscopic and microscopic resistance analysis, although they were both ultimately susceptible to *C. camelliae*. These results suggest that although these hybrids have similar parent species the genetic rearrangements that occur during hybridization are likely to influence the ability of each individual offspring to resist *C. camelliae*. In addition to recombination, additional complex genetic rearrangement can occur during interspecific hybridization that can lead to differences in disease resistance (Johnson, 2008).

The data presented here demonstrate that *Camellia lutchuensis* derived hybrids were the most resistant to infection by *C. camelliae*, with the exception of one highly resistant *C. transnokoensis*-based hybrid. However, for all but one interspecific *Camellia* hybrid (hybrid No. 15), the levels of natural resistance were not sufficient to prevent the development of '*Camellia* flower blight'.

3.4. Conclusions

Comparative analysis revealed a correlation between *Camellia* sections and their levels of incompatibility to *C. camelliae*. Collectively, species of section Theopsis showed the highest levels of incompatibility which makes them preferred candidates for future *C. camelliae* resistance breeding strategies. *Camellia yuhsienensis* also showed increased resistance to *C. camelliae* despite its close taxonomic proximity to susceptible *Camellia* species. The observed incompatible *Camellia lutchuensis*-*C. camelliae* interaction is consistent with an induced polygenic plant defense response (Jones & Dangl, 2006), indicating that *C. camelliae* is only semi-adapted to this species. Interspecific hybrids with high genetic dosages of *C. lutchuensis* displayed the strongest resistance phenotype to *C. camelliae*, although all but one hybrid succumbed to *C. camelliae* infection. Based on these results, the introgression of genetic material from section Theopsis species into hybrids of *Camellia* would be a valid approach for increasing resistance to *C. camelliae.*

4. The development of genomic and transcriptomic resources for the *Camellia*-*Ciborinia camelliae* interaction

4.1. Introduction

A recent estimation based on information from next-generation sequencing (NGS) methods puts the number of fungal species currently inhabiting the earth at as many as 5.1 million (O'Brien et al., 2005), which is more than triple the previous estimation (Hawksworth, 1991). This number has increased dramatically over the last few years, primarily due to the development of cost-effective NGS technology, which has allowed for more thorough taxonomical investigation.

Research organizations such as the Joint Genome Institute (JGI), the Broad Institute and the Welcome Trust Sanger Centre have embarked on large scale fungal genome sequencing projects, which have dramatically increased the amount of publicly available fungal sequence data. Currently, nearly 400 draft fungal genomes are listed on the JGI website (Retrieved from http://genome.jgi-psf.org/programs/fungi/index.jsf 1 Aug 2014). These data have facilitated various studies; from understanding the role of gene duplication in eukaryotic gene evolution (Wapinski et al., 2007) to comparing the genomes of closely related fungi (Amselem et al., 2011).

Transcriptome sequencing projects are often undertaken in parallel with genome sequencing in order to add a second layer of information to the genomic data. Complementary expressed sequence tag (EST) data can facilitate the annotation of genomic contigs and the detection of splice variants (Zuccaro et al., 2011). Furthermore, transcriptomes can be used to profile global gene expression patterns. For example, transcriptome sequencing of temporal life stages of *Colletotrichum higginsianum* enabled the identification of genes involved in the transition from biotrophy to necrotrophy (O'Connell et al., 2012).

This chapter describes the development and validation of three major genetic resources; the *C. camelliae* draft genome, the compatible *Camellia* 'Nicky Crisp'-*C. camelliae* transcriptome and the incompatible *Camellia lutchuensis*-*C. camelliae* transcriptome. The usefulness of these resources for investigating host genetic changes associated with the *Camellia*-*C. camelliae* interaction is demonstrated and discussed.

4.2. Results

4.2.1. *Ciborinia camelliae* draft genome sequencing and assembly

Initial attempts to extract *C. camelliae* genomic DNA using standard gDNA extraction resulted in low yields of low quality gDNA. Due to the highly viscous nature of the fungal DNA pellet it was assumed that an excess of carbohydrate compounds were contaminating the fungal gDNA. In order to eliminate these contaminants from the gDNA a cesium chloride purification step was included following liquid/liquid partitioning (see section 2.5.1). *C. camelliae* gDNA isolated using this protocol was deemed suitable for next generation sequencing with a yield of 70 ng/ul and a 260/280 optical density ratio of 1.88.

The *C. camelliae* genome was sequenced on the Illumina MiSeq platform resulting in a total of ~8.6 GB of 250 bp paired-end raw sequence read data. The SolexaQA software package (Cox et al., 2010) was used to identify and remove low quality sequence reads resulting in a combined total of ~5.66 GB of high quality sequence read data. *C. camelliae* genome coverage was estimated to be 139x, based on a genome size of 40.7 MB (Table 4.1).

The *C. camelliae* genome was assembled using the *de novo* assembly software Velvet (Zerbino et al., 2008). A k-mer value of 69 was chosen for the assembly as it yielded the fewest contigs with the highest n50 (Appendix 9.6). A total of 2664 Velvet-assembled contigs were further assembled into 2581 scaffolds using SSPACE (Boetzer et al., 2011). The effectiveness of the *C. camelliae* draft genome for gene prediction was validated by aligning previously sequenced *C. camelliae* gene sequences and *C. camelliae* ESTs to the *C. camelliae* draft genome (data not shown). Additional validation was performed by comparing *C. camelliae* scaffolds with genomic data previously characterized in *B. cinerea* and *S. sclerotiorum* (Fig. 4.1) (Amselem et al., 2011).

4.2.2. *Ciborinia camelliae* shares genomic characteristics with close relatives *Botrytis cinerea* and *Sclerotinia sclerotiorum*

Ciborinia camelliae is a member of the Sclerotiniaceae family and shares a common ancestor with the necrotrophic phytopathogens *B. cinerea* and *S. sclerotiorum* (Appendix 9.5). The *C. camelliae* draft genome was compared to the previously published genomes of *B. cinerea* (strain B05.10) and *S. sclerotiorum* (strain 1980) (Table 4.1). Statistics derived from genome assembly indicate that the *C. camelliae* genome (40.7 MB) is similar in size to the *B. cinerea* (38.8 MB) and *S. sclerotiorum* (38.0 MB) genomes. The guanidine and cytosine (GC) content of each of the three genomes was also within a similar range, as was the total number of predicted protein coding genes. Despite the generation of a higher amount of sequence coverage, the *C. camelliae* genome assembly produced a much more fragmented genome as compared to *B. cinerea* and *S. sclerotiorum.* The main limitation in the assembly process for *C. camelliae* appears to be during the contig scaffolding process. Scaffolding is primarily hindered by repetitive sequence reads and low genome coverage (Zerbino & Birney, 2008). It is unclear which of these two factors contributed to the high scaffold number in the *C. camelliae* draft genome.

4.2.3. The *Ciborinia camelliae MAT* locus exhibits synteny with the heterothallic *Botrytis cinerea* B05.10 *MAT1-1* mating locus

The sexual behaviour of fungal species in the ascomycota is primarily determined by the genetic composition of the conserved mating locus (*MAT*) (Debuchy et al., 2010). The *MAT* locus traditionally consists of 2 to 4 *MAT* genes flanked by the *APN2* and *SLA2* genes. All four *MAT* genes are required for sexual development. Fungi that are homothallic have all four *MAT* genes within a single *MAT* locus. Fungi that are heterothallic have two *MAT* genes within two mating type-specific *MAT* loci. All 4 *MAT* genes are united following the fusion of two complementary mating type strains. *B. cinerea* and *S. sclerotiorum* have heterothallic and homothallic mating systems respectively, despite their taxonomic similarity (Amselem et al., 2011). The *APN2* and *SLA2* genes of *S. sclerotiorum* and *B. cinerea* were used to determine the flanking regions of the *C. camelliae MAT* locus. These two genes successfully aligned to a 10 kb region located on scaffold 205 of the *C. camelliae* draft genome (Fig. 4.1).

Table 4.1. Comparative analysis of the *Ciborinia camelliae* draft genome with the *Botrytis cinerea* and *Sclerotinia sclerotiorum* genomes[a].

	***C. camelliae* ICMP 19812**	***B. cinerea* B05.10**	***S. sclerotiorum* 1980**
Sequencing platform	Illumina MiSeq™	Sanger	Sanger
Assembly software	Velvet and SSPACE	Arachne	Arachne
Coverage	139x	4.5x	9.1x
Total contig length (Mb)	40.7	38.8	38.0
Number of contigs	2664	4534	679
Contig N50 (kb)	32.0	16.4	123
Number of scaffolds	2581	588	36
Scaffold N50 (kb)	32.1	257	1630
GC content (%)	42.4	43.1	41.8
Predicted protein coding genes	14711	16448	14552

[a.] *B. cinerea* and *S. sclerotiorum* genomes were sequenced, assembled and characterized previously (Amselem et al., 2011). See section 2.10.2 for information regarding the calculation of the values shown. *C. camelliae* protein prediction is described in section 2.7.6.

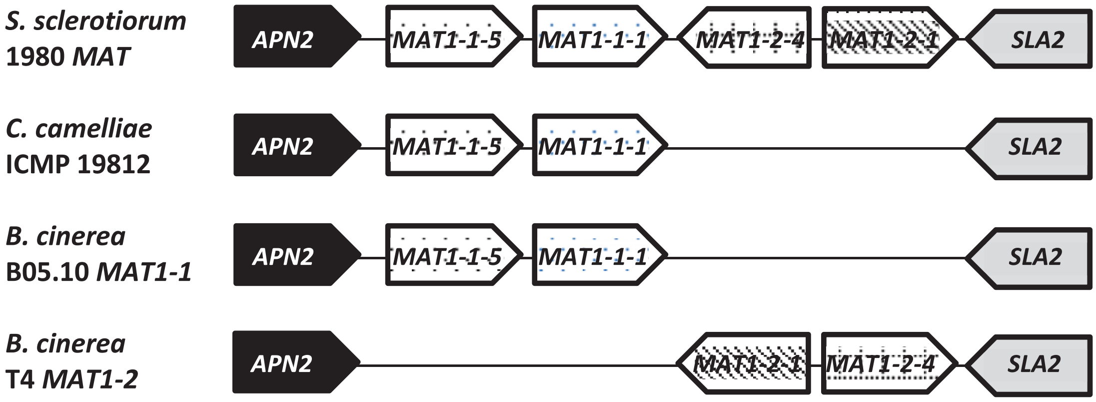

Figure 4.1. Mating (*MAT*) locus synteny comparisons between *Ciborinia camelliae* isolate ICMP 19812, *Sclerotinia sclerotiorum* 1980 and *Botrytis cinerea* mating type strains B05.10 and T4.

The *C. camelliae MAT* locus exhibited strong synteny to the *B. cinerea* B05.10 *MAT1-1* mating locus. BLASTN analysis indicated that the *S. sclerotiorum* 1980 and *B. cinerea* T4-specific *MAT1-2-4* and *MAT1-2-1* genes were absent in the draft genome of the sequenced *C. camelliae* isolate. These findings suggest that the *C. camelliae* mating system may resemble that of the heterothallic *B. cinerea* system, although the presence of a complimentary *C. camelliae* mating type is still to be confirmed. Furthermore, the genomic synteny observed between scaffold 205 of the *C. camelliae* genome with the *MAT* loci of *B. cinerea* and *S. sclerotiorum* further validates the accuracy of the *C. camelliae* genome assembly.

4.2.4. *Camellia* 'Nicky Crisp' infected samples produce mixed origin transcriptomes

Petal tissue samples of *Camellia lutchuensis* and *Camellia* 'Nicky Crisp' were spray inoculated with ascospores or milliQ H_2O as described in section 2.2. Petals were incubated for 48 hpi to allow for the development of disease symptoms on susceptible *Camellia* 'Nicky Crisp' tissue and the development of resistance responses in *Camellia lutchuensis* tissue (see Chapter 3). After 48 hpi petal tissue was snap frozen and total RNA was extracted from pooled *Camellia lutchuensis* mock, *Camellia lutchuensis* infected, *Camellia* 'Nicky Crisp' mock and *Camellia* 'Nicky Crisp' infected samples. All four RNA samples were sequenced on the Illumina HiSeq 2000 platform. A total of ~80 GB of 100 bp paired-end raw sequence read data was generated. The SolexaQA software package (Cox et al., 2010) was used to identify and remove low quality sequence reads resulting in a combined total of ~54.5 GB of high quality sequence read data (Table 4.2). The total number of reads within the infected *Camellia lutchuensis* and *Camellia* 'Nicky Crisp' host-tissue datasets were less than their respective mock control datasets. This observation is counterintuitive considering infected host-tissue should include multiple mRNAs from two different organisms (Table 4.2).

Assembly of the *Camellia lutchuensis* mock, *Camellia lutchuensis* infected, *Camellia* 'Nicky Crisp' mock and *Camellia* 'Nicky Crisp' infected transcriptomes was performed using the *de* novo sequence assembler Trinity (Grabherr et al., 2011). The number of assembled contigs varied from 90080 in the *Camellia* 'Nicky Crisp' infected

Table 4.2. *Ciborinia camelliae-Camellia* transcriptome assembly statistics.

	Camellia lutchuensis **mock**	***Camellia lutchuensis*** **infected**	***Camellia lutchuensis*** **non-redundant ***	***Camellia*** **'Nicky Crisp' mock**	***Camellia*** **'Nicky Crisp' infected**	***Camellia*** **'Nicky Crisp' non-redundant ***
No. of 100 bp paired-end reads	72 M	38 M	-	97 M	65 M	-
Number of contigs	103484	92362	107482	141650	90080	138042
Contig n50 (bp)	1595	1647	1310	1580	1553	1355
Max contig (bp)	14719	15740	15740	13752	10726	13752

*Non-redundant datasets were created by combining the relevant 'mock' and 'infected' EST datasets and removing EST redundancy, including predicted splice variants.

Table 4.3. Comparative analysis of the *Camellia* 'Nicky Crisp' non-redundant transcriptome with the putative *Ciborinia camelliae* transcriptome.

	***Camellia* 'Nicky Crisp' non-redundant transcriptome**	***Ciborinia camelliae* transcriptome**
Assembly software	Trinity	Trinity
Contigs	138042	13245
Contig N50	1355	1882
GC content (%)	40.6	45.2
Min contig length[A] (bp)	201	201
Max contig length (bp)	13752	7622
Median contig length (bp)	403	697
Mean contig length (bp)	1521.2	1099.7

[A]The Trinity software has a default minimum contig length of 200 bp (Grabherr et al., 2011).

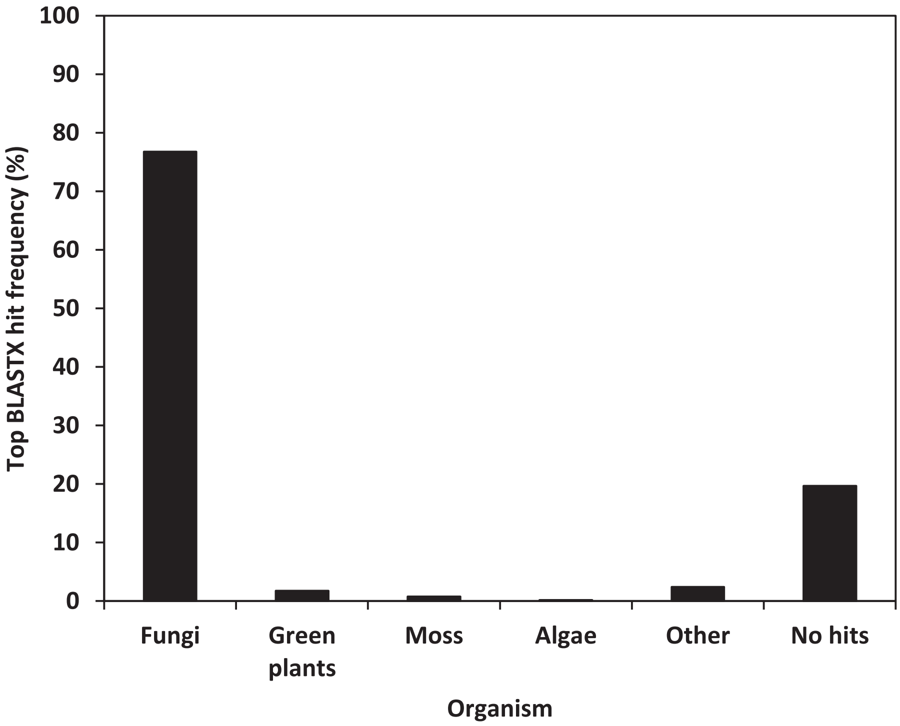

Figure 4.2. Validation of the origin of *Ciborinia camelliae* transcriptome ESTs using BLASTX and the Genbank non-redundant protein database. The organism categories are derived from alignment annotation data. A total of 1325 randomly selected putative *C. camelliae* ESTs were analyzed, which represents 10% of the total *C. camelliae* transcriptome.

transcriptome to 141650 in the *Camellia* 'Nicky Crisp' mock control transcriptome (Table 4.2). Higher numbers of contigs were assembled in the mock transcriptomes as compared to the infected transcriptomes. This pattern is likely to be a direct consequence of the differences in the number of paired-end reads used to assemble these contigs.

The presence of fungal ESTs within each transcriptome was determined by aligning published *B. cinerea* and *S. sclerotiorum* fungal ESTs to local BLAST databases of the *Camellia lutchuensis* mock, *Camellia lutchuensis* infected, *Camellia* 'Nicky Crisp' mock and *Camellia* 'Nicky Crisp' infected transcriptomes (Appendix 9.7). ESTs within the *Camellia* 'Nicky Crisp' infected transcriptome produced high probability alignments (E value = 0) with the published fungal ESTs. In contrast, not a single EST within the *Camellia lutchuensis* infected transcriptome aligned with high probability to the published fungal ESTs. This lack of fungal gene expression confirms *Camellia lutchuensis* as an incompatible host of *C. camelliae.* Previously published *Camellia* mRNA sequences were also aligned to each of the four independent transcriptomes (Appendix 9.7). As expected, *Camellia* ESTs were identified in all four transcriptomes. Notably, all 21 published *Camellia* ESTs produced high probability alignments (E value = 0) with the *C*. 'Nicky Crisp' mock transcriptome, further validating the Trinity transcriptome assembly process.

Non-redundant 'reference' EST datasets were created by combining relevant mock and infected EST transcriptome datasets and removing redundant sequences. The number of contigs within the mock-infected transcriptome datasets was almost equivalent to the non-redundant transcriptome (Table 4.2). This can be explained by differences in the number of splice variants between the two datasets. The redundant mock-control datasets retain splice variants whereas the non-redundant dataset only retain a single variant.

4.2.5. Fungal ESTs make up 10% of the *Camellia* 'Nicky Crisp' non-redundant transcriptome

The *Camellia* 'Nicky Crisp' non-redundant EST library was shown to include fungal ESTs, presumably of *C. camelliae* origin (Appendix 9.7). *C. camelliae* ESTs were separated from all other ESTs based on their ability to align to the *C. camelliae* genome (Appendix 9.9), as well as their absence within mock-inoculated transcriptomes.

A total of 13245 *C. camelliae* ESTs were identified within the *Camellia* 'Nicky Crisp' non-redundant transcriptome which equates to 9.5% of the total transcriptome (Table 4.3). This number is thought to be a conservative estimate, as occasionally 'non-fungal' designated ESTs were found to align best to fungal genomes indicating that the screening process was fallible (data not shown). The longest *C. camelliae* EST (7622 bp) was about half the length of the longest *Camellia* 'Nicky Crisp' non-redundant EST (13752 bp). On average, *C. camelliae* ESTs tended to be shorter and more GC rich than non-fungal ESTs.

BLASTX analysis of 1325 (10%) randomly chosen *C. camelliae* ESTs showed that 76% of these sequences shared homology with fungal protein sequences deposited in the Genbank non-redundant protein database (Fig. 4.2). It is plausible that the majority of the ESTs that did not align with fungal proteins are in fact of *C. camelliae* origin, as they initially aligned with high probability to the *C. camelliae* genome. A total of 5% of the designated *C. camelliae* ESTs aligned with proteins from the green plants, moss, algae and other categories. These alignments are likely to be miscalls. Miscalls often arise when a highly homologous reference protein is absent from the database but a protein with weak homology is present. A total of 19.7% of the ESTs failed to align with any of the Genbank non-redundant protein sequences. Filamentous ascomycete phytopathogens are well known for their high levels of genome innovation as compared to non-filamentous and non-pathogenic fungi (Soanes et al., 2008). Therefore, it is plausible that *C. camelliae* has rare or unique ESTs that do not match the proteins in the Genbank non-redundant protein database.

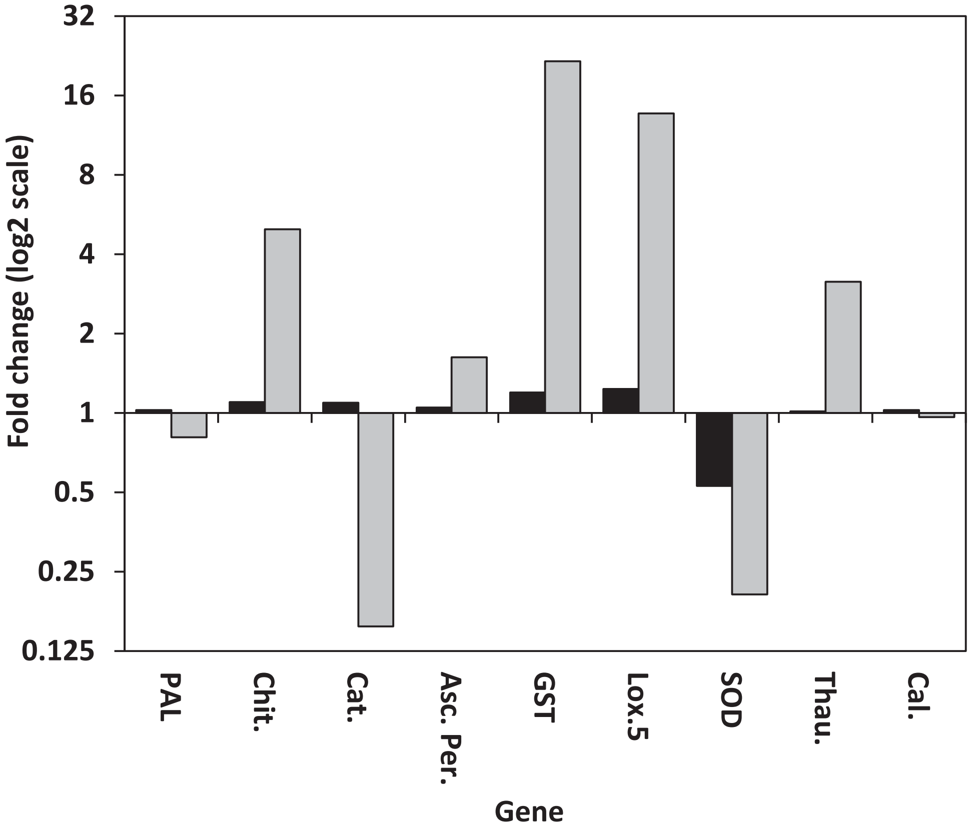

Figure 4.3. *Camellia* 'Nicky Crisp' (grey bars) and *Camellia lutchuensis* (black bars) infection-associated gene expression changes of ESTs homologous to 9 *Camellia* defense-related genes. Gene expression fold changes are based on comparisons between mock-inoculated and infected transcriptomes (P < 0.001) including correction for the false discovery rate (Benjamini et al., 1995). Genes are abbreviated as PAL (phenylalanine ammonia-lyase), Chit. (chitinase), Cat. (catalase), Asc. Per. (ascorbate peroxidase), GST (glutathione s-transferase), Lox. 5 (lipoxygenase), SOD (superoxide dismutase), Thau (thaumatin) and Cal. (calmodulin).

4.2.6. Large changes in host-defense gene expression are induced in compatible *Camellia 'Nicky Crisp-Ciborinia camelliae* interactions

The alignment of 9 published *Camellia* defense gene sequences to the *Camellia* 'Nicky Crisp' and *Camellia lutchuensis* non-redundant transcriptomes identified *Camellia* 'Nicky Crisp' and *Camellia lutchuensis* EST sequence homologs (Appendix 9.8). In response to infection, *Camellia lutchuensis* defense gene expression remained relatively unchanged for all nine EST homologs (Fig. 4.3). The largest change was recorded for the superoxide dismutase homolog which decreased in expression 2 fold. In contrast, large changes in gene expression (> 3 fold) were observed in *Camellia* 'Nicky Crisp' petal tissue for 6 of the 9 EST homologs. The glutathione S-transferase (21 fold), lipoxygenase 5 (13 fold), chitinase (5 fold) and thaumatin (3 fold) homologs all increased in response to infection. Decreases in expression were observed for the catalase (6 fold) and superoxide dismutase (5 fold) homologs, whereas the phenylalanine ammonia-lyase (1.25 fold) ascorbate peroxidase (1.6 fold) and calmodulin (1.04 fold) homologs remained relatively unchanged. In total, 2.9% of the ESTs within the *Camellia lutchuensis* non-redundant transcriptome significantly increased or decreased more than 1.5 fold, as compared to 29.9% within the *Camellia* 'Nicky Crisp' non-redundant transcriptome (excluding the 13245 fungal ESTs).

ESTs exhibiting high gene expression fold increases in response to infection were annotated using BLASTN and the Genbank non-redundant database (Table 4.4). In congruence with the data shown in figure 4.3, *Camellia* 'Nicky Crisp' gene expression changes were more dramatic than those observed for *Camellia lutchuensis* petal tissue. The list of *Camellia* 'Nicky Crisp' ESTs with increasing gene expression was dominated by EST homologs of plant cell wall modifying enzymes (pectinesterases and laccases) and enzymes involved in ROS homeostasis (a peroxidase, an oxidoreductase and a cytochrome P450 enzyme). Also on the list were single EST homologs involved in pH homeostasis (carbonic anhydrase) and ethylene biosynthesis (ACC synthase). In contrast, the highly up-regulated *Camellia lutchuensis* ESTs included a diverse range of ESTs homologous to kinases, carbohydrate modifying enzymes, DNA binding enzymes, cell structure-related genes and amino acid biosynthesis enzymes. Of particular

Table 4.4. The top 10 *Camellia* ‘Nicky Crisp’ and *Camellia lutchuensis* genes undergoing gene expression increases in response to *Ciborinia camelliae* infection.

Plant	EST ID.	Fold increase	BLASTN annotation	E-value	Genbank ID
Camellia ‘Nicky Crisp’	comp38657_c0_seq1_len=1192	998	*Theobroma cacao* pectinesterase	1.06E-128	XM_007038351
	comp31548_c0_seq1_len=1336	890	*Solanum lycopersicum* peroxidase 4-like	5.10E-102	XM_004249006
	comp33767_c0_seq1_len=1786	732	*Populus trichocarpus* hypothetical protein	0.00E+00	XM_002318778
	comp51975_c0_seq1_len=1749	728	*Theobroma cacao* pectinesterase	0.00E+00	XM_007038351
	comp24040_c0_seq1_len=1592	609	*Theobroma cacao* NAD(P)-linked oxidoreductase	1.79E-120	XM_007045353
	comp36892_c0_seq1_len=2114	498	*Prunus mume* laccase-7	3.29E-53	XM_008241698
	comp38851_c0_seq1_len=1401	493	*Solanum lycopersicum* laccase-7	6.77E-85	XM_004240105
	comp39054_c0_seq1_len=2136	469	*Panax ginseng* cytochrome P450	5.96E-175	JN604538
	comp29471_c0_seq1_len=1174	292	*Ricinus communis* carbonic anhydrase	5.56E-124	XM_002519412
	comp38741_c0_seq1_len=1626	260	*Camellia japonica* ACC synthase	0.00E+00	JX503066
Camellia lutchuensis	comp4193_c0_seq1_len=386	22	*Theobroma cacao* AGC Kinase	3.99E-102	XM_007038364
	comp233059_c0_seq1_len=344	18	*Vitis vinifera* beta-galactosidase 8-like	4.15E-66	XM_002285048
	comp1228_c0_seq1_len=335	18	*Ricinus communis* DNA binding protein	2.27E-63	XM_002532936
	comp232700_c0_seq1_len=245	17	*Vitis vinifera* homocysteine S-methyltransferase	4.21E-56	XM_002282513
	comp3293_c0_seq1_len=367	17	*Vitis vinifera* probable serine/threonine protein kinase	5.96E-104	XM_003634254
	comp5243_c0_seq1_len=369	17	*Camellia sinensis* CBF-like protein	1.77E-59	EU563238
	comp120872_c0_seq1_len=301	14	*Vitis vinifera* actin-related protein	2.73E-42	XM_002272449
	comp17522_c0_seq1_len=290	13	*Prunus mume* protein ODORANTI1-like	2.56E-87	XM_008229704
	comp9074_c0_seq1_len=449	11	*Citrus sinensis* Kinesin-like protein	2.11E-43	XM_006490358
	comp2633_c0_seq1_len=386	10	*Ricinus communis* anthranilate phosphoribosyltransferase	1.17E-95	XM_002511332

interest was the identification of homologs of the *CBF-like* and *ODORANTI1-like* transcription factors. These transcription factors have been implicated in the regulation of plant resistance to abiotic stresses (Akhatar et al., 2012) and fragrance biosynthesis (Verdonk et al., 2005) respectively.

4.3. Discussion

Genomic and transcriptomic analyses have been widely utilized in the field of molecular plant pathology. The screening of plant genomes for putative NBS-LRR plant resistance genes (Jupe, et al., 2012; Tamura & Tachida, 2011), the identification of novel antimicrobial secondary metabolites (Douglas et al., 2007) and the discovery of fungal virulence and avirulence factors (De Wit et al., 2009; Koeck et al., 2011), are a few examples of applications that these modern *in silico* technologies have facilitated. In this chapter the *C. camelliae* draft genome was compared and validated against the genomes of the closely related fungal species *Botrytis cinerea* and *Sclerotinia sclerotiorum*. Gene expression changes associated with contrasting *Camellia*-*C. camelliae* interactions were captured, validated and assessed. The preliminary results provide an insight into the extent of genetic changes associated with '*Camellia* flower blight' disease resistance and susceptibility.

4.3.1. RNA sequencing bias and *de novo* assembly limitations

The quality of the final assembly is highly dependent on the quality of the samples submitted for sequencing. RNA sequencing of the two infected host-tissue samples returned a lower number of total reads as compared to their respective mock controls (Table 4.2). From this observation it might be hypothesized that *C. camelliae* infection affects mRNA quality and abundance. However, the four RNA samples submitted for RNA sequencing were all of high quality, with RNA integrity (RIN) values > 8.0. Furthermore, the resulting read sequence quality scores were similar for all four samples, suggesting that the bias in read counts was not due to a difference in mRNA quality. It is possible that a bias arose during cDNA library construction. cDNA library synthesis has previously been shown to lead to biases in transcript uniformity as a result of random hexamer priming (Hansen et al., 2010). However, the large reduction in read counts cannot be explained by random hexamer priming alone. An alternative possibility is that only highly abundant transcripts were retained in the infected mRNA samples. mRNA sequences that had low abundance may have been degraded in the necrotic *in planta* environment created during compatible fungal infection.

Both the *C. camelliae* draft genome and transcriptomes were assembled using the *de novo s*equence assembly software Velvet (Zerbino and Birney, 2008) and Trinity (Grabherr et al., 2011), respectively. The majority of biological organisms lack a reliable genome or transcriptome (Ward et al., 2012), making *de novo* sequence assembly the preferred option for genome or transcriptome assembly. The main challenge with *de novo* genome assembly is associated with contig assembly and scaffolding, although new approaches are being developed to solve these issues (Burton et al., 2013). Contig assembly is usually impeded as a result of low sequence coverage, or the presence of large repeat regions within the endogenous sequence (Salzberg & Yorke., 2005). Without positional information it is difficult to form scaffolds from these contigs (Lai et al., 2011). Scaffolding of the *B. cinerea* and *S. sclerotiorum* genomes was aided by the use of genetic maps, which were not available for *C. camelliae* (Amselem et al., 2011). This may explain why the contig to scaffold conversion rate was much better for the *B. cinerea* and *S. sclerotiorum* genome assemblies as compared to the *C. camelliae* genome (Table 4.1). Furthermore, long Sanger sequenced reads (~800 bp) were used to assemble the *B. cinerea* and *S. sclerotiorum* genomes. Longer reads are able to span repeat regions and extend the length of contigs. Alternatively, *C. camelliae* may have a proportionally higher number of repeat regions as compared to *B. cinerea* and *S. sclerotiorum*, although this was not assessed. Despite the shortfalls associated with contig and scaffold assembly, the *de novo* assembled *C. camelliae* draft genome was suitable for gene prediction and gene discovery, as the average contig length (> 15 kb) was much greater than the average fungal gene length (< 2 kb) (Galagan et al., 2005). Efficient scaffolding was not as crucial for transcriptome assembly, as gene annotation and gene expression information was able to be estimated from truncated ESTs.

<u>4.3.2. Comparative genome analysis reveals potential heterothallism in *Ciborinia camelliae*</u>

Sexual development in ascomycete fungi is controlled by the action of two transcription factors, *MAT1-1* and *MAT1-2*. The coding sequences for these two regulators lie within the mating (*MAT*) locus (Coppin et al., 1997; Debuchy et al., 2010). Homothallic fungi like *S. sclerotiorum* have both the *MAT1-1* and *MAT 1-2* transcription factor genes, giving them the ability to self. In contrast, heterothallic *B. cinerea* fungi have two distinct mating types, each with a single gene within their *MAT* locus. The *MAT* locus of the sequenced *C. camelliae* isolate showed high synteny to the *B. cinerea MAT1-1* locus, suggesting that *C. camelliae* is also likely to be heterothallic (Fig. 4.1). Interestingly, heterothallism is thought to have evolved from homothallism in the Sclerotiniaceae (Amselem et al., 2011), suggesting that the common heterothallic ancestor of *B. cinerea* and *C. camelliae* may have diverged separately from the homothallic ancestor of *S. sclerotiorum*.

Although the complementary mating type is still to be confirmed in *C. camelliae*, this discovery has implications for *C. camelliae in vitro* propagation. Completion of the lifecycle of *C. camelliae in vitro* has not been demonstrated previously, due to the inability to produce apothecia from sclerotia in culture (Taylor, 2004). The discovery of putative heterothallism in *C. camelliae* suggests that apothecia would only be produced if two compatible mating types were grown together on the same petri dish. The creation of mating-type specific primers would aide in the identification of different *C. camelliae* mating types. These results demonstrate how genome sequencing can provide fundamental evidence about the biology of an organism.

4.3.3. The *Ciborinia camelliae* transcriptome is estimated to be 94% complete

Ciborinia camelliae ESTs were identified in the *Camellia* 'Nicky Crisp' non-redundant EST library. Their selection was based initially on BLASTN E-value alignment scores with the *C. camelliae* genome. The alignment E-value threshold of ≤ 1e-100 was chosen based on the distribution of E-value scores from alignments of all *Camellia* 'Nicky Crisp' non-redundant ESTs to the *C. camelliae* genome (Appendix 9.9). Other studies have also used this technique to separate a mixed transcriptome (Kawahara et al., 2012). In addition, ESTs that passed the E-value threshold were required to have a 50 fold increase in gene expression (mock vs infected) and have less than 20 read counts in the mock infected control. These extra stipulations were chosen to minimize non-fungal EST contamination in the final dataset. However, BLASTX analysis indicated that the *C. camelliae* EST dataset was contaminated with non-fungal ESTs (~23%) (Fig. 4.2). It is likely that the ESTs that aligned best with green plant, moss, algae, other and no hit categories are false positives due to the lack of appropriate fungal homologs within the Genbank non-redundant protein database. Translated fungal ESTs in the green plant, moss, algae and other categories are likely to align with conserved eukaryotic proteins in the absence of a more suitable fungal homolog. Due to the strict threshold parameters associated with selecting *C. camelliae* ESTs it is likely that the ESTs that are designated as green plant, moss, algae, other and no hit in figure 4.2, are of *C. camelliae* origin.

The conservative nature of the threshold parameters used to select *C. camelliae* ESTs generated a trade-off between minimizing EST contamination and maximizing *C. camelliae* EST discovery. Several hundred ESTs had E-value scores above the chosen BLASTN E-value cutoff of ≤ 1e-100 but below the common arbitrary E-value cutoff threshold of ≤ 1e-10. BLASTN annotation of a random selection of these genes indicated that at least some of them were fungal in origin (data not shown). It is likely that many of the fungal ESTs that didn't pass the chosen cutoff threshold (≤ 1e-100) were relatively short sequences originating from short coding sequences or poorly assembled transcripts. If this ambiguous set of ESTs were to be included with the 13245 *C. camelliae* ESTs they would only represent 6.2% of the total dataset. Based on this logic, these data suggest that the *C. camelliae* transcriptome is relatively free of contaminating ESTs. Furthermore, around 93.8% of *C. camelliae* transcripts expressed during infection are estimated to be present within the *C. camelliae* EST dataset.

4.3.4. Compatible *Camellia* 'Nicky Crisp'-*Ciborinia camelliae* interactions induce dramatic changes in host gene expression

The establishment of *C. camelliae* within compatible *Camellia* 'Nicky Crisp' petal tissue resulted in large changes in gene expression (Fig 4.4). This phenotype contrasted with the relatively small gene expression changes observed during the incompatible *Camellia lutchuensis-C. camelliae* interaction (Figs. 4.3 & 4.4). Furthermore, the annotated lists of highly expressed genes identified in both interactions were dissimilar from each other (Table 4.4). Taken together, these results highlight the large genotypic differences associated with two ultimately diverse biological processes; host-cell necrosis (compatible) and the host-defense response (incompatible).

The compatible interaction stimulated the expression of several *Camellia* defense gene homologs, including a class 1 chitinase, lipoxygenase 5 and a thaumatin (pathogenesis-related protein 5) gene (Fig. 4.3). Plant chitinases are commonly expressed in response to fungal pathogen attack and act to dissolve chitin in the fungal cell wall (Punja & Zhang, 1993). Lipoxygenase 5 catalyzes the formation of oxylipins, which are implicated in defense signaling during fungal pathogen attack (Porta et al., 2002). Thaumatin overexpression in transgenic plants has led to reduced fungal disease incidence (Datta, et al 1999; Mahdavi et al., 2012). Despite the functional significance of these three genes in host-defense, their expression failed to halt *C. camelliae* infection. Although it is possible that the timing or amplitude of gene expression of these defense genes was not sufficient to influence infection, it is also plausible that *C. camelliae* somehow counters the function of these genes through the action of its own fungal effector proteins. Chitin sequestration by fungal chitin binding effectors has previously been shown as a mechanism for suppressing the host-defense response in the apoplastic biotroph, *Cladosporium fulvum* (van Esse, et al., 2007; Kombrink et al., 2013).

Interestingly, the expression of *Camellia* defense genes remained comparatively low during the *Camellia lutchuensis-C. camelliae* interaction. Of particular interest was the increase in gene expression of two *Camellia lutchuensis* transcription factor homologs, *ODORANTI1* and *CBF-like* (Table 4.4). *ODORANTI1* is involved in the synthesis of benzoids, which are key components of floral scent (Verdonk et al., 2005). It is unknown if *ODORANTI1* also functions in plant defense. However, a positive association between scented *Camellia* species and *C. camelliae* resistance was observed in this study (Fig. 3.4). *CBF-like* transcriptions factors are known to be regulated in response to abiotic stresses such as cold, drought, and salinity (Akhatar et al., 2012). In the absence of functional information, the true role of the homologous *ODORANTI1* and *CBF-like* ESTs expressed in *Camellia lutchuensis* is yet to be determined.

As alluded to in chapters 1 and 3, two well documented host-responses to fungal pathogen attack are the modification of host cell walls and the induction of ROS

(Dickman & de Figueiredo, 2013; Bellincampi et al., 2014). Several cell wall and ROS-scavenging gene homologs were highly upregulated during compatible interactions, including two laccases, two pectinesterases, a peroxidase, and an oxidoreductase gene (Table 4.4). Similar ROS-scavenging gene expression patterns might be expected to be observed during the incompatible interaction, as H_2O_2 accumulation was observed during histological analyses (Fig. 3.3, Table 3.1). However, the expression of EST homologs of catalase, ascorbic peroxidase and glutathione S-transferase remained relatively unchanged (Fig. 4.4). In addition, ROS-scavenging genes were absent from the list of *Camellia lutchuensis* genes that were highly upregulated in response to *C. camelliae* infection (Table 4.4). It is possible that the gene expression of host ROS-scavenging genes is suppressed during incompatible interactions in order to maintain a high-ROS, antimicrobial environment. Plant NADPH oxidases have previously been shown to be active in establishing a ROS environment upon pathogen attack (Dubiella et al., 2013; Torres et al., 2013). Furthermore, the fungal pathogen *Magnaporthe oryzae* relies upon the action of its own ROS detoxification enzymes to reduce levels of ROS within host tissue, and establish compatibility (Tanabe et al., 2009; Huang et al., 2011). Elucidating the temporal and spatial expression patterns of *Camellia lutchuensis* NADPH oxidase homologs would help to elucidate the role of ROS during the incompatible *Camellia lutchuensis-C. camelliae* interaction.

4.4. Conclusions

Sequencing and assembly of the *C. camelliae* draft genome resulted in 2581 scaffolds. Scaffold 206 had high synteny to the mating type-specific *MAT1-1* locus of *Botrytis cinerea* (strain B05.10), suggesting that *C. camelliae* may have a heterothallic mating system. Sequencing and assembly of the *Camellia lutchuensis* mock, *Camellia lutchuensis* infected, *Camellia* 'Nicky Crisp' mock and *Camellia* 'Nicky Crisp' infected transcriptomes resulted in a large number of putative ESTs, especially in transcriptomes derived from mock-infected tissue. A total of 13245 ESTs were deemed to be specific to *C. camelliae* based on alignments to the *C. camelliae* genome and analysis of the differential gene expression data. Several genes were identified in the *Camellia lutchuensis-C. camelliae* interaction that may be involved in resistance to *C. camelliae*, including two putative transcription factors. However, RNA-seq based gene expression data did not include biological replication, due to the high sequencing cost associated with multiple replicates. Therefore, specific changes in gene expression need to be confirmed via additional experimentation. Despite these shortfalls with gene expression interpretation, the transcriptome content was highly informative and can potentially be used for gene prediction and gene discovery investigations. The next chapter of this thesis focuses on utilizing the *C. camelliae* genome and transcriptome data to predict and characterize the *C. camelliae* secretome.

5. Comparative analysis of the secretomes of *Ciborinia camelliae*, *Botrytis cinerea* and *Sclerotinia sclerotiorum*

5.1. Introduction

The establishment of compatible interactions with species of *Camellia* suggests that *C. camelliae* must somehow evade or suppress the host plant immune system during infection. It is widely accepted that fungi secrete virulence factors (effectors) that act to suppress the plant immune system during infection (De Wit et al., 2009).

The majority of fungal effectors have been characterized from obligate biotrophic phytopathogens. Biotrophs must evade the host-immune system in order to complete their lifecycle. Failure to suppress ETI-associated resistance results in a characteristic host hypersensitive response (HR) (Jones & Dangl, 2006). More recently, effectors of necrotrophic pathogens have been described (Tan et al., 2010). Unlike biotrophic effectors, most necrotrophic effectors act to promote host-cell death as these pathogens preferentially feed from dying tissue (Friesen et al., 2007). It has recently been shown that effectors from necrotrophic fungi are able to utilize the plant's own ETI-associated resistance response to promote host-cell death and susceptibility (Lorang et al., 2012).

Traditionally, fungal effectors were identified by their ability to trigger a hypersensitive response on incompatible host-tissue (Lauge & De Wit, 1998). More recently it has become possible to predict fungal effectors using bioinformatic strategies. Typically, fungal effectors are small, secreted, cysteine-rich proteins. Bioinformatic prediction software has successfully utilized these characteristics to predict novel candidate effectors in several unrelated fungal genomes (Godfrey et al., 2010; Guyon et al., 2014). This strategy relies on the premise that effector proteins have conserved characteristics. However, it is well documented that the sequences of fungal effectors are constantly changing to avoid detection from ETI-associated plant resistance proteins (Jones & Dangl, 2006). Therefore, many novel fungal effectors may be overlooked by bioinformatic prediction strategies that only consider characteristics of previously characterized effectors.

This chapter describes the prediction and characterization of the secretomes of *C. camelliae*, *Botrytis cinerea* and *Sclerotinia sclerotiorum*. The composition of each secretome was determined by assigning annotations to each of the predicted proteins. Comparative analysis of the *C. camelliae*, *B. cinerea* and *S. sclerotiorum* secretomes identified conserved and divergent secretome proteins, including a family of conserved small secreted proteins.

5.2. Results

5.2.1. The *Ciborinia camelliae* genome is predicted to contain 14711 non-redundant proteins

Ciborinia camelliae proteins were predicted using the eukaryotic gene prediction software MAKER2 (Holt & Yandell, 2011) together with OrfPredictor (Min et al., 2005). A total of 14711 non-redundant *C. camelliae* protein coding sequences were identified. The predicted *C. camelliae* proteins were validated by aligning a subset (*n* = 1472) of the proteins to the Genbank non-redundant protein database using BLASTP. The best alignments for each *C.* camelliae protein (≤ 1e-03) were categorized into six groups; fungi, bacteria, animal, insect, unknown and no hits (Appendix 9.10A). The 'unknown' category refers to proteins that successfully aligned with unannotated proteins. The 'no hits' category refers to ESTs that did not align with a protein in the Genbank non-redundant database. Nearly 71% of the predicted *C. camelliae* proteins produced their best alignment with fungal proteins, whereas 27% did not align to any of the proteins in the database. *C. camelliae* proteins that produced 'no hits' to the Genbank database are likely to be either unique to *C. camelliae*, or incorrectly predicted. The remaining 2% aligned to bacteria, animal, insect or unknown proteins. E-values of each alignment were plotted to determine the overall quality of the alignments (Appendix 9.10B). The majority of the E-values were associated with high probability alignments, with 55% producing the maximum E value. These data suggest that a large proportion of the 14711 non-redundant *C. camelliae* protein coding sequences are correctly predicted.

5.2.2. The secretomes of *Ciborinia camelliae*, *Botrytis cinerea* and *Sclerotinia sclerotiorum* are estimated to be more than 80% complete.

A total of 14711 *C. camelliae* predicted proteins were used for *C. camelliae* secretome prediction. Predicted protein sequences for *B. cinerea* and *S. sclerotiorum* were downloaded from the Broad Institute's fungal genome database (Retrieved from http://www.Broadinstitute.org/ 1 Jun 2013). Secretome prediction was performed as outlined in the bioinformatic pipeline shown in figure 5.1. Protein sequences were screened for signal peptides, cellular localization signals and transmembrane domains using a suite of bioinformatic tools (Fig. 5.1). A total of 749 *C. camelliae*, 754 *B. cinerea* and 677 *S. sclerotiorum* proteins were predicted to be secreted.

Comparison of the *B. cinerea* secretome pipeline data with previoulsy published *B. cinerea* secreted proteome data (Shah et al., 2009, Espino et al., 2010, Gonzalez-Fernandez et al., 2014) indicated that the *B. cinerea* secretome incorporated at least 82% of proteins that were secreted by *B. cinerea* during *in vitro* growth (Appendix 9.11). Based on this estimate, it was assumed that the predicted *C. camelliae* and *S. sclerotiorum* secretomes were also likely to be more than 80% complete.

5.2.3. Scatterplot analysis reveals differences in secretome composition between *Ciborinia camelliae*, *Botrytis cinerea* and *Sclerotinia sclerotiorum*.

The three secretomes of *C. camelliae*, *B. cinerea* and *S. sclerotiorum* were annotated using BLASTP alignments and enzyme code information. Proteins were then sorted into 32 protein categories (Appendix 9.12).

BLASTP was used to compare the similarities and differences between the three secretomes. Secreted protein sequences from a single species were aligned to the secretomes of the other two species. For each protein sequence, the best alignments to each species were identified and amino acid identity information was extracted. The two amino acid identity scores associated with each query protein were used to plot comparative protein homology scores on a two-dimensional scatterplot. The same analysis was performed independently for each of the three fungal secretomes (Fig. 5.2).

Each of the three scatterplots produced a discernable positive slope from the lower left to the upper right. Query proteins that produced similar amino acid identity scores when aligned to the other two secretomes, mapped along the positive slope. Therefore, this slope can be viewed as a depiction of protein homology between the three fungal species, whereby proteins with high amino acid identity across all secretomes map to the top right of the scatterplot and proteins with low amino acid identity to both secretomes map towards the bottom left. Another feature of the scatterplots is the white space that runs parallel to the x and y axes between values 0

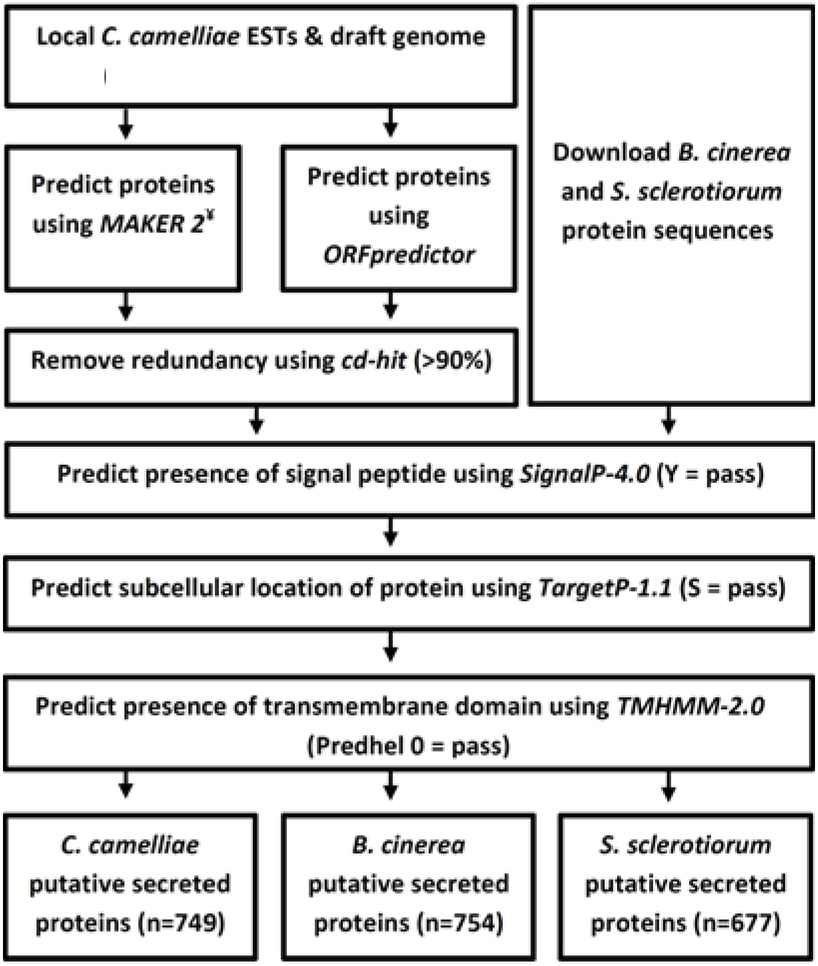

Figure 5.1. The *Ciborinia camelliae*, *Botrytis cinerea* and *Sclerotinia sclerotiorum* secretome prediction pipeline. For detailed descriptions of *C. camelliae* protein prediction and secretome predictions see sections 2.6.6 and 2.6.7.

and 20. No data points were plotted for values between 0% and 20% amino acid identity because alignments ≤ 20% amino acid identity are considered below the acceptable BLASTP alignment threshold. For the purpose of this analysis, alignments ≤ 20% amino acid identity were scored as 0% amino acid identity and were plotted accordingly.

The strongest cluster of proteins (indicated by the increased colour density) formed in the top right of each scatterplot, suggesting that a large proportion of the secreted proteins were highly homologous across all three fungal species. This region of high homology was normalized across all three scatterplots by adding a 'zone of conservation' represented by the square box (≥ 50% amino acid identity for alignments with both subject datasets).

A second densely coloured point routinely appeared at the x,y coordinates 0,0. These proteins had no discernable homology to the other secretomes and are likely to be either species-specific proteins or incorrectly predicted protein sequences. Overlaying the three scatterplots helped to decipher regions of high conservation (Fig 5.2D, arrow I), as well as regions of divergence (Fig 5.2D, arrows II & III). Interestingly, regions designated as 'II' and 'III' both fall within the protein homology trend line and could represent proteins that are under diversifying selection for *C. camelliae* and *B. cinerea* respectively.

5.2.4. Secretome annotation identifies conserved and divergent protein categories

Assigning annotations to each protein allowed further insights to be made into the makeup of each secretome. Between 76% to 80% of the proteins within each secretome were assigned to the predicted protein, CAZyme, oxidoreductase, small secreted protein (SSP) or protease categories. The remaining proteins were distributed among 27 additional categories (Appendix 9.12). The largest annotated category for each of the three secretomes was the predicted protein category, which accounted for

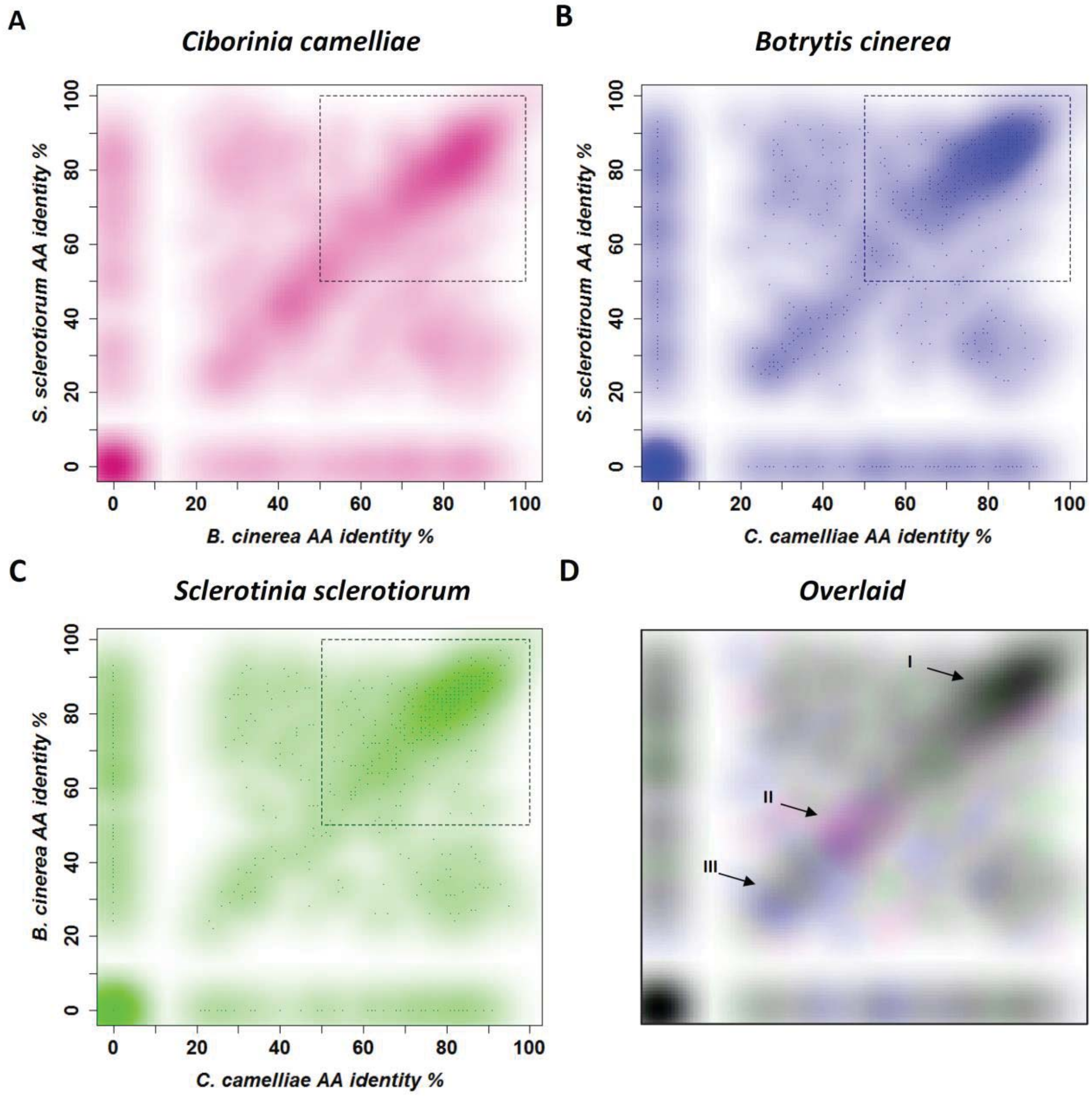

Figure 5.2. Reciprocal scatterplot comparisons of secretome proteins from **A,** *C. camelliae* (pink) **B**, *B. cinerea* (blue) and **C,** *S. sclerotiorum* (green). Proteins are plotted based on their BLASTP amino acid identity scores to homologous proteins identified in the two other fungal secretome datasets. The square box represents a 'zone of conservation' where query proteins have matches of ≥ 50% amino acid identity with proteins from both of the other two datasets. Overlaid scatterplots reveal areas of interest; 'I' indicates a cluster of highly conserved proteins, 'II' indicates a dominant cluster of *C. camelliae*-specific proteins and 'III' indicates a dominant cluster of *B. cinerea*-specific proteins.

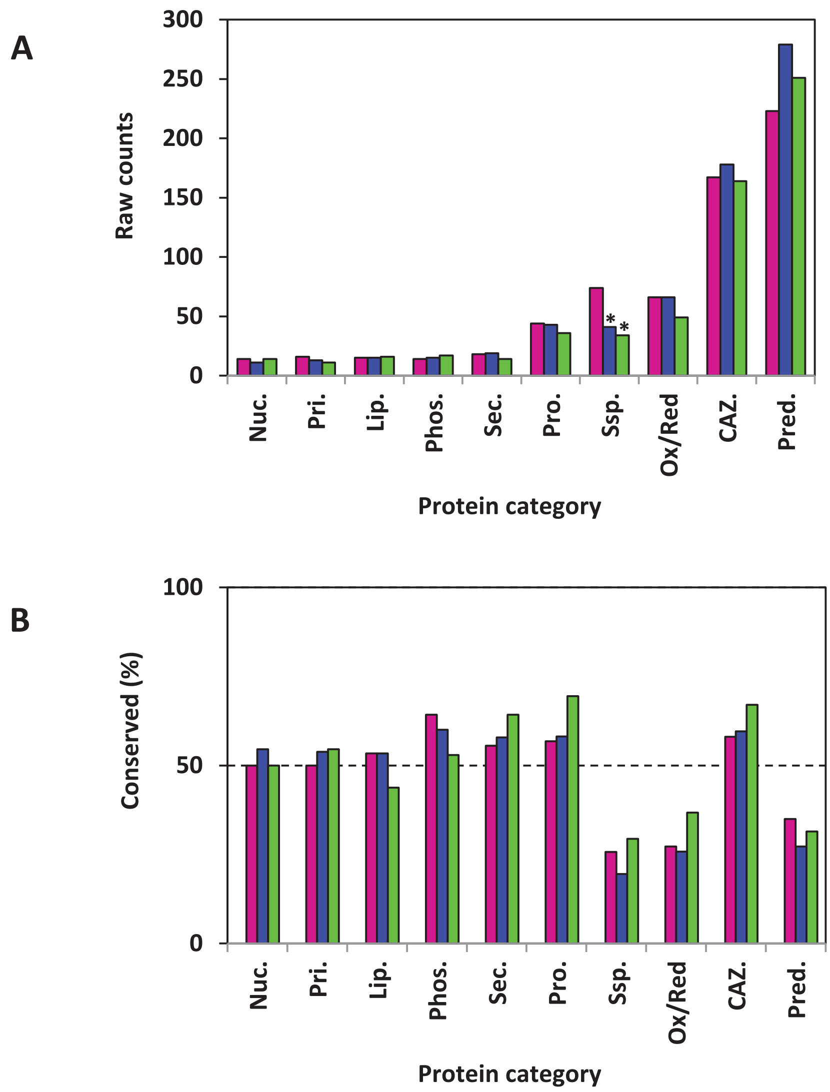

Figure 5.3. A comparison of secretome composition and conservation. *C. camelliae* proteins are represented by pink bars, *B. cinerea* blue bars and *S. sclerotiorum* green bars. **A**, A comparison of the composition of each annotated fungal secretome. Raw counts represent the number of genes in each category. The top ten most common categories are shown (a common category has ≥ 10 genes and has representative proteins in all 3 fungal species). * indicates statistical differences (Fisher's exact test with multiple testing adjustment) to *C. camelliae* raw counts (p = 0.05). **B,** A graphical comparison showing the degree of conservation within annotated secretome categories. Conserved (%) was calculated by counting the number of proteins in the 'zone of conservation' (see Fig 5.2), and dividing this number by the total number of proteins in that category. Conserved % values > 50 indicate protein conservation. Nuc. (Nucleic acid modification proteins), Pri. (Primary metabolism proteins), Lip. (Lipases), Phos. (Phosphatases), Sec. (Secondary metabolism proteins), Pro. (Proteases), SSP. (Small secreted proteins), Ox/Red. (Oxidoreductases), CAZ. (Carbohydrate active enzymes) and Pred. (Predicted proteins).

30 to 35% of each secretome (Fig. 5.3A). Predicted proteins generally refer to proteins that have been predicted from genome sequence information and have not yet been assigned a function. The second largest category was the carbohydrate active enzymes (CAZymes) category, which accounted for 20 to 25% of each secretome. Unlike the predicted protein category, the CAZymes appear to be highly conserved in all three fungal species and are abundant within the zone of conservation (Fig. 5.3B & Appendix 9.13). The third and fourth largest categories are the oxidoreductase and SSP categories, respectively. These categories accounted for 5 to 10% of each secretome. Interestingly, *C. camelliae* had significantly more SSPs as compared to *B. cinerea* and *S. sclerotiorum*. Both oxidoreductase and SSP categories are generally not well conserved between the three species. The fifth largest category is the protease category which also accounts for around 5% of each secretome. Like the CAZymes, the proteases appear to be well conserved in all three secretomes (Fig. 5.3B).

The CAZyme, oxidoreductase, SSP and protease categories were split into subcategories for more detailed characterization (Fig 5.4). The majority of CAZymes (69 to 74%) belonged to the glycosyl hydrolase subcategory which includes enzymes involved in the breakdown of complex carbohydrates like cellulose and hemicellulose. The number of carbohydrate esterase proteins were higher in *B. cinerea* (n = 32) as compared to *C. camelliae* (n = 22) and *S. sclerotiorum* (n = 23).

B. cinerea carbohydrate esterases were not well represented in the zone of conservation (Fig 5.5) and appear to contribute to one of the main differences observed in the overlaid scatterplot analysis (Fig 5.2D, arrow III and Appendix 9.13). The small numbers of polysaccharide lyase enzymes detected were highly conserved across all three species, which may indicate a common role for these enzymes in necrotrophic secretome biology. Strikingly, *S. sclerotiorum* had the strongest CAZyme protein conservation scores for all 5 of the analyzed subcategories (Fig. 5.5).

The well conserved group of protease enzymes identified in each secretome, was dominated by the serine protease subcategory. *C. camelliae* and *B. cinerea* had markedly similar protease repertoires whereas *S. sclerotiorum* had reduced numbers of serine and aspartate proteases and a slightly more diverse range of metalloproteases.

A considerable amount of variation was observed within the oxidoreductase subcategories for each species. The dominant alcohol oxidoreductase and oxygenase subcategories varied in their counts between the three species and were not very well conserved. Like the *B. cinerea* carbohydrate esterases, *B. cinerea* oxygenases contribute to the major cluster difference identified in the overlaid scatterplot (Fig. 5.2D, arrow III and Appendix 9.13), suggesting that *B. cinerea* oxygenases may be undergoing diversifying selection.

The most striking difference between the secretomes of all three species appears within the SSP category. SSPs with ≥ 10% cysteine composition were significantly more abundant within the *C. camelliae* secretome. Interestingly, the small numbers of *B. cinerea* and *S. sclerotiorum* proteins within the same category were well conserved between each other (Fig. 5.4). *C. camelliae* SSPs with ≥8% cysteine content were the main group of proteins contributing to the *C. camelliae*-specific cluster identified in the overlaid scatterplot (Fig. 5.2D, arrow II and Appendix 9.13). Significantly more SSPs with 4 – 5.9% cysteine content were present in the *B. cinerea* and *S. sclerotiorum* secretomes as compared to the *C. camelliae* secretome. This subcategory of SSPs is not well conserved, and may include putative effector candidates that have a species-specific role in *B. cinerea* and *S. sclerotiorum*.

5.2.5. Phylogenetic analysis reveals a conserved family of small secreted proteins that appear to be under diversifying selection in *Ciborinia camelliae*.

To further study the relationships between the SSPs of these three necrotrophic fungi, a cladogram was built based on an alignment of all 149 SSPs (Fig. 5.6). Not all of the SSPs were able to be aligned due to large differences in amino acid composition. However, a highly supported clade of 49 proteins emerged from the cladogram, with 47 proteins belonging to *C. camelliae*, 1 to *B. cinerea* and 1 to *S. sclerotiorum*. Based on

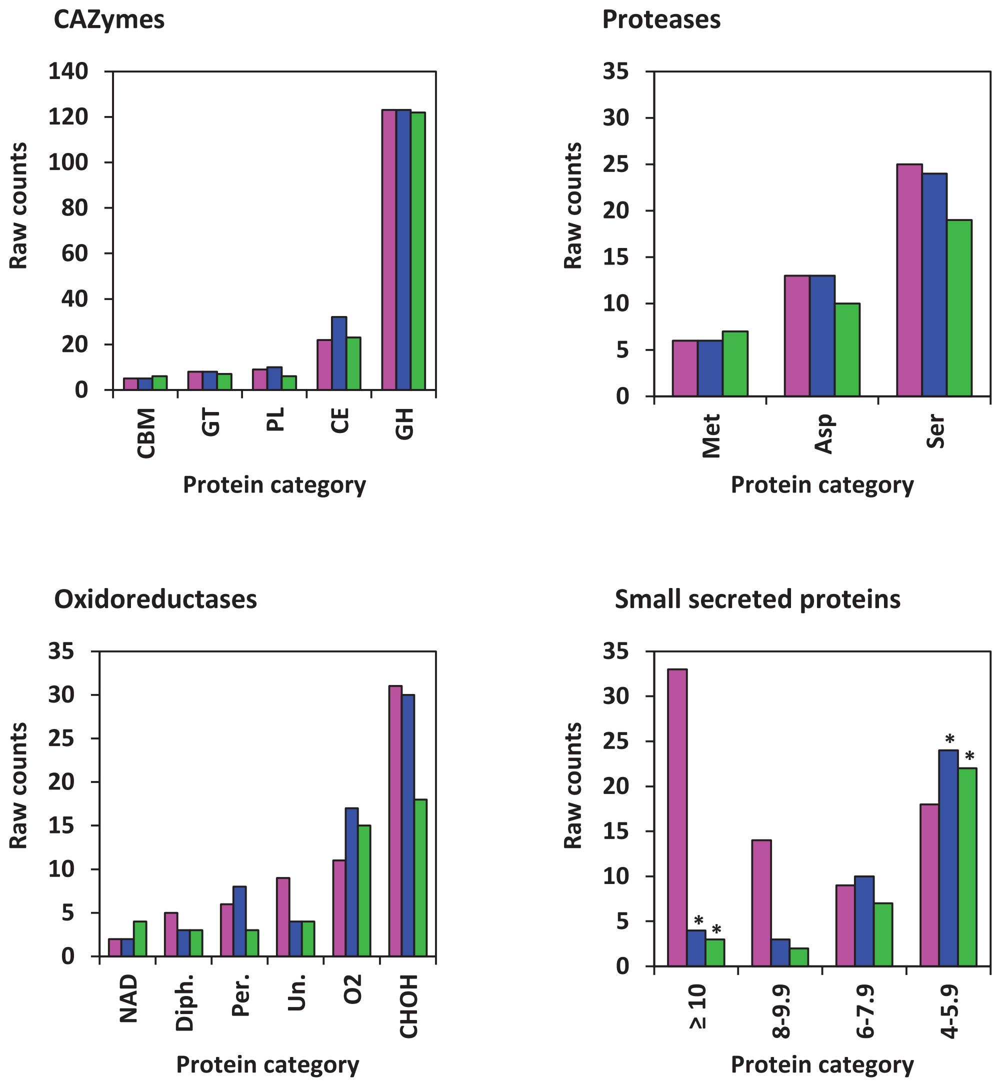

Figure 5.4. Analysis of the composition of the four most common secretome protein categories (excluding predicted proteins). *C. camelliae* proteins are represented by pink bars, *B. cinerea* blue bars and *S. sclerotiorum* green bars. CBM (Carbohydrate binding module), GT (Glycosyl transferase), PL (Polysaccharide lyase), CE (Carbohydrate esterase), GH (Glycosyl hydrolase), Met (Metalloprotease), Asp (Aspartate protease), Ser (Serine protease), NAD (NADH/NADPH oxidoreductase), Diph. (Diphenol oxidoreductase), Per. (Peroxidase), Un. (Uncategorized oxidoreductase), O2 (Oxygenase), CHOH (Alcohol oxidoreductase). Small secreted proteins are categorized based on the cysteine residue percentage present in their peptide sequence. * indicates statistical differences (Fisher's exact test with multiple testing adjustment) to *C. camelliae* raw counts (p = 0.05).

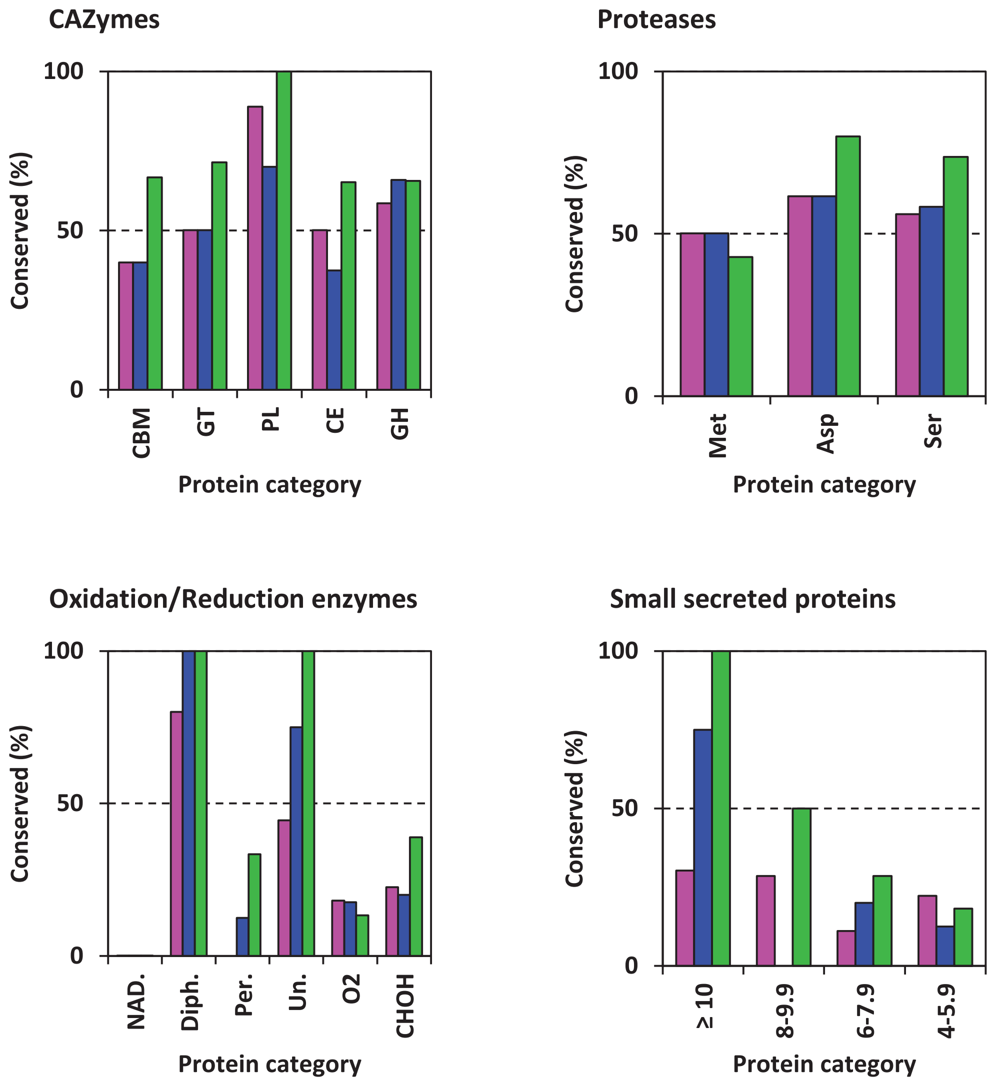

Figure 5.5. Analysis of the conservation of subcategories within the four most common secretome protein categories (excluding predicted proteins). *C. camelliae* proteins are represented by pink bars, *B. cinerea* blue bars and *S. sclerotiorum* green bars. Conserved (%) was calculated by counting the number of proteins in the 'zone of conservation' (see Fig 5.2), and dividing this number by the total number of proteins in the same subcategory. Conserved % values > 50 indicate protein conservation. CBM (Carbohydrate binding module), GT (Glycosyl transferase), PL (Polysaccharide lyase), CE (Carbohydrate esterase), GH (Glycosyl hydrolase), Met (Metalloprotease), Asp (Aspartate protease), Ser (Serine protease), NAD (NADH/NADPH oxidoreductase), Diph. (Diphenol oxidoreductase), Per. (Peroxidase), Un. (Uncategorized oxidoreductase), O2 (Oxygenase), CHOH (CH-OH oxidoreductase). Small secreted proteins are categorized based on the cysteine residue percentage present in their peptide sequence.

their unique identification numbers the *C. camelliae* members were able to be confirmed as those proteins that contribute to the *C. camelliae* dominant cluster observed previously in the secretome (Fig. 5.2D, arrow II).

Mining the *C. camelliae* genome for homologs of this protein family identified an additional 27 proteins. Due to the high conservation of their sequences, coding sequences for all 74 proteins were able to be predicted. CcSSP49 was identified as a duplicate of CcSSP17. This protein had been missed during redundancy processing due to the inclusion of an intron within its sequence. In total, 73 unique coding sequences belonging to this protein family were identified in *C. camelliae*. Protein sequence length ranged from 83 to 118 amino acids with a median length of 98 amino acids (Appendix 9.15). Reciprocal analyses in the *B. cinerea* and *S. sclerotiorum* genomes confirmed that only single copy homologs of this conserved gene family existed within these two species.

A total of 72 of the 73 *C. camelliae* secretome SSPs were detected as ESTs in the transcriptome, indicating that they were expressed during infection. EST abundance measurements varied for each individual protein (Appendix 9.15), but did not correlate with the phylogenetic relationship of the proteins (data not shown). Interestingly, both the *B. cinerea* and *S. sclerotiorum* single copy homologs have previously been reported as being expressed during the onset of disease in *Lactuca sativa* (lettuce) and *Helianthus annuus* (sunflower) respectively (Cremer et al., 2013; Guyon et al., 2014).

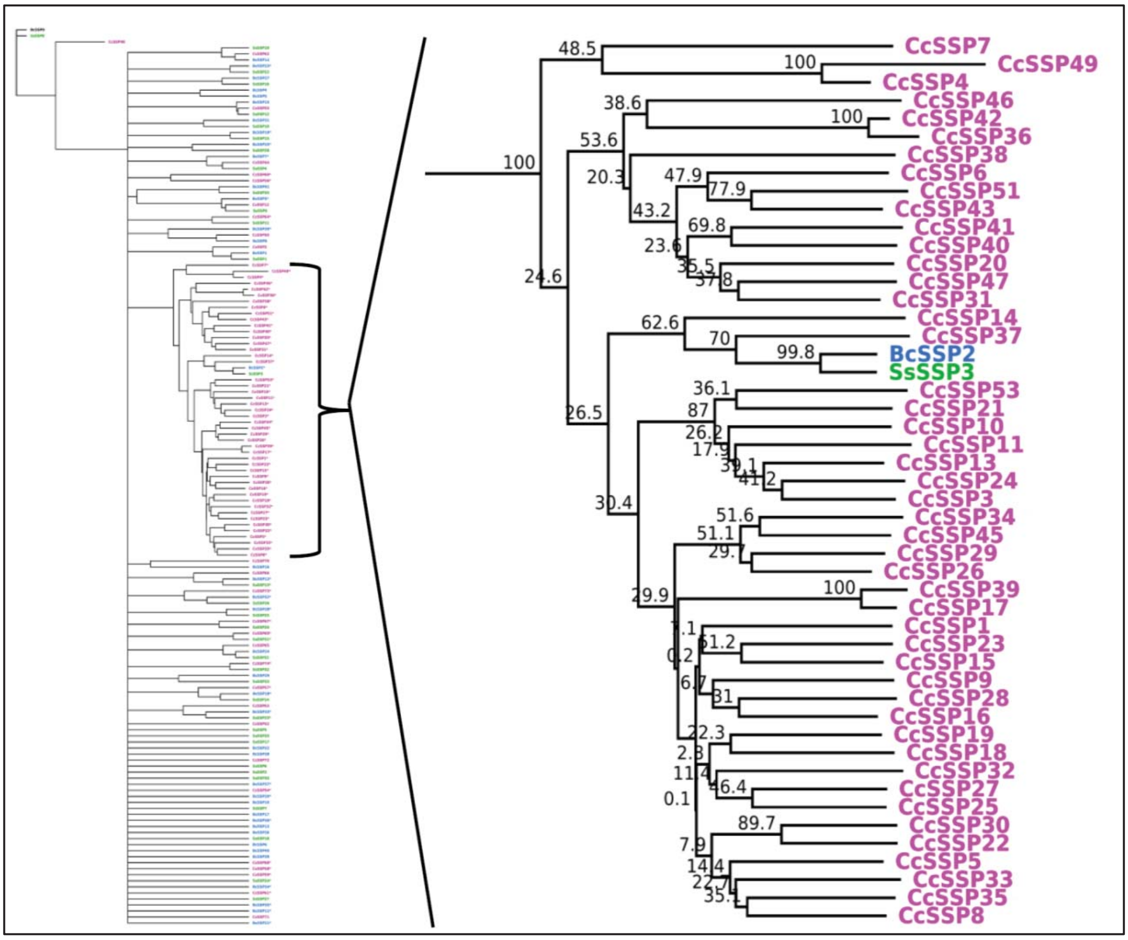

Figure 5.6. A cladogram of the 149 small secreted proteins (SSPs) from *Ciborinia camelliae*, *Botrytis cinerea* and *Sclerotinia sclerotiorum*. The expanded region represents a homologous family (> 41% amino acid identity across all members) of SSPs. Published *B. cinerea* (Cremer et al., 2013) and *S. sclerotiorum* RNA-seq data (Guyon et al., 2014) indicate that BcSSP2 and SsSSP3 proteins are expressed during infection. SSPs were aligned in Geneious™ using CLUSTALW and the phylogenetic tree was constructed using the PHYML plugin from 1000 bootstrap samples.

5.3. Discussion

The fungal secretome consists of a diverse range of proteins that all have characteristic N-terminal signal peptides. The signal peptide directs the translated protein to the endoplasmic reticulum. Following signal peptide cleavage, the mature protein is exported out of the cell via the golgi apparatus (Lippincott-Schwartz et al., 2000). The presence of a signal peptide is a key element in predicting secreted proteins and has led to the development of bioinformatic tools that specialize in this area (Emanuelsson et al., 2000; Petersen et al., 2011). Coupled with the increased availability of genomic data, these tools are commonly being used to predict the secretomes of prokaryotic and eukaryotic organisms (Nielsen et al., 1997). This section discusses the secretome prediction results for three related fungal necrotrophic phytopathogens, *C. camelliae*, *Botrytis cinerea* and *Sclerotinia sclerotiorum*. The composition of each secretome is compared, with a focus on identifying conserved and diversifying secretome proteins. The discovery of a large family of *C. camelliae*-like small secreted proteins (CCL-SSPs) highlights the effectiveness of this secretome prediction process for identifying biological differences across closely related species.

5.3.1. Validating the secretomes of *Ciborinia camelliae*, *Botrytis cinerea* and *Sclerotinia sclerotiorum*

The accuracy of the *C. camelliae* secretome is highly dependent on the accuracy of the preceding protein prediction. A total of 14711 non-redundant *C. camelliae* protein coding sequences were predicted using a split bioinformatic pipeline (Fig. 5.1). This strategy utilized *ab initio* prediction software (Stanke et al., 2004; Holt & Yandell, 2011) as well as software that utilized transcriptome and genomic data (Min et al., 2005; Holt & Yandell, 2011). Due to the absence of an autonomous *C. camelliae* genome/proteome, predicted *C. camelliae* proteins were validated using homology-based methods. BLASTP alignments of a subset (10%) of the predicted proteins to the Genbank non-redundant protein database showed that predicted proteins aligned best with proteins of fungal origin (71%) (Appendix 9.10A). However, a total of 27% of predicted *C. camelliae* proteins did not align to any known proteins in the Genbank non-redundant protein database, indicating that a portion of the predicted proteins are either incorrectly predicted or are not represented in the database. Previous reports suggest a total of 14% of *B. cinerea* predicted proteins are thought to be species-specific (Amselem et al., 2011). Therefore, it is probable that a significant portion of the predicted *C. camelliae* 'no hit' proteins are also species-specific.

Alignment of *C. camelliae* CCL-SSP family members back to the *C. camelliae* draft genome uncovered an example of an intron-containing-predicted protein (CcSSP47). Accurate intron prediction is a major challenge for eukaryotic protein prediction software (Yandell & Ence, 2012) and is likely to be a source of error within the *C. camelliae* predicted protein dataset.

The accuracy of the secretome prediction pipeline was validated through comparisons with previously published *B. cinerea* and *S. sclerotiorum* secretome data. A total of 745 secreted proteins were recently predicted for the *S. sclerotiorum* secretome (Guyon et al., 2014), which is slightly higher than what is reported here (*n* = 678). Guyon et al. focused their study on secreted proteins expressed *in planta* (SPEPs) which accounted for 65% (*n* = 486) of their total secretome dataset. A total of 75% of the SPEP secretome was identical in composition to the *S. sclerotiorum* secretome predicted here. Closer inspection of the Guyon et al., data showed that peptide sequences as low as 2 AAs in length were considered as independent counts, whereas the dataset presented here only considered peptide sequences > 89 AA. This discrepancy may account for part of the 25% difference in sequence composition between the two datasets. In addition, the frequency of SSPs (< 300 AA) within *B. cinerea* and *S. sclerotiorum* secretomes was compared. A total of 521 *B. cinerea* and 363 *S. sclerotiorum* small secreted proteins (< 300 AA) were reported in an alternative study (Amselem et al; 2011). Our estimation of 312 and 267 is much lower but supports the finding that *B. cinerea* has a higher number of SSPs than *S. sclerotiorum*. These two examples exemplify the difficulty associated with comparing predicted fungal secretomes that are derived using slightly different parameters and cutoff thresholds.

An alternative approach was used to validate the secretome prediction pipeline utilizing three published *B. cinerea* secreted proteome data sets (Shah et al., 2009; Espino et al., 2010; Gonzalez-Fernandez et al., 2013). Although each published *B.*

cinerea secreted proteome was sampled from slightly different *in vitro* culture conditions, consistent comparisons were observed (Appendix 9.12). The *B. cinerea* secretome that was predicted here was shown to include more than 80% of the published *B. cinerea* secreted proteome. The remaining 20% may represent proteins that have not been predicted using bioinformatic tools or proteins that are specifically expressed *in vitro* as opposed to *in planta*.

One of the main objectives of studying the *C. camelliae* secretome was to identify putative fungal effector proteins. The host-immune suppressing protein SSITL (SS1G_14133) of *S. sclerotiorum* (Zhu et al., 2013) was successfully predicted using the secretome prediction pipeline (Fig. 5.1), as were the two *S. sclerotiorum* necrosis and ethylene-like inducing proteins (NLP) SsNEP1 (SS1G_03080) and SsNEP2 (SS1G_11912) (Dallal et al., 2010). The *B. cinerea* NLP proteins, BcNEP1 (BC1G_06310) and BcNEP2 (BC1G_10306) (Staats et al., 2007) were also successfully predicted, as was the *B. cinerea* cerato-platanin HR-inducing protein, BcSpl1 (BC1G_02163) (Frías et al., 2011). Therefore, the described secretome prediction pipeline successfully targets effector proteins of *S. sclerotiorum* and *B. cinerea*. Furthermore, their discovery validates the use of the same prediction pipeline for effector discovery in *C. camelliae*.

5.3.2. Two-dimensional scatterplot analysis enables visual comparison of related fungal secretomes.

To discern evolutionary differences and similarities between the secretomes of *C. camelliae*, *B. cinerea* and *S. sclerotiorum*, protein homology was analyzed using two-dimensional scatterplots (Fig. 5.2). Spatial clustering of proteins allowed for an additional level of secretome characterization. Proteins that mapped to the positive slope line were interpreted as being either highly conserved across all species (≥ 50% amino acid identity for alignments with both subject datasets) or changing in the query species (< 50% amino acid identity for alignments with both subject datasets). Focusing specifically on these sets of proteins allowed inferences to be made about what groups of proteins are core to the secretomes of these three necrotophic fungi and what groups are more specific to each species.

Additional spatial clusters were observed that represent alternative evolutionary scenarios. Many fungal effectors are thought to be species or lineage-specific in nature as they are constantly evolving to maintain function within their host (Kombrink & Thomma, 2013). Therefore, species-specific effectors would likely map to the scatterplot x, y coordinates 0, 0. This scatterplot position could also represent incorrectly predicted proteins, or proteins whose homologs were not predicted by the secretome pipeline.

Proteins that were conserved in 2 of the 3 species clustered towards the top left and bottom right corners of the scatterplots. Clusters that fit this description were clearly distinguishable in each scatterplot (Fig. 5.2). Quantitative analysis of the number of homologous genes within clusters of this type may provide evidence for taxonomic relationships of the analyzed species. Indeed, comparatively larger clusters were visible for reciprocal *B. cinerea*/*S. sclerotiorum* comparisons as compared to *B. cinerea*/*C. camelliae* or *S. sclerotiorum*/*C. camelliae* comparisons, suggesting that *B. cinerea* and *S. sclerotiorum* secretomes have proportionally higher numbers of protein homologs (Fig. 5.3). This type of cluster may also include proteins that are shared due to similarities in fungal pathogenicity. For example, *B. cinerea* and *S. sclerotiorum* may have homologous proteins specifically associated with their host-generalist lifestyles that are absent in the host-specialist *C. camelliae*.

5.3.3. CAZymes and proteases are highly conserved in all three secretomes

Protein annotation was used to further characterize proteins that make up the secretomes of *C. camelliae*, *B. cinerea* and *S. sclerotiorum.* Of particular interest were those proteins that mapped within the 'zone of conservation' (≥ 50% amino acid identity for alignments with both subject datasets).

Enzymes involved in carbohydrate modification have previously been reported to be key components in necrotrophic pathogenicity (Bellincampi et al., 2014). The results presented here support this finding, as CAZymes are highly abundant in all three secretomes and are also well represented in the 'zone of conservation' (Figs. 5.3 &

5.5). Many CAZymes occur as multiple isoforms, which is thought to provide greater flexibility to pathogens that have several hosts (Keon et al., 1987). Five *B. cinerea* endo-polygalacturonases have been reported to differ in their necrotizing activity on different host plants (Kars et al., 2005). Furthermore, analysis of several *S. sclerotiorum* polygalacturonase genes, indicate different expression patterns during infection (Li et al., 2004; Kasza et al., 2004). Despite its host-specific lifestyle, *C. camelliae* secretes a similar number of conserved CAZymes as compared to the two host-generalists (Fig. 5.3). Whether *C. camelliae*'s homologous polygalacturonases are as diverse in their activity or expression patterns as the other two pathogens is still to be determined.

The carbohydrate esterase subgroup was the least conserved of the CAZymes (Fig. 5.3). This subgroup includes enzymes that act on xylan, pectin and cutin (Zhao et al., 2013). Carbohydrate esterases of *B. cinerea* were especially divergent and contributed to one of the major differential clusters observed during scatterplot analyses (Fig. 5.2D, arrow III and Appendix 9.13). Closer inspection of this divergent cluster of *B. cinerea* carbohydrate esterase proteins indicated that the majority of them are annotated as homologs of feruloyl esterases (data not shown). Feruloyl esterases catalyse the degradation of hydroxycinnamates, resulting in the degradation of lignocellulose linkages within the plant cell wall (Rumbold et al., 2003). It is not clear whether the divergence of this set of *B.* cinerea feruloyl esterases has any biological significance.

Glycosyl hydrolases catalyze the breakdown of complex carbohydrates (Davies & Henrissat, 1995). Interestingly, glycosyl hydrolases are more prominent in necrotrophs and hemibiotrophs as compared to biotrophs, which may be due to their primary role in host cell wall modification (Zhao et al., 2013). The CAZyme component of the secretomes of *C. camelliae*, *B. cinerea* and *S. sclerotiorum* was dominated by similar numbers of glycosyl hydrolase derivatives, confirming the abundance of these enzymes in these three necrotrophic fungi (Fig. 5.4).

The carbohydrate binding module, glycosyl transferase, and polysaccharide lyase subcategories made up a small portion of the CAZyme secretome group (Fig. 5.4). The polysaccharide lyases formed the most conserved CAZyme secretome group across the three species (Fig. 5.5). These enzymes are primarily involved in pectin degradation (van den Brink & de Vries, 2011). Conservation of these enzymes within all three secretomes suggests that they are an integral part of *C. camelliae*, *B. cinerea* and *S. sclerotiorum* biology.

Proteases were also well conserved across all three fungal secretomes (Fig. 5.3). It is estimated that 10% of the plant cell wall consists of protein (Carpita & Gibeaut, 1993), highlighting a role for secreted fungal proteases in plant cell wall degradation. Serine proteases were the most common form of protease identified in the secretomes of *C. camelliae*, *B. cinerea* and *S. sclerotiorum,* followed by aspartate proteases and metalloproteases (Fig. 5.4). Previous characterization of protease activity in *B. cinerea* culture filtrates suggested that aspartate proteases are the most active form (ten Have et al., 2004). Their high conservation within the secretomes of *C. camelliae*, *B. cinerea* and *S. sclerotiorum,* further supports the significance of this group of proteases (Fig. 5.5). Previous estimations of the number of aspartate proteases in *B. cinerea* (n = 13) and *S. sclerotiorum* (n = 8) (Amselem et al., 2011) matched well with what was predicted here (Fig. 5.4).

<u>5.3.4. Diversity exists within the oxidoreductase and small secreted protein categories of each fungal secretome.</u>

Despite the taxonomic proximity of *C. camelliae*, *B. cinerea* and *S. sclerotiorum* (Appendix 9.5) many of the predicted secretome proteins in one species did not have high amino acid conservation with secretome proteins in the other two species (Fig. 5.2). These differences were particularly prevalent when comparing the oxidoreductase and SSP secretome categories. The lack of conservation within a group of functionally similar proteins can be attributed to adaptive divergence (Gladieux et al., 2014). Furthermore, rapid fungal gene evolution is a hallmark of proteins that are involved in mediating host-pathogen interactions (Sperschneider et al., 2014). Based on the patterns of homology shown in the scatterplots (Appendix 9.13), the oxidoreductase and SSP secretome categories may contain examples of species-specific proteins that are undergoing adaptive divergence.

Oxygenase enzymes were abundant in *B. cinerea* but were not well conserved with the oxygenase enzymes of *C. camelliae* and *S. sclerotiorum* (Figs. 5.4 & 5.5). Identification of the spatial position of these enzymes in the original overlaid scatterplot indicates that they contribute to the diversifying cluster of *B. cinerea*-specific proteins (Fig 5.2D, arrow III). The expansion and diversification of oxygenases in *B. cinerea* may be an adaptive strategy against host-imposed oxidative stress. It is well recognized that *B. cinerea* and *S. sclerotiorum* can survive the plant HR, which includes the establishment of a high ROS environment *in planta* (Govrin and Levine, 2000; Thomma et al.,2001). Therefore, the adaptation of ROS scavenging oxidoreductase enzymes to this type of environment may improve the survival of these pathogens. Oxidoreductase diversity across these three species may be host-driven, although the ultimate reason for diversification of this group of proteins is still to be determined.

Perhaps the most striking difference between the secretomes of *C. camelliae*, *B. cinerea* and *S. sclerotiorum* were the significantly variable SSP compositions (Figs. 5.3, 5.4 & Appendix 9.13). Compared to *B. cinerea* and *S. sclerotiorum*, the *C. camelliae* secretome contained twice as many SSPs including 10 fold more SSPs with > 10% cysteine content. Identification of the spatial position of the *C. camelliae* SSPs in the original overlaid scatterplot showed that they are the major contributing factor to the diversifying cluster of *C. camelliae*-specific proteins identified in the overlaid scatterplot (Fig. 5.2D, arrow II & Appendix 9.13).

5.3.5. Half of the small secreted proteins are homologous.

Phylogenetic analysis of the SSP categories identified a homologous family of *C. camelliae*-like small secreted proteins (CCL-SSPs) that were conserved in *C. camelliae* (*n* = 73), *B. cinerea* (*n* = 1) and *S. sclerotiorum* (*n* = 1) (Fig. 5.6). It is likely that the 73 *C. camelliae CCL-SSP* family members have undergone lineage-specific gene expansion, probably via gene duplication. Lineage-specific gene expansion within the genome of the wheat stem rust pathogen *Puccinia graminis* f. sp. *tritici* is thought to be driven by evolutionary adaptation to the host-pathogen interaction (Duplessis et al., 2011; Raffaele & Kamoun, 2012). Signatures of adaptive expansion have been utilized to predict fungal effector proteins in a recent bioinformatic strategy (Sperschneider et al., 2014). Therefore, it is possible that the expansion of CCL-SSPs observed in *C. camelliae* may be a result of host-driven selection pressure.

Previously characterized fungal effectors that retain conservation at the sequence level belong to the necrosis and ethylene-inducing peptide 1 (NEP1)-like protein (NLPs) family, the cerato-platanin protein family and the ECP2 family (Guyon et al., 2014). Notably, these effectors are usually associated with necrotrophic or hemibiotrophic pathogens and tend to function as host-cell death inducers, as opposed to plant immune system suppressors (Bailey, 1995; Staats et al., 2007; Dallal et al., 2010; Stergiopoulos et al., 2010; Frías et al., 2012). The ability of CCL-SSP family members to cause host-cell necrosis is addressed in the next chapter

5.4. Conclusions

Validation of the *C. camelliae*, *Botrytis cinerea* and *Sclerotinia sclerotiorum* secretomes suggested that over 80% of all secreted proteins were predicted for each species. Comparative secretome homology analysis using two-dimensional scatterplots provided an extra level of scrutiny when comparing the three fungal secretomes. Clusters of proteins that were highly conserved, or undergoing diversifying selection, were clearly distinguishable using the scatterplot method. Protein annotation allowed for in depth analysis of the components of each secretome resulting in the identification of the highly conserved CAZyme and protease categories, as well as the diversifying oxidoreductase and SSP categories. A large family of conserved SSPs were discovered in *C. camelliae* (*n* = 73), *B. cinerea* (*n* = 1) and *S. sclerotiorum* (*n* = 1). The functional characterization of this family of *C. camelliae*-like small secreted proteins (CCL-SSPs) is the subject of the next chapter of this thesis.

6. *In silico* and functional characterization of a conserved family of small secreted proteins from *Ciborinia camelliae*, *Botrytis cinerea* and *Sclerotinia sclerotiorum*

6.1. Introduction

Fungal effector proteins act to promote fungal infection by subverting the host plant's natural defense mechanisms (Jones & Dangl, 2006). *In silico* strategies have previously been employed to characterize fungal effector protein families. Effectors are often described as being in an 'arms race' with their host targets (Jones & Dangl, 2006). Therefore, signs of adaptive selection pressure are often maintained within their nucleotide sequence (Sperschneider et al., 2014). Adaptive selection pressure can also lead to gene family expansions (Gladieux et al., 2014). For example, the ToxB fungal effector protein is predicted to have recently undergone gene duplication in *Pyrenophora tritici-repentis* (Martinez et al., 2004). Therefore, secreted protein sequence information can be analyzed *in silico* for effector-like characteristics.

The biological activity of putative fungal effectors can only be truly determined by examining their behavior *in vivo*. Gene expression studies have been used to analyze the temporal expression patterns of fungal effectors (Marshall et al., 2011). Correlation of putative fungal effector gene expression with stages of disease development can provide hints as to their role *in planta*. The function of a putative effector protein can be elucidated by selectively applying it to the host tissue and observing the host-response. Transient expression (Ma et al., 2012) or recombinant protein infiltration experiments can determine whether the putative effector protein is involved in host-cell necrosis (Liu et al., 2009, Liu et al., 2013), is acting as an avirulence factor (Lauge & De Wit, 1998), or is acting to suppress the host immune system (Dou & Zhou, 2012).

Ciborinia camelliae, *Botrytis cinerea* and *Sclerotinia sclerotiorum* secretome analysis predicted a conserved family of *C. camelliae*-like small secreted proteins (CCL-SSPs). These CCL-SSP homologs appear to have undergone lineage-specific expansion in *C. camelliae*, but remain as single homologs in *B. cinerea* and *S. sclerotiorum.* Proteins within this family exhibit features of fungal effector proteins, including high cysteine content and short peptide sequences (< 300 AA) (De Wit et al., 2009). In this chapter, the ability of these CCL-SSPs to exhibit functional properties of fungal effector molecules is assessed using similar methods to those described above.

6.2. Results

<u>6.2.1. *In silico Ciborinia camelliae*-like small secreted protein (CCL-SSP) characterization reveals conserved primary protein structure</u>

Protein family members from *C. camelliae* (*n* = 73), *Botrytis cinerea* (*n* = 1) and *Sclerotinia sclerotiorum* (*n* = 1) were further characterized using *in silico* analysis. As determined previously (Fig. 5.1), all protein family members had a predicted N-terminal signal peptide (Fig. 6.1). The predicted signal cleavage site was followed by a domain containing 5 conserved cysteine residues. This domain is the basis of the MEME predicted (http://meme.nbcr.net/meme/) conserved amino acid motif 'CTYCQCLFPDGSHCC' and localizes within the first exon of each *CCL-SSP* gene. The second exon is more variable in sequence composition and includes a variable central region that appears to be under positive selection (Fig. 6.1). The protein family's C-terminal region also appears to be under positive selection and varies in length and composition (Appendix 9.16). Interestingly, each of the 10 cysteine residues appear to be located in regions that are not predicted to be undergoing positive selection, suggesting a conserved structural role for these residues (Fig. 6.1). All 10 of the cysteine residues were predicted to form disulphide bonds and predicted connectivity patterns were conserved for all 75 proteins. Of particular significance is the prediction of a Y/F/WxC putative effector motif (Godfrey et al., 2010), present in 70 of the 75 CCL-SSPs (Fig. 6.1). This motif was previously characterized in putative fungal effector proteins of *Blumeria graminis* (Godfrey et al., 2010).

<u>6.2.2. CCL-SSP homologs are present across fungal classes but are confined to species with necrotrophic lifestyles</u>

To search for additional cross-species homologs, all 75 of the CCL-SSPs were aligned to the Genbank non-redundant protein database using BLASTP. A total of 15 additional fungal species were identified as having 1 or more protein homologs to this CCL-SSP family (Table 6.1). All identified species belonged within one of four taxonomical classes; the Leotiomycetes, Dothideomycetes, Eurotiomycetes or Sordariomycetes. Comparatively, *C. camelliae* had by far the largest number of CCL-SSP family members (*n* = 73), with the next largest number belonging to *Cochliobolus miyabeanus* (*n* = 4) and *Cochliobolus heterostrophus* (*n* = 4). Except for *C. camelliae,* all species within the

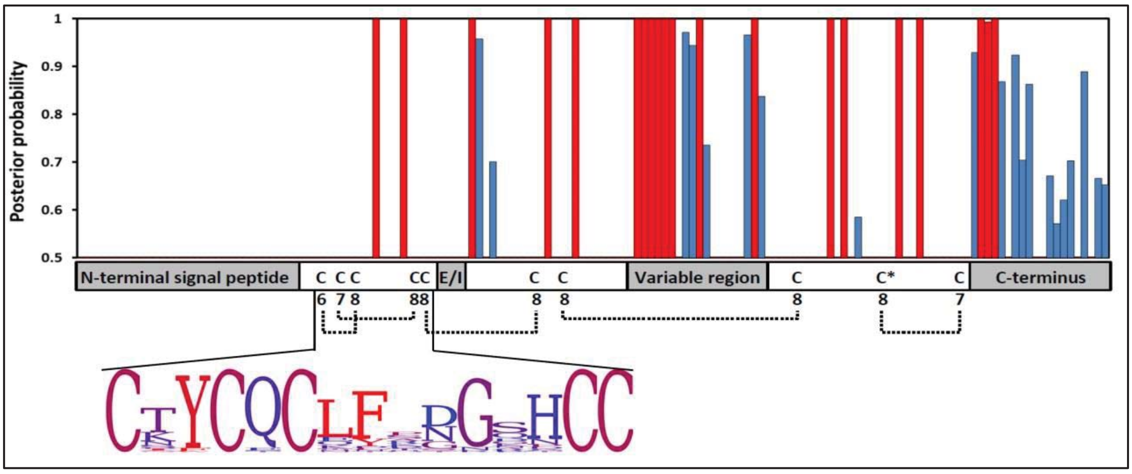

Figure 6.1. *In silico* characterization of the conserved *Ciborinia camelliae*-like small secreted protein (CCL-SSP) family (*n* = 75). Each protein consists of 10 conserved cysteine residues, an N-terminal signal peptide, two exons (E/I = exon/intron boundary), a variable central domain and a variable C-terminus. PAML was used to score the probability that each amino acid residue was under non synonymous (positive) selection (Red bars = P ≥ 0.01, blue bars = P ≥ 0.5) A single Y/F/WxC motif was identified in 70/75 proteins and is associated with the ninth cysteine residue (*). All cysteine residues are predicted to form disulphide bonds using *DiSULPHIND*, with dashed lines indicating the disulphide bond connectivity pattern prediction (0 = low to 9 = high). MEME was used to predict the conserved motif 'CTYCQCLFPDGSHCC', which is associated with the cysteine residues within the first exon.

Table 6.1. Characterization of CCL-SSP family homologs across different taxonomic classes of the fungal kingdom[A].

Species	Class[B]	No of homologs	AA identity (%)[C]	No. of cysteines	Fungal lifestyle	Genbank accessions
Ciborinia camelliae	Leot.	73	41–54	10	Necrotrophic (Kohn & Nagasawa, 1984)	N/A
Botrytis cinerea	Leot.	1	76	10	Necrotrophic (Amselem et al., 2011)	*XP_001559885*
Sclerotinia sclerotiorum	Leot.	1	75	10	Necrotrophic (Amselem et al., 2011)	*XP_001593146*
Sclerotinia borealis	Leot.	1	59	10	Necrotrophic (Mardanov et al., 2014)	*ESZ96062*
Aspergillus flavus	Euro.	1	60	10	Necrotrophic (Kishore et al., 2005)	*XP_002382650*
Aspergillus niger	Euro.	1	56	10	Necrotrophic (Kishore et al., 2005)	*XP_003188958*
Aspergillus kawachii	Euro.	1	56	10	Unknown[D]	*GAA85125*
Aspergillus oryzae	Euro.	1	51	11	Unknown[D]	*EIT77128*
Penicillium digitatum	Euro.	1	25	10	Necrotrophic (Marcet-Houben et al., 2012)	*EKV19894*
Cochliobolus miyabeanus	Doth.	4	22-52	8	Necrotrophic (Condon et al., 2013)	*EUC41471, EUC41469, EUC39656, EUC41470*
Cochliobolus sativus	Doth.	3	24-51	8	Necrotrophic (Condon et al., 2013)	*EMD63959, EMD63957, EMD63958*
Cochliobolus heterostrophus	Doth.	4	23-52	8	Necrotrophic (Condon et al., 2013)	*EMD93168, EMD85486, EMD93170, EMD93169*
Cochliobolus victoriae	Doth.	3	26-50	8	Necrotrophic (Condon et al., 2013)	*EUN20677, EUN20679, EUN20678*
Zymoseptoria tritici	Doth.	1	19	10	Hemibiotrophic (Brunner et al., 2013)	*XP_003855229*
Setosphaeria turcica	Doth.	2	26	9	Hemibiotrophic (Condon et al., 2013)	*EOA90575, EOA90576*
Colletotrichum gloeosporioides	Sord.	2	28-29	9/10	Hemibiotrophic (Gan et al., 2013)	*ELA33475, EQB51326*
Colletotrichum orbiculare	Sord.	2	20-21	11	Hemibiotrophic (Gan et al., 2013)	*ENH77728, ENH80832*
Fusarium pseudograminearum	Sord.	2	23	8	Necrotrophic (Desmond et al., 2005)	*EKJ69295, EKJ69294*

[A]Homologs are qualified by a BLASTP alignment E-value cutoff of ≥ 1e-03 to any member of the identified *C. camelliae* SSP family.

[B]Fungal classes are abbreviated as Leot. (Leotiomycetes), Euro. (Eurotiomycetes), Doth. (Dothideomycetes), and Sord. (Sordariomycetes).

[C]Pairwise amino acid identity as compared to the most ancestral CCL-SSP sequence in *C. camelliae* (CcSSP92).

[D]Sequenced *Aspergillus oryzae* and *A. kawachii* strains have been used in traditional Asian brewing techniques and it is unknown whether they occur naturally (Machida et al., 2008; Futagami et al., 2011).

Leotiomycetes and Eurotiomycetes had only one homolog, whereas the majority of species in the Dothideomycetes and Sordariomycetes had two or more. Pairwise amino acid identity was assessed for each homolog by comparison with CcSSP92 (Table 6.1), which is predicted to be the most ancestral *C. camelliae* CCL-SSP sequence based on its amino acid sequence conservation with BcSSP2 and SsSSP3 (Appendix 9.14). Interestingly, the CcSSP92 sequence has higher amino acid identity with CCL-SSP homologous in *B. cinerea, S. sclerotiorum, Aspergillus flavus, S. borealis, Aspergillus niger,* and *Aspergillus kawachii* than it did with other *C. camelliae* CCL-SSPs (Table 6.1). Homologs that belonged to pathogens with necrotrophic lifestyles were generally more similar to CcSSP92. When ≥ 3 homologs were present in one species, they were generally highly diverse in amino acid composition.

The number of cysteine residues identified in each protein also appeared to correlate with taxonomic class. Homologs from species within the Leotiomycetes and Eurotiomycetes had 10 cysteine residues (with the exception of *A. oryzae*) whereas homologs from the Dothideomycetes and Sordariomycetes had 8 to 11. *Colletotrichum gloeosporioides* was the only species to have multiple isoforms with differing numbers of cysteine residues. An alignment of all known homologs (n = 105) indicated that cysteine residues located from position 2 to 8 were universally conserved within the CCL-SSP family (Appendix 9.16).

Not one biotrophic fungal species was identified as having homology to the CCL-SSP protein family (Table 6.1). With the exception of the domesticated species *A. kawachii* and *A.* oryzae, all of the fungal species have been described in the literature as having a necrotrophic life stage, suggesting that these CCL-SSPs may have a role in necrotrophic fungal biology.

6.2.3. Members of the *CCL-SSP* family share genomic loci.

Alignment of the 73 *C. camelliae CCL-SSP* coding sequences to the *C. camelliae* draft genome revealed localized clustering of 52% of the genes (Fig. 6.2A). Genes were considered to be clustered if they localized within 6 kb of each other and non-clustered

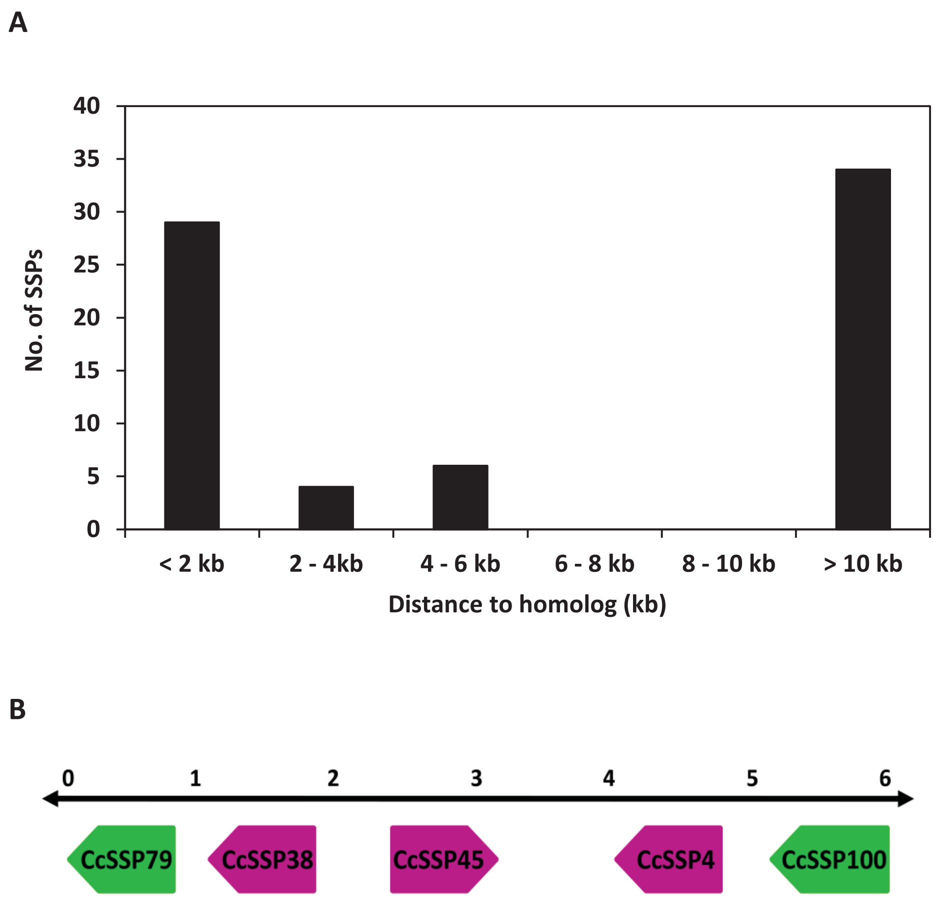

Figure 6.2. Clustering of 73 homologous *Ciborinia camelliae CCL-SSP* gene loci within the *C. camelliae* genome. **A**, A graphical representation of the proximal distance of homologous *CCL-SSP* genes from one another. **B**, An example of a single 6 kb locus from contig 302 (37309kb). Independently identified *C. camelliae CCL-SSP* gene homologs from the secretome (pink) and preceding genome mining process (green) cluster within the same 6 kb locus (see section 5.2.5).

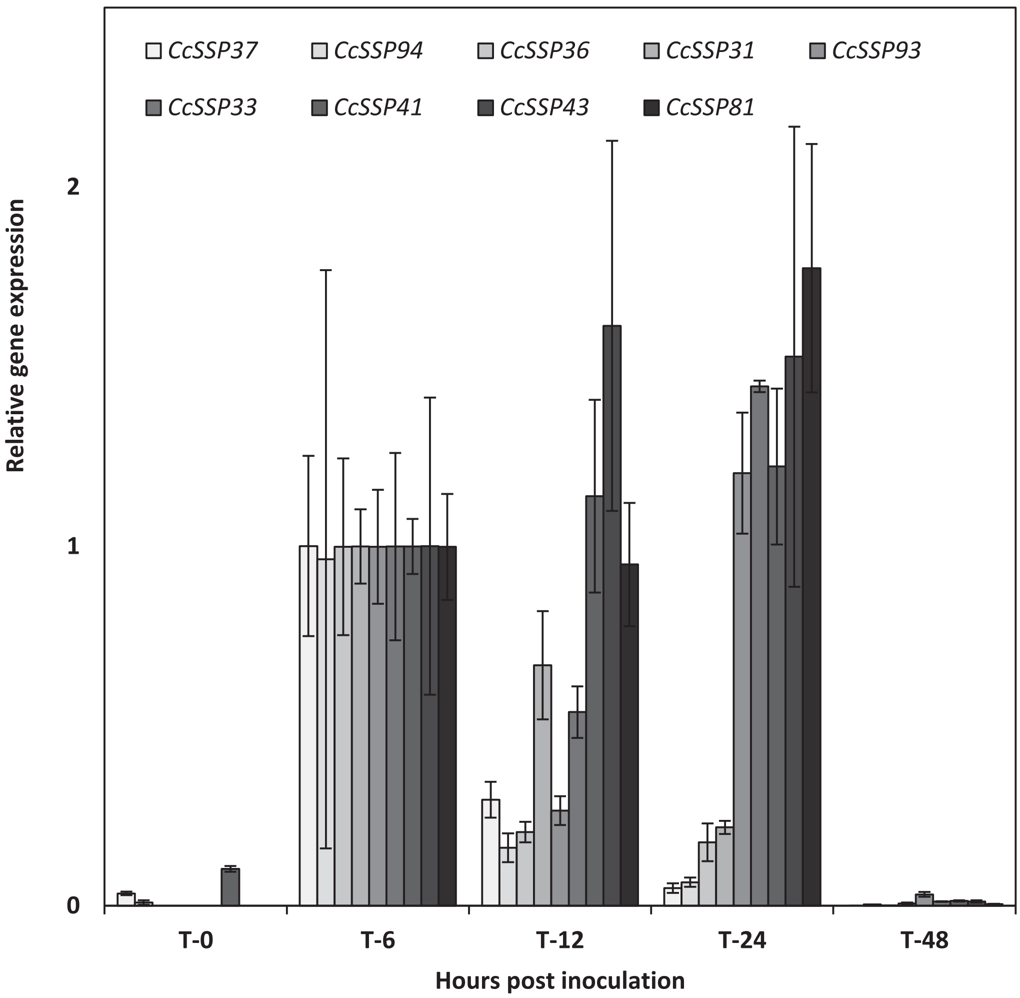

Figure 6.3. Quantitative real-time PCR data for a subset of 9 of the 73 *Ciborinia camelliae CCL-SSP* genes. All data were normalized to Cq (quantification cycle) values of the two fungal housekeeping genes NAD and TUB, which were shown to increase expression in parallel with fungal growth (Appendix 9.17). Relative expression data were normalized to T-6 to allow for comparisons between genes. Large biological variation in T-6 Cq values led to normalized relative expression values that were < 1.

if they were > 10 kb from each other. The majority of clustered genes localized within 2 kb of each other (74%) across 15 scaffolds. *C. camelliae CCL-SSP* genes that were predicted from the initial secretome data localized to the same genomic clusters as genes predicted from the follow-up genome mining screen described in section 5.2.5 (Fig. 6.2B).

6.2.4. *Ciborinia camelliae CCL-SSP* family members are expressed during pre-lesion development

RNA-seq data indicated that 72 out of 73 *C. camelliae CCL-SSP* genes were expressed during infection (Appendix 9.15). To further characterize the expression of these genes, temporal analysis was performed on 9 of the genes using qRT-PCR. The fungal housekeeping genes nicotinamide adenine dinucleotide (NAD) and tubulin (TUB) were selected as reference genes for qRT-PCR analysis. These two housekeeping genes were chosen because their expression levels increased in parallel with *C. camelliae in planta* growth (Appendix 9.17).

Immediately postinoculation (0 h), gene expression was low or non-existent for all 9 genes (Fig 6.3). Gene expression increased for all homologs by 6 h postinoculation (hpi), which coincides with ascospore germination and cuticle penetration (Fig 3.3A). From 6 to 24 hpi individual genes varied in their expression levels, with some consistently increasing, some remaining constant and others declining in expression. Of particular significance was the decline in expression of all genes by 48 hpi. During disease development, 48 hpi represents the period of lesion maturation and the on-set of host-cell necrosis (Fig 3.1). These data show that this sub-set of 9 *C. camelliae CCL-SSPs* are more highly expressed during the asymptomatic pre-lesion period of *in planta* development, suggesting that they may have a role in *C. camelliae* host-establishment.

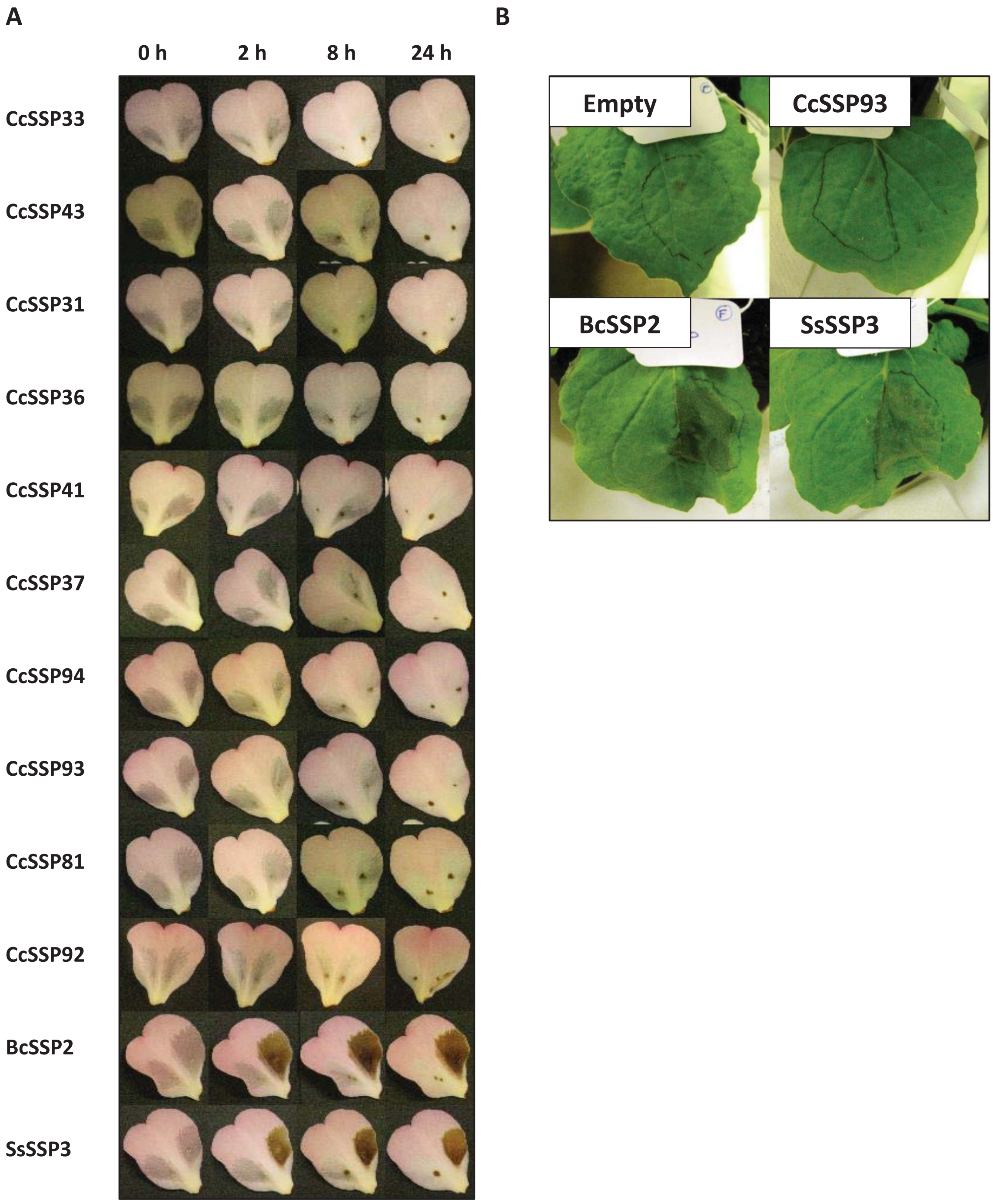

Figure 6.4. Functional assays using native recombinant *Ciborinia camelliae*-like small secreted proteins (CCL-SSPs). **A**, *Camellia* 'Nicky Crisp' petal tissue infiltrated with 'empty vector' culture filtrate (left petal lobe) and 12 individual recombinant proteins (right petal lobe) (n = 3). Photographs were taken at 0, 2, 8 and 24 h postinoculation. **B**, *Nicotiana benthamiana* leaf tissue infiltrated with culture filtrates containing 'empty vector', CcSSP93, BcSSP2 and SsSSP3 recombinant proteins at 48 h. All native *C. camelliae* CCL-SSP recombinant proteins failed to induce cell death in *N. benthamiana* within 48 h (photos not taken). Representative images are shown (n = 3).

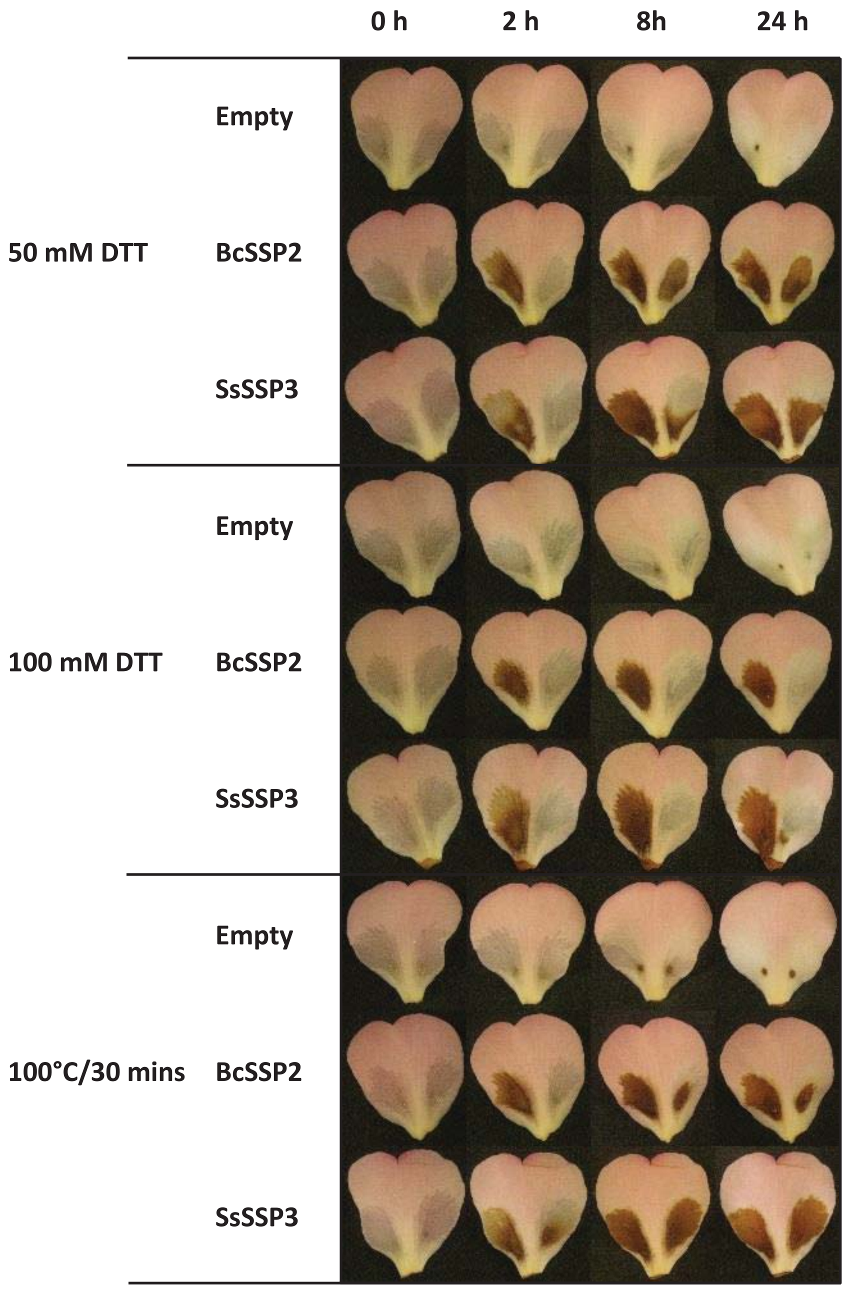

Figure 6.5. Functional stability of the BcSSP2 and SsSSP3 proteins. Culture filtrates were treated for 2 h with either 50 mM dithiothreitol (DTT), 100 mM DTT, or boiling for 30 mins. *Camellia* 'Nicky Crisp' petal tissue was infiltrated with untreated culture filtrate (left petal lobe) or treated culture filtrate (right petal lobe). Photographs were taken at 0, 2, 8 and 24 h postinoculation. Representative images are shown (*n* = 3).

<u>6.2.5. Recombinant *Botrytis cinerea* and *Sclerotinia sclerotiorum* CCL-SSP family members induce host-cell necrosis</u>

In order to gain insights into the cellular function of this family of CCL-SSPs, a sub-set of the CCL-SSP proteins were selected for recombinant protein expression using the *Pichia pastoris* eukaryotic protein expression system. This recombinant protein expression system was chosen over a prokaryotic system due to the assumption that higher eukaryotic protein modifications were likely to be important for correct CCL-SSP folding and function. Ten *C. camelliae CCL-SSP* genes, *CcSSP31*, *CcSSP33*, *CcSSP36*, *CcSSP37*, *CcSSP41*, *CcSSP43*, *CcSSP81*, *CcSSP92*, *CcSSP93*, *CcSSP94* and the single copy *CCL-SSP* genes from *B. cinerea* (*BcSSP2*) and *S. sclerotiorum* (*SsSSP3*) were chosen for cloning and recombinant protein expression. These ten *C. camelliae CCL-SSP* genes are spread across the phylogenetic spectrum of the *C. camelliae CCL-SSP* family and include the two homologs that share the greatest amino acid sequence conservation with BcSSP2 and SsSSP3 (Appendix 9.14).

Filter sterilized culture filtrates were collected for each *P. pastoris* recombinant protein strain and infiltrated into compatible *Camellia* 'Nicky Crisp' host tissue. All ten *C. camelliae* CCL-SSP homolog culture filtrates failed to stimulate a visible host response within 24 hpi (Fig. 6.4A). In contrast, BcSSP2 and SsSSP3 culture filtrates stimulated rapid host-cell necrosis from 2 hpi. Host-cell necrosis was specific to the infiltrated area. Infiltration of the same culture filtrate samples into petal tissue of the incompatible host *C. lutchuensis* produced a similar response, although BcSSP2 and SsSSP3-associated host-cell necrosis wasn't visible until 24 hpi (Appendix 9.20).

Culture filtrates were also inoculated into *Nicotiana benthamiana* leaf tissue. Interestingly, BcSSP2 and SsSSP3 culture filtrates induced a host-cell necrosis response in *N. benthamiana*, suggesting that the activity of these two proteins is conserved in taxonomically distinct host tissues (Fig 6.4B).

6.2.6. *BcSSP2* and *SsSSP3* are expressed in *Pichia pastoris* post-induction and are highly stable

The discovery of a phenotypic response to BcSSP2 and SsSSP3 culture filtrates meant that functional assays could be utilized to further characterize these two proteins. To test whether BcSSP2 and SsSSP3 proteins were responsible for the observed host-cell necrosis phenotype, samples of culture filtrate were collected at different time points post-induction. All culture filtrates collected more than 3 h post-induction stimulated host-cell necrosis (Appendix 9.21). Only culture filtrates that were immediately collected following the addition of induction media failed to stimulate a response, suggesting that the active component of each culture filtrate is accumulated under inducive conditions.

The same phenotypic assay was used to determine whether protein stability was important for maintaining the host-cell necrosis phenotype. To disrupt the conformation of BcSSP2 and SsSSP3 proteins, culture filtrates (including empty vector) were treated for 2 hours prior to inoculation with either 50 mM dithiothreitol (DTT), 100 mM DTT, or were boiled for 30 mins. Initially, culture filtrates containing 50 mM DTT were unable to induce host-cell necrosis. However, by 8 hpi host-cell necrosis had developed in BcSSP2 and SsSSP3-treated host tissue (Fig. 6.5). Increasing the DTT concentration to 100 mM resulted in a near total loss of the host-cell necrosis phenotype, although a small lesion was observed in SsSSP3-treated tissue at 24 h postinoculation. Boiling the BcSSP2 and SsSSP3 culture filtrates failed to completely eliminate the host-cell necrosis phenotype. Together these results suggest that the active component of the BcSSP2 and SsSSP3 culture filtrates is proteinaceous in nature. Furthermore, the active proteins within these culture filtrates are heat stable and are likely to have a robust structure.

6.2.7. Tagged recombinant CCL-SSPs are compromised in their ability to induce host-cell necrosis

The native recombinant proteins BcSSP2 and SsSSP3 induce host-cell necrosis. However, it is unclear whether the lack of necrosis from the native *C. camelliae* CCL-SSP proteins was due to a lack of synonymous function, or due to reduced concentrations of soluble protein as compared to BcSSP2 and SsSSP3. To facilitate protein detection and the determination of protein concentration, a c-Myc 6xHis-tag was included at the C-terminus of each protein by mutating the native stop codon and allowing transcription of the endogenous pPICZA c-Myc 6xHis-tag vector sequence (Appendix 9.19).

The presence of tagged *C. camelliae* proteins in culture filtrates was confirmed by western blot using antibodies raised against the C-terminal c-Myc tag (Appendix 9.22 & Fig. 6.6A). The seven tagged proteins, CcSSP43^{T}, CcSSP37^{T}, CcSSP93^{T}, CcSSP81^{T}, CcSSP92^{T}, BcSSP2^{T} and SsSSP3^{T} were present in detectable concentrations (Appendix 9.22). CcSSP33 ^{T}, CcSSP31^{T} and CcSSP94^{T} were not detected. Site-directed mutagenesis of the native stop codons of CcSSP36 and CcSSP41 failed. Therefore, these two homologs were excluded from further analysis. CcSSP33^{T} was predicted to have a single glycosylation site which may have affected its ability to be successfully secreted in *P. pastoris*.

The three tagged recombinant *C. camelliae* CCL-SSPs CcSSP43^{T}, CcSSP37^{T} and CcSSP81^{T}, were chosen for comparative functional analysis with BcSSP2^{T} and SsSSP3^{T}. Of the 73 *C. camelliae* CCL-SSPs described, CcSSP37T and CcSSP92T, are the most similar to BcSSP2^{T} (55% and 76% identity) and SsSSP3^{T} (58% and 75%) (Fig. 6.6B & Appendix 9.14). These two *C. camelliae* proteins would be the most likely to share functionality with the native BcSPP2 and SsSSP3 proteins. CcSSP43^{T} was included in the analysis as a negative control for sequence conservation, but still retained 40% and 45% amino acid identity to BcSSP2^{T} and SsSSP3^{T} respectively (Fig. 6.6B).

To normalize for variations in protein concentration, the concentration of each tagged protein was quantified using a chemiluminescence-based quantification method (Fig. 6.6C & 6.6D). All tagged proteins were present in culture filtrates at a higher concentration than the 5 fold diluted SsSSP3^{T} protein (Fig. 6.6D). Only SsSSP3^{T} undiluted and diluted (10 fold) culture filtrates were able to induce a host-cell necrosis response (Fig. 6.6E). Compared to the native protein assays, the SsSSP3^{T} host-necrosis response was delayed and never completely necrotized the infiltrated area (Fig. 6.4A &

6.6E). BcSSP3^{T} failed to induce any visible host-cell necrosis response suggesting that the addition of the c-Myc 6xHis-tag to the C-terminus of the native BcSSP3 and SsSSP3 proteins had resulted in a perturbation of protein function. CcSSP43^{T}, CcSSP37^{T} and CcSSP81^{T} also failed to induce any response but it is unclear whether this is due to the addition of the C-terminal tag or due to an absence of host-cell necrosis function.

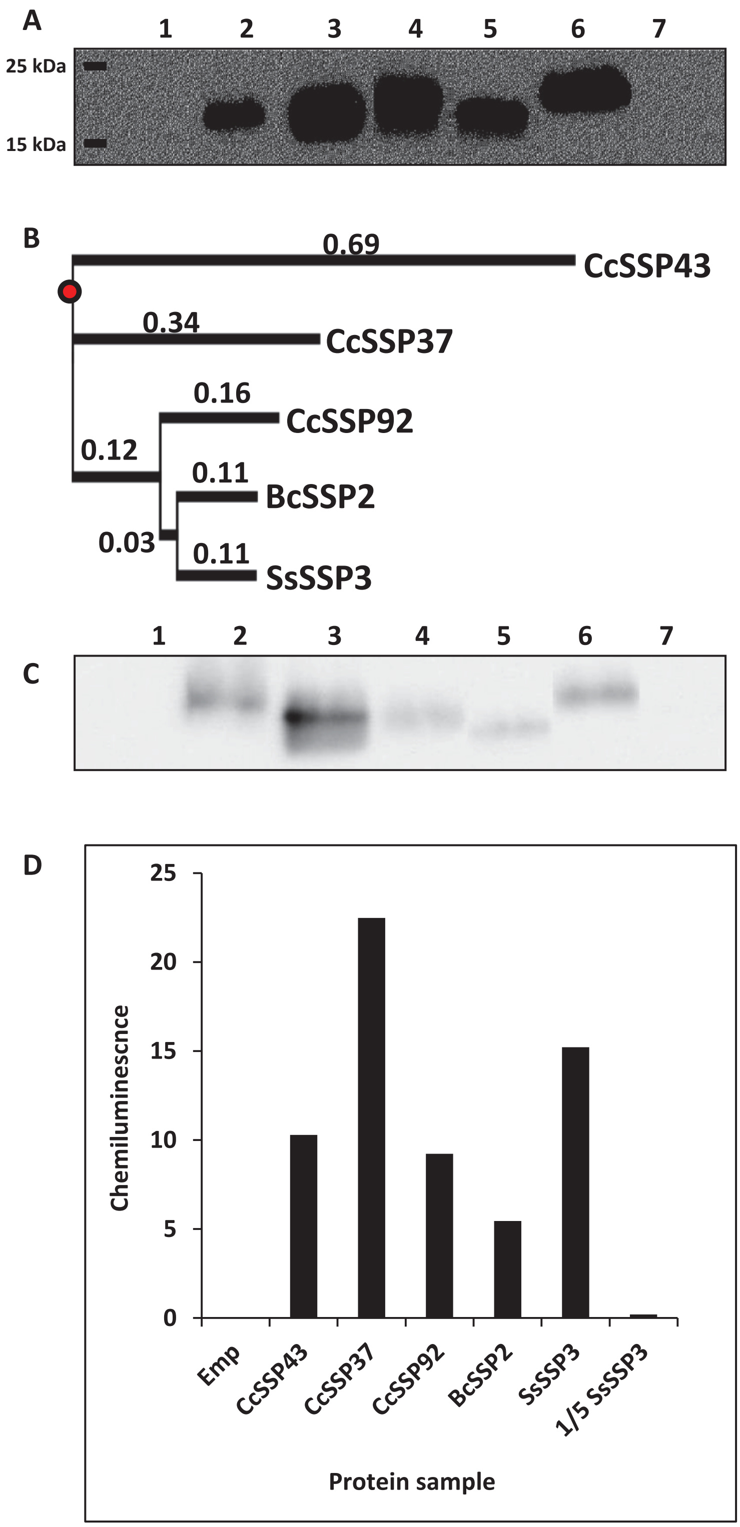
A
1 2 3 4 5 6 7
25 kDa
15 kDa
B
0.69
CcSSP43
0.34
CcSSP37
0.16
CcSSP92
0.12
0.11
BcSSP2
0.03
0.11
SsSSP3
1 2 3 4 5 6 7
C
D
25
20
15
10
5
0
Chemiluminescnce
Emp
CcSSP43
CcSSP37
CcSSP92
BcSSP2
SsSSP3
1/5 SsSSP3
Protein sample

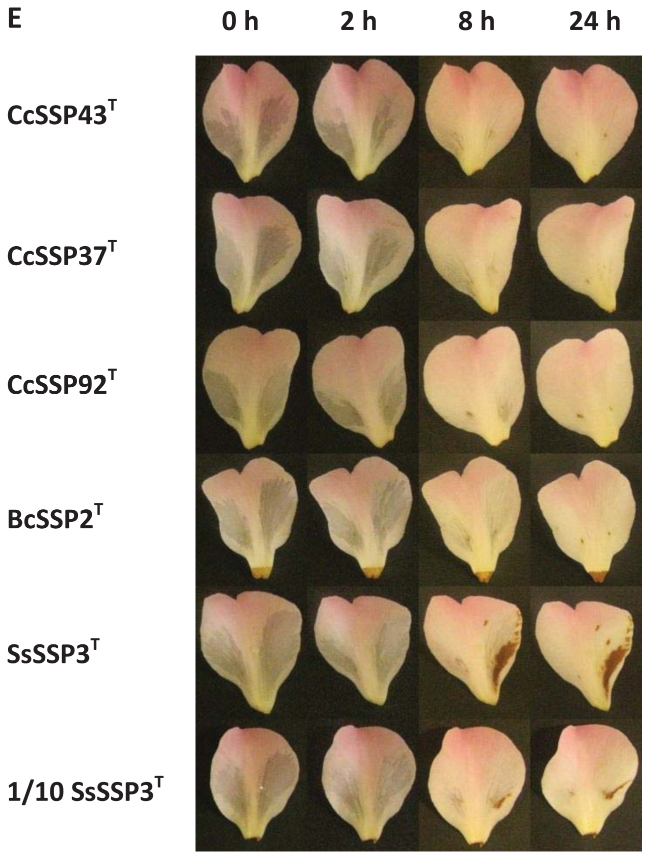

Figure 6.6. Tagged recombinant *Ciborinia camelliae*-like small secreted protein (CCL-SSP) expression and functional assays. **A**, A western blot showing the expression of 5 tagged CCL-SSPs using the anti c-Myc antibody. Empty vector (lane1), CcSSP43^T (lane2), CcSSP37^T (lane 3), CcSSP92^T (lane 4), BcSSP2^T (lane 5), SsSSP3^T (lane 6), 1/10 diluted SsSSP3^T (lane 7). **B**, A phylogenetic tree showing relationships of the expressed tagged proteins. The red circle designates a node with 100% bootstrap support. Values indicate phylogenetic distance based on amino acid substitutions per site. **C**, Chemiluminescent detection of expressed tagged proteins. Lane order is identical to that shown in 6.6A. ***D,*** Semi-quantitative analysis of protein abundance using chemiluminescence data and the ImageJ gel quantification plugin. **E**, *Camellia* 'Nicky Crisp' petal tissue (*n* = 3) infiltrated with 'empty vector' culture filtrate (left petal lobe) and 5 tagged recombinant protein culture filtrates (right petal lobe). Photographs were taken at 0, 2, 8 and 24 h postinoculation. Representative images are shown (*n* = 3).

6.3. Discussion

Comparative secretome analysis identified a family of conserved *C. camelliae*-like small secreted proteins (CCL-SSPs) in the secretomes of *C. camelliae* (*n* = 73), *Botrytis cinerea* (*n* = 1) and *Sclerotinia sclerotiorum* (*n* = 1). Several fungal SSPs have previously been shown to function as effector proteins (De Wit et al., 2009). *In silico* characterization of the conserved CCL-SSP family identified conserved cysteine residues, conserved motifs and protein homologs in other necrotrophic fungal species. In agreement with the necrotrophic lifestyles of *B. cinerea* and *S. sclerotiorum*, functional studies indicated that the single copy CCL-SSPs identified in *B. cinerea* and *S. sclerotiorum* were able to induce host-cell necrosis. Interestingly, homologs in *C. camelliae* were unable to replicate this phenotype. This section discusses features of the identified family of CCL-SSPs, including their primary protein structure, their similarity to other fungal effector families and hypothesizes why *C. camelliae* CCL-SSP homologs are unable to induce host-cell necrosis.

<u>6.3.1. CCL-SSP family members share a robust, heat tolerant structure.</u>

Many fungal effectors have high cysteine content (Templeton et al., 1994; Stergiopoulos & De Wit, 2009). The cysteine residues within fungal effector proteins are proposed to form disulphide bonds, which help maintain protein stability within the plant apoplast (Dou & Zhou, 2012). A total of 10 conserved cysteine residues were present in each *C. camelliae*, *B. cinerea* and *S. sclerotiorum* CCL-SSP homolog. Considering the median CCL-SSP length of 98 amino acids, the cysteine content is extremely high within these proteins (i.e. ~10%). *In silico* predictions showed that all 10 cysteine residues were likely to form disulphide bonds (Fig. 6.1). The conservation of cysteine residues indicates that the secondary structure of these proteins is also likely to be conserved.

Treatment of BcSSP2 and SsSSP3 proteins with DTT, or 30 minutes of boiling, confirmed the stability of these two CCL-SSPs under denaturing conditions and heat stress (Fig. 6.5). The observed results were very similar to what has been shown for the fungal effectors SnTox1 (Liu et al., 2012) and SnTox3 (Liu et al., 2009). SnTox3 has 6 cysteine residues and is 231 AA in length whereas SnTox1 has 16 cysteine residues and is 117 AA in length. DTT concentrations of 5 mM for SnTox3 (2 h incubation) and 40 mM for SnTox1 (4 h incubation) were required to disrupt the necrosis-inducing function of these proteins, which correlates well with their cysteine content.

A small region of necrosis was observed in petals infiltrated with 100mM DTT treated SsSSP3 culture filtrates, but was absent in petals infiltrated with 100mM DDT treated BcSSP2 culture filtrates (Fig. 6.5). This result suggests that SsSSP3 may be slightly more stable than BcSSP2. The SsSSP3^T protein was able to maintain a low level of necrosis-inducing function, which was completely compromised in BcSSP2^T. The differences in functional ability observed in tagged proteins might also be attributed to greater stability in the SsSSP3^T protein.

Screening of the *C. camelliae*, *B. cinerea* and *S. sclerotiorum* CCL-SSPs for previously characterized effector motifs, identified the presence of a Y/F/WxC-motif. This motif was originally identified in the N-terminus of small secreted proteins of *Blumeria graminis* and *Puccinia triticina* (Godfrey et al, 2010). Godfrey et al. hypothesized that the Y/F/WxC motif was exclusive to biotrophic fungi that produce haustoria. The results shown here disprove this hypothesis as *C. camelliae*, *B. cinerea* and *S. sclerotiorum* do not produce haustoria. Furthermore, the same motif has also been recently reported in SSPs of *Mycosphaerella graminicola* (syn. *Zymoseptoria tritici*), a hemibiotroph that also lacks haustoria (Morais do Amaral et al., 2012). Unlike the CCL-SSPs identified in this project, the primary protein structure of *B. graminis* and *P. triticina* SSPs is not highly conserved. Furthermore, the N-terminal location of the *B. graminis* and *P. triticina* Y/F/WxC-motifs contrasted with the C-terminal location of this motif in *C. camelliae*, *B. cinerea* and *S. sclerotiorum* CCL-SSPs. Interestingly, a very similar Y/F/W,C motif was present in the N-terminal conserved motif 'CTYCQCLFPDGSHCC' for 100 of the 105 *C. camelliae*, *B. cinerea* and *S. sclerotiorum* CCL-SSPs (Fig. 6.1). It is possible that the common occurrence of this short motif in fungal effector proteins is by chance. Indeed the functional significance of this motif is yet to be determined.

The ‘CTYCQCLFPDGSHCC’ motif was predicted to be common to all 75 CCL-SSP family members identified in this project (Fig. 6.1). In addition, the majority of the homologs identified in other species also share this domain (data not shown). This motif seems to be specific to the CCL-SSP family, as only low levels of sequence homology were predicted with other known proteins.

6.3.2. CCL-SSP family members share characteristics with other necrosis-inducing fungal effectors.

The CCL-SSP family members identified here are cysteine rich, share conserved and unique sequence motifs (Fig. 6.1) and are found within the genomes of fungi that exhibit necrotrophic life stages (Table 6.1). Furthermore, recombinant *B. cinerea* and *S. sclerotiorum* CCL-SSP family members are heat stable (Fig. 6.5) and are able to induce host cell necrosis in multiple hosts (Fig. 6.4 & Appendix 9.20). Many of these defining characteristics are shared with select families of previously characterized fungal effector proteins.

The TOX family of fungal effectors from *Stagonospora nodorum* and *Pyrenophora tritici-repentis* are generally cysteine rich, are heat stable, are associated with necrotrophic fungi and cause host-cell necrosis within their hosts (Liu et al., 2009; Liu et al., 2012). Sequence conservation varies between each TOX protein, although ToxB has multiple, identical homologs in *Pyrenophora tritici-repentis* (Martinez et al., 2004). The main difference between the CCL-SSP family and the TOX proteins, is host-specificity. TOX proteins are host-specific toxins (HSTs) (Tan et al., 2010). Their ability to cause necrosis and subsequent infection is dependent on the presence of a host-specific plant gene (Liu et al., 2009; Liu et al., 2012; Tan et al., 2010). Based on the results shown in Figure 6.4 and Appendix 9.20, the *B. cinerea* and *S. sclerotiorum* CCL-SSPs are not host-specific toxins as they are able to induce host-cell death in the distinct hosts *Camellia* ‘Nicky Crisp’, *Camellia lutchuensis* and *Nicotiana benthamiana*.

The necrosis and ethylene-inducing peptide 1 (Nep1)-like proteins (NLPs) are virulence factors that are conserved in oomycetes, fungi and bacteria (Qutob et al., 2006). Like their name suggests, they function to induce host-cell necrosis and ethylene production. They are more common in microorganisms that rely on hemibiotrophic or necrotrophic nutrition and often exist as large gene families, especially in *Phytophthora* species (Gijzen & Nurnberger, 2006). A study in *Arabidopsis* showed that oomycete-derived NLPs were more active in the plant apoplast (Qutob et al., 2006). This observation correlates with their hypothesized function as proteins that interact with the plasma membrane of host cells, resulting in cytolysis (Ottman et al., 2009). NLPs are non-host specific, which is similar to what has been observed for BcSSP2 and SsSSP3. However, there are several distinctive differences between NLPs and the described CCL-SSP family. Only two cysteine residues are conserved in NLPs making the mature protein more heat labile (Qutob et al., 2006). Furthermore, they universally share the sequence motif 'GHRHDWE', which has been shown to be involved in necrosis-inducing function (Ottman et al., 2009), and is absent in all of the CCL-SSP homologs. Additional features of NLPs include their light-dependent activity, the restriction of their activity to dicotyledonous plants and their ability to induce ethylene production. These features have not been tested or measured for BcSSP2 or SsSSP3-associated assays. However, many of the species identified as having CCL-SSP homologs are monocot infecting phytopathogens (Table 6.1). The ability of CCL-SSP homologs of monocot-infecting pathogens to induce host-cell necrosis is still to be determined.

The genomes of *B. cinerea* and *S. sclerotiorum* each contain two NLP homologs. Mutant studies of the *B. cinerea* NLP homologs, *BcNEP1* and *BcNEP2*, indicated that they are not required for full virulence (Arenas et al., 2010). *S sclerotiorum* NLP homologs *SsNEP1* and *SsNEP2* share the 'GHRHDWE' domain with *BcNEP1* and *BcNEP2* but their role in virulence has not been determined (Dallal et al., 2010). The protein products of all four genes have been shown to induce necrosis in host tissue, much like that observed for BcSSP2 and SsSSP3. However, due to the lack of a 'GHRHDWE' domain in BcSSP2 and SsSSP3 these two proteins cannot be classed as NLPs.

The third family of proteins that share similarities to the CCL-SSP family are the <u>h</u>omologs of <u>*C*</u>*ladosporium fulvum* <u>E</u>cp<u>2</u> (Hce2) proteins. <u>E</u>xtracellular <u>*C*</u>*. fulvum* <u>p</u>rotein <u>2</u> (Ecp2) was originally described in the non-obligate biotroph *C. fulvum*, as part of a group of extracellular proteins that induce an HR in *Cf-Ecp* resistant tomato lines (Stergiopoulos & de Wit, 2009). Ecp2 has been shown to contribute to the virulence of *C. fulvum*, but its fundamental function is still to be resolved (Lauge et al., 1997). The recent finding that Ecp2 has conserved homologs in many other fungi sets it apart from other species-specific fungal effectors of *C. fulvum* (Stergiopoulos et al., 2012). Hce2 proteins have 4 conserved cysteine residues and conserved exon/intron boundaries. The *Mycosphaerella fijiensis* Hce2 protein induces necrosis in tomato lines that lack a *C. fulvum* resistance gene (Stergiopoulos et al., 2010). Interestingly, the same *M. fijiensis* Hce2 protein induces an HR in tomato lines that contain a *C. fulvum* resistance gene. It is hypothesized that the *M. fijiensis* Hce2 protein induces necrosis and compatibility through its interaction with a host protein. When the host protein is guarded an ETI-associated defense response ensues, resulting in cell death. It was unknown whether *M. fijiensis* can survive the ETI-associated defense response as assays were performed using an artificial PVX-expression system (Stergiopoulos et al., 2010). It is unclear whether Hce2 homologs in other species share the same function as *M. fijiensis* Hce2. Hce2 homologs do not share sequence conservation with the CCL-SSP homologs identified here. Furthermore, no Hce2 homologs have been identified in *B. cinerea* or *S. sclerotiorum*, or any other species of the Leotiomycetes (Stergiopoulos et al., 2012).

Generally, members of the TOX, NLP, Ecp2 and CCL-SSP families induce host-necrosis and are confined to fungal species that exhibit necrotrophic life stages. The CCL-SSP family described here shares multiple characteristics with these previously defined fungal effector families. However, differences in sequence information, primary protein structure and host specificity suggest that they are not equivalent.

6.3.3. *Ciborinia camelliae CCL-SSP* family members are likely to have undergone gene duplication.

The lineage-specific expansion of CCL-SSPs in *C. camelliae* is likely to have resulted through the process of gene duplication. The close proximity of these genes to each other in the *C. camelliae* draft genome (Fig. 6.2), their nucleotide conservation (Fig. 5.8) and their conserved exon/intron structure (Fig. 6.1) support this hypothesis. A very similar scenario has been reported for small secreted proteins in the biotrophic fungus *Ustilago maydis*, where twelve genomic clusters of two to five SSP genes were discovered (Kamper et al., 2006). *Ustilago maydis* SSP genes are expressed together and are upregulated in infected tissue. These observations parallel the expression data observed for *C. camelliae CCL-SSPs* (Fig 6. 3). Deletion of individual *U. maydis* SSP clusters resulted in variable virulence phenotypes suggesting that they are involved in host-pathogen interactions.

Several fungal effector families that cause host cell necrosis are thought to have evolved through gene duplication. All six copies of *ToxB* in *Pyrenophora tritici-repentis* have identical open reading frames (Martinez et al 2004). Duplication of *ToxB* is hypothesized to be a result of transposable element integration and mobilization. The presence of transposable elements and repeat-induced point (RIP) mutation signatures within *C. camelliae CCL-SSP* genomic clusters was not determined and could be a contributing factor to the expansion and diversification of this gene family. The *Ecp2* fungal effector superfamily is also thought to have duplicated and diversified in adaptation to stress (Stergiopoulos et al., 2012). Therefore, gene duplication is a characteristic of at least two families of necrosis-inducing fungal effectors and is likely to have contributed to the expansion of the conserved CCL-SSP genes in *C. camelliae.*

6.3.4. *Ciborinia camelliae CCL-SSP* gene expression precedes host-cell necrosis

Temporal gene expression patterns can provide the first clues to the function of a gene product. Previous RNAseq datasets indicate that *BcSSP2* and *SsSSP3* genes are expressed at the onset of visible disease symptoms in *Lactuca sativa* (lettuce) and *Helianthus annuus* (sunflower) respectively (Cremer et al., 2013; Guyon et al., 2014). This expression pattern correlates well with their necrosis-inducing function. Other studies have also utilized temporal gene expression information to characterize putative fungal effector proteins (Marshall et al., 2011; Cantu et al., 2013). A subset of 9 *C. camelliae CCL-SSP* genes was shown to be expressed strongly from 6 to 24 hpi, with a marked decrease in expression at 48 hpi (Fig. 6.3). During infection assays, *C. camelliae*-mediated host-cell necrosis consistently occurred around 30 hpi (Fig. 3.1).

Therefore, the expression of all 9 *C. camelliae CCL-SSP* genes correlated well with the establishment stage of infection, not the onset of visible disease. This temporal expression pattern suggests that *C. camelliae CCL-SSP* genes function during the establishment of *C. camelliae* in petal tissue.

6.3.5. There is no evidence to suggest *Ciborinia camelliae* CCL-SSPs are functional homologs of BcSSP2 and SsSSP3.

Of the 12 native recombinant CCL-SSP proteins tested, only culture filtrates containing the two species-specific homologs BcSSP2 and SsSSP3 were able to induce host-cell necrosis (Fig. 6.4). Attempts to rule out protein concentration as a delimiting factor in the function of the 10 tested *C. camelliae* CCL-SSP homologs failed, due to the loss of function in tagged proteins (Fig. 6.6). In this section technical reasons for the absence of function in native *C. camelliae* CCL-SSP homologs are discussed.

Infiltrated culture filtrates were originally buffered to pH 6.0. This slightly acidic environment may have had an effect on the activity of the recombinant CCL-SSP proteins. *B. cinerea* and *S. sclerotiorum* acidify host tissue during infection (Godoy et al., 1990; Andrew et al., 2012), although it is unclear whether *C. camelliae* does the same. Furthermore, the regulation of pathogenicity in *B. cinerea* and *S. sclerotiorum* has shown to be influenced by pH (Rollins & Dickman, 2001; Rollins, 2003; Billon-Grand et al., 2011). Therefore, it is likely that the BcSSP2 and SsSSP3 proteins have evolved to be functional in acidic conditions. Interestingly, the isoelectric points of BcSSP2, SsSSP3 and CcSSP92 are all below pH 6.0 indicating that these proteins were negatively charged in culture filtrates. The other 9 *C. camelliae* CCL-SSP recombinant proteins were positively charged at pH 6.0 (Appendix 9.23). The marked difference in isoelectric point values among this group of proteins may have contributed to their ability to induce host-cell necrosis. In disagreement with this hypothesis, CcSSP92 did not induce necrosis despite having similar isoelectric properties to BcSSP2 and SsSSP3 (Figs. 6.4, 6.6 & Appendix 9.23). The addition of the c-Myc 6xHis-tag to the native proteins changed the isoelectric points of BcSSP2^{T} and SsSSP3^{T}. This change in sequence led to the proteins having a net positive charge at pH 6.0, which may have contributed to the reduction in necrosis-inducing activity of BcSSP2^{T} and SsSSP3^{T} (Fig. 6.5).

Only 10 of the 73 *C. camelliae* CCL-SSPs were assessed for necrosis-inducing function (Fig. 6.4). It is possible that active *C. camelliae* CCL-SSPs were overlooked. Previous studies have shown that large fungal effector families may contain a high proportion of non-functional genes. For example, only 2 out of 9 *Verticillium dahliae* NLP recombinant protein family members were able to induce host-cell necrosis (Zhou et al., 2009). The assumption was made that *C. camelliae* CCL-SSPs with the greatest sequence homology to BcSSP2 and SsSSP3 would be most likely to share the host-cell necrosis-inducing function. However, CcSSP92 and CcSSP37 were unable to induce any visible phenotype (Figs. 6.4 & 6.6). As opposed to primary sequence homology, tertiary structure homology may correlate better with protein function. NLP proteins share a common fold in their tertiary structure that is required for function (Ottman et al., 2009). Therefore, the possibility that necrosis-inducing *C. camelliae* CCL-SSPs were overlooked, cannot be ruled out.

6.4. Conclusions

The functional characterization of 12 recombinant CCL-SSP proteins revealed a species-specific split in their ability to induce host-cell necrosis. Culture filtrates of the single CCL-SSP homologs identified in *B. cinerea* and *S. sclerotiorum* induced host-cell necrosis in taxonomically diverse plants. *C. camelliae* CCL-SSPs were unable to trigger host-cell necrosis despite having similar primary structures to the host-cell necrosis inducing proteins BcSSP2 and SsSSP3. The lineage-specific expansion of *C. camelliae CCL-SSP* genes appears to have arisen through gene duplication and resembles host-mediated adaptive evolution. Multiple CCL-SSP homologs are present in other necrotrophic fungi ($n \leq 4$), but no other fungal species in the Genbank database has as many CCL-SSP homologs as *C. camelliae* ($n = 73$). Gene expression studies suggest that *C. camelliae* CCL-SSPs are most likely to function during the asymptomatic establishment phase of disease development. Whether *C. camelliae* CCL-SSPs suppress the host immune system during the initial stages of infection is still to be determined.

7. General discussion

7.1. Breeding for *Ciborinia camelliae* resistance

The initial incursion of *C. camelliae* into New Zealand in the early 1990s prompted research into mechanisms to control '*Camellia* flower blight' (Taylor, 1999; Van Toor et al., 2001; Vingnanasingam, 2002; Taylor, 2004; Van Toor et al., 2005a; Van Toor et al., 2005b; Van Toor et al., 2005c). The discovery of natural resistance to *C. camelliae* in certain species of *Camellia* uncovered a new opportunity to potentially control this pathogen using a traditional plant breeding strategy (Taylor et al., 2004). This discovery formed the initial basis for the research presented in this thesis.

It was demonstrated that natural resistance to *C. camelliae* was variable across the *Camellia* genus with higher levels of resistance observed in species of section Theopsis (Fig. 3.4). It is likely that this variation is due to differences in plant defense responses as well as differences in *C. camelliae* effector efficiency. Interestingly, the natural host range of several section Theopsis species is restricted to offshore islands (Wu et al., 2007). Therefore, incompatible *Camellia* species may have evolved in an environment isolated from *C. camelliae*, resulting in effector/host protein incompatibilities.

Microscopic analyses of the incompatible interaction with *Camellia lutchuensis* showed that more than half of the infection attempts were halted at the point of penetration, suggesting that early detection of *C. camelliae* occurred (Table 3.1). The majority of hyphae that managed to invade the apoplast of incompatible host tissue appeared to be retarded in growth, indicating that additional extracellular defense mechanisms were likely to be involved. This defense response resembles a polygenic PAMP–triggered immunity (PTI)-associated defense response, and fits with the theory that polygenic resistance responses are indicative of discordant host-pathogen interactions (Schulze-Lefert & Panstruga, 2011).

Monogenic effector triggered immunity (ETI)-associated plant resistance is determined by the presence of a single plant resistance gene (Jones & Dangl, 2006). Although it is relatively simple to introgress a single resistance gene into a susceptible host, the durability of this acquired resistance is often questionable and resistance can quickly be overcome (Palloix et al., 2009). Introgression of polygenic resistance into susceptible hosts is an attractive, but challenging alternative.

With the help of molecular mapping techniques and marker-assisted breeding, genomic loci that contribute to disease resistance can be identified and introgressed into susceptible plant lines (Lindhout, 2002). Due to the lack of genetic maps and suitable mapping populations of *Camellia*, it is currently not possible to use these methods to identify genomic loci in *Camellia lutchuensis* that confer resistance to *C. camelliae*. Instead, a 'blind' selection strategy has been proposed, based on backcrossing *Camellia lutchuensis* to hybrids with established *Camellia lutchuensis* parentage. This strategy aims to increase the proportion of *Camellia lutchuensis* in the hybrid, and in turn, increase the chance of inheriting multiple genes that contribute to *C. camelliae* resistance. Offspring that have increased *C. camelliae* resistance, together with desirable ornamental characteristics, would be selected for (Fig. 7.1). This strategy is currently being implemented by staff associated with the *Camellia* plant collection at Auckland Botanic Gardens, New Zealand.

7.2. Utilizing bioinformatics for fungal gene discovery

The advent of next generation sequencing has unlocked the ability of molecular biologists to expand their interest to non-model organisms like *C. camelliae*. Prior to this study, molecular information pertaining to *C. camelliae* was limited to a total of 10 publicly available gene sequences (www.ncbi.nlm.nih.gov/nuccore/?term= Ciborinia %20camelliae retrieved 15 Oct 2014). Sequencing of the complementary *C. camelliae* draft genome and transcriptome have unlocked the possibility to study molecular genetics of *C. camelliae* in detail. Although these datasets are far from complete, they have proven to be useful for gene discovery and gene prediction. Analysis of the *MAT* locus of *C. camelliae* provided strong evidence for heterothallism in *C. camelliae* (Fig. 4.1). Furthermore, the classification of *C. camelliae* expressed sequence tags (ESTs) from the mixed transcriptome dataset would have been difficult without a reference *C. camelliae* draft genome. It is likely that these molecular resources will provide valuable information for future studies of *C. camelliae*.

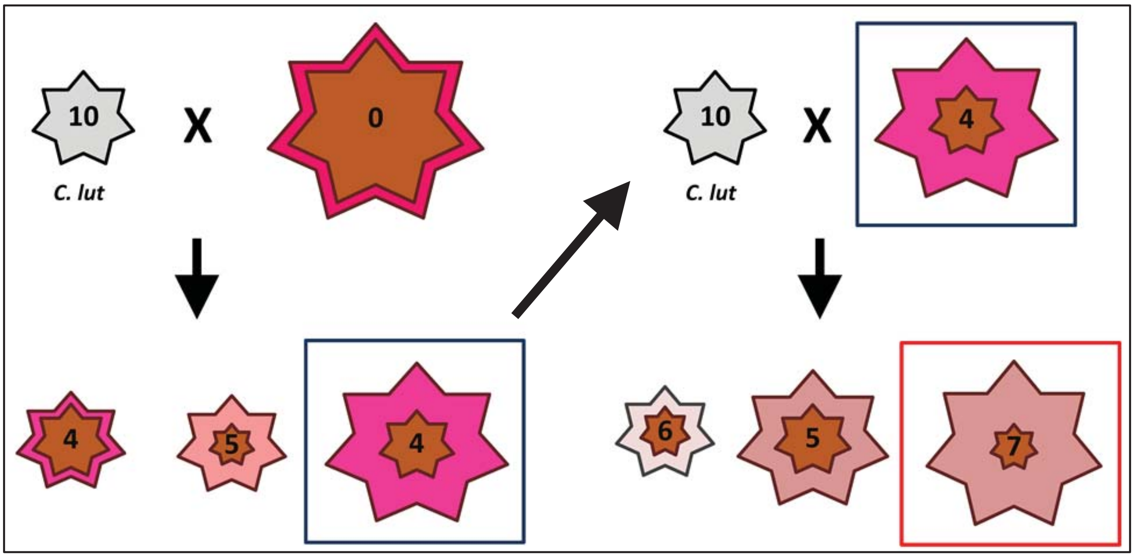

Figure. 7.1. Backcrossing interspecific *Camellia* hybrids with *Camellia lutchuensis*. Values represent the hypothetical number of resistance genes within each genotype. Brown stars denote the degree of susceptibility to petal blight. Bloom size and the intensity of the pink colour, represent desirable characteristics. The blue square highlights an established hybrid that has reduced petal blight incidence together with desirable characteristics. The red square highlights a bloom from the backcrossed population that has reduced petal blight incidence together with desirable characteristics.

Fungal secretome prediction has become a popular strategy used by molecular pathologists to identify fungal genes that may contribute to fungal virulence (Amselem et al., 2011; Morais do Amaral et al., 2012; Hacquard et al., 2012; Cantu et al., 2013; Guyon et al., 2014). The objective of this study was to identify and characterize compositional similarities and differences between the secretomes of three closely related fungi, *C. camelliae*, *Botrytis cinerea* and *Sclerotinia sclerotiorum*. Unexpectedly, the composition of small secreted proteins (SSPs) varied significantly between these three fungi (Figs. 5.3 & 5.4). Further analysis led to the identification of a family of conserved *C. camelliae*-like small secreted proteins (CCL-SSPs) that appear to have specifically expanded in *C. camelliae* (Fig. 5.6).

Fungal effectors are often small (< 300AA) cysteine rich proteins that are secreted extracellularly during infection (Stergiopoulos & De Wit, 2009). In the past, these three basic features have been utilized by bioinformaticians to screen fungal secretomes for putative fungal effectors (De Wit et al., 2009; Hacquard et al., 2012). More recently effector screening strategies have begun to incorporate complex information, including temporal and tissue-specific gene expression patterns, evidence for positive selection and 3-dimensional protein structure prediction (Pedersen et al., 2012; Pendleton et al., 2014; Guyon et al., 2014). The comparative secretome strategy demonstrated in this thesis could be incorporated into a complex fungal effector prediction pipeline. This would add the ability to identify putative effectors that are species-specific, or those that are conserved across different fungal families.

The comparative secretome approach could also be scaled up to incorporate more fungal species. Correlations between the conserved components of each secretome and the lifestyle of the chosen fungi could be made. Identification of horizontal gene transfer events between unrelated fungi that share similar niche environments could also be facilitated. Similar bioinformatic analyses successfully identified putative horizontal gene transfers in *Fusarium pseudograminearum* (Gardiner et al., 2012). Furthermore, the strategy described here could be used to compare the secretomes of near isogenic fungi that have different phenotypes. Recent attempts were made to identify secretome proteins that contributed to pathogenicity in *Fusarium* *graminearum* by comparing a pathogenic isolate with a non-pathogenic isolate (Rampitsch et al., 2013). Providing that phenotypic differences between the two isolates were due to gene loss, gene gain or gene diversification, a comparative secretome analysis strategy could also be used in this instance.

Previously described necrosis-inducing fungal proteins generally belong to conserved fungal families (Martinez et al., 2004; Qutob et al., 2006; Stergiopoulos et al., 2012; Zhou et al., 2012). Therefore, it is likely that the discovery of necrosis-inducing fungal proteins could be targeted by screening for small, secreted, cysteine rich proteins that share homology. The identification of necrosis-inducing proteins BcSSP2 and SsSSP3 validate this proposal as their identification was based on these characteristics. In contrast, host-immune suppression-associated fungal effectors are likely to be highly specific to their host (Guyon et al., 2014). Screening for non-conserved, small, secreted, cysteine-rich proteins may facilitate the discovery of this class of fungal effectors.

7.3. Putative necrosis-inducing mechanisms of BcSSP2 and SsSSP3

Culture filtrates containing recombinant BcSSP2 and SsSSP3 proteins induced host-cell necrosis when infiltrated into host-tissue (Fig. 6.4). Evidence presented in this thesis suggests that host-cell necrosis was due to the action of BcSSP2 and SsSSP3. These proteins are proposed to be functionally homologous, although differences in their activity have been observed. It is hypothesized here that the mechanism that BcSSP2 and SsSSP3 use to induce host-cell necrosis may parallel those mechanisms used by other necrotrophic necrosis-inducing proteins.

Several of the Tox proteins of *Stagonospora nodorum* are known to cause necrosis and susceptibility through indirect interactions with specific plant proteins in wheat (Faris et al., 2010; Liu et al., 2009; Liu et al., 2012). These types of interactions have been termed inverse gene-for-gene interactions, because susceptibility is determined by the interaction of a single Tox protein with a single plant protein. These interactions contrast directly with the gene-for-gene hypothesis, where interactions between a single fungal effector protein and a single plant protein can result in ETI-associated resistance (Flor, 1942 & 1956). Wheat cultivars that lack susceptibility genes are resistant to infection by *S. nodorum*. A similar mechanism has been characterized for the non-proteinaceous host selective toxin victorin, which is secreted by *Cochliobolus victoriae* during infection (Lorang et al., 2012). *C. victoriae* has evolved to have an effector that tricks the host-immune system into inducing cell death, which benefits its necrotrophic lifestyle. Although the guarded protein is still to be discovered, this same mechanism is proposed for *S. nodorum*'s Tox proteins. It is hypothesized that the BcSSP2 and SsSSP3 proteins may also cause necrosis through the action of a guarded host protein (Fig. 7.2). For this to be the case, the targeted host-protein would be required to be universally guarded in diverse hosts, as these two proteins act in a nonhost-specific manner (Fig. 6.4).

The Ecp2 effector of *Mycosphaerella fijiensis* is also thought to interact with a guarded host-protein. Transient expression of Ecp2 in tomato lines containing a cognate Ecp2 resistant gene results in severe ETI (Stergiopoulos et al., 2010). In tomato lines that lack a cognate Ecp2 resistance gene, *M. fijiensis* infection results in host-cell necrosis and susceptibility. It is assumed that *M. fijiensis* Ecp2 interacts with the same host-protein in susceptible and resistant tomato lines. *M. fijiensis* Ecp2 homologs exist in other fungi, although it is unclear whether they are functionally conserved (Stergiopoulos et al., 2012). It is hypothesized that BcSSP2 and SsSSP3 also employ a necrosis-inducing mechanism analogous to that of the *M. fijiensis* Ecp2 protein (Fig. 7.2). Additional experimentation is required to determine whether the observed necrosis-inducing function of BcSSP2 and SsSSP3 is the result of an HR or the result of an alternative cell-death mechanism.

NLP proteins also induce necrosis and are common in fungi that have a necrotrophic life stage (Qutob et al., 2006). The universally conserved domain 'GHRHDWE' is required for NLP-mediated host-cell necrosis (Arenas et al., 2010). NLP proteins are active in the plant apoplast (Qutob et al., 2006), localise to cell membranes (Schouten et al., 2007) and are thought to induce host-cell necrosis by disrupting the integrity of the plasma membrane (Ottman et al., 2009). The molecular mechanism that leads to

NLP-induced host-cell necrosis is still to be determined. As an alternative to the Tox/victorin-like and Ecp2-like hypotheses, it is proposed that BcSSP2 and SsSSP3 may interact with host-cell membranes to induce a NLP-like host-cell necrosis response, although there is no current evidence for this (Fig. 7.2).

It is also possible that BcSSP2 and SsSSP3 induce host-cell necrosis via a novel pathway that has not been considered in this thesis. Additional studies are required to determine the mechanism that leads to BcSSP2/SsSSP3 host-cell necrosis.

7.4. Adaptive evolution of *Ciborinia camelliae CCL-SSP* genes correlates with a loss of necrosis-inducing activity

Initial results suggest that the *C. camelliae* members of the conserved CCL-SSP family do not share the necrosis-inducing function attributed to their *B. cinerea* and *S. sclerotiorum* homologs (Figs. 6.4 & 6.6). The gene expansion pattern observed for *C. camelliae CCL-SSP* homologs is indicative of diversifying selection via gene duplication and has previously been described as a characteristic of fungal effector evolution in *Puccinia graminis* f. sp. *tritici* (Sperschneider et al., 2014). Therefore, it is likely that the expansion and diversification of these genes occurred due to selection pressure from the host, much like that reported for the RXLR effectors of *Phytophthora* species (Win et al., 2007). In contrast, *BcSSP2* and *SsSSP3* exist as single copy genes and do not appear to be undergoing adaptive evolution. It is hypothesized here, that the lack of *C. camelliae* CCL-SSP-associated necrosis-inducing function is a consequence of adaptive evolution.

Despite the lack of necrosis-inducing function, *C. camelliae* CCL-SSPs may still interact with the same host proteins as BcSSP2 and SsSSP3. The *Phytophthora infestans* EPIC1 and EPIC2 effectors bind to the same target as *Cladosporium fulvum's* Avr2 effector (Song et al., 2009). The function of these two sets of effectors is to inhibit the apoplastic tomato Rcr3 protease. In resistant tomato lines Rcr3 is guarded by an R-protein. Contrastingly, the Avr2 effector triggers ETI in resistant tomato lines, whereas the EPIC1 and EPIC2 effectors do not. EPIC1 and EPIC2 are likely to target a domain of the Rcr3 protein that doesn't de-stabilize the guard protein. Based on this example it is

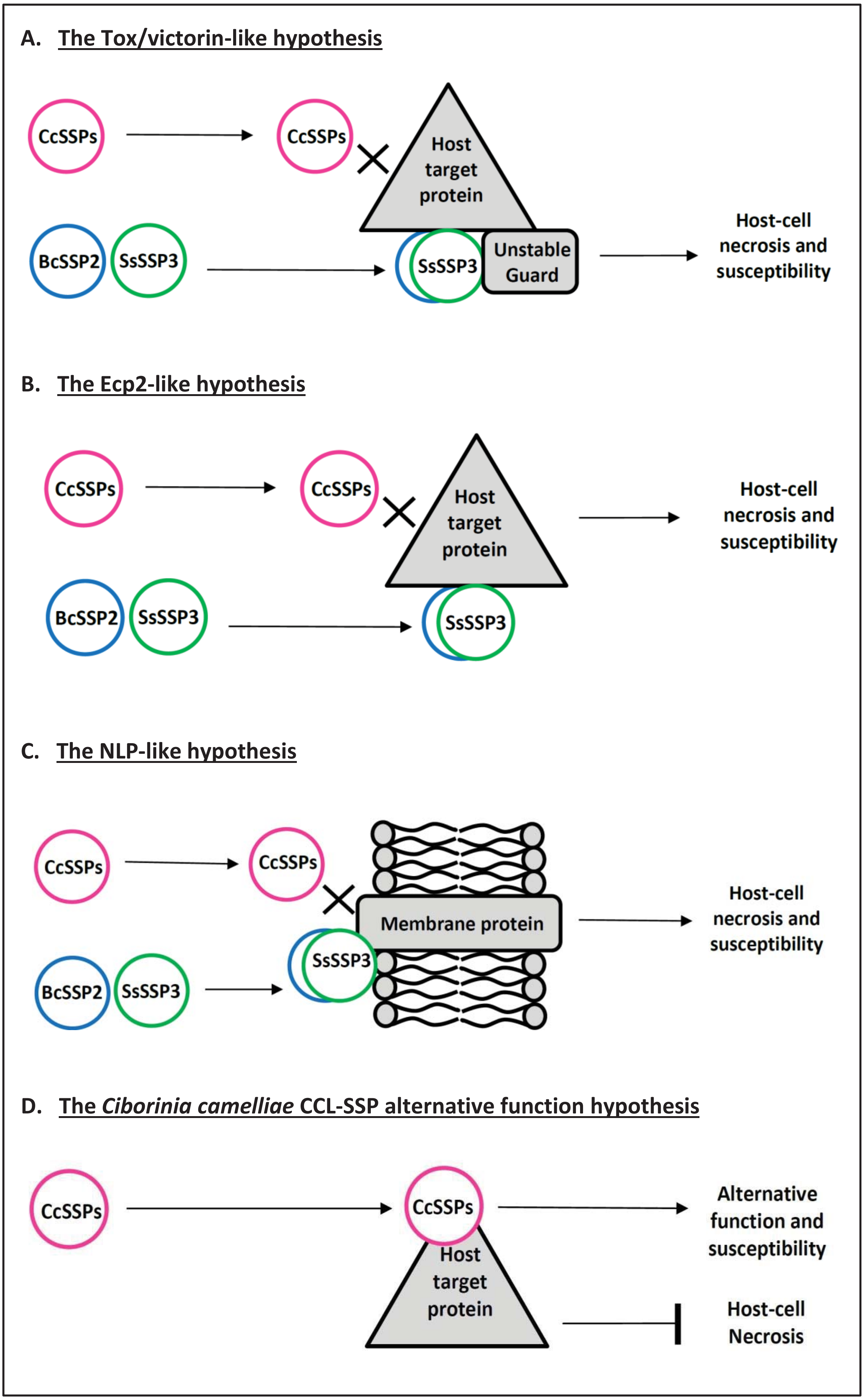
A. The Tox/victorin-like hypothesis
CcSSPs
CcSSPs
Host target protein
BcSSP2
SsSSP3
SsSSP3
Unstable Guard
Host-cell necrosis and susceptibility
B. The Ecp2-like hypothesis
CcSSPs
CcSSPs
Host target protein
Host-cell necrosis and susceptibility
BcSSP2
SsSSP3
SsSSP3
C. The NLP-like hypothesis
CcSSPs
CcSSPs
Membrane protein
Host-cell necrosis and susceptibility
SsSSP3
BcSSP2
SsSSP3
D. The Ciborinia camelliae CCL-SSP alternative function hypothesis
CcSSPs
CcSSPs
Host target protein
Alternative function and susceptibility
Host-cell Necrosis

Figure 7.2. Hypothesized molecular mechanisms of BcSSP2, SsSSP3 and the *C. camelliae* CCL-SSP homologs (CcSSPs). Hypotheses are based on molecular mechanisms proposed for other fungal effectors. **A,** The Tox/victorin-like hypothesis. BcSSP2 and SsSSP3 induce host-cell necrosis by de-stabilizing a guard protein. *C. camelliae* CCL-SSP homologs are unable to interact with the host protein, resulting in a stable guard/guardee interaction and no host-cell necrosis. **B,** The Ecp2-like hypothesis. BcSSP2 and SsSSP3 induce host-cell necrosis by interacting with a host protein. *C. camelliae* CCL-SSP homologs are unable to interact with the host protein and do not cause host-cell necrosis. **C,** The NLP-like hypothesis. BcSSP2 and SsSSP3 induce host-cell necrosis through interactions with host-cell membranes or membrane proteins. *C. camelliae* CCL-SSP homologs are unable to interact with the host membrane or host membrane protein in the same way as BcSSP2 and SsSSP3 and do not cause host-cell necrosis. **D,** The *C. camelliae* CCL-SSP alternative function hypothesis. *C. camelliae* CCL-SSP homologs interact with a host protein to induce host-susceptibility. Notably, the alternative function of the *C. camelliae* CCL-SSP homologs does not induce host-cell necrosis.

possible that the *C. camelliae* CCL-SSP homologs bind to the same host target protein as BcSSP2 and SsSSP3, but do not induce host-cell necrosis (Fig. 7.2).

Homologous Ecp2 proteins from *C. fulvum* and *M. fijiensis* are proposed to have similar host target proteins (Stergiopoulos et al., 2012). During susceptible interactions *C. fulvum* Ecp2 is thought to contribute to virulence by suppressing the host immune system (Lauge et al., 1997). Contrastingly, the *M. fijiensis* Ecp2 homolog contributes to virulence by inducing host-cell necrosis (Stergiopoulos et al., 2012). Despite their homology and shared contribution to virulence, these two effectors function in completely different ways. Like the proposed function of the *C. fulvum* Ecp2 protein, *C. camelliae* CCL-SSPs may act to suppress the host-immune system as an alternative to inducing host-cell death. Indeed, the early expression pattern of 9 *C. camelliae CCL-SSP* genes agrees with this hypothesis (Fig. 6.3). Furthermore, fungal effectors that suppress the host immune system are often required to diversify in order to maintain function in the host (Guyon et al. 2014). Therefore, it is hypothesized that *C. camelliae* CCL-SSP homologs have evolved to suppress the host immune system, resulting in increased fitness of *C. camelliae* in host *Camellia* petal tissue.

How a loss of *C. camelliae* CCL-SSP-associated necrosis-inducing ability would lead to increased fitness can only be speculated. During adaptation to a host-specific lifestyle, *C. camelliae* may have no longer required rapid host-cell necrosis ability. Rapid necrosis of resource rich *Camellia* petal tissue may have promoted increased competition from other microbes. Furthermore, rapid death of the host petal tissue may have limited the ability of *C. camelliae* to spread throughout the petal tissue and hence maximize the sequestration of nutrients. Until *C. camelliae* CCL-SSP homologs have been proven to lack *in planta* necrosis-inducing function, hypotheses about their evolution remain speculative.

7.5. Future directions

Confirming the lack of necrosis-inducing function of recombinant C. camelliae CCL-SSP homologs.

Differences in recombinant protein culture filtrate concentration may explain the lack of necrosis observed during infiltration of host petal tissue with *C. camelliae* CCL-SSPs. Protein-specific antibodies would alleviate the need for a tag on the recombinant protein and would facilitate ELISA-based protein quantification methods. The concentrations of each recombinant protein could be normalized prior to infiltration into host tissue. The effect of pH on the necrosis-inducing ability of native BcSSP2, SsSSP3 and CcSSP92 proteins should also be determined.

Characterizing the molecular basis of the BcSSP2 and SsSSP3 cell-death phenotype

It is unclear whether BcSSP2 and SsSSP3 are necrosis-inducing factors or avirulence proteins. Infiltration of purified BcSSP2 and SsSSP3 proteins into ETI-compromised *Nicotiana benthamiana* lines would determine whether ETI is required for the BcSSP2 and SsSSP3 cell-death phenotype. ETI-comprimized lines of *Nicotiana benthamiana* would be produced by silencing key genetic components of the ETI pathway (e.g. *SGT1*, *EDS1* or *HSP90*) using virus-induced gene silencing (VIGS).

Identifying the functional domains of BcSSP2 and SsSSP3.

An alignment of the polypeptide sequences of BcSSP2, SsSSP3 and CcSSP92 reveals that 11 amino acid residues (12%) differ between the two necrosis-inducing proteins and the non-functional CcSSP92 protein (Fig. 7.3). Site-directed mutagenesis of these target amino acids would help to identify which domains of the recombinant proteins are most important for function. It is speculated that amino acid changes that result in the largest changes in hydrophobicity are likely to affect the conformation and function of these proteins (Fig. 7.3).

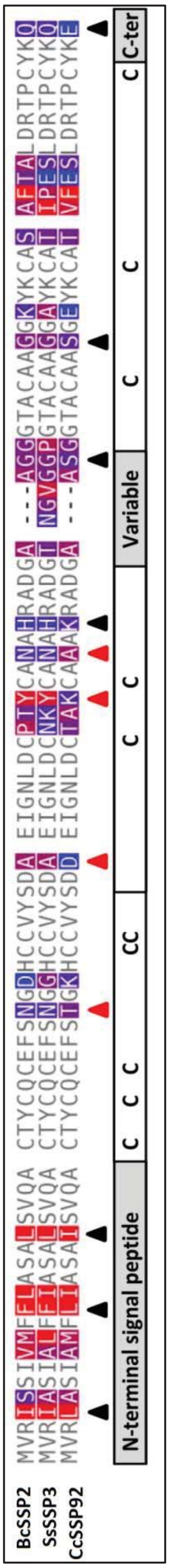

Figure 7.3. A comparison of the native BcSSP2, SsSSP3 and CcSSP92 protein sequences. Coloured amino acid residues represent hydrophobicity levels (Red = Hydrophobic, Blue = Hydrophilic). Triangles indicate amino acid changes that are specific to CcSSP92. Red triangles represent amino acid changes that are hypothesized to affect protein folding based on changes in hydrophobicity.

Determining the role of conserved CCL-SSPs in pathogenicity.

The creation and characterization of *B. cinerea Bcssp2* knockouts would elucidate whether the *BcSSP2* gene has a role in pathogenicity. Complementation of the *Bcssp2* mutant with the WT *BcSSP2* gene would confirm the role of this gene. Additional *Bcssp2* complementation experiments using either *CcSSP92* or *SsSSP3*, would determine if these genes are functionally redundant to *BcSSP2*. The inability of *CcSSP92* to complement the *Bcssp2* mutant would provide additional evidence that *C. camelliae CCL-SSP* genes do not function to induce host-cell necrosis.

Determining the interacting protein partners of BcSSP2 and SsSSP3.

To determine the likely interaction partners of BcSSP2 and SsSSP3, protein-protein interaction experiments would be conducted. The results of these experiments would also provide molecular information about the mechanism that leads to host-cell necrosis. A yeast-2-hybrid screen using a *Camellia* cDNA library as bait would be developed to identify putative interacting partners. Alternatively, a *N. benthamiana* cDNA library could be used, or a cDNA library from another suitable host. Bimolecular fluorescence complementation analysis would be utilized to confirm promising protein-protein interactions *in planta*.

Screening hosts for BcSSP2 and SsSSP3 necrosis-inducing phenotypes.

To determine whether the necrosis-inducing function of BcSSP2 and SsSSP3 follows the inverse gene-for-gene hypothesis, recombinant proteins could be in infiltrated into near isogenic host lines that vary in their *R* gene content. *Arabidopsis* accessions would be ideal for this screen, providing the host-cell necrosis phenotype is reproducible in this host species. Recombinant inbred lines of *Arabidopsis* could be used to facilitate the mapping of the reciprocal host gene.

7.5. Concluding remarks

In conclusion, *C. camelliae* is a necrotrophic fungus that has evolved to efficiently establish infection in the floral tissue of *Camellia* species and interspecific hybrids. Resistance to *C. camelliae* is present in several species of *Camellia*, namely those that are classified in section Theopsis. The type of resistance observed involves the induction of the plant immune system and results in characteristic PTI-associated downstream responses. Host genes involved in plant resistance were identified based on their differential expression patterns but still require functional validation. Interspecific hybrids of *Camellia* are reduced in their ability to resist *C. camelliae*. A strategy to increase interspecific hybrid resistance via backcrossing to section Theopsis species has been proposed and is currently being implemented by *Camellia* breeders at the Auckland Botanic Gardens (Fig. 7.1).

An asymptomatic period of fungal growth was observed during the initial establishment of *C. camelliae* within compatible *Camellia* petal tissue and was hypothesized to be mediated by *C .camelliae* fungal effectors. Comparative analysis of the predicted *C. camelliae*, *B. cinerea* and *S. sclerotiorum* secretomes identified proteins that conformed to the small secreted, cysteine rich profile of previously reported fungal effectors. A family of conserved *C. camelliae*-like small secreted proteins (CCL-SSPs) were identified in *C. camelliae* (n = 73) *B. cinerea* (n = 1) and *S. sclerotiorum* (n = 1). Functional characterization of this family indicated that the *B. cinerea* and *S. sclerotiorum* recombinant protein homologs were able to induce host-cell necrosis. If BcSSP2 or SsSSP3 are shown to contribute significantly to the virulence of their host organisms these recombinant proteins could be utilized to screen for disease resistance. The necrosis-inducing function of recombinant BcSSP2 and SsSSP3 was not observed for recombinant *C. camelliae* CCL-SSPs. Based on the lineage-specific expansion of the *C. camelliae CCL-SSP* genes and their lack of necrosis-inducing function, it is hypothesized that they may act to suppress the immune system of *Camellia*.

Unlike the host-generalist necrotrophs *B. cinerea* and *S. sclerotiorum, C. camelliae* has evolved to maintain the viability of its host by restricting infection to a single, renewable plant organ. The loss of necrosis-inducing ability in *C. camelliae* CCL-SSPs correlates with the evolution of *C. camelliae* host-specificity. Whether host-specificity has led to the functional diversification of *CCL-SSP* genes in *C. camelliae* is still to be determined. The elucidation of the function of *C. camelliae* CCL-SSP homologs and the mechanism that leads to BcSSP2/SsSSP3 host-cell necrosis will help to answer this question.

8. References

Ackerman, W. L. (1973). Species compatibility relationships within the genus *Camellia*. *J. Hered*, *64*, 356-358.

Adaskaveg, J. E., Dieguez-Uribeondo, J., Forster, H., Soto-Estrada, A. (2005). Subcuticular-intracellular hemibiotrophic and intercellular necrotrophic development of *Colletotrichum acutatum* on almond. *Phytopathology*, *95*(7), 751-758.

Aghnoum, R., & Niks, R. E. (2010). Specificity and levels of nonhost resistance to non-adapted *Blumeria graminis* forms in barley. *New Phytologist*, *185*(1), 275-284.

Akhatar, M., Jaiswal, A., Taj, G., Jaiswal, J. P., Qureshi, M. I., Singh, N. K. (2012) *DREB1/CBF* transcription factors: their structure, function and role in abiotic stress tolerance in plants. *J. Genet*, *91*, 385–395.

Amselem, J., Cuomo, C. A., van Kan, J. A., Viaud, M., Benito, E. P., Couloux, A., . . . Dickman, M. (2011). Genomic analysis of the necrotrophic fungal pathogens *Sclerotinia sclerotiorum* and *Botrytis cinerea*. *PLOS Genetics*, *7*(8), 1-27.

Andrew, M., Barua, R., Short, S. M., Kohn, L. M. (2012). Evidence for a common toolbox based on necrotrophy in a fungal lineage spanning necrotrophs, biotrophs, endophytes, host generalists and specialists. *PLOS One*, *7*(1), 1-12.

Anzalone, L. J. (1959). Studies on flower blight of *Camellia* and *Cercospora* leaf spot of *Photinia serrulata*. PhD Dissertation, Louisiana State University Baton Rouge.

Arenas, Y. C., Kalkman, E. R. I. C., Schouten, A., Dieho, M., Vredenbregt, P., Uwumukiza, B., Ruiz, M. O., van Kan, J. A. L. (2010). Functional analysis and mode of action of phytotoxic Nep1-like proteins of *Botrytis cinerea*. *Physiol. Mol. Plant Pathol*, *74*, 376–386.

Assaad, F. F., Qiu, J. L., Youngs, H., Ehrhardt, D., Zimmerli, L., Kalde, M., . . . Thordal-Christensen, H. (2004). The PEN1 syntaxin defines a novel cellular compartment upon fungal attack and is required for the timely assembly of papillae. *Molecular Biology of the Cell*, *15*(11), 5118-5129.

Azevedo, H., Lino-Neto, T., Tavares, R. M. (2008). The necrotroph *Botrytis cinerea* induces a non-host type II resistance mechanism in *Pinus pinaster* suspension-cultured cells. *Plant & cell physiology*, *49*(3), 386-395.

Bailey, B. (1995). Purification of a protein from culture filtrates of *Fusarium oxysporum* that induces ethylene and necrosis in leaves of *Erythroxylum coca*. *Phytopathol*, *85*, 1250–1255.

Bailey, T. L, Williams, N., Misleh, C., Li, W. W. (2006) MEME: discovering and analyzing DNA and protein sequence motifs. *Nucleic Acids Research*, *34*, 369–373.

Batra, L. R., & Korf, R. P. (1959). The species of *Ciborinia* pathogenic to herbaceous angiosperms. *American Journal of Botany*, *46*(6), 441-450.

Bellincampi, D., Cervone, F., Lionetti, V. (2014). Plant cell wall dynamics and wall-related susceptibility in plant–pathogen interactions. *Front. Plant Sci*, *5*, 228.

Benjamini, Y., & Hochberg, J. (1995). Controlling the false discovery rate - a practical and powerful approach to multiple testing. *J. R. Stat. Soc. Ser. B Stat. Methodol*, *57*(1), 289-300.

Bhuiyan, N. H., Selvaraj, G., Wei, Y., King, J. (2009). Gene expression profiling and silencing reveal that monolignol biosynthesis plays a critical role in penetration defence in wheat against powdery mildew invasion. *Journal of experimental botany*, *60*(2), 509-521.

Billon-Grand, G., Rascle, C., Droux, M., Rollins, J. A., Poussereau, N. (2011). pH modulation differs during sunflower cotyledon colonization by the two closely related necrotrophic fungi *Botrytis cinerea* and *Sclerotinia sclerotiorum*. *Molecular Plant Pathology*, *3*(6), 568-78.

Boetzer, M., Henkel, C. V., Jansen, H. J., Butler, D., Pirovano, W. (2011) Scaffolding pre-assembled contigs using SSPACE. *Bioinformatics*, *27*, 578-579.

Boland, G. J., & Hall, R. (1994). Index of plant hosts of *Sclerotinia sclerotiorum*. *Canadian Journal of Plant Pathology*. *16*(2), 93-108.

Bolton, M. D., Thomma, B. P. H. J., Nelson, B. D. (2006). *Sclerotinia sclerotiorum* (Lib.) de Bary: biology and molecular traits of a cosmopolitan pathogen. *Molecular Plant Pathology*, *7*(1), 1-16.

Bowyer, P., Clarke, B. R., Lunness, P., Daniels, M. J., Osbourn, A. E. (1995). Host range of a plant pathogenic fungus determined by a saponin detoxifying enzyme. *Science*, *267*(5196), 371-374.

Bradley, D. J., Kjellbom, P., Lamb, C. J. (1992). Elicitor and wound-induced oxidative cross-linking of a proline-rich plant cell wall protein: a novel, rapid defense response. *Cell*, *70*(1), 21-30.

Brunner, P. C., Torriani, S. F. F., Croll, D., Stukenbrock, E. H., McDonald, B. A. (2012). Coevolution and life cycle specialization of plant cell wall degrading enzymes in a hemibiotrophic pathogen. *Mol Biol Evol*, *30*, 1337-1347.

Burton, J. N., Adey, A., Patwardhan, R. P., Qiu, R., Kitzman, J. O., Shendure, J. (2013). Chromosome-scale scaffolding of *de novo* genome assemblies based on chromatin interactions. *Nat Biotech*, *31*(12), 1119-1125.

Cantu, D., Segovia, V., MacLean, D., Bayles, R., Chen, X., Kamoun, S., Dubcovsky, J.,Saunders, D, G, O., Uauy, C. (2013). Genome analyses of the wheat yellow (stripe) rust pathogen *Puccinia striiformis* f. sp. *tritici* reveal polymorphic and haustorial expressed secreted proteins as candidate effectors. *BMC Genomics*, *14*, 270.

Cantu, D., Vicente, A. R., Labavitch, J. M., Bennett, A. B., Powell, A. L. T. (2008). Strangers in the matrix: plant cell walls and pathogen susceptibility. *Trends in Plant Science*, *13*(11), 610-617.

Caracuel, Z., Roncero, M. I., Espeso, E. A., Gonzalez-Verdejo, C. I., Garcia-Maceira, F. I., Di Pietro, A. (2003). The pH signalling transcription factor *PacC* controls virulence in the plant pathogen *Fusarium oxysporum*. *Molecular microbiology*, *48*(3), 765-779.

Carpita, N. C., & Gibeaut, D. M. (1993). Structural models of primary cell walls in flowering plants: consistency of molecular structure with the physical properties of the walls during growth. *The Plant Journal*, *3*(1), 1–30.

Ceroni, A., Passerini, A., Vullo, A., Frasconi, P. (2006) DISULFIND: a disulfide bonding state and cysteine connectivity prediction server. *Nucleic Acids Res*, *34*, 177–181.

Chen, L., Zhou, Z. X., Yang, Y. J. (2006). Genetic improvement and breeding of tea plant (*Camellia sinensis*) in China: from individual selection to hybridization and molecular breeding. *Euphytica*, *154*(1-2), 239-248.

Collins, N. C., Thordal-Christensen, H., Lipka, V., Bau, S., Kombrink, E., Qiu, J. L., . . . Schulze-Lefert, P. (2003). SNARE-protein-mediated disease resistance at the plant cell wall. *Nature*, *425*(6961), 973-977.

Condon, B. J., Leng, Y., Wu, D., Bushley, K. E., Ohm, R. A., ...Mohdzainudin, N. (2013) Comparative genome structure, secondary metabolite, and effector coding capacity across *Cochliobolus pathogens*. *PLOS Genetics*, *9*(1), e1003233.

Conesa, A.,& Götz, S. (2008) Blast2GO: A comprehensive suite for functional analysis in plant genomics. *International Journal of Plant Genomics*, 1-13.

Coppin, E., Debuchy, R., Arnaise, S., Picard, M. (1997). Mating types and sexual development in filamentous ascomycetes. *Microbiol Mol Biol Rev*, *61*, 411–428.

Cox, M. P., Peterson, D. A., Biggs, P. J. (2010). SolexaQA: At-a-glance quality assessment of Illumina second-generation sequencing data. *BMC Bioinformatics*, *11*, 1-6.

Cremer, .K, Mathys, J., Vos, C., Froenicke, L., Michelmore, R. W., Cammue, B., de Coninck, B. (2013). RNAseq-based transcriptome analysis of *Lactuca sativa* infected by the fungal necrotroph *Botrytis cinerea*. *Plant Cell Environ*, *36*, 1992-2007.

Dallal, B. Z., Hegedus, D. D., Buchwaldt, L., Rimmer, S. R., Borhan, M. H. (2010). Expression and regulation of *Sclerotinia sclerotiorum* necrosis and ethylene–inducing peptides (NEPs). *Mol Plant Pathol*, *11*(1), 43-53.

Datta, K., Velazhahan, R., Oliva, N., Ona, I., Mew, T., Kush, G. S., Muthukrishnan, S., Datta, S. K. (1999). Over-expression of the cloned rice thaumatin-like protein (*PR-5*) gene in transgenic rice plants enhances environmental friendly resistance to *Rhizoctonia solani* causing sheath blight disease. *Theor. Appl. Genet*, *98*, 1138–1145.

Davies, G., & Henrissat, B. (1995). Structures and mechanisms of glycosyl hydrolases. *Structure*, *3*, 853–859

De Lorenzo, G., Brutus, A., Savatin, D. V., Sicilia, F., Cervone, F. (2011). Engineering plant resistance by constructing chimeric receptors that recognize damage-associated molecular patterns (DAMPs). *FEBS letters*, *585*(11), 1521-1528.

De Wit, P. J. (1977). A light and scanning-electron microscopic study of the infection of tomato plants by the virulent and avirulent races of *Cladosporium fulvum*. *Neth. J. Plant Path*, *83*, 109-122.

De Wit, P. J. G. M., Spikman, G. (1982). Evidence for the occurrence of race and cultivar-specific elicitors of necrosis in intercellular fluids of compatible interactions of *Cladosporium fulvum* and tomato. *Physiological Plant Pathology*, *21*, 1-11.

De Wit, P. J. G. M., Mehrabi, R., van den Burg, H. A., Stergiopoulos, I. (2009). Fungal effector proteins: past, present and future. *Molecular Plant Pathology*, *10*(6), 735-747.

Dean, R., van Kan, J. A. L., Pretorius, Z. A., Hammond-Kosack, K. E., Pietro, D. S., Spanu, P. D., . . . Foster, G. D. (2012). The top 10 fungal pathogens in molecular plant pathology. *Molecular Plant Pathology*, *13*(4), 414-430.

Debuchy, R., Berteaux-Lecellier, V., Silar, P. (2010) Mating systems and sexual morphogenesis in Ascomycetes. In: Borkovich KA, Ebbole DJ, editors. Cellular and molecular biology of filamentous fungi. Washington: ASM Press. pp. 501–535.

Deller, S., Hammond-Kosack, K. E., Rudd, J. J. (2011). The complex interactions between host immunity and non-biotrophic fungal pathogens of wheat leaves. *Journal of Plant Physiology*, *168*(1), 63-71.

Desmond, O. J., Edgar, C. I., Manners, J. M., Maclean, D. J., Schenk, P. M., Kazan, K. (2005). Methyl jasmonate induced gene expression in wheat delays symptom development by the crown rot pathogen *Fusarium pseudograminearum*. *Physiol. Mol. Plant Pathol*, *67*, 171–179.

Di Matteo, A., Federici, L., Mattei, B., Salvi, G., Johnson, K. A., Savino, C., . . . Cervone, F. (2003). The crystal structure of polygalacturonase-inhibiting protein (PGIP), a leucine-rich repeat protein involved in plant defense. *Proceedings of the National Academy of Sciences of the United States of America*, *100*(17), 10124-10128.

Dickman, M. B., de Figueiredo, P. (2013) Death be not proud—cell death control in plant fungal interactions. *PLOS Pathog*. *9*(9), e1003542.

Dickman, M. B., Podila, G. K., Kolattukudy, P. E. (1989). Insertion of cutinase gene into a wound pathogen enables it to infect intact host. *Nature*, *342*(6248), 446-448.

Dixon, R. A. (2001). Natural products and plant disease resistance. *Nature*, *411*(6839), 843-847.

Dodds, P. N., Lawrence, G. J., Catanzariti, A. M., Teh, T., Wang, C. I., Ayliffe, M. A., . . . Ellis, J. G. (2006). Direct protein interaction underlies gene-for-gene specificity and coevolution of the flax resistance genes and flax rust avirulence genes. *Proceedings of the National Academy of Sciences of the United States of America*, *103*(23), 8888-8893.

Dodds, P. N., & Rathjen, J. P. (2010). Plant immunity: towards an integrated view of plant-pathogen interactions. *Nature Reviews Genetics*. *11*(8), 539-548.

Dou, D., Zhou, J.-M. (2012). Phytopathogen effectors subverting host immunity: Different foes, similar battleground. *Cell Host Microbe*, *12*, 484–495.

Douglas, C. J., Hamberger, B., Ellis, M., Friedmann, M., Souza, C. D. A., Barbazuk, B. (2007). Genome-wide analyses of phenylpropanoid-related genes in Populus trichocarpa, *Arabidopsis thaliana*, and Oryza sativa: the Populus lignin toolbox and conservation and diversification of angiosperm gene families. *Canadian Journal of Botany-Revue Canadienne De Botanique*, *85*(12), 1182-1201.

Dubiella, U., Seybold, H., Durian, G., Komander, E., Lassig, R., Witte, C. P., Schulze, W. X., Romeis, T. (2013). Calcium-dependent protein kinase/NADPH oxidase activation circuit is required for rapid defense signal propagation. *Proceedings of the National Academy of Sciences*, *110*, 8744–8749.

Dufresne, M., Perfect, S., Pellier, A. L., Bailey, J. A., Langin, T. (2000). A GAL4-like protein is involved in the switch between biotrophic and necrotrophic phases of the infection process of *Colletotrichum lindemuthianum* on common bean. *The Plant Cell*, *12*(9), 1579-1590.

Duplessis, S., Cuomo, C. A., Lin, Y. C., Aerts, A., Tisserant, E., Veneault-Fourrey, C., . . . Martin, F. (2011). Obligate biotrophy features unravelled by the genomic analysis of rust fungi. *Proceedings of the National Academy of Sciences of the United States of America*, *108*(22), 9166-9171.

Eaton, C. J., Cox, M. P., Ambrose, B., Becker, M., Hesse, U., Schardl, C. L., Scott, B. (2010). Disruption of signaling in a fungal-grass symbiosis leads to pathogenesis. *Plant Physiol*. *153*, 1780-1794.

Emanuelsson, O., Nielsen, H., Brunak, S., von Heijne, G. (2000). Predicting subcellular localization of proteins based on their N-terminal amino acid sequence. *J. Mol. Biol*, *300*, 1005-1016.

Espino, J. J.; Gutiérrez-Sánchez, G.; Brito, N.; Shah, P.; Orlando, R.; González, C. (2010). The *Botrytis cinerea* early secretome. *Proteomics*, *10*, 3020-3034.

Fan, J., & Doerner, P. (2012). Genetic and molecular basis of nonhost disease resistance: complex, yes; silver bullet, no. *Curr. Opin. Plant Biol*, *15*(4), 400-406.

Faris, J. D., Zhang, Z. C., Lu, H. J., Lu, S. W., Reddy, L., Cloutier, S., . . . Friesen, T. L. (2010). A unique wheat disease resistance-like gene governs effector-triggered susceptibility to necrotrophic pathogens. *Proceedings of the National Academy of Sciences of the United States of America*, *107*(30), 13544-13549.

Flor, H. H. (1942). Inheritance of pathogenicity in *Melampsora lini*. *Phytopathology*, *32*(8), 653-669.

Flor, H. H. (1956). The complementary genic systems in flax and flax Rust. *Advances in Genetics Incorporating Molecular Genetic Medicine*, *8*, 29-54.

Fourie, J. F., & Holz, G. (1995). Initial infection processes by *Botrytis cinerea* on nectarine and plum fruit and the development of decay. *Phytopathology*, *85*(1), 82-87.

Frías, M., González, C., Brito, N. (2011). BcSpl1, a cerato–platanin family protein, contributes to *Botrytis cinerea* virulence and elicits the hypersensitive response in the host. *New Phytol*, *192*, 483-495.

Friedman, A. R., & Baker, B. J. (2007). The evolution of resistance genes in multi-protein plant resistance systems. *Current opinion in genetics & development*, *17*(6), 493-499.

Friesen, T. L., Meinhardt, S. W., Faris, J. D. (2007). The *Stagonospora nodorum*-wheat pathosystem involves multiple proteinaceous host-selective toxins and corresponding host sensitivity genes that interact in an inverse gene-for-gene manner. *The Plant journal*, *51*(4), 681-692.

Fu, L., Niu, B., Zhu, Z., Wu, S., Li, W. (2012). CD-HIT: accelerated for clustering the next generation sequencing data. *Bioinformatics*, *28*(23), 3150-3152.

Futagami, T., Mori, K., Yamashita, A., Wada, S., Kajiwara, Y., Takashita, H., Omori, T., Takegawa, K., Tashiro, K., Kuhara, S., Goto, M. (2011). Genome sequence of the white koji mold *Aspergillus kawachii* IFO 4308, used for brewing the Japanese distilled spirit shochu. *Eukaryot. Cell*, *10*, 1586–1587.

Galagan, J, E., Henn, M. R., Ma, L., Cuomo, C. A., Birren, B. (2005). Genomics of the fungal kingdom: Insights into eukaryotic biology. *Genome Res*, *15*, 1620-1631.

Gan, P., Ikeda, K., Irieda, H., Narusaka, M., O'Connell, R. J., Narusaka, Y., Takano, Y., Kubo, Y. and Shirasu, K. (2013). Comparative genomic and transcriptomic analyses reveal the hemibiotrophic stage shift of *Colletotrichum* fungi. *New Phytologist*, *197*, 1236–1249.

Gardiner, D. M., McDonald, M. C., Covarelli, L., Solomon, P. S., Rusu, A. G., Marshall, M., Kazan, K., McDonald, B., Manners, J. (2012) Comparative pathogenomics reveals horizontally acquired novel virulence genes in fungi infecting cereal hosts. *PLOS Pathog*, *8*(9), e1002952.

Gijzen, M., & Nürnberger, T. (2006). Nep1-like proteins from plants pathogens: Recruitment and diversification of the NPP1 domain across taxa. *Phytochemistry*, *16*(67), 1800-1807.

Gladieux, P., Ropars, J., Badouin, H., Branca, A., Aguileta, G., de Vienne, D. M., Rodríguez de la Vega, R. C., Branco, S. and Giraud, T. (2014). Fungal evolutionary genomics provides insight into the mechanisms of adaptive divergence in eukaryotes. *Molecular Ecology*, *23*, 753–773.

Glazebrook, J. (2005). Contrasting mechanisms of defense against biotrophic and necrotrophic pathogens. *Annual Review of Phytopathology*, *43*, 205-227.

Godfrey, D., Böhlenius, H., Pedersen, C., Zhang, Z., Emmersen, J., and Thordal-Christensen, H. (2010). Powdery mildew fungal effector candidates share N-terminal Y/F/WxC-motif. *BMC Genomics*, *11*, 317.

Godoy, G., Steadman, J. R., Dickman, M. B., Dam, R. (1990). Use of mutants to demonstrate the role of oxalic acid in pathogenicity of *Sclerotinia sclerotiorum* on *Phaseolus vulgaris*. *Physiological and Molecular Plant Pathology*, *37*(3), 179-191.

Gomez-Gomez, L., & Boller, T. (2002). Flagellin perception: a paradigm for innate immunity. *Trends in Plant Science*, *7*(6), 251-256.

Gomez-Gomez, L., Bauer, Z., Boller, T. (2001). Both the extracellular leucine-rich repeat domain and the kinase activity of FSL2 are required for flagellin binding and signalling in *Arabidopsis*. *The Plant Cell*, *13*(5), 1155-1163.

Gonzalez-Fernandez, R., Aloria, K., Valero-Galvan, J., Redondo, I., Arizmendi, J. M., Jorrin-Novo, J. V. (2013). Proteomic analysis of mycelium and secretome of different *Botrytis cinerea* wild-type strains. *J. Proteomics*, *97*, 195-221.

Govrin, E. M., Rachmilevitch, S., Tiwari, B. S., Soloman, M., Levine, A. (2006). An elicitor from *Botrytis cinerea* induces the hypersensitive response in *Arabidopsis thaliana* and other plants and promotes the gray mold disease. *Phytopathology*, *96*(3), 299-307.

Grabherr, M. G., Haas, B.J., Yassour, M., Levin, J. Z., Thompson, D. A., Amit, I., . . . Regev, A. (2011). Full-length transcriptome assembly from RNA-seq data without a reference genome. *Nat Biotechnol*, *29*(7), 644-52.

Groves, J. W., & Bowerman, C. A. (1955). The species of *Ciborinia* on *Populus*. *Canadian Journal of Botany-Revue Canadienne De Botanique*, *33*(6), 577-590.

Gu, K., Yang, B., Tian, D., Wu, L., Wang, D., Sreekala, C., . . . Yin, Z. (2005). R gene expression induced by a type-III effector triggers disease resistance in rice. *Nature*, *435*(7045) 1122-5.

Guyon, K., Balague, C., Roby, D., Raffaele, S. (2014). Secretome analysis reveals effector candidates associated with broad host range necrotrophy in the fungal plant pathogen *Sclerotinia sclerotiorum*. *BMC Genomics*, *15*, 336.

Hacquard, S., Joly, D. L., Lin, Y-C., Tisserant, E., Feau, N., Delaruelle, C., Legue, V., Kohler, A., Tanguay, P., Petre, B., Frey, P., Van de Peer, Y., Rouze, P., Martin, F., Hamelin, R. C., Duplessis, S. (2012). A comprehensive analysis of genes encoding small secreted proteins identifies candidate effectors in *Melampsora larici-populina* (poplar leaf rust). *Mol Plant Microbe Interact*, *25*(3), 279-293.

Hadwiger, L. A., & Culley, D. E. (1993). Nonhost resistance genes and race-specific resistance. *Trends in microbiology*, *1*(4), 136-141.

Hahn, M. G., Darvill, A. G.,Albersheim, P. (1981). Host-pathogen interactions : XIX. The endogenous elicitor, a fragment of a plant cell wall polysaccharide that elicits phytoalexin accumulation in soybeans. *Plant Physiology*, *68*(5), 1161-1169.

Hammerschmidt, R. (1999). Phytoalexins: what have we learned after 60 years? *Annu. Rev. Phytopathol*, *37*, 285-306.

Hammond-Kosack, K. E., & Rudd, J. J. (2008). Plant resistance signalling hijacked by a necrotrophic fungal pathogen. *Plant signaling & behavior*, *3*(11), 993-995.

Hansen, H. H., & Thomas, H. E. (1940). Flower blight of Camellias. *Phytopathology*, *30*, 166-170.

Hansen, K., Brenner, S., Dudoit, S. (2010). Biases in Illumina transcriptome sequencing caused by random hexamer priming. *Nucleic Acids Research*, *38*, 1-7.

Hao, B. L., Wang, H., Xu, Z., Gao, L. (2009). A fungal phylogeny based on 82 complete genomes using the composition vector method. *BMC Evolutionary Biology*, 9, 195.

Hao, X. Y., Yu, K., Ma, Q., Song, X. H., Li, H. L., Wang, M. G. (2011). Histochemical studies on the accumulation of H_2O_2 and hypersensitive cell death in the nonhost resistance of pepper against *Blumeria graminis* f. sp *tritici*. *Physiological and Molecular Plant Pathology*, *76*(2), 104-111.

Hara, K. (1919). On a *Sclerotinia* disease of camellia. *Dainippon Saurinkwaiho*, *436*, 29-31.

Hawksworth, D. L. (1991). The fungal dimension of biodiversity: Magnitude, significance, and conservation. *Mycological Research*, *95*, 641-655.

Heath, M. C. (2000). Nonhost resistance and nonspecific plant defenses. *Curr. Opin. Plant Biol*, *3*(4), 315-9.

Henson, L., & Valleau, W. D. (1940). The production of apothecia of *Sclerotinia scleotiorum* and *S. trifoliorum* in culture. *Phytopathology*, *30*, 869-873.

Holt, C., & Yandell, M. (2011). MAKER2: an annotation pipeline and genome-database management tool for second-generation genome projects. *BMC Bioinformatics*, *12*, 491.

Howard, R. J., Ferrari, M. A., Roach, D. H., Money, N. P. (1991). Penetration of hard substrates by a fungus employing enormous turgor pressures. *Proceedings of the National Academy of Sciences of the United States of America*, *88*(24), 11281-11284.

Huang, K., Czymmek, K. J., Caplan, J. L., Sweigard, J. A., Donofrio, N. M. (2011). HYR1-mediated detoxification of reactive oxygen species is required for full virulence in the rice blast fungus. *PLOS Pathog*, *7*(4), e1001335.

Huckelhoven, R., & Kogel, K. H. (1998). Tissue-specific superoxide generation at interaction sites in resistant and susceptible near-isogenic barley lines attacked by the powdery mildew fungus (*Erysiphe graminis* f. sp. *hordei*). *Molecular Plant-Microbe Interactions*, *11*(4), 292-300.

Huckelhoven, R., Dechert, C., Kogel, K. H. (2001). Non-host resistance of barley is associated with a hydrogen peroxide burst at sites of attempted penetration by wheat powdery mildew fungus. *Molecular Plant Pathology*, *2*(4), 199-205.

Jabs, T., Tschope, M., Colling, C., Hahlbrock, K., Scheel, D. (1997). Elicitor-stimulated ion fluxes and O^{2-} from the oxidative burst are essential components in triggering defense gene activation and phytoalexin synthesis in parsley. *Proceedings of the National Academy of Sciences of the United States of America*, *94*(9), 4800-4805.

Jacobs, A. K., Lipka, V., Burton, R. A., Panstruga, R., Strizhov, N., Schulze-Lefert, P., Fincher, G. B. (2003). An *Arabidopsis* callose synthase, *GSL5*, is required for wound and papillary callose formation. *The Plant Cell*, *15*(11), 2503-2513.

Jia, Y., McAdams, S. A., Bryan, G. T., Hershey, H. P., Valent, B. (2000). Direct interaction of resistance gene and avirulence gene products confers rice blast resistance. *The EMBO journal*, *19*(15), 4004-4014.

Johnson, N. (2008) Hybrid incompatibility and speciation. *Nature Education*, *1*(1), 20.

Jones, J. D. G., & Dangl, J. L. (2006). The plant immune system. *Nature*, *444*(7117), 323-329.

Joosten, H. J., Han, Y., Niu, W. L., Vervoort, J., Dunaway-Mariano, D., Schaap, P. J. (2008). Identification of fungal oxaloacetate hydrolyase within the isocitrate lyase/PEP mutase enzyme superfamily using a sequence marker-based method. *Proteins-Structure Function and Bioinformatics*, *70*(1), 157-166.

Jupe, F., Pritchard, L., Etherington, G. J., Mackenzie, K., Cock, P. J., Wright, F., . . . Hein, I. (2012). Identification and localisation of the NB-LRR gene family within the potato genome. *BMC Genomics*, *13*, 75.

Jurick, W. M., & Rollins, J. A. (2007). Deletion of the adenylate cyclase (sac1) gene affects multiple developmental pathways and pathogenicity in *Sclerotinia sclerotiorum*. *Fungal Genet. Biol*. *44*(6), 521-530.

Kamper, J., Kahmann, R., Bolker, M., Ma, L. J., Brefort, T., ... Birren, B. W. (2006) Insights from the genome of the biotrophic fungal plant pathogen *Ustilago maydis*. *Nature*, *444*, 97–101.

Kang, Z. S., Wang, C. F., Huang, L. L., Zhang, H. C., Han, Q. M., Buchenauer, H. (2010). Cytochemical localization of reactive oxygen species O^{2-} and H_2O_2 and peroxidase in the incompatible and compatible interaction of wheat *Puccinia striiformis* f. sp *tritici*. *Physiological and Molecular Plant Pathology*, *74*(3-4), 221-229.

Kars, I., Krooshof, G., Wagemakers, C. A. M., Joosten, R., Benen, J. A. E. and Van Kan, J. A .L. (2005). Necrotising activity of five *Botrytis cinerea* endopolygalacturonases produced in *Pichia pastoris*. *Plant J*, *43*, 213–225.

Kasza, Z., Vagvölgyi, C., Fèvre, M. and Cotton, P. (2004). Molecular characterization and *in planta* detection of *Sclerotinia sclerotiorum* endopolygalacturonase genes. *Curr. Microbiol*, *48*, 208–213.

Kawahara, Y., Oono, Y., Kanamori, H., Matsumoto, T., Itoh, T., Minami, E. (2012) Simultaneous RNA-Seq analysis of a mixed transcriptome of rice and blast fungus Interaction. *PLOS ONE*, *7*(11) e49423.

Kelley, B. S., Lee, S. J., Damasceno, C. M., Chakravarthy, S., Kim, B. D., Martin, G. B., Rose, J. K. (2010). A secreted effector protein (SNE1) from *Phytophthora infestans* is a broadly acting suppressor of programmed cell death. *The Plant journal*, *62*(3), 357-366.

Keon, J. P. R., Byrde, R .J . W., Cooper, R. M. (1987) Some aspects of fungal enzymes that degrade plant cell walls. In Fungal Infection of Plants (Pegg, G.F. and Ayres, P.G., eds). Cambridge: Cambridge University Press, pp. 133–157.

Keon, J., Antoniw, J., Carzaniga, R., Deller, S., Ward, J. L., Baker, J. M., . . . Rudd, J. J. (2007). Transcriptional adaptation of *Mycosphaerella graminicola* to programmed cell death (PCD) of its susceptible wheat host. *Molecular Plant-Microbe Interactions*, *20*(2), 178-193.

Kiba, A., Takata, O., Ohnishi, K., Hikichi, Y. (2006). Comparative analysis of induction pattern of programmed cell death and defense-related responses during hypersensitive cell death and development of bacterial necrotic leaf spots in eggplant. *Planta*, *224*(5), 981-994.

Kim, C. Y., & Zhang, S. (2004). Activation of a mitogen-activated protein kinase cascade induces WRKY family of transcription factors and defense genes in tobacco. *The Plant Journal*, *38*(1), 142-151.

Kim, H. J., Chen, C. B., Kabbage, M., Dickman, M. B. (2011). Identification and characterization of *Sclerotinia sclerotiorum* NADPH oxidases. *Appl. Environ. Microb*. *77*(21), 7721-7729.

Kim, K. S., Min, J. Y., Dickman, M. B. (2008). Oxalic acid is an elicitor of plant programmed cell death during *Sclerotinia sclerotiorum* disease development. *Molecular Plant-Microbe Interactions*, *21*(5), 605-612.

Kishore, G.K., Pande, S, Podile, A. R. (2005). Biological control of collar rot disease with broad-spectrum antifungal bacteria associated with groundnut. *Can J Microbiol*. *51*(2), 123-32.

Kleemann, J., Rincon-Rivera, L. J., Takahara, H., Neumann, U., van Themaat, E. V. L., van der Does, H. C., . . . O'Connell, R. J. (2012). Sequential delivery of host-induced virulence effectors by appressoria and intracellular hyphae of the phytopathogen *Colletotrichum higginsianum*. *PLOS Pathogens*, *8*(4), e1002643.

Kobayashi, Y., Yamada, M., Kobayashi, I., Kunoh, H. (1997). Actin microfilaments are required for the expression of nonhost resistance in higher plants. *Plant and Cell Physiology*, *38*(6), 725-733.

Kobe, B., & Kajava, A. V. (2001). The leucine-rich repeat as a protein recognition motif. *Current opinion in structural biology*, *11*(6), 725-732.

Koeck, M., Hardham, A. R., Dodds, P. N. (2011). The role of effectors of biotrophic and hemibiotrophic fungi in infection. *Cellular Microbiology*, *13*(12), 1849-1857.

Kogel, K. H., Huckelhoven, R., Fodor, J., Preis, C. (1999). Hypersensitive cell death and papilla formation in barley attacked by the powdery mildew fungus are associated with hydrogen peroxide but not with salicylic acid accumulation. *Plant Physiology*, *119*(4), 1251-1260.

Kohn, L. M., & Nagasawa, E. (1984). A taxonomic reassessment of *Sclerotinia camelliae* Hara (*Ciborinia camelliae* Kohn), with observations on flower blight of *Camellia* in Japan. *Transactions of the Mycological Society of Japan*, *25*(2), 149-161.

Kombrink, A., Thomma, B. P. H. J. (2013). LysM effectors: Secreted proteins supporting fungal life. *PLOS Pathog*, *9*(12), e1003769.

Krogh, A., Larsson, B., von Heijne, G., Sonnhammer, E. L. L. (2001). Predicting transmembrane protein topology with a hidden markov model: application to complete genomes. *J. Mol. Biol*, *305*, 567-580.

Lai, A. G., Denton-Giles, M., Mueller-Roeber, B., Schippers, J. H. M., Dijkwel, P. P. (2011). Positional information resolves structural variations and uncovers an evolutionarily divergent genetic locus in accessions of *Arabidopsis thaliana*. *Genome Biology and Evolution*, *3*, 627–640.

Lamb, C., & Dixon, R. A. (1997). The oxidative burst in plant disease resistance. *Annu. Rev. Plant Physiol*, *48*, 251-275.

Langmead, B., Salzberg, S. (2012). Fast gapped-read alignment with Bowtie 2. *Nature Methods*, *9*, 357-359.

Lauge, R., & De Wit, P. J. (1998). Fungal avirulence genes: structure and possible functions. *Fungal Genet. Biol*, *24*, 285–297.

Lauge, R., Joosten, M. H. A. J., van den Ackerveken, G. F. J. M., van den Broek, H. W. J., and de Wit, P. J. G. M. (1997). The *in planta*-produced extracellular proteins ECP1 and ECP2 of *Cladosporium fulvum* are virulence factors. *Mol. Plant Microbe Interact*, *10*, 725–734.

Lee, M. H., & Bostock, R. M. (2006). Induction, regulation, and role in pathogenesis of appressoria in *Monilinia fructicola*. *Phytopathology*, *96*(10), 1072-1080.

Lee, S. J., & Rose, J. K. (2010). Mediation of the transition from biotrophy to necrotrophy in hemibiotrophic plant pathogens by secreted effector proteins. *Plant signaling & behavior*, *5*(6), 769-772.

Levine, A., Tenhaken, R., Dixon, R., Lamb, C. (1994). H_2O_2 from the oxidative burst orchestrates the plant hypersensitive disease resistance response. *Cell*, *79*(4), 583-593.

Li, H., Goodwin, P. H., Han, Q., Huang, L., Kang, Z. (2012). Microscopy and proteomic analysis of the non-host resistance of *Oryza sativa* to the wheat leaf rust fungus, *Puccinia triticina* f. sp. *tritici*. *Plant Cell Reports*, *31*(4), 637-650.

Li, R., Rimmer, R., Buchwaldt, L., Sharpe, A. G., Senguin-Swartz, G. and Hegedus, D. D. (2004). Interaction of *Sclerotinia sclerotiorum* with *Brassica napus*: cloning and characterization of endo- and exo-polygalacturonases expressed during saprophytic and parasitic modes. *Fungal Genet. Biol*, *41*, 754–765.

Li, W., Godzic, A. (2006). Cd-hit: a fast program for clustering and computing large sets of protein or nucleotide sequences. *Bioinformatics*, *22*, 1658-1659.

Lindhout, P., (2002). The perspectives of polygenic resistance in breeding for durable disease resistance. *Euphytica*, *124*, 217–226.

Lipka, U., Fuchs, R., Kuhns, C., Petutschnig, E., Lipka, V. (2010). Live and let die: *Arabidopsis* nonhost resistance to powdery mildews. *European journal of cell biology*, *89*(2-3), 194-199.

Lipka, U., Fuchs, R., Lipka, V. (2008). *Arabidopsis* non-host resistance to powdery mildews. *Curr. Opin. Plant Biol*, *11*(4), 404-11.

Lipka, V., Dittgen, J., Bednarek, P., Bhat, R., Wiermer, M., Stein, M., . . . Schulze-Lefert, P. (2005). Pre- and postinvasion defences both contribute to nonhost resistance in *Arabidopsis*. *Science*, *310*(5751), 1180-1183.

Lippincott-Schwartz, J., Roberts, T. H., Hirschberg, K. (2000). Secretory protein trafficking and organelle dynamics in living cells. *Annu. Rev. Cell Dev. Biol*, *16*, 557–589.

Liu, Z., Faris, J. D., Oliver, R. P., Tan, K-C., Solomon, P. S., McDonald, M. C., McDonald, B. A., Nunez, A., Lu, S., Rasmussen, J. B., Friesen, T. L. (2009). SnTox3 acts in effector triggered susceptibility to induce disease on wheat carrying the *Snn3* gene. *PLOS Pathog*, *5*(9), e1000581.

Liu, Z., Zhang, Z., Faris, J. D., Oliver, R. P., Syme, R., McDonald, M. C., McDonald, B. A., Solomon, P. S., Lu, S., Shelver, W, L., Xu, S., Friesen, T. L. (2012). The cysteine rich necrotrophic effector SnTox1 produced by *Stagonospora nodorum* triggers susceptibility of wheat lines harboring *Snn1*. *PLOS Pathog*, *8*(1), e1002467.

Lorang, J., Kidarsa, T., Bradford, C., Gilbert, B., Curtis, M., Tzeng, S. C., Maier, C. S., Wolpert, T. J. (2012). Tricking the guard: exploiting plant defense for disease susceptibility. *Science*, *338*, 659–62.

Lotze, M. T., Zeh, H. J., Rubartelli, A., Sparvero, L. J., Amoscato, A. A., Washburn, N. R., . . . Billiar, T. (2007). The grateful dead: damage-associated molecular pattern molecules and reduction/oxidation regulate immunity. *Immunological reviews*, *220*, 60-81.

Ma, L., Lukasik, E., Gawehns, F., Takken, F. L. (2012). The use of agroinfiltration for transient expression of plant resistance and fungal effector proteins in *Nicotiana benthamiana* leaves. *Methods Mol. Biol*, *835*, 61-74.

Ma, W., & Berkowitz, G. A. (2007). The grateful dead: calcium and cell death in plant innate immunity. *Cellular Microbiology*, *9*(11), 2571-2585.

Machida, M., Yamada, O., Gomi, K. (2008). Genomics of *Aspergillus oryzae*: learning from the history of Koji mold and exploration of its future. *DNA Res*, *15*, 173-183.

Mahdavi, F., Sariah, M., Maziah, M. (2012). Expression of rice thaumatin-like protein gene in transgenic banana plants enhances resistance to fusarium wilt. *Appl Biochem Biotechnol*, *166*(4), 1008–1019.

Marcet-Houben, M., Ballester, A. R., de la Fuente, B., Harries, E., Marcos, J. F., Gonzalez-Candelas, L., Gabaldon, T. (2012). Genome sequence of the necrotrophic fungus *Penicillium digitatum*, the main postharvest pathogen of citrus. *BMC Genomics*, *13*, 646.

Mardanov, A. V., Beletsky, A. V., Kadnikov, V. V., Ignatov, A. N., Ravin, N. V. (2014). Draft genome sequence of *Sclerotinia borealis*, a psychrophilic plant pathogenic fungus. *Genome Announc*, *2*(1), e01175-13.

Marshall, R., Kombrink, A., Motteram, J., Loza-Reyes, E., Lucas, J., Hammond-Kosack, K. E., Thomma, B. P. H. J. and Rudd, J .J. (2011). Analysis of two in planta expressed LysM effector homologs from the fungus *Mycosphaerella graminicola* reveals novel functional properties and varying contributions to virulence on wheat. *Plant Physiol*, *156*, 756–769.

Martinez, J. P., Oesch, N. W., Ciuffetti, L. M. (2004). Characterization of the multiple-copy host-selective toxin gene, *ToxB*, in pathogenic and nonpathogenic isolates of *Pyrenophora tritici-repentis*. *Mol Plant-Microbe Interact*. *17*(5), 467-474.
McDowell, J. M. (2011). Genomes of obligate plant pathogens reveal adaptations for obligate parasitism. *Proceedings of the National Academy of Sciences of the United States of America*, *108*(22), 8921-8922.
Min, X. J., Butler, G., Storms, R., Tsang, A. (2005) OrfPredictor: predicting protein-coding regions in EST-derived sequences. *Nucleic Acids Res*, *33*, 677-680.
Mithen, R. (1992). Leaf glucosinolate profiles and their relationship to pest and disease resistance in oilseed rape. *Euphytica*, *63*, 71-83.
Molina, L., & Kahmann, R. (2007). An *Ustilago maydis* gene involved in H_2O_2 detoxification is required for virulence. *Plant Cell*, *19*(7), 2293-309.
Moose, S. P., & Mumm, R. H. (2008). Molecular plant breeding as the foundation for 21st century crop improvement. *Plant Physiol*, *147*(3), 969-977.
Morais do Amaral, A., Antoniw, J., Rudd, J. J., Hammond-Kosack, K. E. (2012). Defining the predicted protein secretome of the fungal wheat leaf pathogen *Mycosphaerella graminicola*. *PLoS ONE*, *7*(12), e49904.
Mur, L. A., Carver, T. L., Prats, E. (2006). NO way to live; the various roles of nitric oxide in plant-pathogen interactions. *Journal of experimental botany*, *57*(3), 489-505.
Mysore, K. S., & Ryu, C. M. (2004). Nonhost resistance: how much do we know? *Trends in Plant Science*, *9*(2), 97-104.
Ngugi, H. K., & Scherm, H. (2006). Biology of flower-infecting fungi. *Annual Review of Phytopathology*, *44*, 261-282.
Nielsen, H., Engelbrecht, J., Brunak, S., von Heijne, G. (1997). Identification of prokaryotic and eukaryotic signal peptides and prediction of their cleavage sites. *Protein Engineering*, *10*, 1-6.
Niks, R. E., & Marcel, T. (2009). Nonhost and basal resistance: how to explain specificity? *New Phytol*, *182*(4), 817-28.
Nishimura, M. T., Stein, M., Hou, B. H., Vogel, J. P., Edwards, H., Somerville, S. C. (2003). Loss of a callose synthase results in salicylic acid-dependent disease resistance. *Science*, *301*(5635), 969-972.
Noda, J., Brito, N., Gonzalez, C. (2010) The *Botrytis cinerea* xylanase Xyn11A contributes to virulence with its necrotizing activity, not with its catalytic activity. *BMC Plant Biol*, *10*, 38.
O'Brien, H. E., Parrent, J. L., Jackson, J. A., Moncalvo, J. M., Vilgalys, R. (2005). Fungal community analysis by large-scale sequencing of environmental samples. *Applied and environmental microbiology*, *71*(9), 5544-5550.
O'Connell, R. J., Thon, M. R., Hacquard, S., Amyotte, S. G., Kleemann, J., Torres, M. F., . . . Vaillancourt, L. J. (2012). Lifestyle transitions in plant pathogenic *Colletotrichum* fungi deciphered by genome and transcriptome analyses. *Nature Genetics*, *44*(9), 1060-1065.

Oliver, R. P., & Ipcho, S. V. S. (2004). *Arabidopsis* pathology breathes new life into the necrotrophs vs. biotrophs classification of fungal pathogens. *Molecular Plant Pathology*, *5*(4), 347-352.

Oliver, R. P., & Solomon, P. S. (2004). Does the oxidative stress used by plants for defence provide a source of nutrients for pathogenic fungi? *Trends in Plant Science*, *9*(10), 472-473.

Oliver, R. P., Lord, M., Rybak, K., Faris, J. D., Solomon, P. S. (2008). Emergence of tan spot disease caused by toxigenic *Pyrenophora tritici-repentis* in Australia is not associated with increased deployment of toxin-sensitive cultivars. *Phytopathology*, *98*(5), 488-491.

Olivier, C. Y., Gossen, B. D., Seguin-Swartz, G. (2008). Impact of flower age and colour on infection of bean and alfalfa by *Sclerotinia sclerotiorum*. *Canadian Journal of Plant Pathology-Revue Canadienne De Phytopathologie*, *30*, 1-8.

Osbourn, A. E. (1996). Preformed antimicrobial compounds and plant defense against fungal attack. *Plant Cell*, *8*(10), 1821-1831.

Ottmann, C., Luberacki, B., Kufner, I., Koch, W., Brunner, F., Weyand, M., Mattinen, L., Pirhonen, M., Anderluh, G., Seitz, H. U., Nurnberger, T., Oecking, C. (2009). A common toxin fold mediates microbial attack and plant defense. *Proc Natl Acad Sci*, (25),10359*106*-10364.

Pajonk, S., Kwon, C., Clemens, N., Panstruga, R., Schulze-Lefert, P. (2008). Activity determinants and functional specialization of *Arabidopsis* PEN1 syntaxin in innate immunity. *The Journal of biological chemistry*, *283*(40), 26974-26984.

Palloix, A., Ayme, V., Moury, B. (2009). Durability of plant major resistance genes to pathogens depends on the genetic background, experimental evidence and consequences for breeding strategies. *New Phytol*, *183*, 190–199.

Papadopoulou, K., Melton, R. E., Leggett, M., Daniels, M. J., Osbourn, A. E. (1999). Compromised disease resistance in saponin-deficient plants. *Proceedings of the National Academy of Sciences of the United States of America*, *96*(22), 12923-12928.

Park, H. C., Kang, Y. H., Chun, H. J., Koo, J. C., Cheong, Y. H., Kim, C. Y., . . . Cho, M. J. (2002). Characterization of a stamen-specific cDNA encoding a novel plant defensin in Chinese cabbage. *Plant molecular biology*, *50*(1), 59-69.

Pedersen, C., van Themaat, E. V., McGuffin ,L. J., Abbott, J. C., Burgis, T. A., Barton, G., Bindschedler, L. V., Lu, X., Maekawa, T., Wessling, R., . . . Spanu, P. D. (2012). Structure and evolution of barley powdery mildew effector candidates. *BMC* Genomics, *13*, 694.

Pedras, M. S., Minic, Z., Sarma-Mamillapalle, V. K. (2009). Synthetic inhibitors of the fungal detoxifying enzyme brassinin oxidase based on the phytoalexin camalexin scaffold. *Journal of Agricultural and Food Chemistry*, *57*(6), 2429-2435.

Pendleton, A. L., Smith, K. E., Feau, N., Martin, F. M., Grigoriev, I. V., Hamelin, R., Nelson, C. D., Burleigh, J. G., Davis, J. M. (2014). Duplications and losses in gene families of rust pathogens highlight putative effectors *Front Plant Sci*. *5*, 299.

Perfect, S. E., & Green, J. R. (2001). Infection structures of biotrophic and hemibiotrophic fungal plant pathogens. *Molecular Plant Pathology*, *2*(2), 101-108.

Petersen, T. N., Brunak, S., von Heijne, G., Nielsen, H. (2011). SignalP 4.0: discriminating signal peptides from transmembrane regions. *Nature Methods*, *8*, 785-786.

Porta, H,. & Rocha-Sosa, M. (2002). Plant lipoxygenases. Physiological and molecular features. *Plant Physiology*, *130*, 15–21.

Punja, Z. K., & Zhang, Y. Y. (1993). Plant chitinases and their roles in resistance to fungal diseases. *J. Nematol*, *25*, 526–540.

Qutob, D., Kemmerling, B., Brunner, F., Kufner, I., Engelhardt, S., Gust, A. A., Luberacki, B., Seitz, H. U., Stahl, D., Rauhut, T., . . . Nurnberger, T. (2006). Phytotoxicity and innate immune responses induced by Nep1-like proteins. *Plant Cell*, *18*, 3721–3744.

Raffaele, S., and Kamoun, S. (2012). Genome evolution in filamentous plant pathogens: why bigger can be better. *Nat. Rev. Microbiol*, *10*, 417–430.

Rampitsch, C.; Day, J.; Subramaniam, R.; Walkowiak, S. (2013). Comparative secretome analysis of *Fusarium graminearum* and two of its non-pathogenic mutants upon deoxynivalenol induction in vitro. *Proteomics*, *13*, 1913– 1921.

Ranf, S., Eschen-Lippold, L., Pecher, P., Lee, J., Scheel, D. (2011). Interplay between calcium signalling and early signalling elements during defence responses to microbe or damage-associated molecular patterns. *The Plant journal*, *68*(1), 100-113.

Ribot, C., Hirsch, J., Balzergue, S., Tharreau, D., Notteghem, J. L., Lebrun, M. H., Morel, J. B. (2008). Susceptibility of rice to the blast fungus, *Magnaporthe grisea*. *Journal of Plant Physiology*, *165*(1), 114-124.

Richter, T. E., & Ronald, P. C. (2000). The evolution of disease resistance genes. *Plant molecular biology*, *42*(1), 195-204.

Rojas, C. M., Senthil-Kumar, M., Wang, K., Ryu, C. M., Kaundal, A., Mysore, K. S. (2012). Glycolate oxidase modulates reactive oxygen species-mediated signal transduction during nonhost resistance in *Nicotiana benthamiana* and *Arabidopsis*. *The Plant Cell24*, (1), 336-352.

Rolke, Y., Liu, S., Quidde, T., Williamson, B., Schouten, A., Weltring, K. M., . . . Tudzynski, P. (2004). Functional analysis of H_2O_2-generating systems in *Botrytis cinerea*: the major Cu-Zn-superoxide dismutase (BCSOD1) contributes to virulence on French bean, whereas a glucose oxidase (BCGOD1) is dispensable. *Molecular Plant Pathology*, *5*(1), 17-27.

Rolland, S., Bruel, C., Rascle, C., Girard, V., Billon-Grand, G., Poussereau, N. (2009). pH controls both transcription and post-translational processing of the protease BcACP1 in the phytopathogenic fungus *Botrytis cinerea*. *Microbiology*, *155*(6), 2097-2105.

Rollins, J. A. (2003). The *Sclerotinia sclerotiorum* Pac1 gene is required for sclerotial development and virulence. *Molecular Plant-Microbe Interactions*, *16*(9), 785-795.

Rollins, J. A., & Dickman, M. B. (2001). pH signaling in *Sclerotinia sclerotiorum*: identification of a *pacC/RIM1* homolog. *Applied and environmental microbiology*, *67*(1), 75-81.

Rooney, H. C., Van't Klooster, J. W., van der Hoorn, R. A., Joosten, M. H., Jones, J. D., de Wit, P. J. (2005). *Cladosporium* Avr2 inhibits tomato Rcr3 protease required for Cf-2-dependent disease resistance. *Science*, *308*(5729), 1783-1786.

Rumbold, P., Biely, M., Mastihubova, M., Gudelj, G., Guebitz, K. H., Robra, B. A. (2003) Prior purification and properties of a feruloyl esterase involved in lignocellulose degradation by *Aureobasidium pullulans*. Appl Environ Microbiol, *69*, 5622–5626.

Saito, I., & Kaji, K. (2006). *Ciborinia gentianae* sp. nov., the casual organism of sclerotial flower blight of cut-flower gentians. *Mycoscience*, *47*, 41-47.

Salzberg, S. L., Yorke, J. A. (2005). Beware of mis-assembled genomes. *Bioinformatics*, *21*, 4320-4321.

Schouten, A., Tenberge, K. B., Vermeer, J., Stewart, J., Wagemakers, L., Williamson, B., van Kan, J. A. (2002). Functional analysis of an extracellular catalase of *Botrytis cinerea*. *Molecular Plant Pathology*, *3*(4), 227-238.

Schouten, A., van Baarlen, P., van Kan, J. A. L. (2008). Phytotoxic Nep1-like proteins from the necrotrophic fungus *Botrytis cinerea* associate with membranes and the nucleus of plant cells. *New Phytologist*, 177, 493–505.

Schulze-Lefert, P., & Panstruga, R, (2011). A molecular evolutionary concept connecting nonhost resistance, pathogen host range, and pathogen speciation. *Trends Plant Sci*, *16*(3), 117-125.

Segmuller, N., Ellendorf, U., Tudzynski, B., Tudzynski, P. (2007). BcSAK1, a stress-activated mitogen-activated protein kinase, is involved in vegetative differentiation and pathogenicity in *Botrytis cinerea*. *Eukaryotic cell*, *6*(2), 211-221.

Segmuller, N., Kokkelink, L., Giesbert, S., Odinius, D., van Kan, J., Tudzynski, P. (2008). NADPH oxidases are involved in differentiation and pathogenicity in *Botrytis cinerea*. *Molecular Plant-Picrobe Interactions*, *21*(6), 808-819.

Sfondrini, N., and De Guadenzi. (2012). Web camellia register. International Camellia Society Web Register, Pavia, Italy. Retrieved November 03, 2012 from http://camellia.unipv.it/camelliadb2/.

Shah, P.; Atwood, J. A.; Orlando, R.; El Mubarek, H.; Podila, G. K.; Davis, M. R.(2009). Comparative proteomic analysis of *Botrytis cinerea* secretome. *J. Proteome Res*, *8*, 1123– 1130.

Shi, C., Yang, H., Wei, C., Yu, O., Zhang, Z., Jiang, C., . . . Wan, X. (2011). Deep sequencing of the *Camellia sinensis* transcriptome revealed candidate genes for major metabolic pathways of tea-specific compounds. *BMC Genomics*, *12*(1), 131.

Skibbe, D. S., Doehlemann, G., Fernandes, J., Walbot, V. (2010). Maize tumors caused by *Ustilago maydis* require organ-specific genes in host and pathogen. *Science*, *328*(5974), 89-92.

Smith, D. A., Harrer, J. M., Cleveland, T. E. (1981). Simultaneous detoxification of phytoalexins by *Fusarium solani* f. sp. *phaseoli*. *Phytopathology*, *71*, 1212-1215.

Soanes, D. M., Alam, I., Cornell, M., Wong, H. M., Hedeler, C., Paton, N. W., Rattray, M., Hubbard, S. J., Oliver, S. G., Talbot, N. J. (2008) Comparative genome analysis of filamentous fungi reveals gene family expansions associated with fungal pathogenesis. *PLoS ONE*, *3*(6), e2300.

Solomon, P. S., Oliver, R. P. (2001). The nitrogen content of the tomato leaf apoplast increases during infection by *Cladosporium fulvum*. *Planta*, *213*(2), 241-9.

Solomon, P. S., Oliver, R. P. (2002). Evidence that gamma-aminobutyric acid is a major nitrogen source during *Cladosporium fulvum* infection of tomato. *Planta*, *214*(3), 414-420.

Song, J., Win, J., Tian, M. Y., Schornack, S., Kaschani, F., Ilyas, M., . . . Kamoun, S. (2009). Apoplastic effectors secreted by two unrelated eukaryotic plant pathogens target the tomato defense protease Rcr3. *Proceedings of the National Academy of Sciences of the United States of America*, *106*(5), 1654-1659.

Song, X., Rampitsch, C., Soltani, B., Mauthe, W., Linning, R., Banks, T., . . . Bakkeren, G. (2011). Proteome analysis of wheat leaf rust fungus, *Puccinia triticina*, infection structures enriched for haustoria. *Proteomics*, *11*(5), 944-963.

Sperschneider, J., Ying, H., Dodds, P. N., Gardiner, D. M., Upadhyaya, N. M., Singh, K. B., Manners, J. M., Taylor, J. M. (2014). Diversifying selection in the wheat stem rust fungus acts predominantly on the pathogen-associated gene families and reveals candidate effectors. *Frontiers in Plant Science*, *5*, 1-13.

Staats, M., Van Baarlen, P., Schouten, A., Van Kan, J. A. L., Bakker, F. T. (2007). Positive selection in phytotoxic protein-encoding genes of *Botrytis* species. *Fungal Genetics and Biology*, *4*, 52–63.

Stakman, E. C. (1915). Relation between *Puccinia graminis* and plants highly resistant to its attack. *Journal of Agricultural Research*, *4*, 193-199.

Stanke, M., Steinkamp, R., Waack, S., Morgenstern, B. (2004) AUGUSTUS: a web server for gene finding in eukaryotes. *Nucleic Acids Research*, *32*, 309-312.

Staskawicz, B. J., Dahlbeck, D., Keen, N. T. (1984). Cloned avirulence gene of *Pseudomonas syringae* pv. *glycinea* determines race-specific incompatibility on

Glycine max (L) Merr. *Proceedings of the National Academy of Sciences*, *81*(19), 6024-6028.

Stein, M., Dittgen, J., Sanchez-Rodriguez, C., Hou, B. H., Molina, A., Schulze-Lefert, P., . . Somerville, S. (2006). *Arabidopsis* PEN3/PDR8, an ATP binding cassette transporter, contributes to nonhost resistance to inappropriate pathogens that enter by direct penetration. *Plant Cell*, *18*(3), 731-746.

Stergiopoulos, I., de Wit, P. J. (2009). Fungal effector proteins. *Annu Rev Phytopathol*, *47*, 233–263.

Stergiopoulos, I., Kourmpetis, Y. A., Slot, J. C., Bakker, F. T., De Wit, P. J., Rokas, A. (2012). *In silico* characterization and molecular evolutionary analysis of a novel superfamily of fungal effector proteins. *Mol Biol Evol*, *29*(11), 3371-3384.

Stergiopoulos, I., van den Burg, H. A., Okmen, B., Beenen, H. G., van Liere, S., Kema, G. H., de Wit, P. J. G. M. (2010). Tomato Cf resistance proteins mediate recognition of cognate homologous effectors from fungi pathogenic on dicots and monocots. *Proc. Natl. Acad. Sci*, *107*, 7610–7615.

Sweat, T. A., Lorang, J. M., Bakker, E. G., Wolpert, T. J. (2008). Characterization of natural and induced variation in the *LOV1* gene, a CC-NB-LRR gene conferring victorin sensitivity and disease susceptibility in *Arabidopsis*. *Molecular Plant-Microbe Interactions*, *21*(1), 7-19.

Takemoto, D., & Hardham, A. R. (2004). The cytoskeleton as a regulator and target of biotic interactions in plants. *Plant Physiology*, *136*(4), 3864-3876.

Takemoto, D., Jones, D. A., Hardham, A. R. (2003). GFP-tagging of cell components reveals the dynamics of subcellular re-organization in response to infection of *Arabidopsis* by oomycete pathogens. *The Plant journal*, *33*(4), 775-792.

Tamura, M., & Tachida, H. (2011). Evolution of the number of LRRs in plant disease resistance genes. *Molecular genetics and genomics*, *285*, 393-402.

Tan, K. C., Oliver, R. P., Solomon, P. S., Moffat, C. S. (2010). Proteinaceous necrotrophic effectors in fungal virulence. *Functional Plant Biology*, *37*, 907–912.

Tanabe, S., Nishizawa, Y., Minami, E. (2009). Effects of catalase on the accumulation of H_2O_2 in rice cells inoculated with rice blast fungus, *Magnaporthe oryzae*. *Physiol Plant*, *137*, 148–154.

Tanaka, S., Ishihama, N., Yoshioka, H., Huser, A., O'Connell, R., Tsuji, G., . . . Kubo, Y. (2009). The *Colletotrichum orbiculare ssd1* mutant enhances *Nicotiana benthamiana* basal resistance by activating a mitogen-activated protein kinase pathway. *The Plant Cell*, *21*(8), 2517-2526.

Taylor, C. H. (1999). Studies of Camellia Flower Blight (*Ciborinia camelliae*) in New Zealand. MSc dissertation, Massey University, Palmerston North.

Taylor, C. H. (2004). Studies of Camellia flower blight (*Ciborinia camelliae* Kohn). Doctoral dissertation, Massey University, Palmerston North.

Taylor, C. H., Long, P. G. (2000). Review of literature on camellia flower blight caused by *Ciborinia camelliae*. *New Zeal. J. Crop Hort*, *28*(2), 123-138.

Temme, N., & Tudzynski, P. (2009). Does Botrytis cinerea ignore H_2O_2-induced oxidative stress during infection? Characterization of botrytis activator protein 1. *Molecular plant-microbe interactions*, *22*(8), 987-998.

Templeton, M. D., Rikkerink, E. H. A., and Beever, R. E. (1994). Small, cysteine-rich proteins and recognition in fungal-plant interactions. *Mol. Plant-Microbe Interact*. *7*, 320–325.

ten Have, A., Dekkers, E., Kay, J., Phylip, L. H., van Kan, J. A. (2004). An aspartic proteinase gene family in the filamentous fungus *Botrytis cinerea* contains members with novel features. *Microbiology*, *150*(7), 2475-2489.

Thomazella, D. P., Teixeira, P. J., Oliveira, H. C., Saviani, E. E., Rincones, J., Toni, I. M., . . . Pereira, G. A. (2012). The hemibiotrophic cacao pathogen *Moniliophthora perniciosa* depends on a mitochondrial alternative oxidase for biotrophic development. *The New phytologist*. *194*(4), 1025-34.

Thomma, B. P. H. J., Penninckx, I. A. M. A., Broekaert, W .F., Cammue, B. P. A. (2001) The complexity of disease signaling in *Arabidopsis*. *Curr. Opin. Immunol*, *13*, 63–68.

Thomma, B. P., Van Esse, H. P., Crous, P. W., De Wit, P. J. G. M. (2005). *Cladosporium fulvum* (syn. *Passalora fulva*), a highly specialized plant pathogen as a model for functional studies on plant pathogenic Mycosphaerellaceae. *Molecular Plant Pathology*, *6*(4), 379-393.

Thomma, B. P., Nelissen, I., Eggermont, K., Broekaert, W. F. (1999). Deficiency in phytoalexin production causes enhanced susceptibility of *Arabidopsis thaliana* to the fungus *Alternaria brassicicola*. *The Plant journal*, *19*(2), 163-171.

Thordal-Christensen, H., Zhang, Z. G., Wei, Y. D., Collinge, D. B. (1997). Subcellular localization of H_2O_2 in plants. H_2O_2 accumulation in papillae and hypersensitive response during the barley-powdery mildew interaction. *Plant Journal*, *11*(6), 1187-1194.

Thornburg, R. W., Carter, C., Powell, A., Mittler, R., Rizhsky, L., Horner, H. T. (2003). A major function of the tobacco floral nectary is defense against microbial attack. *Plant Systematics and Evolution*, *238*, 211-218.

Torres, M. A., Dangl, J. L., Jones, J. D. (2002). *Arabidopsis* gp91phox homologues AtrbohD and AtrbohF are required for accumulation of reactive oxygen intermediates in the plant defense response. *Proceedings of the National Academy of Sciences of the United States of America*, *99*(1), 517-522.

Torres, M. A., Morales, J., Sánchez-Rodríguez, C., Molina, A., Dangl, J. L. (2013). Functional interplay between *Arabidopsis* NADPH oxidases and heterotrimeric G protein. *Mol. Plant-Microbe Interact*, *26*, 686-694.

Tsuda, K., & Katagiri, F. (2010). Comparing signaling mechanisms engaged in pattern-triggered and effector-triggered immunity. *Current Opinion in Plant Biology*, *13*(4), 459-465.

Tsuda, K., Sato, M., Stoddard, T., Glazebrook, J., Katagiri, F. (2009). Network properties of robust immunity in plants. *PLOS Genetics*, *5*(12).

Uma, B., Rani, T. S., & Podile, A. R. (2011). Warriors at the gate that never sleep: Non-host resistance in plants. *Journal of Plant Physiology*, *168*(18), 2141-2152.

van den Brink, J., & de Vries, R. P. (2011). Fungal enzyme sets for plant polysaccharide degradation. *Appl. Microbiol. Biotechnol*, *91*, 1477–1492.

Van der Biezen, E. A., & Jones, J. D. (1998). Plant disease-resistance proteins and the gene-for-gene concept. *Trends in biochemical sciences*, *23*(12), 454-456.

van Esse, H. P., Bolton, M. D., Stergiopoulos, I., de Wit, P. J., Thomma, B. P. (2007). The chitin-binding *Cladosporium fulvum* effector protein Avr4 is a virulence factor. *Mol. Plant-Microbe Interact*, *20*(9), 1092-101.

van Esse, H. P., van Klooster, J. W., Bolton, M. D., Yadeta, K. A., van Baarlen, P., Boeren, S., Vervoort, J., de Wit, P. J., Thomma, B. P. (2008). The *Cladosporium fulvum* virulence protein Avr2 inhibits host proteases required for basal defense. *Plant Cell*, *20*(7), 1948-63.

van Toor, R. F., Jaspers, M. V., Stewart, A. (2001). Evaluation of acibenzolar-S-methyl for induction of resistance in camellia flowers to *Ciborinia camelliae* infection. *New Zealand Plant Protection*, *54*, 209-212

van Toor, R. F., Dench, M. W., MJaspers, M. V., Stewart, A. (2005a). Tree mulches reduce sclerotial numbers and apothecial production by *Ciborinia camelliae*. *New Zeal. J. Crop Hort*. *33*(2), 161-168.

van Toor, R. F., Jaspers, M. V., Stewart, A. (2005b). Effect of soil microorganisms on viability of sclerotia of *Ciborinia camelliae*, the causal agent of camellia flower blight. *New Zeal. J. Crop Hort*, *33*(2), 149-160.

van Toor, R. F., Jaspers, M. V., Stewart, A. (2005c). Wood rotting fungi and pine mulches enhance parasitism of *Ciborinia camelliae* sclerotia *in vitro*. *New Zeal. J. Crop Hort*, *33*(4), 389-397.

van Etten, H. D., Mansfield, J. W., Bailey, J. A., Farmer, E. E. (1994). Two classes of plant antibiotics: phytoalexins versus ‘phytoanticipins’. The Plant Cell, 6(9), 1191-1192.

Vargas, W. A., Martin, J. M., Rech, G. E., Rivera, L. P., Benito, E. P., Diaz-Minguez, J. M., . . . Sukno, S. A. (2012). Plant defense mechanisms are activated during biotrophic and necrotrophic development of *Colletotricum graminicola* in maize. *Plant Physiology*, *158*(3), 1342-1358.

Verdonk, J. C., Haring, M. A., van Tunen, A. J., Schuurink, R. C. (2005).ODORANT1 regulates fragrance biosynthesis in petunia flowers. *The Plant Cell*, *17*, 1612–1624.

Veronese, P., Ruiz, M. T., Coca, M. A., Hernandez-Lopez, A., Lee, H., Ibeas, J. I., . . . Narasimhan, M. L. (2003). In defense against pathogens. Both plant sentinels and foot soldiers need to know the enemy. *Plant Physiology*, *131*(4), 1580-1590.

Vijayan, K., Zhang, W., Tso, C. (2009). Molecular taxonomy of *Camellia* (Theaceae) inferred from nrITS sequences. *Am. J. Bot*, *96*(7), 1348-1360.

Vingnanasingam, V. (2002). Confocal microscopy of infection by, and resistance to, *Ciborinia camelliae* in *Camellia* species and the potential for biocontrol. PhD Dissertation, Massey University, Palmerston North.

Vleeshouwers, V. G., Rietman, H., Krenek, P., Champouret, N., Young, C., Oh, S. K., . . . Van der Vossen, E. A. (2008). Effector genomics accelerates discovery and functional profiling of potato disease resistance and *Phytophthora infestans* avirulence genes. *PLOS one*, *3*(8).

Voegele, R. T., Struck, C., Hahn, M., Mendgen, K. (2001). The role of haustoria in sugar supply during infection of broad bean by the rust fungus *Uromyces fabae*. *Proceedings of the National Academy of Sciences of the United States of America*, *98*(14), 8133-8138.

Wang, L., Feng, Z., Wang, X., Zhang, X: (2010) DEGseq: an R package for identifying differentially expressed genes from RNA-seq data. *Bioinformatics*, *26*, 136-138.

Wang, Z., Mao, H., Dong, C. H., Ji, R. Q., Cai, L., Fu, H., Liu, S. Y. (2009). Overexpression of *Brassica napus* MPK4 enhances resistance to *Sclerotinia sclerotiorum* in oilseed rape. *Molecular Plant-Microbe Interactions*, *22*(3), 235-244.

Wapinski, I., Pfeffer, A., Friedman, N., Regev, A. (2007). Natural history and evolutionary principles of gene duplication in fungi. *Nature*, *449*, 54–61.

Ward, J. A., Ponnala, L., Weber, C. A. (2012). Strategies for transcriptome analysis in non-model plants. *American Journal of Botany*, *99*(2), 267-276.

Wasmann, C. C., & Van Etten, H. (1996). Transformation-mediated chromosome loss and disruption of a gene for pisatin demethylase decreases the virulence of *Nectria haematococca* on pea. *Molecular Plant Microbe Interactions*, *9*, 793-803.

Whetzel, H. H. (1945). A synopsis of the genera and species of the Sclerotiniaceae, a family of stromatic inoperculate Discomycetes. *Mycologia*, *37*, 648-714.

Williams, B., Kabbage, M., Kim, H. J., Britt, R., Dickman, M. B. (2011). Tipping the balance: *Sclerotinia sclerotiorum* secreted oxalic acid suppresses host defenses by manipulating the host redox environment. *PLOS Pathogens*, *7*(6).

Williamson, B., Tudzynski, B., Tudzynski, P., van Kan, J. A. (2007). *Botrytis cinerea*: the cause of grey mould disease. *Molecular Plant Pathology*, *8*(5), 561-580.

Wilson, R. A., & Talbot, N. J. (2009). Under pressure: investigating the biology of plant infection by *Magnaporthe oryzae*. *Nature Rev. Microbiol*, *7*(3), 185-95.

Win, J., Morgan, W., Bos, J., Krasileva, K. V., Cano, L. M., Chaparro-Garcia, A., Ammar, R., Staskawicz, B. J., and Kamoun, S. (2007). Adaptive evolution has targeted the C-Terminal domain of the RXLR effectors of plant pathogenic oomycetes. *Plant Cell*, *19*, 2349–2369.

Wu, Z. Y., Raven, P. H., Hong, D. Y. (2007). Flora of China (Hippocastanaceae through Theaceae). Pages 367-412. Science Press, Beijing.

Xu, B., Yang, Z. (2013). PamlX: A graphical user interface for PAML. *Mol Biol Evol*, *30*, 2723-2724.

Yamaguchi, Y., Huffaker, A., Bryan, A. C., Tax, F. E., Ryan, C. A. (2010). PEPR2 is a second receptor for the Pep1 and Pep2 peptides and contributes to defense responses in *Arabidopsis*. *The Plant Cell*, *22*(2), 508-522.

Yandell, M., Ence, D. (2012). A beginner's guide to eukaryotic genome annotation. *Nature Reviews Genetics*, *13*, 329–342.

Yun, B. W., Atkinson, H. A., Gaborit, C., Greenland, A., Read, N. D., Pallas, J. A., Loake, G. J. (2003). Loss of actin cytoskeletal function and EDS1 activity, in combination, severely compromises non-host resistance in *Arabidopsis* against wheat powdery mildew. *The Plant Journal*, *34*(6), 768-777.

Zeier, J., Delledonne, M., Mishina, T., Severi, E., Sonoda, M., Lamb, C. (2004). Genetic elucidation of nitric oxide signaling in incompatible plant-pathogen interactions. *Plant Physiology*, *136*(1), 2875-2886.

Zerbino, D.R., Birney, E. (2008). Velvet: algorithms for *de novo* short read assembly using de Bruijn graphs. *Genome Res*, *18*, 821-829.

Zhang, Z., Feechan, A., Pedersen, C., Newman, M. A., Qiu, J. L., Olesen, K. L., and Thordal-Christensen, H. (2007). A SNARE-protein has opposing functions in penetration resistance and defence signalling pathways. *Plant J*, *49,* 302-312.

Zhao, Z. T., Liu, H. Q., Wang, C. F., Xu, J. R. (2013). Comparative analysis of fungal genomes reveals different plant cell wall degrading capacity in fungi. *BMC Genomics*, *14*, 274.

Zhou B. J., Jia P. S., Gao F., Guo H. S. (2012). Molecular characterization and functional analysis of a necrosis- and ethylene-inducing, protein-encoding gene family from *Verticillium dahliae*. *Mol. Plant Microbe Interact*. *25*, 964–975.

Zhu, W., Wei, W., Fu, Y., Cheng, J., Xie, J., Li, G., Yi, X., Kang, Z., Dickman, M. B., Jiang, D. (2013). A secretory protein of necrotrophic fungus *Sclerotinia sclerotiorum* that suppresses host resistance. *PLOS ONE*, *8*(1), e53901.

Zimmerli, L., Stein, M., Lipka, V., Schulze-Lefert, P., Somerville, S. (2004). Host and non-host pathogens elicit different jasmonate/ethylene responses in *Arabidopsis*. *The Plant journal*, *40*(5), 633-646.

Zuccaro, A., Lahrmann, U., Guldener, U., Langen, G., Pfiffi, S., Biedenkopf, D., Kogel, K. H. (2011). Endophytic life strategies decoded by genome and transcriptome analyses of the mutualistic root symbiont *Piriformospora indica*. *PLOS Pathogens*, *7*(10).

Zummo, N. (1960). Studies on chemical control of petal blight of *Camellia* incited by *Sclerotinia camelliae*. PhD Dissertation, Louisiana State University, Baton Rouge.

Zummo, N., & Plakidas, A. G. (1961). Spread of petal blight of camellias by air-borne ascospores of *Sclerotinia camelliae*. *Phytopathology*, *51*(1), 69.

9. Appendices

Appendix 9.1A. Taxonomy, distribution and accession number information for *Camellia* species harvested from Auckland Botanic Gardens, New Zealand

Camellia species/ interspecific hybrids	Camellia subgenus	Camellia section	Natural Distribution[A]	ABG accession no.
C. 'Nicky Crisp'	N/A	N/A	N/A	850001
C. japonica ssp. *japonica var. macrocarpa*	Camellia	Camellia	China, Japan, South Korea, Taiwan	890167
C. bailinshanica	Camellia	Camellia	China	20010655
C. chekiangoleosa	Camellia	Camellia	China	941420
C. huiliensis	Camellia	Camellia	China	981156
C. jinshajiangica	Camellia	Camellia	China	20010661
C. mairei var. mairei	Camellia	Camellia	China	981159
C. pitardii var. pitardii	Camellia	Camellia	China	850090
C. pitardii var. yunnanica	Camellia	Camellia	China	981163
C. polyodonta	Camellia	Camellia	China	930311
C. saluenensis	Camellia	Camellia	China	930704
C. subintegra	Camellia	Camellia	China	941309
C. xichengensis	Camellia	Camellia	China	20010665
C. oleifera	Camellia	Oleifera	China, Laos, Myanmar, Vietnam	890164
C. brevistyla	Camellia	Paracamellia	China, Taiwan	950744
C. fluviatilis	Camellia	Paracamellia	China, India, Myanmar	None
C. grijsii	Camellia	Paracamellia	China	930319
C. kissi var. kissi	Camellia	Paracamellia	Bhutan, Cambodia, China, India, Laos, Myanmar, Nepal, Thailand, Vietnam	920181
C. microphylla	Camellia	Paracamellia	China	950747
C. miyagii	Camellia	Paracamellia	Ryukyu Islands *(Chang)*	950746
C. puniceiflora	Camellia	Paracamellia	China, Taiwan	No tag
C. yuhsienensis	Camellia	Paracamellia	China	970744
C. henryana	Camellia	Pseudocamellia	China	981155
C. trichocarpa	Camellia	Pseudocamellia	China	951182
C. caudata	Metacamellia	Eriandria	China, India, Myanmar, Nepal, Taiwan, Vietnam.	970729
C. melliana	Metacamellia	Eriandria	China	951159
C. crassipes	Metacamellia	Theopsis	China	930320
C. cuspidata var. cuspidata	Metacamellia	Theopsis	China	890165

Camellia species/interspecific hybrids	Camellia subgenus	Camellia section	Natural Distribution[A]	ABG accession no.
C. euryoides	Metacamellia	Theopsis	China, Taiwan	941280
C. fraterna	Metacamellia	Theopsis	China	890165
C. longicarpa	Metacamellia	Theopsis	China	921481
C. rosiflora	Metacamellia	Theopsis	China *(Chang)*	921473
C. transarisanensis	Metacamellia	Theopsis	China, Taiwan	20040761
C. transnokoensis	Metacamellia	Theopsis	Ryuku Islands, Taiwan	960895
C. tsaii var. tsaii	Metacamellia	Theopsis	China, Myanmar, Vietnam	941313
C. lutchuensis	Camellia	Theopsis	China, Ryukyu Islands, Taiwan	981158
C. granthamiana	Protocamellia	Archecamellia	China	890166
C. yunnanensis	Protocamellia	Stereocarpus	China	890174
C. nitidissima var. nitidissima	Thea	Chrysantha	China, Vietnam	20070466
C. sinensis var. assamica	Thea	Thea	China, Laos, Myanmar, Thailand, Vietnam	930308
C. sinensis var. sinensis	Thea	Thea	China, India, Japan, South Korea, Taiwan	941308

[A] Natural distribution information referenced from Wu, Z. Y., P. H. Raven, and D. Y. Hong. 2007. Flora of China (Hippocastanaceae through Theaceae). Pages 367-412. Science Press, Beijing.

Appendix 9.1B. *Camellia* species and interspecific hybrids harvested from Heartwood Nursery, CA

No.	Parentage	Cultivar names	Mean bloom diameter (mm)
1.	(*C. reticulata* x *C. japonica*) x [*C. reticulata* x (*C. saluenensis* x *C. transnokoensis*)]	Heartwood '0216'	70
2.	*C. pitardii* var. *pitardii* x *C. japonica* (Cont.)	*Camellia* 'Nicky Crisp'	63
3.	*C. pitardii* var. *yunnanica* x (*C. reticulata* x [*C. reticulata* x *C. fraterna*])[A]	Heartwood '9619'	63
4.	*C. japonica* x *C. transnokoensis*	Heartwood unknown	42
5.	(*C. reticulata* x *C. japonica*) x (*C. reticulata* x [*C. reticulata* x *C. fraterna*])	Heartwood '0333'	65
6.	(*C. pitardii* var. *yunnanica* x *C. reticulata*) x (*C. saluenensis* x *C. transnokoensis*)	Heartwood '201'	90 [C]
7.	(*C. pitardii* var. *yunnanica* x *C. reticulata*) x [(*C. pitardii* var. *yunnanica* x *C. reticulata*) x (*C. japonica* x *C. fraterna*)]	*Camellia* 'Avalon Sunrise'	68
8.	*C. pitardii* var. *yunnanica* x (*C. reticulata* x [*C. reticulata* x *C. fraterna*])[A]	Heartwood '9612'	72
9.	*C. pitardii* var. *yunnanica* x (*C. pitardii* var. *yunnanica* x *C. fraterna*)	Heartwood unknown	47
10.	(*C. japonica* x *C. lutchuensis*) x (*C. pitardii* var. *yunnanica* x *C. yunnanensis*)	Heartwood unknown	68
11.	{*C. japonica* x [(*C. saluenensis* x *C. japonica*) x (*C. japonica* x *C. lutchuensis*)]} x (*C. pitardii* var. *yunnanica* x *C. yunnanensis*)	Heartwood '9934' x *Camellia* 'High Fragrance'	73
12.	(*C. reticulata* x *C. fraterna*) x (*C. japonica* x *C. fraterna*)	Heartwood '370376'	57
13.	*C. fraterna* x (*C. pitardii* var. *yunnanica* x *C. reticulata*)	Heartwood '77D'	45
14.	*C. grijsii* x (*C. pitardii* var. *yunnanica* x *C. reticulata*)	Heartwood '9860'	60 [C]
15.	*C. japonica* x (*C. reticulata* x *C. forrestii*)	Heartwood '0990'	82
16.	(*C. pitardii* var. *yunnanica* x *C. yunnanensis*) x (*C. japonica* x *C. lutchuensis*)	Heartwood '9934' x *Camellia* 'Minato-no-haru'	78
17.	*C. saluenensis* x *C. lutchuensis*	*Camellia* 'Salute'	38
18.	*C. japonica* x *C. lutchuensis*	*Camellia* 'Scentuous'	52
19.	*C. japonica* x *C. transnokoensis*	*Camellia* 'Sweet Jane'	50
20.	*C. lutchuensis*[B]	*Camellia lutchuensis*	27
21.	*C. lutchuensis*[B]	*Camellia lutchuensis*	23

[A] Morphologically diverse offspring from the same original cross.
[B] *C. lutchuensis* from two different localities.
[C] Data based on two biological replicates.

Appendix 9.2. Primers used in this study

Primer	Target	Sequence (5' to 3')
CAL-228F	Calmodulin gDNA of *C. camelliae*	GAATTCAAGGAGGCCTTCTCCC
CAL-737R	Calmodulin gDNA of *C. camelliae*	CATCTTTCTTGCCATCATAG
G3PDH-Fbis	Glyceraldehyde-3-phosphate dehydrogenase gDNA of *C. camelliae*	GCTGTCAACGATCCTTTCAT
G3PDH-Rbis	Glyceraldehyde-3-phosphate dehydrogenase gDNA of *C. camelliae*	ACCAGGAAACCAACTTGACG
HSP60fwd-deg	Heat-shock protein 60 gDNA of *C. camelliae*	CAACAATTGAGATTCGCCCATAAG
HSP60rev-deg	Heat-shock protein 60 gDNA of *C. camelliae*	GATAGATCCAGTGGTACCGAGCAT
nc-gACT2 F	Actin gDNA of *Camellia* 'Nicky Crisp'	CCTTCACCATTCCAGTTCCAT
nc-gACT2 Re	Actin gDNA of *Camellia* 'Nicky Crisp'	CGTCTTCTCCGTCTCCTCACT
f-gTUB2 F	Tubulin gDNA of *C. camelliae*	CGGTATGGGTACGCTTTTGAT
f-gTUB2 R	Tubulin gDNA of *C. camelliae*	AACTGATGGACGGAGAGGGTA
f-gNAD1 F	Nicotinamide adenine dinucleotide gDNA of *C. camelliae*	AATACTGGGGCATTGTGAAGG
f-gNAD1 R	Nicotinamide adenine dinucleotide gDNA of *C. camelliae*	TCTGCGAACCATAGAAGACGA
nc-gGAPDH1 F	Glyceraldehyde-3-phosphate dehydrogenase cDNA of *Camellia* 'Nicky Crisp'	GTGTCAACCGACTTTATTGGTGA
nc-gGAPDH1 R	Glyceraldehyde-3-phosphate dehydrogenase cDNA of *Camellia* 'Nicky Crisp'	CTGTAACCCCATTCGTTGTCATA
nc-gACT1 F	Actin cDNA of *Camellia* 'Nicky Crisp'	CCAGAATCCAGCACAATACCA
nc-gACT1 R	Actin cDNA of *Camellia* 'Nicky Crisp'	ACCCCAAAGCAAACAGAGAAA
cdna-nad1 F	Nicotinamide adenine dinucleotide cDNA of *C. camelliae*	AATGGAAGCAATATGAAGAAGCTC
cdna-nad1 R	Nicotinamide adenine dinucleotide cDNA of *C. camelliae*	CATCACCGCAAACATAGAAGTAAG
cdna-tub3 F	Tubulin cDNA of *C. camelliae*	ACAAATGTACGACCCCAAGAAC
cdna-tub3 R	Tubulin cDNA of *C. camelliae*	ACCTTACCACGGAAGATAGCAG
cdna-166b F	CcSSP33 cDNA of *C. camelliae*	CCTCCACACTCATTTTGAATCG
cdna-166b R	CcSSP33 cDNA of *C. camelliae*	GTCCTGGAATACACAGCAATGG
cdna-410c F	CcSSP94 cDNA of *C. camelliae*	CCACACTCTCTTCAAATCATCAAA
cdna-410c R	CcSSP94 cDNA of *C. camelliae*	CTATCATCCCTGGCTAAACAACAG
cdna-409b F	CcSSP41 cDNA of *C. camelliae*	CCTCAGGACTCTGCTGTCGTTAT
cdna-409b R	CcSSP41 cDNA of *C. camelliae*	CCCTCCAGATATACGCCATTTAC
cdna-203a F	CcSSP43 cDNA of *C. camelliae*	GTTACACCGACTCAGACCTCAAC
cdna-203a R	CcSSP43 cDNA of *C. camelliae*	TAACACATTGAAAATTGCCTCCT
cdna-123a F	CcSSP37 cDNA of *C. camelliae*	ATTCATCTCCCTCGCTTTATTTGT
cdna-123a R	CcSSP37 cDNA of *C. camelliae*	GCTCGAATATACACAACAATGTGC
cdna-4090a F	CcSSP93 cDNA of *C. camelliae*	TGAGAACTCTCTTATGGGCAACAT
cdna-4090a R	CcSSP93 cDNA of *C. camelliae*	TAAGCGACCCTAATAAGTGTTTCG
cdna-1753a F	CcSSP81 cDNA of *C. camelliae*	GGTCAACTGGGACACCAAGA

Primer	Target	Sequence (5' to 3')
cdna-1753a R	CcSSP81 cDNA of *C. camelliae*	GGGAGCAGCAGTGTTACGAG
cdna-243.6a F	CcSSP31 cDNA of *C. camelliae*	CCGTCTTATACCTCAAGTGTCGAT
cdna-243.6a R	CcSSP31 cDNA of *C. camelliae*	CATTTATAATTTCCACCCCCATT
cdna-243.5a F	CcSSP36 cDNA of *C. camelliae*	AGCCTTTTTCCTCATCGCTACTAT
cdna-243.5a R	CcSSP36 cDNA of *C. camelliae*	TACCGATCTTGGTTGGAGTTACAC
AOX 5'	pPICZA plasmid DNA	GACTGGTTCCAATTGACAAGC
Cc33_nostop R	CcSSP33 construct pPICZA plasmid DNA	TTGTTCGGGCCCTTTGTTTCTAAA
Cc94_nostop R	CcSSP94 construct pPICZA plasmid DNA	TTGTTCGGGCCCCTTCCATCCTCT
Cc43_nostop R	CcSSP43 construct pPICZA plasmid DNA	TTGTTCGGGCCCCTTCTTAGGCAT
Cc37_nostop R	CcSSP37 construct pPICZA plasmid DNA	TTGTTCGGGCCCTTTAGGCTGTGG
Cc93_nostop R	CcSSP93 construct pPICZA plasmid DNA	TTGTTCGGGCCCTTTATAAGTATT
Cc81_nostop R	CcSSP81 construct pPICZA plasmid DNA	TTGTTCGGGCCCTTTCTCGGCACC
Cc31_nostop R	CcSSP31 construct pPICZA plasmid DNA	TTGTTCGGGCCCTTTCTTTGGTGA
Bc2-nostop R	BcSSP2 construct pPICZA plasmid DNA	TTGTTCGGGCCCTTTTTGCTTATA
Ss3 nostop R	SsSSP3 construct pPICZA plasmid DNA	TTGTTCGGGCCCTTTTTGTTTATA

Appendix 9.3. Aerial secondary hyphae of *Ciborinia camelliae* during infection of *Camellia* 'Nicky Crisp'

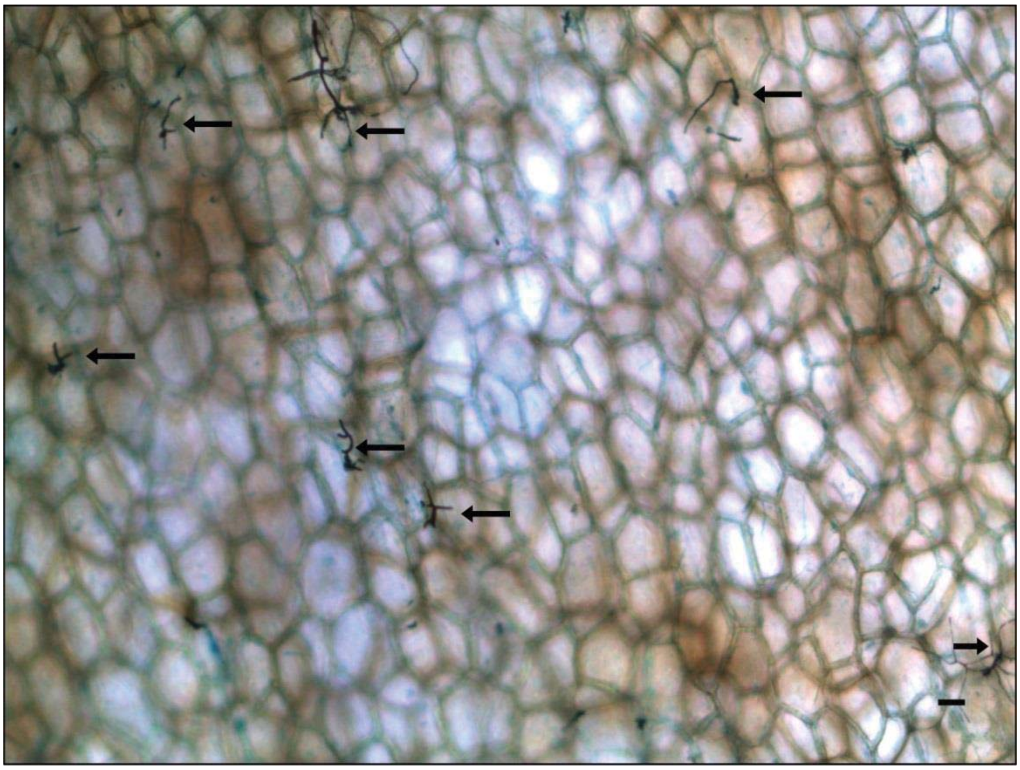

A light micrograph showing Trypan blue stained aerial hyphae of *Ciborinia camelliae* (arrows) protruding above the petal cuticle at 48 hpi. Scale bar = 25µm.

Appendix 9.4. Comparisons of host-resistance between *Camellia* sections using Tukey's range test.

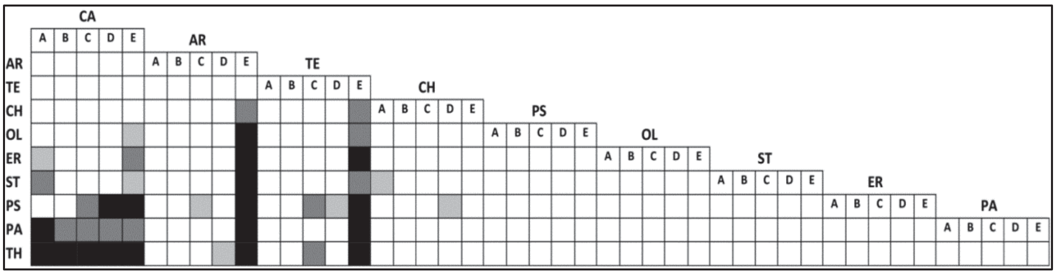

Columns correspond to the assessed parameters. Column A = percent lesion area at 72 hpi; B = papillae absence, C = primary hyphal length; D = sub-cuticular hyphal growth and E =sub-epidermal hyphae at 24 hpi. Black, grey and light grey tiles indicate significant differences between *Camellia* sections at P ≤ 0.05, 0.01 and 0.001 respectively. White tiles indicate no significant difference. *Camellia* sections are abbreviated to CA (Camellia), AR (Archecamellia), TE (Thea), CH (Chrysantha), PS (Pseudocamellia), OL (Oleifera), ST (Stereocarpus), ER (Eriandria), PA (Paracamellia) and TH (Theopsis).

Appendix 9.5. A phylogenetic tree of the Sclerotiniaceae

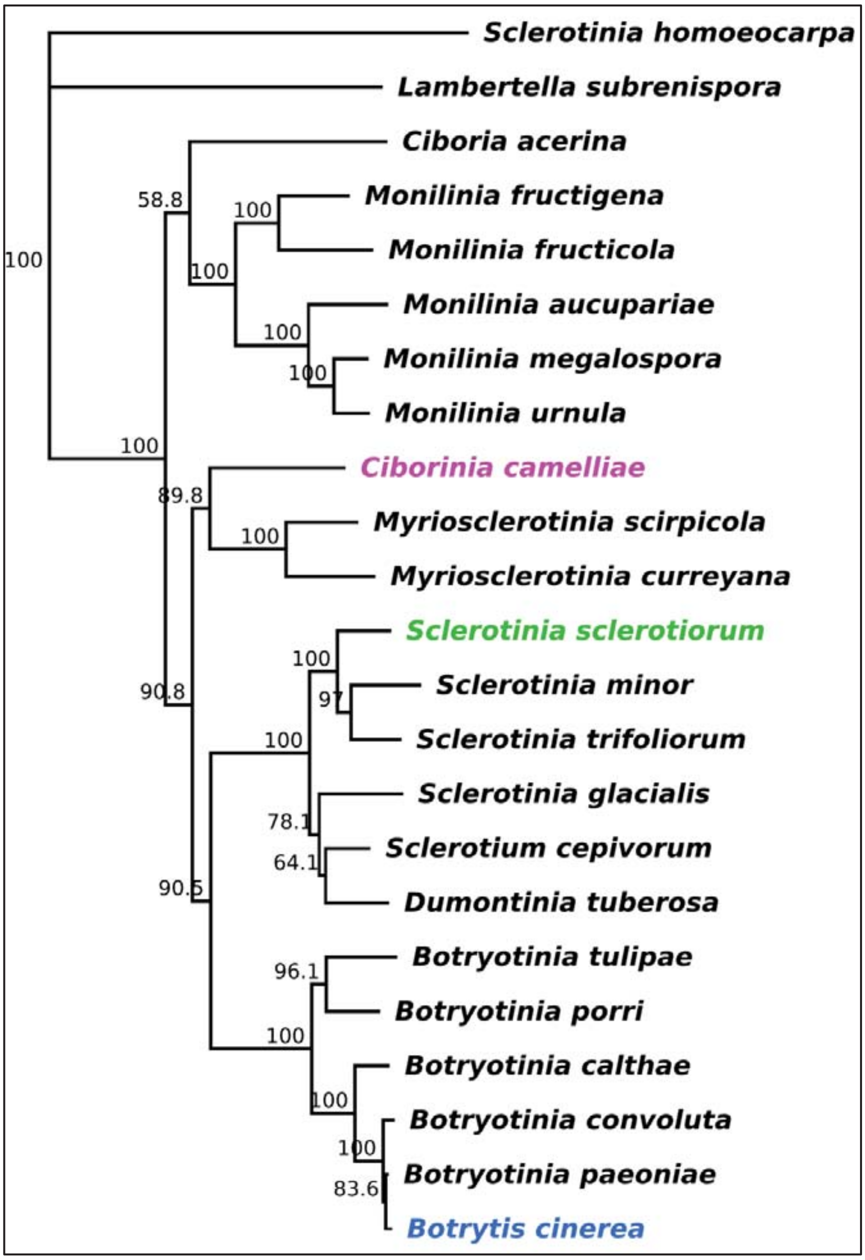

A phylogenetic representation of the Sclerotiniaceae inferred from a CLUSTALW alignment of a 2.2 kb concatenated sequence. The sequence was derived from three housekeeping gene loci (calmodulin, glyceraldehyde-3-phosphate dehydrogenase and heat-shock protein 60). The default Geneious™ neighbour-joining algorithm was used to produce the phylogenetic tree from 1000 bootstrap samples. *Sclerotinia homeocarpa* was designated as the out-group based on the recommendation published in Andrew et al., 2012.

Appendix 9.6. Determination of the 'best' k-mer length for *Ciborinia camelliae* genome assembly (Velvet)

k	n_contigs	n50	Max length	Tot_length	Used reads	Available reads
31	18080	9048	70132	41762321	29045505	29327065
41	16535	14033	116143	44553069	29204646	29327065
49	349946	39	1181	98078507	24096770	29327065
51	2851	31921	247524	40668435	28493696	29327065
53	4453	22012	222390	40160530	28447587	29327065
55	4193	22816	226654	40178017	28426676	29327065
57	3891	23546	221416	40133368	28369849	29327065
61	3417	26586	166427	40276439	28353840	29327065
63	3303	26919	166424	40255401	28326629	29327065
65	3164	27260	194240	40281449	28311826	29327065
69	2664	32026	247718	40712493	28100116	29327065
71	2706	30416	247707	40643437	27933500	29327065
73	2742	29926	167352	40658389	27789014	29327065
75	3793	22216	120486	40001542	27552849	29327065
77	2783	29299	194338	40624111	27498378	29327065
81	2815	28435	174142	40605247	27211165	29327065
91	2879	28233	162157	40759124	26575262	29327065
101	4230	18317	91827	39883677	25657032	29327065
111	3879	20080	101958	40068605	24813393	29327065
121	3667	20714	137856	40259460	23595343	29327065

K-mer 69 yielded the fewest contigs with the highest n50 (yellow row).

Appendix 9.7. Transcriptome validation results using BLASTN

Transcriptome	*Camellia* Sanger (21)		*Botrytis* Sanger (53)		*Sclerotinia* Sanger (16)	
	E = 0	E ≤ -05	E = 0	E ≤ -05	E = 0	E ≤ -05
C. lut mock.	86%	95%	0%	6%	0%	0%
C. lut inf.	86%	95%	0%	15%	0%	6%
C. Nic. Cri. mock	100%	100%	0%	13%	0%	6%
C. Nic. Cri. inf.	90%	100%	43%	92%	50%	93%

Published *Camellia*, *Botrytis cinerea* and *Sclerotinia sclerotiorum* ESTs were aligned to the 4 transcriptomes using BLASTN. Percentage values represent the proportion of published genes that had successful alignment scores.

***Camellia, Botrytis cinerea and Sclerotinia sclerotiorum* ESTs used for transcriptome validation**	
Gene name	Accession number
Botryotinia fuckeliana endopolygalacturonase 2 (BcPGA2) gene	U68716
Botryotinia fuckeliana fructose transporter 1 (frt1) gene	AY738713
Botryotinia fuckeliana PalH (PalH) gene	AY575014
Botryotinia fuckeliana endopolygalacturonase 5 (pg5) mRNA	AY665556
Botryotinia fuckeliana endopolygalacturonase 3 (pg3) mRNA	AY665554
Botryotinia fuckeliana endopolygalacturonase 1 (pg1) gene	AY665552
Botryotinia fuckeliana endo-beta-1,4-glucanase precursor (cel5A) gene	AY618929
Botryotinia fuckeliana aspartic proteinase precursor (ap4) gene	AY507156
Botryotinia fuckeliana aspartic proteinase precursor (AP2) gene	AY361913
Botryotinia fuckeliana strain SAS56 endopolygalacturonase 6 (PGA6) gene	U68722
Botryotinia fuckeliana endopolygalacturonase 4 (BcPGA4) gene	U68719
Botryotinia fuckeliana endopolygalacturonase 1 (BcPGA1) gene	U68715
Botryotinia fuckeliana endopolygalacturonase 3 (PG3) gene	U68717
Botryotinia fuckeliana aspartic proteinase precursor (ap3) gene	AY507155
Botryotinia fuckeliana cyclophilin 1 (BCP1) gene	AY277722
Botryotinia fuckeliana endopolygalacturonase 5 (BcPGA5) gene	U68721
Botryotinia fuckeliana Ras protein (BFRAS1) gene	U79558
Botryotinia fuckeliana phosphoinositide-specific phospholipase C (BCPLC1) gene	U65685
Botryotinia fuckeliana 3-ketosteroid reductase (Erg27) gene	AY220532
Botryotinia fuckeliana chitin synthase class III (chsIIIb) gene	AF529208
Botryotinia fuckeliana MAP kinase (BMP1) gene	AF205375
Botryotinia fuckeliana isolate Bd90 chitin synthase class III (bcchsIII) gene	AF494188
Botryotinia fuckeliana aspartic proteinase precursor (AP1) gene	AF121229
Botryotinia fuckeliana ornithine decarboxylase antizyme (antizyme) mRNA	AF291578
Botryotinia fuckeliana eburicol 14 alpha-demethylase (CYP 51) gene	AF279912
Botryotinia fuckeliana monoubiquitin/carboxy extension protein fusion (UBI1CEP79) gene	AF060232
Botryotinia fuckeliana polyubiquitin (UBI4) gene	AF060501
Botryotinia fuckeliana kinesin gene	AY230425
Botryotinia fuckeliana kinesin (KLP9)	AY230423
Botryotinia fuckeliana kinesin (KLP7)	AY230421
Botryotinia fuckeliana kinesin (KLP5)	AY230419

Gene name	Accession number
Botryotinia fuckeliana kinesin (KLP3)	AY230417
Botryotinia fuckeliana kinesin (KLP1)	AY230415
Botryotinia fuckeliana kinesin (KLP10)	AY230424
Botryotinia fuckeliana kinesin (KLP8)	AY230422
Botryotinia fuckeliana kinesin (KLP6)	AY230420
Botryotinia fuckeliana kinesin (KLP4)	AY230418
Botryotinia fuckeliana kinesin (KLP2)	AY230416
Botryotinia fuckeliana acidic protease 1 (acp1) gene	DQ151453
Botryotinia fuckeliana PIC5 protein (PIC5) gene	DQ140393
Botryotinia fuckeliana laccase 2 (lcc2) gene	AF243855
Botryotinia fuckeliana laccase 1 (lcc1) gene	AF243854
Botryotinia fuckeliana DHA14-like major facilitator (Bcmfs1) gene	AF238225
Botryotinia fuckeliana catalase (cat2) gene	AF243853
Botryotinia fuckeliana EBDP4 gene	EF173621
Botryotinia fuckeliana EBDP2 gene	EF173622
Botryotinia fuckeliana strain B05.10 glucokinase (glk) mRNA	EF156463
Botryotinia fuckeliana strain B05.10 hexokinase (hxk) mRNA	EF156464
Botryotinia fuckeliana B05.10 necrosis- and ethylene-inducing protein 2 precursor (nep2) gene	DQ211825
Botryotinia fuckeliana B05.10 necrosis- and ethylene-inducing protein 1 precursor (nep1) gene	DQ211824
Botryotinia fuckeliana trehalose-6-phosphate synthase gene	DQ632610
Botryotinia fuckeliana neutral trehalase gene	DQ632611
Botryotinia fuckeliana endo-beta-1,4-xylanase precursor (xyn11A) gene,	DQ057980
Camellia sinensis alpha tubulin mRNA	DQ444294.1
Camellia sinensis lipoxygenase (lox1) mRNA	EU195885.2
Camellia sinensis histone 3 mRNA	AY787658.1
Camellia sinensis dihydroflavonol 4-reductase mRNA	AY574920.1
Camellia sinensis flavanone 3-hydroxylase (F3H) mRNA	AY641730.1
Camellia sinensis cultivar UPASI-10 dihydroflavonol 4-reductase (dfr) mRNA	AY648027.1
Camellia sinensis ATP sulfurylase (APS1) mRNA	EF218618.1
Camellia sinensis ATP sulfurylase (APS2) mRNA	EF218619.1
Camellia sinensis maturase K (matK) gene	AF380077.1
Camellia sinensis cytosolic glutamine synthetase mRNA	EF055882.1
Camellia sinensis selenocysteine methyltransferase mRNA	DQ480337.1
Camellia sinensis ribulose-1,5-bisphosphate carboxylase/oxygenase small subunit (rbcS) mRNA	EF011075.1
Camellia sinensis cultivar UPASI-10 anthocyanidin reductase (ANR) mRNA	AY641729.1
Camellia sinensis alpha tubulin 1 (Tua1) mRNA	DQ340766.2
Camellia sinensis CHS2 mRNA for chalcone synthase	D26594.1
Camellia sinensis PAL mRNA for phenylalanine ammonia-lyase	D26596.1
Camellia sinensis CHS3 mRNA for chalcone synthase	D26595.1
Camellia sinensis CHS1 mRNA for chalcone synthase	D26593.1
Camellia sinensis mRNA for PR-1 like protein	AB015047.1
Camellia sinensis mRNA for beta-primeverosidase	AB088027.1
Camellia sinensis TCS1 mRNA for caffeine synthase	AB031280.1
Sclerotinia sclerotiorum acid protease gene	AF221843
Sclerotinia sclerotiorum arom (arom) gene	AY746008
Sclerotinia sclerotiorum hexose transporter (hxt1) gene	AY647267
Sclerotinia sclerotiorum ras protein mRNA	AY664402
Sclerotinia sclerotiorum hexose transporter (hxt2) gene	AY647268
Sclerotinia sclerotiorum cAMP-dependent protein kinase A (pka1) gene	AY545583
Sclerotinia sclerotiorum polygalacturonase 5 (pg5) mRNA	AY496277

Gene name	Accession number
Sclerotinia sclerotiorum mitogen activated protein kinase SMK1 mRNA,	AY351633
Sclerotinia sclerotiorum acidic endopolygalacturonase 3 (PG3) mRNA,	AY312510
Sclerotinia sclerotiorum neutral endopolygalacturonase SSPG6 (sspg6)	AF501308
Sclerotinia sclerotiorum neutral endopolygalacturonase SSPG1d (sspg1d)	AF501307
Sclerotinia sclerotiorum putative zinc finger protein Pac1 (pac1) gene,	AY005467
Sclerotinia sclerotiorum aspartyl protease gene	AF271387
Sclerotinia sclerotiorum adenylate cyclase (sac1) gene	DQ526020
Sclerotinia sclerotiorum endopolygalacturonase gene	L12023
Sclerotinia sclerotiorum calcineurin (cna1) gene	DQ182488

Appendix 9.8. Defense gene homolog identification using BLASTN

Defense gene	BLASTN Query Reference	BLASTN E value	BLASTN Subject *Camellia sinensis* EST homologs (Shi et al., 2011)	Reciprocal BLASTN result using EST as query. Top hit	Reciprocal BLASTN E value
Phenylalanine ammonia-lyase	*Vitis vinifera* EF192469	0.00E+00	HP734547	*Rhus chinensis PAL*	0.00E+00
	Arabidopsis thaliana NM_111869	2.00E-177			
	Solanum lycopersicum M83314	00.00E+00			
Chitinase Class I	*V. vinifera* DQ267094	5.00E-149	HP747422	*V. vinifera Chitinase I*	0.00E+00
	A. thaliana NM_112085	1.00E-49			
	S. lycopersicum NM_001247474	1.00E-92			
Catalase 2	*V. vinifera* AF236127	2.00E-42	HP769724	*Theobroma cacao catalase 2*	2.00E-44
	A. thaliana NM_119675	7.00E-29			
	S. lycopersicum NM_001247257	3.00E-26			
Ascorbate Peroxidase (APX)	*V. vinifera* EU280159	2.00E-77	HP771679	*Theobroma cacao ascorbate peroxidase 2*	1.00E-58
	A. thaliana NM_001123772	4.00E-43			
	S. lycopersicum NM_001247853	1.00E-36			
Glutathione S-Transferase	*V. vinifera* AF501625	5.00E-72	HP742154	*Camellia sinensis glutathione S-tranferase*	3.00E-108
	S. lycopersicum NM_001247293	3.00E-62			
Lipoxygenase 5	*V. vinifera* AY159556	0.00E+00	HP701190	*Camellia sinensis LOX 1*	0.00E+00
	A. thaliana AJ302043.	0.00E+00			
	S. lycopersicum NM_001247944	0.00E+00			
Manganese Superoxide Dismutase	*V. vinifera* EU280161	9.00E-119	HP751734	*Camellia sinensis SOD*	0.00E+00
	A. thaliana NM_001035593	1.00E-86			
PR5 (Thaumatin)	*A. thaliana* NM_106161	3.00E-17	HP734660	*Solanum tuberosum thaumatin-like protein*	9.00E-70
Calmodulin	*Camellia oleifera* FJ649316	2.00E-71	HP766724	*Prunus mume calmodulin-like protein*	7.00E-126

Camellia sinensis defense-associated ESTs were identified (grey column) by aligning defense gene query sequences to a *C. sinensis* EST database (Shi et al., 2011). Reciprocal analysis was performed by querying the Genbank *nr* database using *C. sinensis* ESTs. The selected *C. sinensis* ESTs were then used to identify the best EST homologs in *C.* 'Nicky Crisp' and *C. lutchuensis* (< 1e-20).

Appendix 9.9. BLASTN alignments of the *Camellia* 'Nicky Crisp' non-redundant transcriptome to the *Ciborinia camelliae* genome.

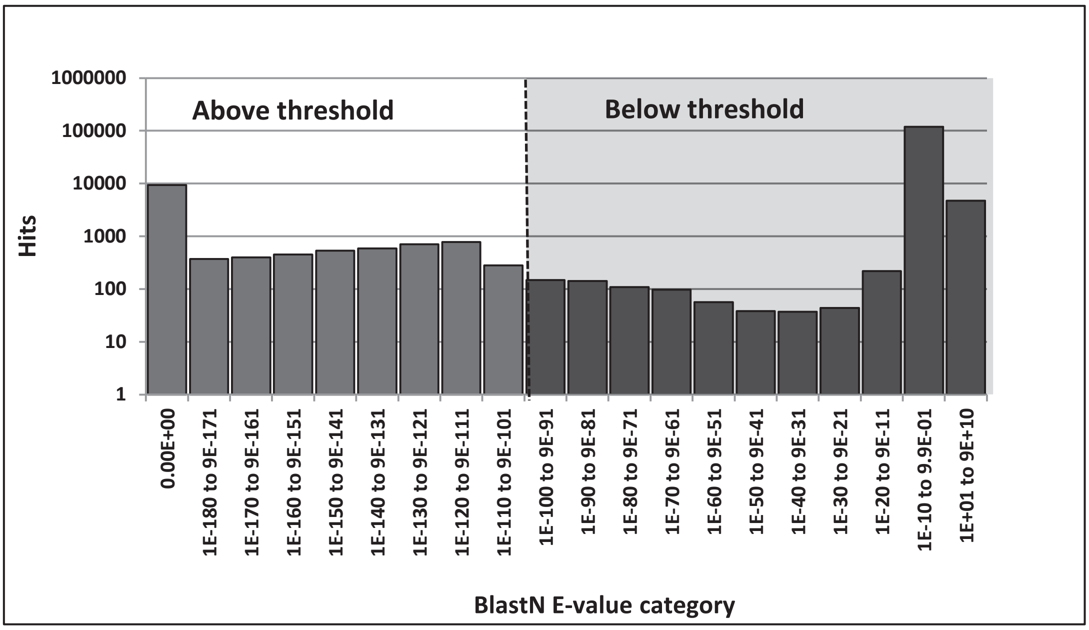

Appendix 9.10A. Validation of a subset of *Ciborinia camelliae* proteins (*n* = 1472) using BLASTP and the Genbank non-redundant protein database

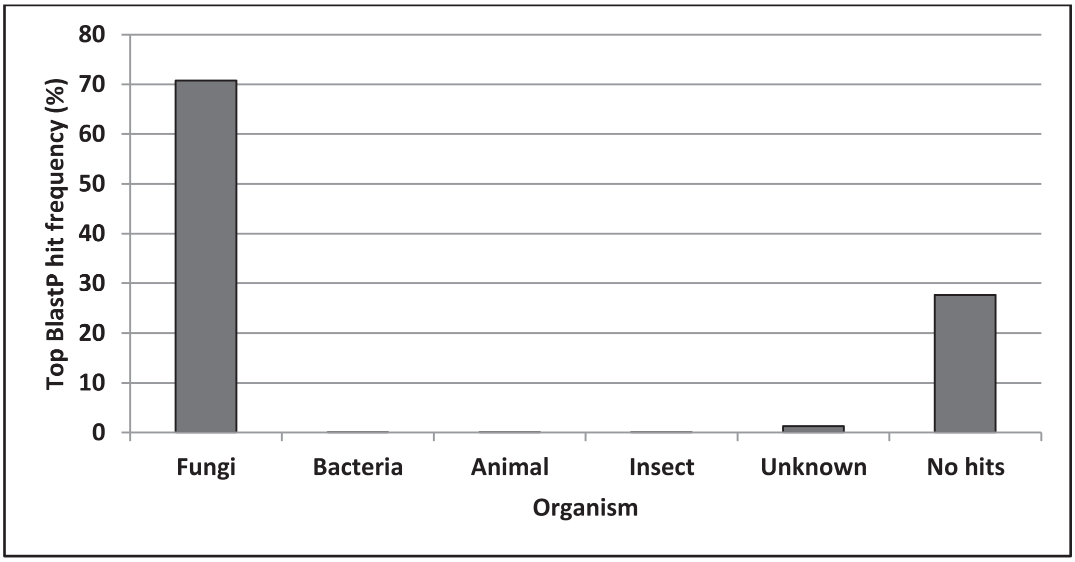

Appendix 9.10B. Validation of a subset of *Ciborinia camelliae* proteins (*n* = 1472) using BLASTP and the Genbank non-redundant protein database - top hit E-value distribution.

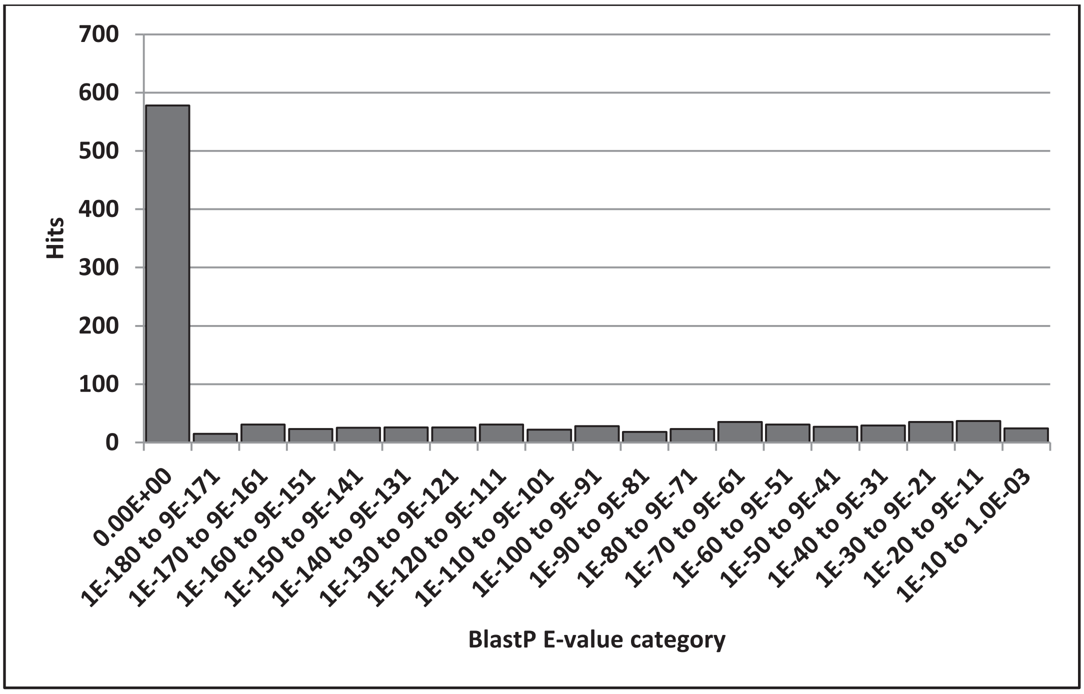

Appendix 9.11. Secretome validation using previously published *Botrytis cinerea* secreted proteome data.

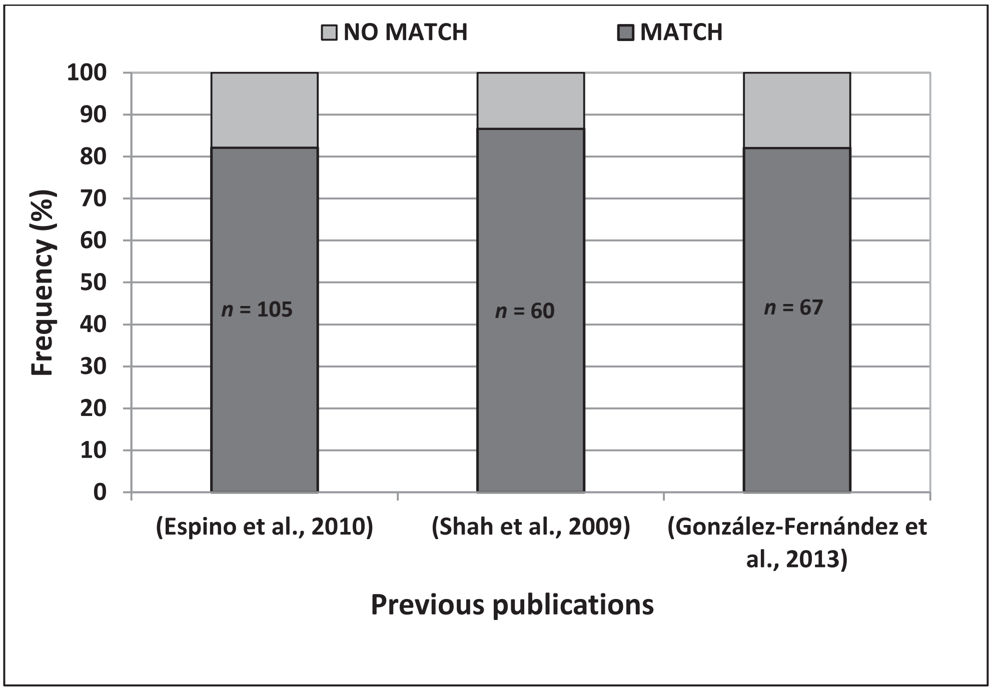

Appendix 9.12. Secretome annotation categories and protein counts.

Category	*C. camelliae*	*B. cinerea*	*Cc vs Bc P-value*	*S. sclerotiorum*	*Cc vs Ss P-value*
Adhesion protein	1	1	1	1	1
Appressorial protein	3	3	1	4	1
CAZyme	167	178	1	164	1
Cell cycle protein	2	4	1	2	1
ER protein	7	8	1	11	1
Fungal cell wall biosynthesis	1	1	1	1	1
Lipase	15	15	1	16	1
Mating	4	5	1	4	1
Membrane protein	8	5	1	6	1
Nucleic acid modification	14	11	1	14	1
Oxidation/Reduction	66	66	1	49	1
Palmitoyl-protein hydrolase	1	1	1	1	1
Peptidase	1	1	1	1	1
pH homeostasis	1	1	1	1	1
Phosphatase	14	15	1	17	1
Phosphoesterase	3	2	1	0	1
Phosphatidylinositide phosphatase	0	1	1	0	1
Predicted protein	223	279	0.42	251	0.47
Primary metabolism	16	13	1	11	1
Protease	44	43	1	36	1
Protease inhibitor	2	0	1	1	1
Protein biosynthesis	1	2	1	1	1
Protein degradation	1	0	1	2	1
Protein Kinase	4	4	1	3	1
Putative effector	10	8	1	6	1
Ribosomal protein	5	4	1	3	1
Secondary metabolism	18	19	1	14	1
Signalling	0	1	1	1	1
Small secreted proteins	74	41	**0.043***	34	**0.021***
Transcription factor	1	1	1	3	1
Transport	9	14	1	14	1
Unknown	33	7	**0.0012****	5	**0.0006*****
TOTAL	749	754		677	

CAZYMES	*C. camelliae*	*B. cinerea*	*Cc vs Bc P-value*	*S. sclerotiorum*	*Cc vs Ss P-value*
Carbohydrate binding module	5	5	1	6	1
Glycosyl transferase	8	8	1	7	1
Polysaccharide lyase	9	10	1	6	1
Carbohydrate esterase	22	32	1	23	1
Glycosyl hydrolase	123	123	1	122	1
Total	167	178		164	

SSPs	*C. camelliae*	*B. cinerea*	*Cc vs Bc P-value*	*S. sclerotiorum*	*Cc vs Ss P-value*
≥ 10	33	4	**0.014***	3	**0.025***
8-9.9	14	3	0.20	2	0.20
6-7.9	9	10	0.20	7	0.40
4-5.9	18	24	**0.04***	22	**0.025***
Total	74	41		34	

Proteases	*C. camelliae*	*B. cinerea*	*Cc vs Bc P-value*	*S. sclerotiorum*	*Cc vs Ss P-value*
Metalloprotease	6	6	1	7	1
Aspartate protease	13	13	1	10	1
Serine protease	25	24	1	19	1
Total	44	43		36	

Proteases	*C. camelliae*	*B. cinerea*	*Cc vs Bc P-value*	*S. sclerotiorum*	*Cc vs Ss P-value*
NADH/NADPH oxidoreductase	2	2	1	4	0.40
Diphenol oxidoreductase	5	3	0.72	3	1
Peroxidase	6	8	0.78	3	0.73
Uncategorized	9	4	0.25	4	0.56
Oxygenase	11	17	0.40	15	0.19
CH-OH oxidoreductase	31	30	1	18	0.60
Total	64	64		47	

Fisher's exact test was chosen to look for significant differences between *C. camelliae* and *B. cinerea*, or *C. camelliae* and *S. sclerotiorum protein categories* P values were adjusted for multiple testing using a false discovery rate correction (Benjamini et al., 1995). *, ** and *** indicate p = 0.05, 0.01 and 0.001 respectively.

Appendix 9.13. Secretome subcategory annotation and scatterplot analyses

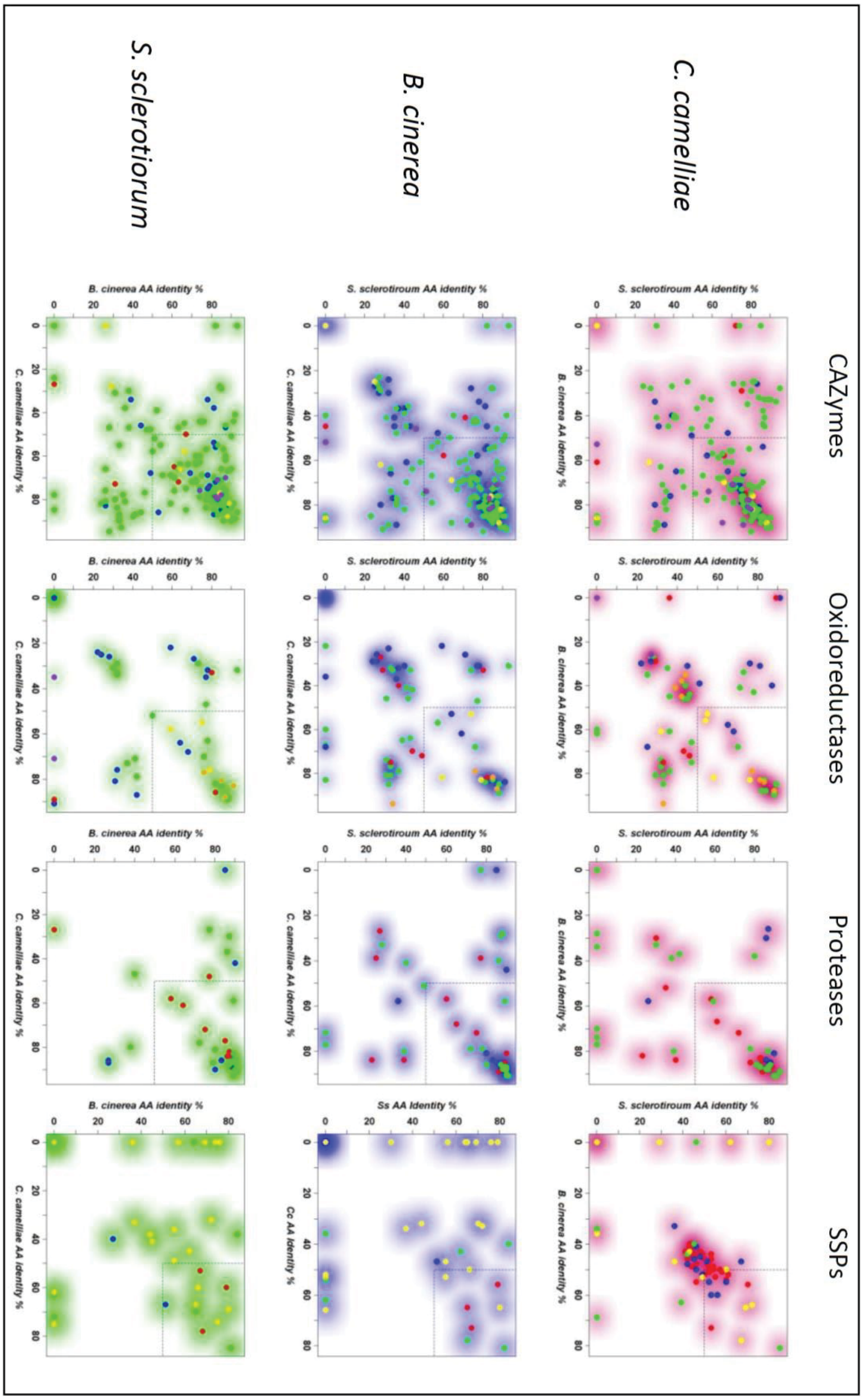

CAZymes: Carbohydrate binding module (●), Glycosyl transferase (●), Polysaccharide lyase (●), Carbohydrate esterase (●), Glycosyl hydrolase (●). Oxidoreductases: NADH/NADPH oxidoreductase (●), Diphenol oxidoreductase (●), Peroxidase (●), Uncategorized oxidoreductase (●), Oxygenase (●), alcohol oxidoreductase (●). Proteases: Metalloprotease (●), Aspartate protease (●), Serine protease (●). Small secreted proteins: ≥ 10 cysteines (●), 8-9.9 cysteines (●), 6-7.9 cysteines (●), 4-5.9 cysteines (●).

Appendix 9.14. A phylogenetic tree of the conserved CCL-SSP family highlighting proteins chosen for recombinant analysis.

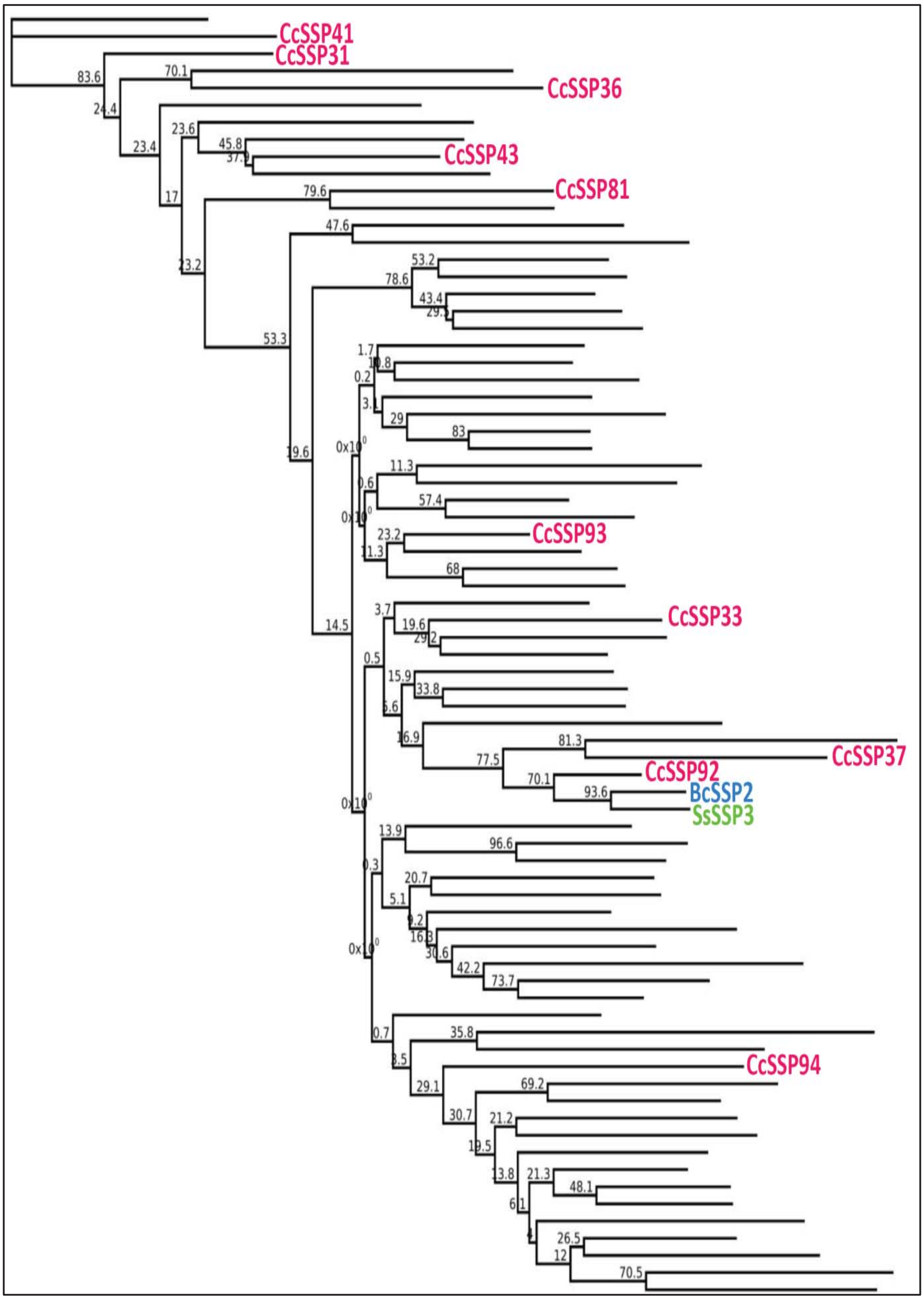

The labelled nodes indicate those proteins that were chosen for recombinant protein expression. *C. camelliae* proteins (pink), *B. cinerea* (blue) and *S. sclerotiorum* (green). The phylogenetic tree was created from a CLUSTALW protein alignment of the CCL-SSP protein data. The Geneious™ PHYML plugin was used to build the tree from 1000 bootstrap samples.

Appendix 9.15. CCL-SSP family statistics

Name	AA length	CDS length	Intron length	Intron/Exon boundary		Genome Scaffold locus	Relative EST abundance
CcSSP39	97	291	54	K/D	37/38	1338	N/A
CcSSP16	97	291	76	T/Q	37/38	1338	2.07792
CcSSP7	94	282	107	E/N	38/39	843	2.00745
CcSSP20	98	294	73	K/P	40/41	18	1.64242
CcSSP35	104	312	69	E/D	39/40	724	0.77802
CcSSP51	114	342	87	K/A	40/41	81	0.08868
CcSSP53	98	294	60	K/D	37/38	10	2.77273
CcSSP32	101	303	87	Q/D	37/38	186	0.59686
CcSSP30	100	300	131	Y/Q	36/37	279	0.12766
CcSSP40	109	327	52	K/E	41/42	139	0.02823
CcSSP37	106	318	76	S/S	38/39	67	0.10577
CcSSP47	117	351	74	T/P	39/40	476	0.49393
CcSSP45	116	348	106	T/T	39/40	302	0.40766
CcSSP17	97	291	52	Q/D	37/38	1338	0.79412
CcSSP4	93	279	61	A/N	37/38	302	0.75787
CcSSP33	101	303	66	Q/D	38/39	724	6.05579
CcSSP5	93	279	108	R/N	37/38	1297	0.26492
CcSSP26	99	297	62	K/T	39/40	1576	0.4977
CcSSP6	93	279	149	R/T	42/43	141	0.50645
CcSSP43	115	345	136	Q/T	41/42	1691	0.21384
CcSSP21	98	294	75	K/D	37/38	1513	1.36142
CcSSP8	95	285	110	E/D	37/38	5	0.78993
CcSSP9	95	285	104	E/D	37/38	736	0.1722
CcSSP31	100	300	79	Y/T	39/40	1650	0.87705
CcSSP36	104	312	56	K/I	39/40	1650	0.39813
CcSSP38	106	318	62	A/L	40/41	302	0.39089
CcSSP27	99	297	66	Q/D	38/39	1716	1.625
CcSSP18	97	291	60	H/D	37/38	697	9.13881
CcSSP41	110	330	73	Q/D	41/42	139	4.09163
CcSSP10	95	285	153	K/D	38/39	493	1.98473
CcSSP46	116	348	Unknown	V/S	53/54	1689	1.5739
CcSSP19	97	291	204	Q/D	37/38	419	2.12155
CcSSP34	103	309	131	W/T	41/42	372	2.18496
CcSSP22	98	294	80	Q/N	37/38	219	0.85314
CcSSP13	96	288	51	K/D	37/38	655	0.85714
CcSSP3	92	276	114	K/D	37/38	118	0.23929
CcSSP23	98	294	87	Q/D	39/40	93	2.39665
CcSSP24	98	294	113	K/D	37/38	697	0.5505
CcSSP1	90	270	145	R/A	37/38	52	0.57486
CcSSP28	99	297	54	K/D	37/38	107	0.11224
CcSSP14	96	288	72	S/G	40/41	419	0.98327
CcSSP25	98	294	64	Q/N	38/39	1297	0.07219
CcSSP11	95	285	59	K/D	37/38	1513	0.48398
CcSSP15	96	288	97	R/N	38/39	477	2.78372
CcSSP29	99	297	78	K/T	41/42	469	0.14123
CcSSP42	110	330	82	K/T	39/40	1650	0.47939
CcSSP75	95	285	113	E/N	37/38	9	0.220803

Name	AA length	CDS length	Intron length	Intron/Exon boundary	Genome Scaffold locus	Relative EST abundance	Name
CcSSP76	96	288	155	K/D	38/39	419	0.315891
CcSSP77	101	303	68	Q/I	37/38	1713	0.819421
CcSSP78	83	249	100	V/D	37/38	1175	0.594744
CcSSP79	84	252	65	V/G	38/39	302	0.669034
CcSSP80	100	300	91	K/D	37/38	2128	0.156134
CcSSP81	118	354	56	V/N	41/42	308	2.699844
CcSSP82	83	249	107	T/N	37/38	799	2.39399
CcSSP83	83	249	93	S/N	38/39	97	1.545024
CcSSP84	97	291	79	K/D	37/38	469	0.808743
CcSSP85	105	315	90	R/D	36/37	1513	0.135922
CcSSP86	97	291	75	M/D	37/38	1650	0.619681
CcSSP87	95	285	60	K/D	37/38	1011	0.854154
CcSSP88	98	294	123	E/D	38/39	121	0.588448
CcSSP89	98	294		K/D	37/38	492	1.866524
CcSSP90	102	306	93	E/D	39/40	159	0.639922
CcSSP91	97	291	76	E/D	39/40	736	3.387358
CcSSP92	91	273	66	S/D	38/39	62	8.479791
CcSSP93	86	258	77	E/N	37/38	1691	4.171717
CcSSP94	101	303	73	R/D	36/37	1576	3.38806
CcSSP95	89	267	101	K/G	38/39	851	1.735703
CcSSP96	98	294	75	Q/D	38/39	162	1.824051
CcSSP97	105	315	95	K/D	38/39	1912	1.469169
CcSSP98	86	258	64	K/N	37/38	655	1.165138
CcSSP99	84	252	73	G/D	37/38	147	0.908463
CcSSP100	87	261	56	T/S	37/38	302	1.268627
CcSSP101	84	252	115	Q/N	37/38	139	0.466102
BcSSP2	90	270	70	S/D	38/39	N/A	N/A
SsSSP3	93	279	71	S/D	38/39	N/A	N/A

Appendix 9.16. An alignment of all CCL-SSP family members showing the conserved cysteine residues.

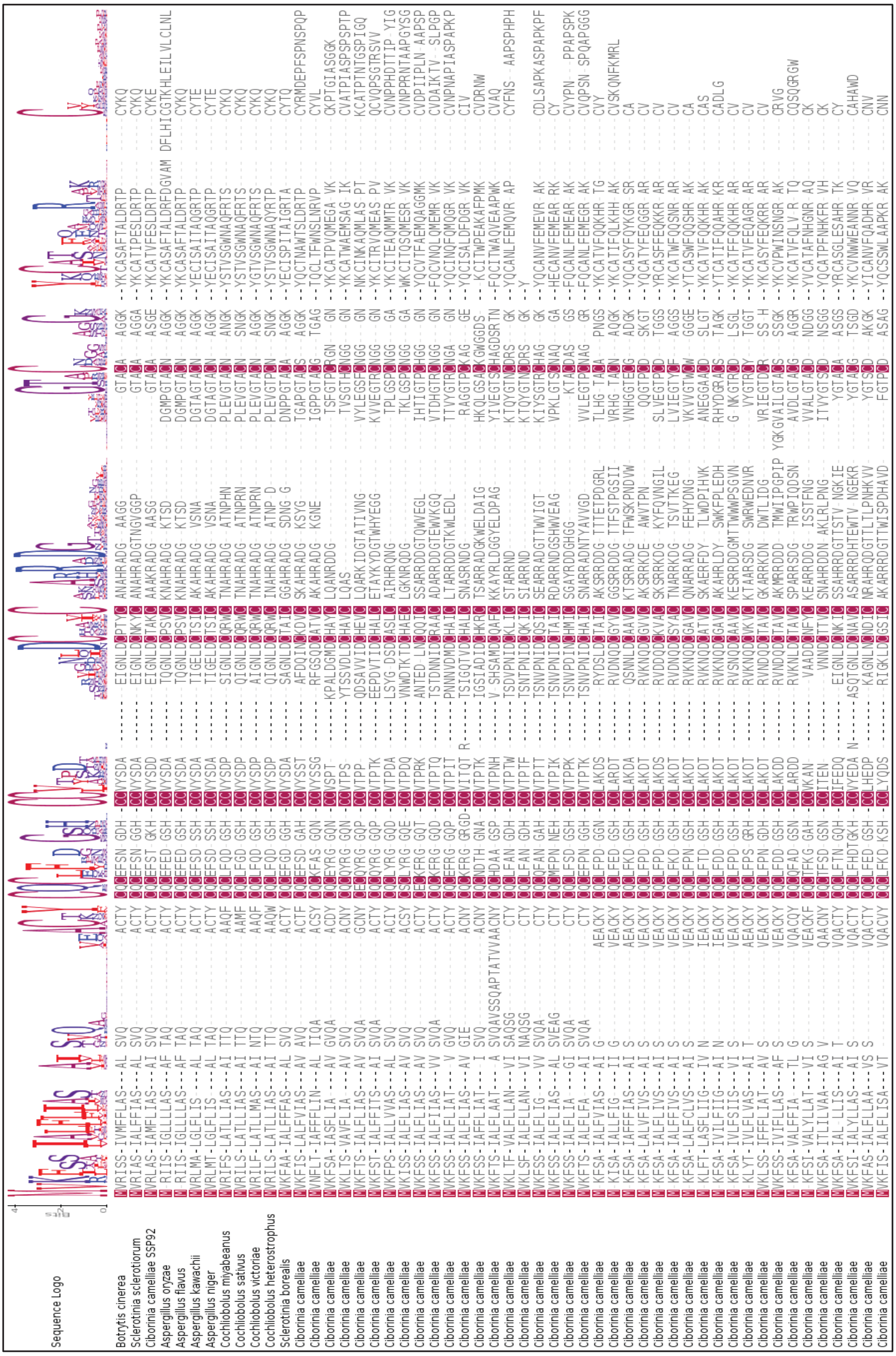

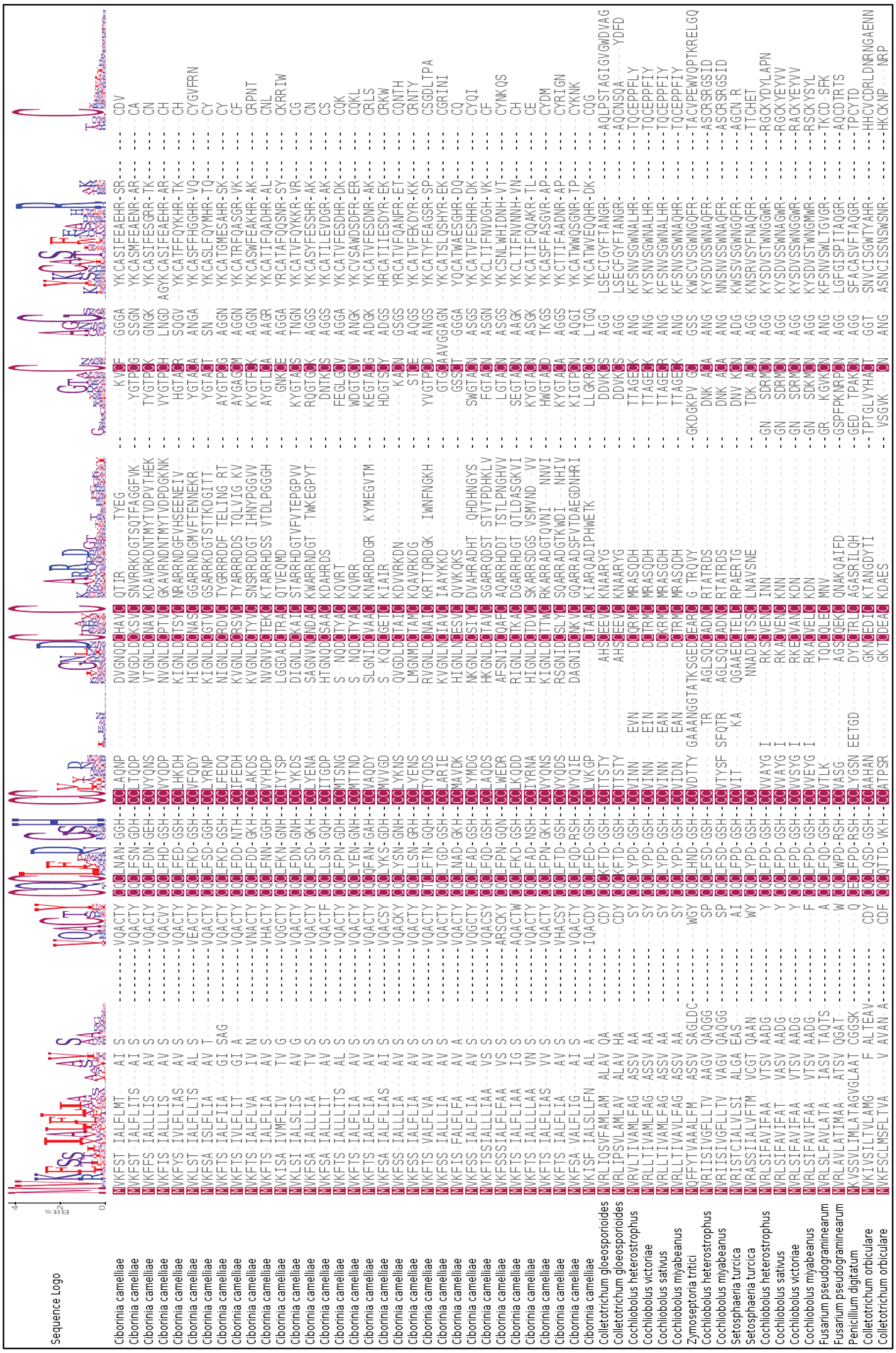
Sequence Logo

Appendix 9.17. Fungal gDNA accumulation *in planta* correlates with fungal NAD and TUB mRNA accumulation.

A

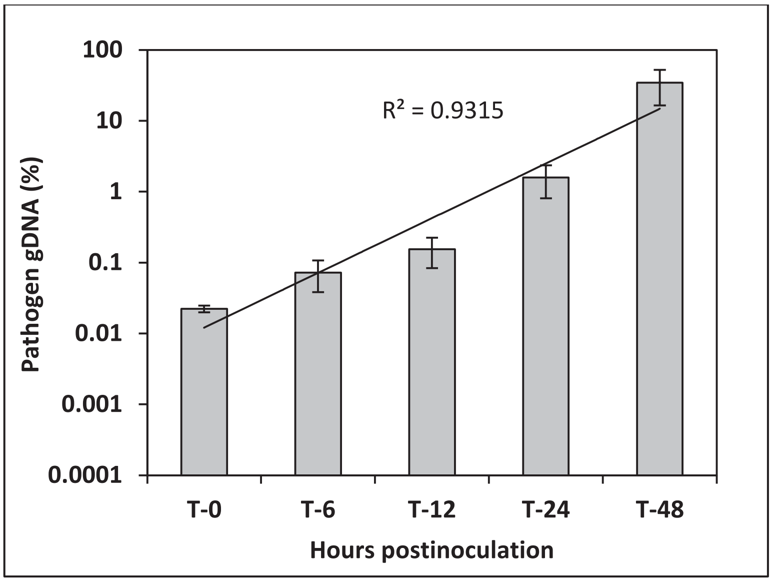

B

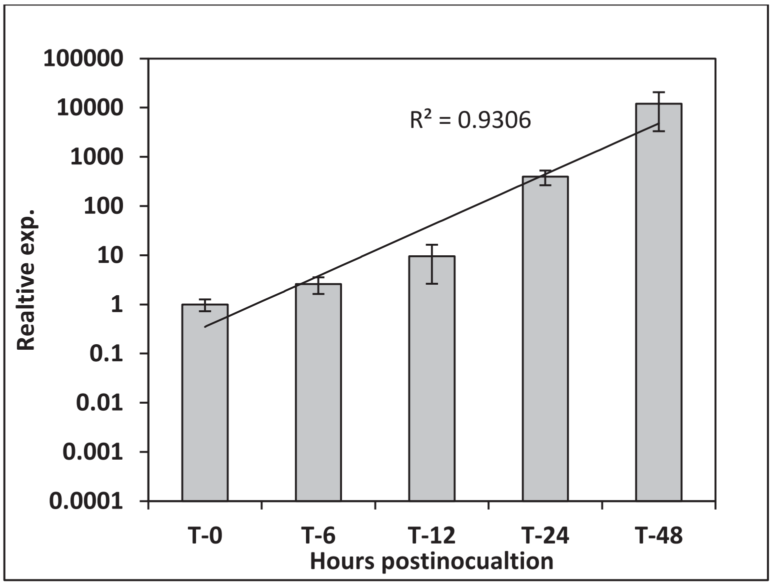

A, qRT-PCR analysis of fungal gDNA abundance using the geo-mean of the two fungal genes NAD and TUB normalized to plant Actin gDNA. Relative expression is presented on a logarithmic scale (base 10). gDNA was quantified using standard curves produced from known concentrations of plant and fungal gDNA (data not shown). Pathogen gDNA is presented as a percentage of total gDNA (plant & pathogen). Error bars = ±1 SE.

B, qRT-PCR analysis of fungal mRNA abundance using the geo-mean of the two fungal genes NAD and TUB normalized to the geo-mean of the plant GADPH and Actin mRNA. Relative expression is presented on a logarithmic scale (base 10). Error bars = ±1 SE.

Appendix 9.18. Recombinant CCL-SSP construct sequences optimized for *P .pastoris* codon usage (note: these are not endogenous nucleotide sequences).

CcSSP33
GAATTCACTATGGTCAAACTTTCAACTATCGCTCTTTTCCTTCTTACCTCAGCCTTGTCTGTCGAAGCCTG
TACCTATTGCCAGTGCCTTTTTAAGGATGGTTCTCATTGTTGCGTTTTTCAAGATTACCACATTGGAAACT
TGGACTGTAATGCCTCCTGCGGTGGAGCTAGAAGAAACGACGGTATGGTCTTCACTGAAAACAATGAG
AAGAGATACGGTACAGCTTGTGCTGCCAATGGAGCATATAAATGCGCTTCATTTTTCCATGGTGGACAC
AGAGTTCAGTGTTATGGAGTCTTTAGAAACTAAGGGCCC

CcSSP43
GAATTCACTATGGTCAAGTTCTCCAGTATCGCCCTTTTCATCATCGCCTCAGTCGTCTCAGTCCAAGCCG
CCTGTACCTATTGTCAGTGTAAATTCAGAGGTGGACAAGATTGTTGCGTTACTCCAACACAGACCTCTAC
TGATAACAATATTGACTGTAGAGCTGCCTGCGCAGATGCTAGAAGAGATGACGGAACTGAATGGGTTA
AGGGTCAAGTCACAGACCATGGAACTAGATGTAACGGTGGTGGTAATTTCCAGTGCGTTAACCAATTG
CAGATGGAGATGAGAGTCAAGTGTGTTGACGCCATTAAGACCGTTTCCTTGCCTGGACCTTCCCCTATG
CCTAAGTAGGGGCCC

CcSSP31
GAATTCACTATGGTTAAGTTGACCTCCGTCGCAGTCTTTTTGATTGCCGCAGTTTCAGTCCAGGCTTGTA
ATTATTGCCAGTGCCAGTATAGAGGTGGACAAAACTGTTGCGTCACTCCTTCCTACACATCTTCCGTTGA
TTTGGACTGTCATGCCGTCTGCCTTCAGGCTTCCACCGTTTCAGGAACTCACTGTAACGGTGGTGGTAAT
TATAAGTGCGCTACTTGGGCCGAAATGAGTGCTGGTATTAAATGTGTTGCAACACCAATCGCTTCACCA
AGTCCTTCTCCAACTCCTTCACCAAAGTAAGGGCCC

CcSSP36
GAATTCACTATGGTCAAATTCTCCTCAATCGCTTTCTTTCTTATCGCCACTATCTCCGTCCAGGCTTGTAA
CTACTGCCAATGTAACGACACCCATGGAAACGCCTGTTGCGTTACTCCAACAAAAATTGGTTCAATCGC
TGATATTGACTGTCACAAGAGATGCACTTCTGCTAGAAGAGCCGATGGAAAATGGGAATTGGACGCAA
TCGGTCATAAGCAACTTGGATCTGCTTGTAAAGGTTGGGGTGGAGATTCCAAGTGTATCACCTGGCCTG
AAGCAAAAGCATTCCCTATGAAGTGCGTTGACAGAAACTGGTAGGGGCCC

CcSSP41
GAATTCACTATGGTCAAGTTCACCTCTATTGCTTTGTTTCTTATTGCTTCAGCCGTCTCTGTCCAGGCAGG
ATGTAACTATTGCGAGTGTCAGTACAGAGGTGGACAACCTTGTTGCGTTACTCCACCTCAGGATTCAGC
CGTTGTCATTGACTGTCATGAAGTCTGCTTGCAAGCAAGAAAGATTGATGGAACTGCTACAATCGTTAA
CGGAGTCTATCTTGAGGGTTCTTTTTGTAACGGTGGTGGTAACAATAAGTGCATTAACAAGGCTCAAAT
GTTGGCCTCTCCAACTAAATGTGCTACCCCTACTAATACAGGATCCCCAATCGGACAGTAAGGGCCC

CcSSP37
GAATTCACTATGGTTAAGTTTATCTCTCTTGCTCTTTTCGTCATCGCATCTGCCGTCGCCGTTCAGGCTTG
TACCTTCTGTCAGTGTGAGTTTTCAGATGGTGCCCATTGTTGCGTTTACTCTTCCACAGCATTCGATCAA
ATTAACTGTAAGGACGTCTGCTCTAAAGCTCACAGAGCCGACGGTAAATCCTACGGTACCGGTGCTCCA
GGAACTGCATGTTCAGCTGGTGGAAAATATCAATGCACTAACGCCTGGACAAGTTTGGATAGAACTCCT
TGTTACAGAATGGACGAACCATTCTCACCTAATAGTCCACAGCCTTAAGGGCCC

CcSSP94
GAATTCACTATGAAGTTCTCTGCTGTTGCTCTTTTCTTTATTGCCACCTTGGGAGTCCAGGCTTGTCAGTA
TTGTCAGTGCCAGTTTGCCGATGGTTCAAACTGTTGCTTGGCCAGAGATGACAGAGTTAAGAATCTTGA
TTGTACTGCAGTCTGCTCTCCAGCTAGAAGATCCGACGGAACAAGATGGCCTATTCAAGATTCTAACGC
TGTTGACTTGGGTACTGCTTGTGGAGCCGGTGGAAGATACAAATGCGCCACAGTCTTTCAGTTGGTCA
GAACACAATGCCAGTCACAAGGTAGAGGATGGTAGGGGCCC

CcSSP93
GAATTCACAATGGTCAAGTTCTCTTCAATCGCTCTTTTTCTTATCGCTGCTGTTTCTGTCCAGGCTTGCAC
CTACTGTCAATGTTTGCTTTCAAACGGTAGACATTGTTGCTTGTACGAAAACTCACTTATGGAAATATG
GATTGTACCGCTATGTGCAAGCAAGCCGTTAGAAAAGACGGTTCTACTTGTGAAGCACAGGGATCCTA
TAAGTGCGCTACAGTCTTCGAGAAGGATTACAGAAAGAAATGTAGAAATACTTATTAAGGGCCC

CcSSP81
GAATTCACTATGGTCAAAATCTCATCTATCGCATTGTTTCTTATCGCATCCGCCGTTTCTGTTCAGGCTTG
CTCCTACTGTTCATGTCTTTATAGAGGTGGACAAGAATGTTGCGTTACTCCAGATCAGGTCAACTGGGA
TACTAAGACAGACTGTCATGCAGAGTGCTTGGGAAAGAACAGACAAGACGGAACAAAACTTGGTTCCC
CTTGTAATGGTGGAGGTGCTTGGAAGTGCATTACTCAATCTCAGATGGAATCCAGAGTTAAATGTGTCA
ACCCACCTAGAAATACCGCTGCCCCAGGATACTCAGGTATTGATACTCCTATCCCACCTAGTTGGGGAA
AACACGGTGCCGAGTAAGGGCCC

CcSSP92
GAATTCACTATGGTCAGACTTGCTTCTATCGCTATGTTTCTTATCGCTTCCGCTATCTCCGTCCAGGCTTG
TACTTATTGTCAGTGTGAGTTCTCAACTGGTAAACATTGTTGCGTTTACTCTGATGACGAAATTGGAAAC
TTGGATTGTACTGCCAAGTGCGCTGCCGCAAAAAGAGCTGACGGTGCTGCCTCTGGTGGAACAGCTTG
TGCAGCTTCCGGAGAATACAAGTGTGCCACCGTTTTTGAGAGTTTGGATAGAACCCCATGCTACAAGGA
ATAAGGGCCC

BcSSP2
GAATTCACTATGGTCAGAATCTCCTCTATCGTTATGTTTTTCCTTGCCAGTGCCCTTTCCGTCCAGGCTTG
TACCTATTGCCAGTGTGAGTTCTCTAACGGAGATCATTGTTGCGTTTACTCCGACGCCGAAATTGGTAAC
TTGGATTGTCCAACCTATTGCGCCAATGCACACAGAGCAGACGGAGCTGCCGGTGGAGGTACTGCTTG
TGCAGCTGGTGGTAAATACAAATGCGCTTCAGCCTTTACTGCTCTTGATAGAACACCTTGTTATAAGCAA
TAAGGGCCC

SsSSP3
GAATTCACTATGGTCAGAATCGCATCTATCGCATTGTTCTTTATCGCATCCGCTCTTTCCGTTCAAGCCTG
CACCTATTGTCAGTGTGAGTTTTCTAACGGTGGACATTGTTGCGTTTACTCCGATGCTGAAATCGGTAAC
TTGGACTGTAATAAGTACTGCGCAAACGCTCACAGAGCTGATGGTACTAATGGAGTCGGTGGACCAGG
AACAGCCTGTGCTGCCGGTGGAGCCTACAAGTGCGCAACCATCCCAGAGTCACTTGACAGAACTCCTTG
TTATAAACAATAAGGGCCC

Native stop codons were mutated (STOP to LYSINE) to allow for transcription of the pPICZA incorporated c-Myc epitope and His tag sequences shown below.

AAAGGGCCCGAACAAAAACTCATCTCAGAAGAGGATCTGAATAGCGCCGTCGACCATCATCATCATCAT
CATTGA

Restriction sites *EcoRI* and *ApaI* (grey), start codon (green), stop codon (red).

Appendix 9.19. Vector maps

pUC57

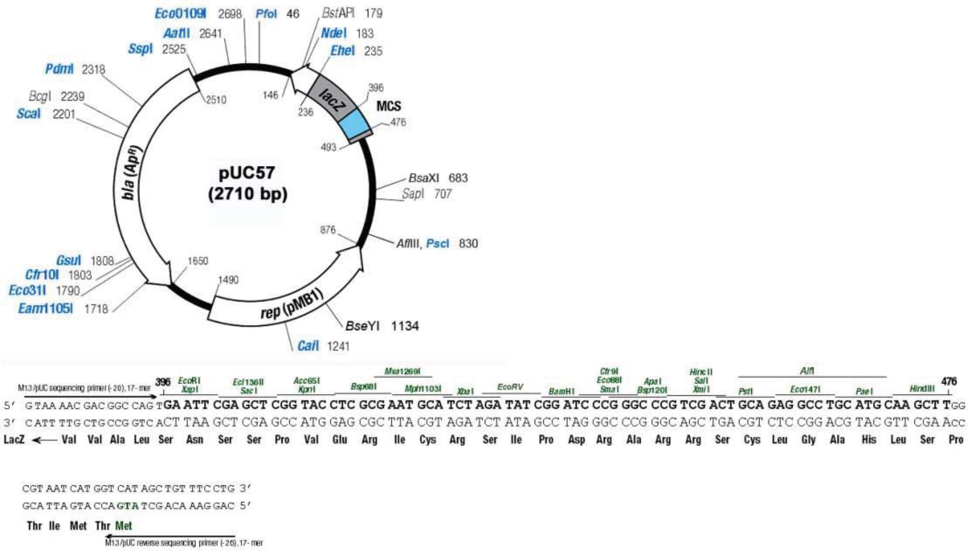

pPICZA

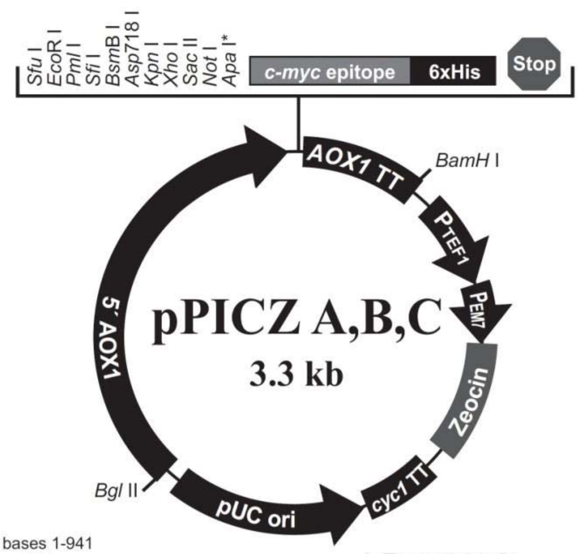

Comments for pPICZ A:
3329 nucleotides

5´ *AOX1* promoter region: bases 1-941
5´ end of *AOX1* mRNA: base 824
5´ *AOX1* priming site: bases 855-875
Multiple cloning site: bases 932-1011
c-myc epitope tag: bases 1012-1044
Polyhistidine tag: bases 1057-1077
3´ AOX priming site: bases 1159-1179
3´ end of mRNA: base 1250
AOX1 transcription termination region: bases 1078-1418
Fragment containing TEF1 promoter: bases 1419-1830
EM7 promoter: bases 1831-1898
Sh ble ORF: bases 1899-2273
CYC1 transcription termination region: bases 2274-2591
pUC origin: bases 2602-3275 (complementary strand)

* The restriction site between *Not* I and the *myc* epitope is different in each version of pPICZ:

Apa I in pPICZ A
Xba I in pPICZ B
*Sna*B I in pPICZ C

pGEM-T Easy

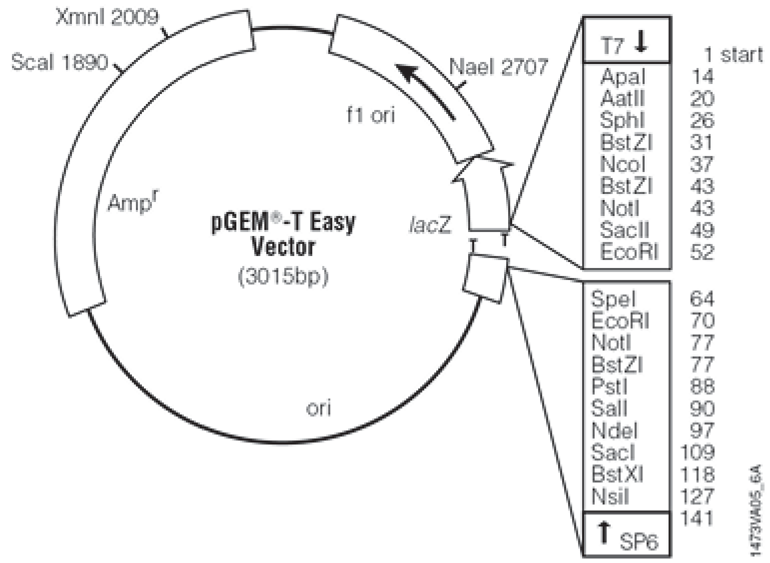
XmnI 2009
ScaI 1890
NaeI 2707
f1 ori
Amp^r
pGEM®-T Easy Vector
(3015bp)
lacZ
ori
T7
1 start
ApaI 14
AatII 20
SphI 26
BstZI 31
NcoI 37
BstZI 43
NotI 43
SacII 49
EcoRI 52
SpeI 64
EcoRI 70
NotI 77
BstZI 77
PstI 88
SalI 90
NdeI 97
SacI 109
BstXI 118
NsiI 127
141
SP6
1473VA05_6A

Appendix 9.20. Functional protein assays using native recombinant CCL-SSPs infiltrated into *Camellia lutchuensis* petal tissue.

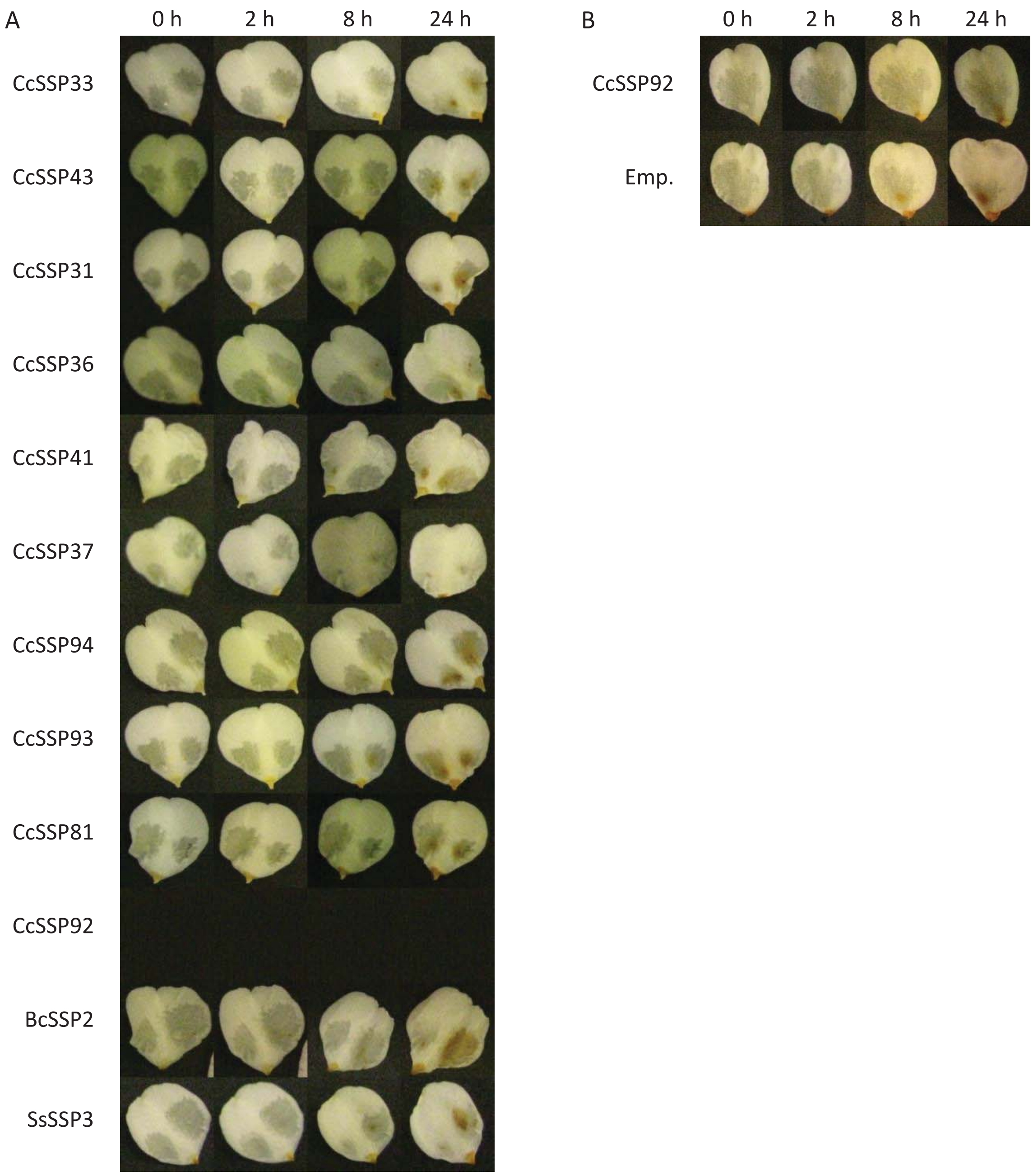

A, *Camellia lutchuensis* petal tissue infiltrated with 'empty vector' culture filtrate (left petal lobe) and 11 individual recombinant proteins (right petal lobe) (n = 3).**B**, Individual *Camellia lutchuensis* petals infiltrated with CcSSP92culture filtrate and 'empty vector' (n = 3). Photographs were taken at 0, 2, 8 and 24 h postinoculation.

Appendix 9.21. Functional protein assays using culture filtrate aliquots of BcSSP2 and SsSSP3 collected at different time-points post-induction.

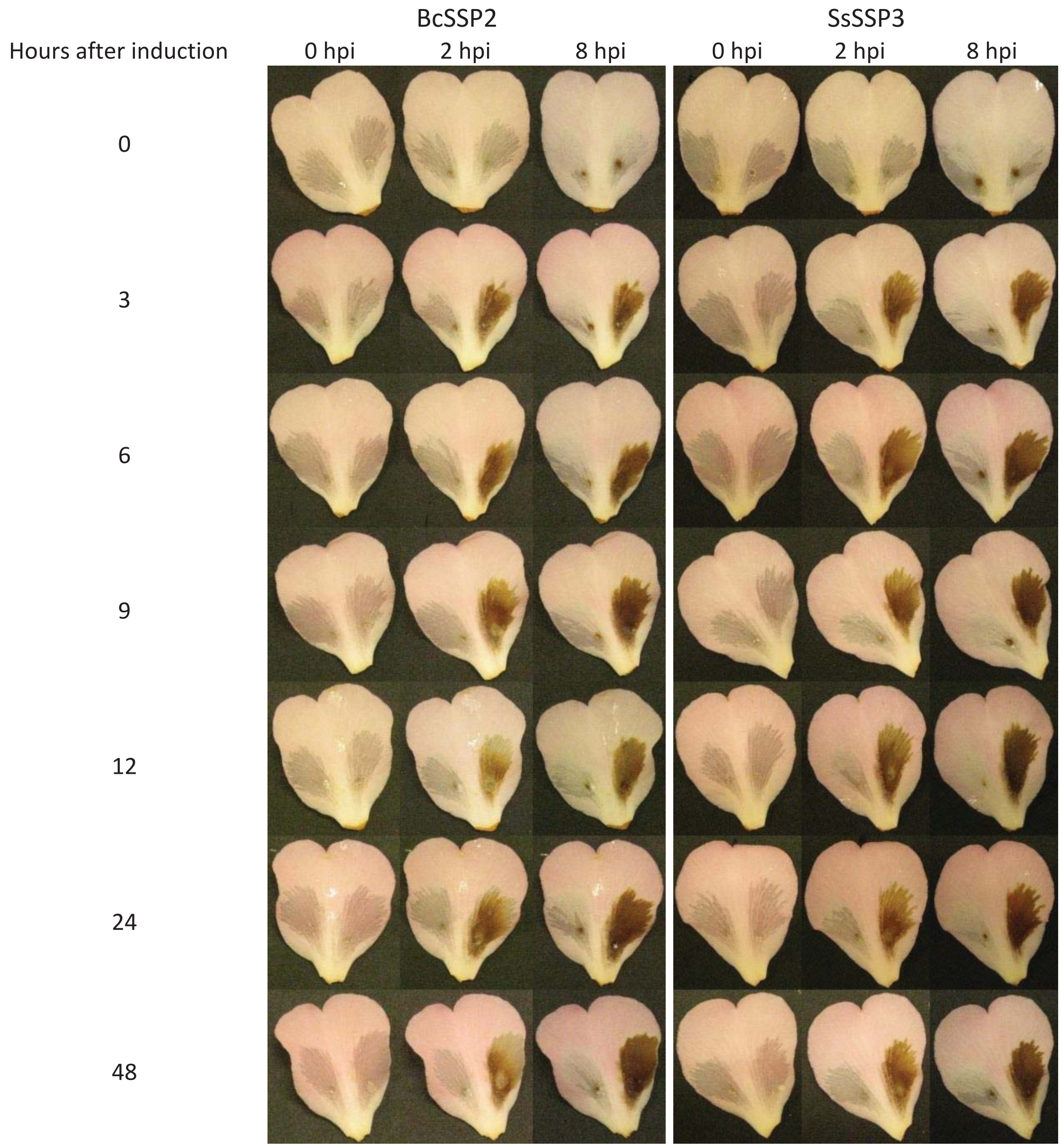

Camellia ‘Nicky Crisp’ petal tissue infiltrated with ‘empty vector’ culture filtrate (left petal lobe) and BcSSP2 or SsSSP3 culture filtrates collected at different time-points post-induction (right petal lobe) (*n* = 3). Photographs were taken at 0, 2 and 8 h postinoculation.

Appendix 9.22. Western blot of tagged recombinant CCL-SSPs.

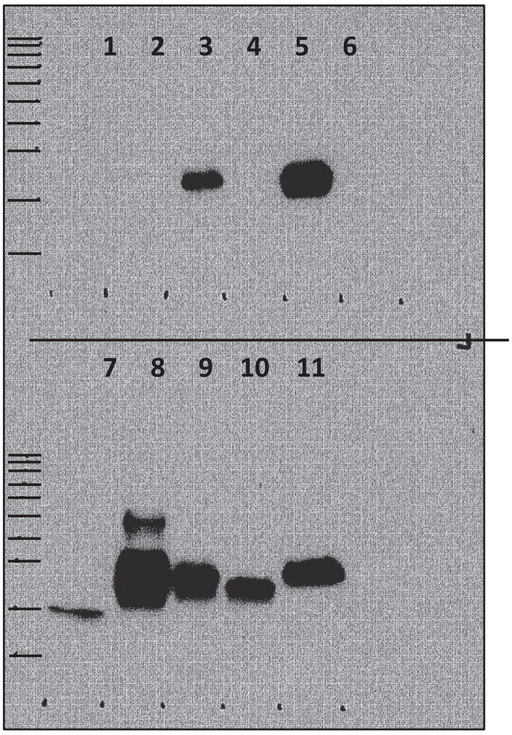

Lane legend: Empty vector (1), CcSSP33 (2), CcSSP43 (3), CcSSP31 (4), CcSSP37 (5), CcSSP94 (6), CcSSP93 (7), CcSSP81 (8), CcSSP92 (9), BcSSP2 (10), SsSSP3 (11). Protein standard values shown are in kDa. Horizontal lines represent protein standard molecular weights. From top to bottom; 170 kDa, 130 kDa, 100 kDa, 70 kDa, 55 kDa, 40 kDa, 35 kDa, 25 kDa, 15 kDa and 10 kDa.

Appendix 9.23. Isoelectric point values of native and tagged recombinant proteins, not including the signal peptide.

SSP ID	Cleavage site (1st amino acid)	Amino acid length (no sig.)	IEP (native)	IEP (tagged)
CcSSP33	20,21 (C)	80	7.89	7.23
CcSSP43	20,21 (A)	94	7.55	6.84
CcSSP31	19,20 (C)	80	7.57	6.90
CcSSP36	19,20 (C)	84	8.09	7.46
CcSSP41	20,21 (G)	89	6.92	6.60
CcSSP37	20,21 (C)	85	6.44	6.49
CcSSP94	18,18 (C)	82	8.08	7.36
CcSSP93	19,20 (C)	66	8.25	7.68
CcSSP81	20,21 (C)	97	7.57	6.91
CcSSP92	20,21 (C)	70	4.63	5.82
BcSSP2	20,21 (C)	70	5.52	6.28
SsSSP3	20,21 (C)	73	5.54	6.28

Appendix 9.24. Coding sequences of all conserved CCL-SSPs from *Ciborinia camelliae, Botrytis cinerea* and *Sclerotinia sclerotiorum* (*n* = 75).

>CcSSP1
ATGGTTAAATTCTCATCCATCGCCTTACTCCTCATCGCCGCTGTCAGTGTACAAGCTTGTACATATTGCCAATGTTTAACCGGTGATGGCAGCCATT
GTTGTTTAGCCAGGATCGAAAAAGTCGGTAACCTTAATTGTATCGCCGTTTGCATAGCAGCCTATAAAAAAGATGGTACGGGCTGTGCTGCTGTA
GGTGGTGCAGGGAACTATAAATGTGCTACTTCTCTTCAATCTCATTACCGTGAGAAGTGTGGGAGGATCAATATATAG

>CcSSP3
ATGAAATTCTCCGCCCTTGCTTTAGTTTTCATCGTTAGCGCTATCAGTGTTGAAGCCTGCAAGTATTGCCAGTGCCTATTCCCAGATGGTTCTCACT
GTTGTCTAGCCAAGGACACTCGAGTCAAGAACCAAGATTGTGGTGTCGTTTGCGCAAAATCCAGGCGTAAGGATGAGGCGTGGGTGACTCCAA
ACCAACAGGGTACTCCTTGTGATAGCAAGGGAACATATCAGTGTGCTACTTATTTCGAACAAGGGGGTCGCGCGAGATGTGTGTAG

>CcSSP4
ATGAAATTCTCTATTGTTGCTTTGTATCTCCTTGCCACTGTTATCAGTGTGGAAGCCTGCAAGTTTTGCCAATGTACATTCAAAGGTGGCGCTCATT
GTTGCGTTAAAGCGAACGTTGCGGCCGACGATTGTAACTTTTATTGCAAAGAGGCTCGTCGTGATGATGGCATATCATCAACATTCAATGGTGTA
GTCGCCCTCGGCACTGCTTGCGACAATGACGGCGGATACGTATGCGCTACTGCTTTCAACCATGGGAATCGTGCTCAATGCAAATAA

>CcSSP5
ATGGTTAAATTCTCTGCCATTAGCTTATTTCTTATCGCCGCTGTAACTGTACAAGCGTGTACTTATTGCCAATGCCTATTTTCGGATGGCGGTCATT
GCTGTCTTTACAGGAACCCTAAAATCGGCAACCTCGATTGCGGAACAGTTTGTGGAAGCGCGCGTCGCAAGGATGGTACATCAACGACGAAAGA
TGGTATAACGACATATGGCACTGCTTGTACTTCAAATTACAAATGTGCTTCTCTTTTCCAGTACATGCATCGTACTCAGTGCTACTAG

>CcSSP6
ATGGTTAAATTCTCCTCCATCGCTTTATTCCTTATCGCTAGCGCGGTCGGTATTGAAGCTTGCAACTATTGTCAATGCAAATTTCGAGGTGGTCGG
GGCGATTGTTGTGTGATAACACAGACTAGGACATCAATTGGCCAAACTGTCGATTGTCACGCCCTATGTTCCAACGCTTCTCGTAATGATGGTAG
AGCAGGAGGTACTCCCTGCAAAGCAGGTGGAGAATATCAATGTATTTCTGCTCTCGATTTCGATGGAAGGGTTAAGTGCATTGTGTAA

>CcSSP7
ATGGTTAAATTCTCTGCCATTACCTTAATCCTCGTCGCCGCTGCTGGTGTCCAAGCCGCATGCAATTATTGCCAATGTACATTCTCCGATGGCTCTA
ATTGTTGTATTACTGAGAACGTAAACAATGATTGTACCACTGTTTGCTCAAATGCGCATCGTGACGATAACGCAAAATTGAGATTGCCCAATGGA
ATTACCGTATATGGAACTTCTTGCGACAACTCAGGCGGATACCAATGCGCTACTCCTTTCAACCACAAATTTCGTGTTCACTGCAAATAG

>CcSSP8
ATGGTCAAATTCTCTGCCATCGCTTTGCTTCTCATCAGCGCTATCACTGTACAAGCTTGTACCTACTGTCAATGTCTATTCACCAATGGCCAGCATT
GTTGTATATTTGAGGACCAGGAGATCGGCAACCTCGATTGTAATAAGATTTGCTCCAGTGCTCATCGTAGGGATGGCACTACGTCGACTGTAAAT
GGCAAAATCGAATATGGCACTGCCTGTGCAGCTTCAGGAAGTTACAGATGCGCTAGTGGTCTCGAATCTGCTCATCGTACCAAGTGTTACTAG

>CcSSP9
ATGGTTAAATTCACGTCCATCGTCTTGTTCCTCATCACTGGTATCGCTGTACAAGCTTGTACATATTGTCAATGTTTATTCGACGATAACACTCACT
GTTGTATATTCGAGGATCACAAAGTCGGCAACCTAGACTGCCGCTCCGTATGCACGTATGCGCGTCGCCGAGACGACTCCACCCAGCTAGTCATT
GGGAAGGTTGCGTATGGAGCGGGCTGTATGGCCGGGGGAAATTATAAGTGCGCAACGAGGTTTCAGGCGTCGGGCCGGGTTAAGTGTTTTTA
G

>CcSSP10ATGGTCAAACTCTCCTCCATTTTTTTCTTTCTCATCGCCACCGCTGTCAGTGTGGAAGCTTGCAAGTATTGCCAGTGCCTATTTCCAAAT
GGTGACCACTGTTGTCTAGCCAAGGACACTCGGGTCAATGACCAAGATTGTACAGCTGTTTGCGGAAAAGCCCGTCGTAAGGATAACGATTGGA
CTTTGATCGATGGAGTTAGGATAGAGGGTACGGATTGTAGATCCAGTCACTACAAGTGTGCTTCTTATTTCGAACAAAAGAGGCGTGCCAGGTG
TGTCTAG
>CcSSP11
ATGAAACTCTATACCATTGTTCTATTTCTCGTCGCAAGCGCTATCACCGCAGAAGCCTGCAAGTATTGTCAATGCTTGTTCCCAAGTGGAAGACAT
TGCTGTCTCGCCAAGGATACGCGAGTTAAAAACCAAGATTGTGTCAAAGTTTGCAAAACAGCTGCTCGTAGCGATGGGAGTTGGCGCTGGGAA
GATAATGTTAGGGTTTATGGTACTCGATGTTATACTGGAGGCACTTATAAATGTGCTACCGTGTTTGAACAAGCTGGTCGTGCTAGATGTGTTTA
G

>CcSSP13
ATGAAATTCTCTGCCATAGCATTGTTTTTCATCGTCAGCGCTATCAGTGTAGAAGCCTGCAAGTATTGCCAATGCTTATTCAAAGATGGCAGTCAC
TGTTGTTTAGCTAAAGACACTCGAGTCGATAACCAAGATTGTTCATACGCTTGCACAAACGCCCGTCGTAAGGATGGAACTTCGGTTACTACCAA
GGAAGGGCTTGTTATTGAGGGTACTTATTGTTTCGCCGGAGGAAGCTACAAGTGTGCTACTTGGTTTCAACAATCGAATCGTGCCAGATGTGTCT
GA

>CcSSP14
ATGGTTAACTTCCTCACCATCGCCTTTTTCTTCCTCATCAACGCCCTCACCATCCAAGCCGCCTGCAGTTACTGCCAATGTAAATTCGCTAGTGGTC
AAAACTGCTGTGTTTATTCGAGCGGTCGATTCGGCAGCCAAGACTGCGCAACCGTTTGTGCCAAAGCCCATCGTGCGGATGGCAAGGGCAATGA
GATTGGCCCCCCAGGAACTGCTTGTGGCACTGGAGCAGGAACCCAGTGTCTCACCTTTTGGAACTCTCTTAATCGCGTTCCGTGCTATGTGTTGTA
G

>CcSSP15
ATGGTTAAATTCACCTCCATCGCTCTCCTCCTCCTTGCCGCCGTCAACAGCGTACAAGCTTGCACATATTGTCAATGTCTCTTCGCAGATAACTCTC
ATTGTTGTATATACCGGAACGCTCATATCGGCAACCTCGATTGTACCGACGTTTGCTCGAAAGCCCGTCGTAGCGATGGTTCAGTATCGATGGTT

AACGATGTGGTTAAATATGGAACGGCTTGTAACGCAAGTGGAAAATATAAATGTGCGACTATTTTCCAACAAGCGAAGCGTACTCTTTGTGAATA
G

>CcSSP16
ATGGTCAAATTCTCTACCATCGCTTTGTTTCTCATCACTAGCGCCATCAGTGTGCAAGCTTGTACTTATTGCCAATGCCTATTCAGCAATGGCGACC
ATTGTTGTCTGACCCAGGACCCTAATGTCGGCGACCTCGATTGTAAATCCGTTTGTTCCAATGTCCGTCGTAAGGATGGTACATCTCAAACATTCG
CAGGAGGTTTTGTCAAATATGGTACTCCTTGTGGGTCTAGTGGAAATTACAAGTGTGCTAGTATGTTCGAAGCCGAGAATCGTGCTAGATGTGCT
TAG

>CcSSP17
ATGGTTAAATTCATCTCCATCGCTCTATTCCTTATTTCCGCCGTCACCGTGCAAGCTTGCGTTTATTGTCAATGCTTGTTTAAAGACAAATCACATTG
TTGTCTATATCAGGATTCTCGTATAGGCAAGCTCGATTGTGGTAGCATCTGCGCCAAAGCCCGTCGTAGAGATGGCACTACATGGATTTCCCCTG
ATCATGCCGTCGATTTTGGTACTCCTTGTGACGCGAGCGCTGGATACCAGTGTTCTAGTTGGCTCGCAGCCCCGAAACGTGCTAAATGTAACAAC
TAA

>CcSSP18
ATGGTCAAATTCACCTCTATCGCTTTGTTTCTGATTGCTGCTGTCAGCGTACACGCTTGCACCTATTGCCAATGTCTGTTCAACAATGGCGGACATT
GTTGTGTGTATCATGACCCTAATGTTGGCAACGTCGATTGTACTGAGAAATGCAAAACCGCTCGTCGTCATGATAGCTCAGTAACTGATTTACCC
GGAGGTGGACATGCATACGGTACTCTCTGTGCGGCTGCAGGAAGATACAAGTGTGCTACTATTTTCCAAGCCGATCATCGCGCTCTATGTAACTT
GTAA

>CcSSP19
ATGGTCAAGTTTACCTCCATCGCTCTATTCCTCATTGCCGCCGTTAGCGTCCAAGCATGTACATATTGTCAATGCCAATTTGCAAATGGTGCGCATT
GTTGTGTAGCTCAGGACTACAGTCTCGGCAACATTGATTGTGTCGCCGCTTGCAAAAATGCCCGTCGCGACGATGGAAGAAAATATATGGAAGG
CGTTACAATGAAGGAAGGAACTGCTTGTGGGGCTGATGGAAAATATAAGTGTGCTACGGTTTTCGAATCCGACAATCGTGCTAAGTGTCGTTTG
TCGTAA

>CcSSP20
ATGGTTAAATTCTCTGCTATCGCCTCCTTCCTCATCGCCGCTGTTGGTGTACAAGCTGCTTGTGATTATTGCCAATGCGAGTATCGAGGTGGCCAG
AATTGCTGTGTATCACCGACCAAGCCCGCACTTGACGGAATGGATTGTCACGCCTATTGTCTTCAAGCCAATCGTGATGATGGCACATCATTTGGT
ACTCCTTGTAGAGGGAATGGAAATTATAAATGCGCTACTCCTGTTCAAATGGAGGGAGCAGTTAAGTGTAAGCCTACTGGGATTGCCAGTGGTG
GCAAATGA

>CcSSP21
ATGAAATTCTCTGCTATAGCATTCTTTTTCATCGCCAGCGCTATCAGTGCAGAAGCTTGCAAATATTGTCAATGCTTATTCAAAGATGGTTCCCATT
GTTGTTTAGCAAAGGATGCTCAAAGCAACAATCTAGATTGTGCCGCCGTTTGCAAAACATCCCGTCGTGCGGATGGAACCTTTTGGTCCAAACCC
AATGACGTTTGGGTCAACCATGGAGGTACTGAGTGTGGTGCCGATGGAAAATATCAATGTGCTTCGTATTTTCAATACAAGGGTCGTTCTAGGTG
TGCTTGA

>CcSSP22
ATGGTTAAATTCTTCTCCATCGCCCTGTTGCTCATTTCCGCTGTCAGCGTGCAAGCTTGCATCTATTGTCAATGCCTGTTTGACAATGGCGAGCATT
GTTGTGTTTATCAGAACTCTGTTACCGGCAACCTCGATTGTAATGCTGTCTGCAAAGACGCCGTTCGTAAAGATAACACGATGTATACTGTTGACC
CCGTTACTCACGAGAAGACATATGGTACTCCTTGTAAGGGTAACGGAAAATACAAGTGTGCTAGCATTTTCGAATCCGGCCGTCGTACTAAATGT
AACTAG

>CcSSP23
ATGGTTAAATTCACCTCCTCCATCGCTCTACTCCTCATTGCGGCTGTCAGCAGTGTACAAGCTTGTAGCTATTGCCAATGCCTCTTTCAAGATGGCT
CGCATTGTTGTCTCGCCCAGGACTCTCATAAAGGCAATCTCGATTGTACAGCCGTCTGCTCCGGAGCCCGTCGTCAGGATAGCACATCGACTGTT
ACCCCTGATCACAAACTTGTATTTGGTACTGCTTGTAATGCTAGTGGAAATTACAAGTGTCTTACTATTTTCAACGTCGATGGTCATGTTAAGTGTT
TTTAG

>CcSSP24
ATGAAATTTTCCGCCATTGTTTTGTTCTCCATCATTAGCGTTATTAGTGTTGAAGCTTGCAAGTATTGCCAATGTTTGTTCCCAGATGGTTCTCATTG
TTGTTTGGCTAAGGATACTCGAGTCAGCAATCAAGATTGTGCTGCTGTTTGCAAAGAATCCCGTCGTGATGATGGCATGACGACGTGGTGGTGG
CCAAGCGGTGTCAACGGGAACAAGGGTACACGTTGTGATCTCAGTGGGTTATACAAGTGTGCTACTTTTTTCCAACAAAAGCATCGTGCTAGATG
TGTCTAG

>CcSSP25
ATGGTTAAATTCACTTCCATCGCCTTATTCCTCATCGCTAGCGTTGTTAGTGTACAAGCTTGCACCTATTGCCAGTGCTTGTTCCCAAATGGAAAGC
ATTGTTGTGTATACCAGAACTCTAAGATCGGCAACCTCGACTGTACTACTTGGTGCCGTAAAGCCCGTCGTGCTGATGGTACACAAGTGAACATA
AACAATGTTATTCATTGGGGTACTGCTTGTGATACCAAAGGAAGTTACAAATGTGCCTCTTTTTTCGCAAGTGGTGTACGTGCTCCTTGTTATGAT
ATGTAG

>CcSSP26
ATGGTCAAATTCTCCTCCATCGCTTTATTCCTTATCGCTGGTATCAGTGTACAAGCTTGTACTTATTGTCAATGCCTATTTTCAGATGGTTCACATTG
TTGTGTAACACCCCCCAAGACCTCAAATGTTCCCGATATCAACTGTCACATGATATGTTCCGGCGCTTATCGTGATGACGGTCACGGAGGTAAAA
CTGCTTGTGATGCAAGTGGAAGTTTTCAATGTGCCAATCTTTTTGAAATGGAGGCTAGGGCTAAATGTGTTTACCCCAACCCACCGGCGCCAAGT
CCAAAATAA

>CcSSP27
ATGGTTAAATTCACCTCTATCGCTCTGTTCCTCATTGCCGCTGTCAGCGTGCACGCTTGTAGCTATTGTCAATGCCTTTTCACAGATGGCTCGCATT
GTTGTGTATATCAGGACTCTAGGTCCGGCAATATCGATTGCAGTTTGTATTGCAGCCAAGCCCGTCGTGCGGATGGCACAAAGTGGGATATCAA

CCATATTGTCAAATATGGTACTGCTTGTGCAGCTGGAGGAAGTTACAAGTGTACTACTATTTTCGCCGCCGACAACCGTGCTCCGTGTTACCGTAT
CGGGAATTAG

>CcSSP28
ATGGTTAAATTCACCTCTATCGCTCTATTCCTCGTTGCTATCGTTAACGTCAACGCTTGCACCTATTGTCAATGCCTGTTCGATGATGGTAAGCATT
GTTGCCTGGCTAAGGACTCTAAGGTTGGCAACCTCGATTGTACTTACGTCTGTTCCAACTCTCGACGCGATGATGGTACAATACATAATTATCCGG
GAGGGGTAGTTAAATATGGTACTTTTTGTAAGGCGGGTGGAAATTATAAGTGTGCTAGTTGGTTTGAGGCCAAGCATCGTGCAAAATGTCGACC
TAATACGTAA

>CcSSP29
ATGGTTAAATTCTCCTCCATCGCTTTATTCCTCATCGCTAGCGCTCTTAGTGTAGAAGCAGGATGCACTTATTGCCAATGCATGTTTCCAAATAATG
AACATTGTTGTGTAACTCCAATCAAGACCTCTAATGTCCCCAACATCGATTGTACAGCCATTTGCAGAGACGCCCGTCGTAACGATGGCTCACACT
GGGTCGAAGCAGGGGTACCTAAATTGGGTACTTCTTGTAATGCCCAAGGAGCCCATGAATGTGCCAATGTTTTCGAAATGGAGGCTCGTAGGAA
GTGTTATTAA

>CcSSP30
ATGGTTAAATTCATTTCCATCGCTCTGCTCCTCATTTCCGCCGTCAGCGTCCAAGCTTGCGTTTATTGTCAATGTCTATTCCACGATGGATCGCATT
GCTGTGTATATCAGGACCCTAATGTCGGCAACCTCGACTGTCCTACCGTCTGCGGCAAAGCCGTTCGCAACGATAATACTATGTACACTGTTGAC
CCTGATGGAAAAAATAAAGTATACGGGACGCCGTGTCACTTGAATGGTGATGCGGGATACAAGTGTGCTAGCATTTTCGAAGCGGAGCATCGT
GCGAGATGTCATTAG

>CcSSP31
ATGGTTAAACTCACCTCCGTCGCTGTCTTCCTTATCGCAGCTGTCAGTGTACAAGCTTGCAATTATTGCCAATGTCAATATCGAGGTGGTCAAAAT
TGCTGTGTAACACCGTCTTATACCTCAAGTGTCGATCTCGATTGTCACGCCGTTTGTCTCCAAGCCAGTACTGTTAGTGGTACTCATTGTAATGGG
GGTGGAAATTATAAATGTGCCACATGGGCCGAAATGTCGGCGGGGATTAAGTGTGTTGCTACTCCGATTGCTAGCCCGTCCCCTAGCCCAACTCC
AAGTCCCAAGTAG

>CcSSP32
ATGGTTAAATTCACCTCCGTCGCCTTATTCCTCGTCGCCGCCGTCAGTGTACAGGCTTGCACTTACTGCACATGCTTATTCACCAATGGCCAACATT
GTTGTACATACCAGGACAGTCGTGTTGGCAACCTTGATTGTAACGCGATTTGCAAGAGAACGACTCAACGTGATGGCAAGATCTGGAATTTCAA
CGGAAAACACTACGTCGGTACTCCTTGTGATGCCAATGGAAGTTACAAGTGCGCTACTTATTTCGAGGCCGGTAGCCGTTCTCCATGCAGCGGG
GACTTGACCCCCGCATAG

>CcSSP33
ATGGTCAAACTCTCTACCATCGCTTTATTTCTCCTCACTAGCGCTCTCAGTGTAGAAGCTTGTACATATTGCCAATGTCTATTCAAAGATGGCTCCC
ATTGCTGTGTATTCCAGGACTATCATATCGGCAACCTAGATTGCAACGCCTCTTGCGGTGGGGCTCGTCGTAACGACGGCATGGTGTTTACTGAA
AACAACGAAAAGAGATATGGTACTGCTTGTGCAGCTAATGGAGCATACAAGTGTGCTAGCTTTTTCCACGGGGGGCATCGTGTTCAGTGTTACG
GTGTTTTCAGAAACTAG

>CcSSP34
ATGGTTAAACTTACCTTCGTCGCTTTGTTCCTTCTCGCCAATGTTATTAGTGCACAATCGGGTTGCACTTACTGTCAATGTCTCTTTGCTAATGGTG
ATCATTGTTGTGTAACACCAACTTGGACCTCCGATGTCCCCAACATCGATTGCAAGTTGATTTGTTCGACCGCCCGTCGCAACGACAAAACGCAAT
ACGGAACCAACTGCGATCGATCGGGAAAATACCAATGCGCCAATCTTTTTGAAATGCAGGTTAGGGCTCCATGTTACTTTAATTCGGCGGCACCT
AGTCCCCACCCTCACCCTTAG

>CcSSP35
ATGGTCAAATTCTCCATCATCGCCCTATATCTCCTCGCTAGCGCCATCAGTGTGCAAGCTTGCACATATTGTCAGTGCTTATTCCACGACACCGGCA
AACATTGCTGTGTATACGAGGACGCCAATGCCAGCCAAACTGGCAACCTTGATTGCAACGCCGTCTGCGCCTCCGCTCGTCGTAGGGATCATACC
GAGTGGACTGTCAATGGCGAAAAAAGATATGGAACTGCTTGTGGTACTTCGGGAGACTACAAGTGTGTTAACTGGTGGGAGGCGAACAACCGT
GTTCAGTGTGCCCATGCTTGGGATTAG

>CcSSP36
ATGGTTAAATTCAGTTCTATAGCCTTTTTCCTCATCGCTACTATTAGTGTACAAGCTTGCAATTATTGTCAATGCAACGATACACATGGTAACGCAT
GTTGTGTAACTCCAACCAAGATCGGTAGCATTGCCGATATAGATTGTCATAAGCGTTGTACAAGTGCTCGTAGAGCAGATGGGAAATGGGAGTT
GGATGCAATTGGTCATAAGCAATTGGGTTCTGCTTGTAAAGGTTGGGGAGGAGATAGTAAATGTATTACTTGGCCGGAAGCTAAAGCCTTTCCC
ATGAAATGCGTTGATCGAAATTGGTAA

>CcSSP37
ATGGTTAAATTCATCTCCCTCGCTTTATTTGTCATCGCCAGCGCCGTTGCCGTGCAAGCATGCACCTTTTGCCAGTGCGAGTTTTCAGATGGAGCA
CATTGTTGTGTATATTCGAGCACTGCATTCGACCAAATCAACTGTAAGGACGTATGCAGCAAGGCGCATCGAGCCGATGGCAAAAGTTATGGAA
CAGGTGCCCCTGGTACCGCTTGTTCTGCCGGAGGCAAATATCAGTGCACCAATGCTTGGACTTCCCTTGATCGTACTCCCTGCTACAGAATGGAT
GAGCCATTCAGTCCAAACTCCCCCCAGCCATAG

>CcSSP38
ATGGTCAAATTCCCTTCCATCGCTTTACTCGTCGTCGCCAGCGCGCTTAGTGTACAGGCTTGCATCTATTGTCAATGCCTCTATCGTGGTGGTCAA
GATTGTTGTGTGACACCTGATGCGCTTTCATACGGCGACAGTGATTGTGCATCTTTATGTGCAATTAGGCATCGTCAAAACGGCACACCCCTTGG
GTCTCCTTGCAATGGAGGTGGAGCTTATAAATGTATTACTGAAGCCCAAATGATGACAAGGGTTAAATGTGTTAATCCTCCTCATGACACTACAA
TTCCATATATTGGTCCTCCTCGCAGGGTTTGA

>CcSSP39
ATGGTTAAACTCTCTATTATCGCTTTATCCCTGATTTCCGCTGTTGGCGTACAAGCTTGCACTTATTGCCAATGTCTATTCGATAATGGCAATCATT
GTTGTCTATATAAGGACTCTGATATCGGCAATCTCGATTGTAAAGCCATTTGCTCTACAGCCCGACGTCATGATGGCACAGTGTTTGTTACAGAGC

CGGGACCTGTAGTTAAATATGGTACTGCTTGTTCCACCAATGGAAATTACAAGTGTGCTACTGTTTTCCAATACAAGAAGCGGGTTAGATGCGGC
TAG

>CcSSP40
ATGGTTAAATTCTCTACCATTGCTTTGTTTTTCATCACTAGTGCTATCAGTGTCCAAGCAGCTTGCACTTATTGCCAATGCCAATATCGAGGTGGTC
AACCTTGTTGTGTCACTCCCACTAAGGAGGAGCCTGATGTAACCATCGATTGTCACGCCCTTTGCGAAACAGCTTATAAATATGATGGTACATGG
CATTATGAAGGGGGGAAGGTTGTAGAGGGTACCCGTTGTAACGGCGGAGGAAACTACAAATGTATCACTCGTGTTCAAATGGAGGCTTCTCCC
GTTCAATGTGTTCAGCCTAGTGGAACTCGTTCAGTCGTTTGA

>CcSSP41
ATGGTCAAATTCACCTCCATCGCCTTATTCCTCATCGCCAGCGCTGTTAGTGTGCAAGCAGGCTGCAATTATTGTGAATGCCAATATCGAGGTGGC
CAGCCTTGTTGTGTAACTCCGCCTCAGGACTCTGCTGTCGTTATCGATTGTCATGAAGTGTGCTTACAAGCCCGTAAAATTGATGGCACAGCTACG
ATCGTAAATGGCGTATATCTGGAGGGTAGCTTTTGTAATGGTGGAGGAAACAATAAATGTATCAATAAGGCCCAAATGTTGGCGTCTCCTACTAA
GTGTGCTACACCTACTAATACTGGGTCACCCATTGGTCAGTAG

>CcSSP42
ATGGTCAAATTTACCTCAATCGCTTTATTCCTCTTCGCCGCTATCAGCGTACAAGCTTGCACTTATTGCCAATGCGAGTTCCCAAACGGAGGACATT
GTTGCGTAACTCCAACTAAGACCTCTAATGTTCCCAACATCGATTGCCATGCCATTTGCTCAAACGCACGTCGTGCCGATAATACATATGCGGTCG
TAGGAGATGTGGTTCTAGAGGGCACCCCTTGTAATGCTGGAGGAAGATTTCAATGTGCCAATCTTTTCGAGATGGAGGGGAGGGCTAAGTGTGT
TCAACCTAGCAATAGTCCTCAAGCTCCAGGTGGTGGAAGATAA

>CcSSP43
ATGGTTAAATTCTCCTCCATCGCCTTATTCATTATCGCCAGCGTGGTTAGTGTACAAGCTGCTTGCACTTATTGTCAGTGTAAATTTCGTGGTGGTC
AAGATTGTTGTGTTACACCGACTCAGACCTCAACCGACAACAACATCGACTGTCGCGCCGCTTGTGCCGATGCCCGTCGTGATGATGGCACAGAA
TGGGTGAAAGGTCAAGTGACTGATCATGGTACGCGTTGCAATGGAGGAGGCAATTTTCAATGTGTTAATCAGTTGCAAATGGAGATGAGGGTT
AAATGTGTGGATGCTATTAAGACTGTTAGTCTCCCTGGTCCGAGTCCTATGCCTAAGTAG

>CcSSP45
ATGGTTAAATTCTCCTCTATCGCGTTATTCCTCATCGGTGTTGTCAGTGTACAAGCTTGTACTTATTGTCAATGCCAGTTTGCAAACGGTGCTCATT
GTTGTGTAACACCAACTACGACCTCCAACGTTCCAAACATTGATTGTCAATCTATATGTTCCGAAGCCCGTCGTGCTGATGGTACAACGTGGGTTA
TCGGAACAAAGATTTATTCTGGTACTCGTTGTCATGCGGGTGGAAAATATCAATGTGCGAATGTTTTCGAAATGGAGGTGAGGGCTAAGTGTGA
TCTCTCTGCTCCAAAGGCTAGTCCGGCTCCTAAGCCATTCCCAAGTCCTAAATCTAGTTAG

>CcSSP46
ATGGTTAAATTCACCTCGATCGCTTTATTCCTCGCCGCGACTGCTAGCGTGCAAGCAGTATCCAGTCAAGCACCAACCGCCACCGTAGTTGCAGCT
TGCAATTACTGCCAATGCCACGATGCAGCCGGCAGCCCATGTTGCGTAACACCCAACCATGTATCCCACAGCGCAATGGATTGCCAAGCCTTCTG
CAAAAAGGCGTACCGCCTCGACGGGGGTTACGAACTAGATCCCGCGGGGTACATTGTCGAGGGAACATCGTGCCACGCCGGGGATTCCAGAAC
GAACTTTCAATGTATTACATGGGCACAAGTGGAGGCCGCTCCATGGAAGTGTGTTGCTCAGTAG

>CcSSP47
ATGGTCAAATTCTCCTCCATCGCCTTATTCCTCATCGCCACTGTTGGTGTACAAGCTTGCACTTATTGCCAATGCGAATTTCGAGGTGGTCAGCCTT
GCTGTGTAACACCAATTACACCCAACAATAATGTCGATATGGATTGCCACGCCATTTGTCTCACAGCTCGTCGTGATGATGGCACAAAATGGCTT
GAAGATCTAACGACCGTGTACGGTACTCGTTGTAATGGGGCTGGAAATTATCAATGTATCAATCAATTCCAAATGCAAGGGAGGGTTAAGTGTG
TTAACCCTAATGCTCCTATTGCTAGTCCGGCTCCTAAGCCGTCTCCTACTCCTATCCATCAGTAG

>CcSSP51
ATGGTTAAATTCTCCTCCATCGCTTTATTCCTCATCGCCAGCGCGGTCAGTGTACAAGCTTGTACCTATTGTGAATGCAAATTTCGTGGTGGACAG
ACATGTTGCGTTACACCTCGAAAGGCCAACACCGAAGACCTGAACTGCCAGCAAATCTGTTCCAGCGCCCGTCGAGACGACGGCACGCAATGGG
TTGAAGGTCTCATCCATACCATTGGCACCCCGTGTCATGGAGGGGGAAATTATCAATGTGTTACTTTTGCGGAAATGCAAGCCGGGGGGATGAA
ATGTGTGGATCCCATCATTCCGTTGAATGCGGCGCCTAGTCCGTCGCCTCACCCTTAG

>CcSSP53
ATGAAATTCTCCGCCATTGCTTTGTTTGTCATCGCTAGCGCCATCGGCGCTGAAGCTTGCAAGTATTGCCAATGCTTGTTCCCAGATGGAGGTAAC
TGCTGTCTCGCCAAGGACAGTAGATACGACAGCCTAGATTGTACCGCCATTTGCGCAAAGTCCCGTCGTGATGATGGTACGACTACGGAGACTC
CCGATGGGCGTCTCACACTACACGGTACTGCTTGTGCCCCCAATGGAAGCTACAAGTGTGCTACTGTGTTTCAACAAAAGCATCGTACCGGTTGT
GTGTATTGA

>CcSSP75
ATGGTTAAATTCTCTGCCATTGCCTTGTTGCTCATCGCAACTGTTAGTGTACAAGCTTGTACTTATTGTCAATGTCTATTCTCAGATGGCAAACATT
GTTGTCTGTATGAGAACGCGAGCGCAGGCAACGTCAATTGTAATGATGCTTGCAAATGGGCCCGTCGTAATGATGGCACAACATGGAAGGAAG
GGCCATACACCAGGCAGGGTACTGGCTGCAAGGCCGGAGGAAGCTACAAATGTGCTAGTTATTTCGAATCCAGTCACCGTGCTAAGTGTAATTA
G

>CcSSP76
ATGGTCAAATTCTACTCCATCGTTCTGTTTCTCATCGCCAGCGCTGTTAGTGTGCAAGCTTGCACTTATTGTCAATGCCTTTTTGAAGATGGCTCAC
ATTGTTGTCTGCACAAGGATCATAAAATCGGCAACCTAGATTGTACATCTTATTGCAATCGAGCCCGTCGTAATGATGGGTTTGTGCATTCTGAAG
AGAATGAAATCGTGCATGGTACAGCCTGCAGATCTCAGGGAGTTTATAAGTGTGCTACTTTTTTTCAATACAAGCATCGTACGAAGTGTCATTAG

>CcSSP77
ATGGTCAAATTCTCTGCCGTCGCTTTGTTTCTCATTGGCGCCATCAGTGTGCAAGCTTGCACTTATTGCCAATGCCTCTTCCAAGATAGGTCTCATT
GTTGTGTATATCAAATCGAGGATGCTGGCAACATCGATTGCAATAAGGTTTGCGGCCAAGCTCGTCGTGCTGATAGCTTTGTTACGGATGCCGAA

GGGGACAACCATAGAATCAAAATCGGTACTCCTTGCAATGCTCAAGGAATATACAAGTGTGCTACTTGGTGGCAAAGTGGAAATCGCACTCCAT
GTTACAAAAACAAGTAG

>CcSSP78
ATGGTTAAATTCATCTCCTTCGCCTTGTTCCTCTTCGCTGCTGTCGCTGTGCAAGCTTGCACTTATTGCCAATGTTTAAACGCAGATGGTAAACATT
GTTGTATGGCCGTGGACAAACATATCGGCAACCTCAACTGCGAATCCGTGTGCCAAGTCGTCAAGCAAAAATCCGGTTCCAGCTGTACCGGTGG
CGGCGCATACCAATGTGCTACTTGGGCGGAATCTGGCCATCGCGATCAGTGTCAGTAG

>CcSSP79
ATGGTTAAATTCTCCGCCATCGCTCTATTCCTCATCGCCAGCGCAATCAGCGTACAAGCTTGCAGCTATTGCCAATGTCTATACAAAAGTGGTGAT
CATTGTTGTATGGTCGTGGGTGATAGCAAGCAAGATTGCGGTGAAACTTGCAAAATTGCCATTCGTCATGATGGCACTAGCTGTTATGCTGATGG
ATCACACAGATGTGCTACTATCATTGAATCCGATTATCGCGAGAAGTGTCGCAAGTGGTAG

>CcSSP80
ATGAAATTCTCCGCCATTGTCATATTATTCATCATTGGAGCCATCAACATTGAAGCATGCAAATATTGTCAATGTTTATTCGACGATGGATCCCACT
GTTGTTTAGCCAAGGATACTCGCGTCAAGAATCAAGATTGTGGCGCCGTTTGCGCCAAAGCCCATCGTTTAGATTACTCGTGGAAATTTCCCCTC
GAAGACCATCGTCATTATGATGGTCGTGCGTGTAGCACGGCGGGAAAATACACGTGCGCGACGATTTTTCAACAGGCGCATCGGAAAAGATGC
GCGGATCTGGGGTGA

>CcSSP81
ATGGTTAAAATCTCCTCCATCGCTTTATTCCTCATCGCTAGCGCAGTCAGCGTACAAGCTTGTTCTTATTGCTCATGTCTATATCGTGGTGGTCAAG
AATGTTGTGTTACACCTGATCAGGTCAACTGGGACACCAAGACGGATTGTCATGCCGAATGTTTGGGAAAGAATCGCCAGGACGGTACCAAACT
TGGGTCTCCTTGTAATGGAGGTGGAGCTTGGAAATGTATTACTCAATCCCAAATGGAGTCGAGGGTCAAGTGTGTTAACCCTCCTCGTAACACTG
CTGCTCCCGGATATAGCGGTATTGACACACCCATCCCACCCTCGTGGGGAAAGCATGGGGCAGAATGA

>CcSSP82
ATGGTTAAATTCACCTCCATCGCTCTATTCCTCATCGCCGCTGTCAGTGTACAAGCTTGCACCTACTGTCAATGTCTATACGAAAACGGCAACCACT
GTTGCATGACCACGAACGATAGCAACCAAGATTGCACGTACGCTTGCAAACAAGTCCGTCGTTGGGATGGCACGGGCTGTGTTGCGAATGGAA
AATACAAGTGTGTTAGTGCGTGGGATTCGGACTTCCGTGAGAGATGCCAGAAACTTTAG

>CcSSP83
ATGGTTAAATTCACTTCCATCGCTTTACTCCTCATTACCAGTGCACTTAGTGTACAAGCTTGCACATATTGTCAATGTCTATTCCCAAATGGAGATC
ATTGTTGTATGACATCGAACGGTAGCAACCAAGATTGCACTTACGCTTGCAAACAAGTCCGAACTTTCGAGGGCCTTGGTTGCGTTGCTGGAGGA
GCATACAAATGCGCTACTGTATTCGAATCCGACCATCGCGATAAGTGTCAAAAATAG

>CcSSP84
ATGAAATTCTCCGCCATTGCTTTGTTTTTGATTGTTAGCGCTATCAGTGTGGAAGCTTGCAAGTATTGCCAGTGCCTGTTTCCAGATGGTTCCCATT
GTTGTCTAGCCAAGGACAGTCGAGTTGACGACCAAGATTGTAAGGTCGCTTGCTCAAAATCCCGTCGTAAGGATGGCAAATACTTTCAAGTAAA
CGGCATTTTGAGTCTGGTAGAGGGCACTCCTTGTGATACCGGAGGAAGTTACAGATGTGCTTCTTTTTTCGAGCAAAAGAAACGTGCCAGATGT
GTGTGA

>CcSSP85
ATGAAAATCTCGGCCATTGCTTTACTTTTTATCGGCATTATCGGTGTCGAAGCTTGCAAATATTGTCAATGCTTATTTGAAGACGGGTCTCATTGTT
GCCTGGCTAGGGATACTCGAGTCGATAATCAAGATTGCGGCTACGTTTGCGGAGGATCCCGTCGTGATGATGGTACAACCTTTAGTACACCCGG
TAGCATTATTGTAAGACATGGTACTGCCTGTAATGCCCAAGGAAAATACAAGTGTGCTACTATTTTCCAACTGAAGCACCATGCTAAGTGCGTTTC
AAAACAAAACTTCAAAATGAGATTGTAG

>CcSSP86
ATGGTCAAATTCTCCTCCATCGCCTTATTCCTCATCGCTGCTGTCAGTGTACAAGGTTGCACTTATTGCCAATGCCTATTCGCAGATGGCTCTCACT
GTTGTCTATATATGGACGGTAACAAAGGCAACCTCGATTGTTCGATCTATTGCGATGTAGCCCATCGTGCTGATCACACACAACACGACCACAAC
GGTTATAGCTCATGGGGTACGGCTTGTAATGCTTCGGGATCATATAAGTGTGCTACAGTTTTTGAATCCCATCACCGTGATAAATGTTACCAAATC
TAA

>CcSSP87
ATGAAGTTTTCAGCCCTCGCTTTATTTTGCCTTGTCAGCGCTATTAGTGTGGAAGCTTGCAAGTATTGCCAATGCTTGTTTCCAAATGGTAGTCATT
GTTGTTTAGCTAAAGATACTCGAGTCAAAAACCAAGATTGTGGAGCCGTGTGTCAAAACGCCCGTCGTGCTGATGGCTTTGAGCATTACGATAAT
GGGGTTAAGGTAGTTGGTACTTGGTGTTGGGGCGGAGGAGAATACACGTGTGCTTCTTGGTTTCAACAATCGCATCGTGCGAAGTGTGCCTAA

>CcSSP88
ATGGTCAAATTCGCCTCCATCGCTCTATTCCTCCTTGCTGCTGTCAGCAGCGTACAAGCTTGTACCTACTGCCAATGTCTATTTGAAGATGGCTCAC
ATTGTTGTCTACACGAGGATCCTAAAGCCGGCAACCTCAACTGTAATGACATCTGCAACAGAGCCCATCGTCAAGATGGCACCACGTTGACTCTC
CCTAACCACAAGGTTGTCTACGGTACTTCCTGTGATGCTAAGGGAAAATACATCTGTGCCAATGTTTTCCAGGCCGATCACCGTGTCCGATGTAAT
GTTTAA

>CcSSP89
ATGAAACTTTTTACTCTCGCTTCATTTTTAATTATTGGAATTGTCAACATTGAAGCTTGCAAATATTGTCAATGTCTATTTACAGATGGTTCTCATTG
TTGTTTGGCCAAGGATACTCGAGTCAAAAACCAAGATTGTGCAACCGTTTGCTCAAAGGCCGAACGTTTTGATTATACATTATGGGATCCAATAC
ATGTCAAAGCCAACGAAGGCGGTGCTGCTTGTGATTCATTAGGAACATACAAGTGTGCTACTGTTTTCCAACAAAAGCATCGTGCAAAGTGTGCA
TCATAG

>CcSSP90
ATGGTTAAATTCAGCTCCTCCATCGCCCTGTTCCTCTTTGCCGCCGTCAGCAGCGCACGCAGTTGTAAATATTGCCAATGCCTATTTCCAAATGGCC
AGAATTGTTGTCTATGGGAGGACAGAGCTTTCAGCAACATCGATTGTCAAGCCTTTTGCGCCCAAGCCCGTCGTCACGATGATACAACCTCTACT
CTCCCTAATGGCCATGTTGTACTTGGCACTGCTTGTAATGCTTCTGGAAGTTACAAGTGTTCAAATCTTTGGCATATCGATAATCATGTCACATGTT
ATAATAAGCAAAGCTAG

>CcSSP91
ATGGTTAAATTCACCTCCATCGCCTTGTTCATCATCGCTGGTATCAGTGCAGGTGTCCAAGCTTGCACTTACTGTCAATGTTTATTCAAAGACGGT
AGTCACTGTTGTTTATTCGAGGATCAAAACATCGGCAACCTCGACTGTCGTGACGTATGCACTTACGGTCGTCGTAGAGATGATTTTACCGAGCT
CATCAATGGAAGAACGGCATATGGTACCCCATGTGGGGCCGGTGGAAATTATAAGTGCGCGACGGGTATGGAATCCGCTCATCGATCCAAGTG
TTACTAG

>CcSSP92
ATGGTCCGCCTCGCATCCATCGCTATGTTCCTCATCGCCAGCGCCATCTCCGTGCAAGCATGCACCTACTGCCAGTGCGAGTTCTCCACTGGAAAG
CACTGCTGTGTCTACTCCGATGATGAAATAGGAAACCTCGACTGCACCGCCAAGTGCGCCGCTGCCAAGCGTGCTGATGGTGCCGCTTCCGGTG
GTACCGCTTGTGCAGCTTCAGGAGAATACAAGTGCGCTACCGTTTTCGAGTCTCTCGACCGTACTCCATGTTACAAGGAGTAA

>CcSSP93
ATGGTTAAATTCTCCTCCATCGCTCTCTTCCTCATCGCTGCTGTCAGTGTACAAGCTTGCACTTATTGCCAATGTTTATTATCAAACGGCAGACATT
GTTGTTTATATGAGAACTCTCTTATGGGCAACATGGACTGTACTGCTATGTGCAAACAAGCGGTTCGAAAAGATGGCTCTACTTGTGAAGCTCAA
GGATCATACAAATGTGCGACTGTTTTTGAAAAAGACTATCGTAAGAAATGTCGAAACACTTATTAG

>CcSSP94
ATGAAGTTCTCTGCCGTTGCCTTGTTTTTCATCGCCACTCTCGGTGTACAAGCTTGCCAGTACTGCCAATGCCAGTTCGCAGATGGTTCCAACTGTT
GTTTAGCCAGGGATGATAGAGTTAAGAACCTCGACTGTACTGCTGTTTGCTCACCTGCCCGCCGTTCGGATGGTACCAGATGGCCTATCCAAGAT
TCTAATGCCGTGGACCTTGGTACTGCTTGTGGTGCCGGTGGAAGATATAAGTGTGCTACTGTTTTCCAACTTGTCCGTACCCAATGCCAATCCCAA
GGCAGAGGTTGGTAA

>CcSSP95
ATGGTCAAGATATCCTTCATCGCCCTATCCCTCCTCTTTAATGCTCTCGCCATTCAAGCGTGCGATTATTGCCAATGCCTATTCGAAGATGGTTCCC
ACTGTTGTCTAGTCAAGGGCCCTGATTGTACAGCCGCTTGCAAAATAGCCCGCCAGGCGGATATTCCGCATTGGGAGACAAAGTTGCTAGGAAA
GCGATGTGGTCTTACAGGACAATATAAGTGTGCTACTTGGGTCGAACAGCAACATCGTGACAAATGTCAAGGGTAG

>CcSSP96
ATGGTCAAATTCACCTCCATCGCTCTGTTCCTCATTGCCGCCATCGGCAGCGCGCAGGCTTGTACCTGGTGTCAATGCCTCTTCAAGGATGGCTCG
CATTGTTGTCTCAAACAGGACGATCGTATTGGTAACCTCGATTGTACAAAGGCCTGCGACGGAGCCCGTCGTCACGATGGCACACAGACTCTTGA
CGCTAGTGGCAAGGTCATTAGTGAGGGTACCGCTTGTAATGCGGCTGGAAAATACAAGTGTCTTACTATTTTCAATGTCAACAATCATGTAAACT
GTCATTAG

>CcSSP97
ATGGTCAAATTCTCATCCATTGTCATATTCCTTCTCGCCAGCGCTTTTAGTGTGGAAGCTTGCAAATATTGTCAATGTTTATTCGATGATGGATCAC
ACTGTTGTCTAGCAAAGGACGATCGAGTCAATGACCAAGATTGTACTGCGGTTTGCGCAAAGATGCGTCGTGACGACGATACAATGTGGATTAT
ACCCGGACCAATACCCTACGGAAAAGGCGTAGCAATACTTGGCACAGCTTGTTCGTCCTCGGGAAAATACAAGTGTGTTCCTTGGATTAATTCGA
ATGGTCGTGCGAAATGTAGAGTAGGATAG

>CcSSP98
ATGGTTAAATTTTCCTCCATCGCACTACTCCTCATCGCCGCTGTCAGCGTACAAGCTTGCAAGTATTGCCAATGTTTATACTCCAATGGCAACCATT
GCTGCTTGTATAAGAACTCTCAGGTTGGGGATCTTGATTGCACTGCCATTTGCAAAGACGTCGTTCGTAAAGATAACAAAGCATGTAATGGTTCG
GGATCATACAGATGTGCTACTGTTTTTCAAGCCAACTTTCGTGAGACCTGTCAGAACACTCATTAA

>CcSSP99
ATGGTTAAATTCTCTGCCATCGCCTTACTCCTTATCACCGCTGTTAGTGTGCAAGCTTGTACTTTCTGTCAATGCTTATTATCAAATGGCCAACATT
GTTGCATTACTGGGGACCCTCATACCGGTAATCAAGATTGTAGTGCGGCTTGCAAGGATGCCCATCGTGACAGCGATAACACTAAATGTAGCGC
CGGTGGAAGCTACAAATGTGCTACTATTCTCGAAGTCGATGGCCGTGCTAAGTGTTCCTAG

>CcSSP100
ATGGTTAAAATCTCCGCTATCGTCATGTTCCTCATAGTTACTGTGGGTGTACAAGGTTGTACATACTGTCAATGTCTATTCAAGAATGGGAACCAT
TGTTGTATTTATACGAGCCCTCTCGGTGGTGATGCTGATTGCACACGCGCCTGTCAAACTGTCGAACAAATGGATGGCAACAAATGTGAAGCTGG
AGGAGCTTACCGATGTGCTACTGCTTTTCAACAGAGCAACCGTAGCTACTGTAAGCGTCGAATTTGGTAG

>CcSSP101
ATGGTTAAATTCAGCACCATCGCCTTATTCCTTATGACCGCTATCAGTGTACAAGCTTGTACCTATTGCCAATGTCTAAACGCTAATGGTGGGCAT
TGTTGTTTAGCCCAGAACCCTGATGTTGGCAATCAAGATTGTCACGCTGTATGCCAAACCATCCGTACATATGAAGGGAAAGTTTGTTTTGGTGG
TGGTGCATACAAATGTGCATCTATTTTCGAAGCCGAGCATCGTTCTAGATGTGATGTTTAG

>SsSSP3/SS1G_06068
T0ATGGTCCGCATCGCCTCTATCGCCTTATTCTTCATCGCCAGCGCCCTTTCGGTGCAAGCTTGCACATACTGCCAGTGCGAGTTCTCAAACGGTG
GTCACTGCTGTGTCTACTCAGATGCTGAGATTGGAAACCTCGATTGCAACAAGTACTGCGCTAATGCTCACCGCGCTGACGGTACCAACGGTGTC
GGAGGTCCTGGAACTGCTTGCGCCGCTGGAGGAGCTTACAAGTGCGCCACCATCCCTGAGTCTCTTGACCGTACTCCATGCTAG

>BcSSP2/BC1T_01444
ATGGTCCGCATCTCCTCCATCGTCATGTTCTTCCTTGCCAGCGCTTTATCAGTGCAAGCATGCACCTATTGCCAGTGCGAATTCTCAAACGGTGATC
ACTGCTGTGTCTATTCGGATGCTGAAATTGGCAACCTCGATTGCCCAACCTATTGCGCTAATGCTCATCGCGCAGATGGTGCAGCTGGTGGTGGA
ACTGCATGCGCAGCTGGAGGAAAATACAAGTGCGCGAGTGCTTTCACAGCTCTTGATCGTACCCCATGTTAG

10. Publication

The majority of the research presented in chapter 3 was published in the journal *Phytopathology*. A copy of the title page is shown here

Genetics and Resistance

e-Xtra*

Ciborinia camelliae (Sclerotiniaceae) Induces Variable Plant Resistance Responses in Selected Species of *Camellia*

Matthew Denton-Giles, Rosie E. Bradshaw, and Paul P. Dijkwel

Institute of Molecular Biosciences, Massey University, Palmerston North, Manawatu, 4442 New Zealand.
Accepted for publication 6 February 2013.

ABSTRACT

Denton-Giles, M., Bradshaw, R. E., and Dijkwel, P. P. 2013. *Ciborinia camelliae* (Sclerotiniaceae) induces variable plant resistance responses in selected species of *Camellia*. Phytopathology 103:725-732.

Ciborinia camelliae is the causal agent of Camellia flower blight. This fungal pathogen is a significant pest of the *Camellia* floriculture industry because it specifically infects the floral tissue of ornamental camellia cultivars leading to the rapid development of necrotic lesions and blight. This study aims to characterize natural resistance to *Ciborinia camelliae* within a selection of *Camellia* spp. Based on macroscopic lesion development, *Camellia* 'Nicky Crisp' and *Camellia lutchuensis* were chosen as compatible and incompatible hosts, respectively. Microscopic analyses of the incompatible *Camellia lutchuensis–Ciborinia camelliae* interaction revealed several hallmarks of induced plant resistance, including papillae formation, H_2O_2 accumulation, and localized cell death. The compatible *Camellia* Nicky Crisp–*Ciborinia camelliae* interaction failed to trigger a similar resistance response. *Ciborinia camelliae* growth in compatible tissue demonstrated a switch from biotrophy to necrotrophy, evident from the simultaneous development of secondary hyphae and necrotic lesions. Extension of resistance analyses to 39 additional *Camellia* spp. identified variable levels of resistance within the *Camellia* genus. The evidence presented supports a resistance breeding strategy for controlling *Ciborinia camelliae* on ornamental *Camellia* hybrids.

Additional keywords: appressoria, hypersensitive response.

The genus *Camellia* is the largest and most economically important of the family Theaceae (5,45). The two most economically important species are *Camellia sinensis* var. *sinensis* and *Camellia sinensis* var. *assamica*, which are cultivated for the production of tea (5). *Camellia* spp. are also valued as ornamental shrubs, being especially popular in temperate regions of the world, including North America, Europe, and Australasia (1,37). Intraspecific and interspecific hybrids of *Camellia japonica*, *Camellia sasanqua*, and *Camellia reticulata* form the basis of more than 20,000 registered ornamental *Camellia* cultivars (33).

Many ornamental *Camellia* spp. and cultivars are susceptible to infection by the fungal phytopathogen *Ciborinia camelliae* L. M. Kohn (Sclerotiniaceae) (21). This pathogen specifically infects the floral tissue of *Camellia* spp. following the dissemination of ascospores from sclerotia-germinated apothecia. Commonly referred to as "Camellia flower blight," compatible interactions result in the development of brown petal lesions, blight, and premature flower fall (21). Prior to the 1990s, *Ciborinia camelliae* had been described only in Japan and North America (11,13). However, recent introductions have been reported in New Zealand (1993) and Europe (1999) and the disease is now widespread in these regions (37).

A number of methods have been tried to control *Ciborinia camelliae* infection, including pest management approaches (42), fungicide applications (37), and the use of biological control agents (43,44). Although several of these strategies have shown promise in reducing the infection rate of *Ciborinia camelliae*, none have been able to stop the annual reincursion of this pathogen into treated areas. The discovery of natural resistance to *Ciborinia camelliae* in several species of *Camellia* has revealed a new opportunity for controlling this pathogen on ornamental *Camellia* hybrids (36).

The identification of incompatibility in several *Camellia* spp.–*Ciborinia camelliae* interactions suggests that the effector repertoire of *Ciborinia camelliae* is not adapted for all species of the genus *Camellia*. The attempted colonization of a plant by a nonadapted microbial pathogen can result in the induction of plant resistance (14,39). Induced plant resistance responses are under complex genetic control and are mediated by the plant immune system (16,28). The plant immune system consists of two branches that have separate molecular mechanisms for detecting pathogen infection (16). The first branch recognizes conserved microbial-associated molecular patterns (MAMPS) at the cell wall, through the action of pathogen recognition receptors (PRRs) (10). MAMP-triggered immunity (MTI) characteristically stimulates downstream defense responses that include cell wall modifications, papillae formation, phytoalexin biosynthesis, and reactive oxygen species (ROS) accumulation (15,25,38). A host-adapted pathogen that successfully suppresses MTI through the action of its effectors is said to have established effector-triggered susceptibility (ETS) (16). The second branch of the plant immune system involves the detection of pathogen effector molecules by plant resistance (R) proteins. Effector-triggered immunity (ETI) characteristically culminates in a hypersensitive response (HR) and is a more rapid response than MTI (16). Many plant–pathogen interactions stimulate characteristics of both branches of the plant immune system (15,31).

In the present work, we aimed to characterize the host responses associated with the compatible *Camellia* 'Nicky Crisp'–*Ciborinia camelliae* and incompatible *Camellia lutchuensis–Ciborinia camelliae* interactions. In addition, we sought to identify further sources of resistance to *Ciborinia camelliae* within the genus *Camellia*.

Corresponding author: P. P. Dijkwel; E-mail address: P.Dijkwel@massey.ac.nz

* The *e*-Xtra logo stands for "electronic extra" and indicates that the online version contains three supplementary figures and two supplementary tables. Figures 1 and 3 appear in color online.

http://dx.doi.org/10.1094/PHYTO-11-12-0289-R

The full paper can be accessed via the following link:
http://apsjournals.apsnet.org/doi/abs/10.1094/PHYTO-11-12-0289-R